Role of the glucocorticoid pathway in skeletal muscle wasting and hepatic metabolism rewiring during cancer cachexia in ApcMin/+ mice – Functional implication of myostatin gene invalidation

Agnès Martin

N° d'ordre NNT : 2020LYSES034

THESE de DOCTORAT DE L'UNIVERSITE DE LYON

opérée au sein de
L'Université Jean Monnet Saint Etienne

Ecole Doctorale N° 488
Ecole doctorale Sciences, Ingénierie, Santé (EDSIS)

Spécialité / discipline de doctorat : Biologie, Médecine, Santé

Soutenue publiquement le 21/10/2020, par :

Agnès Martin

Role of the glucocorticoid pathway in skeletal muscle wasting and hepatic metabolism rewiring during cancer cachexia in *Apc*$^{Min/+}$ mice – Functional implication of myostatin gene invalidation

Rôle de la voie des glucocorticoïdes dans la perte de masse musculaire et le remaniement du métabolisme hépatique pendant la cachexie associée au cancer dans les souris *Apc*$^{Min/+}$ – implications fonctionnelles de l'inactivation du gène de la myostatine

---

Devant le jury composé de :

Rébillard Amélie, Professeur des universités Université de Rennes, France	Rapporteure
Thissen Jean-Paul, MD, Professeur des universités Université Catholique de Louvain, Belgique	Rapporteur
Blaauw Bert, Associate Professor University of Padova, Italie	Examinateur
Busquets Silvia, Agregate Professor University of Barcelone, Espagne	Examinatrice
Rohm Maria, PhD Helmholtz Center Munich, Germany	Examinatrice
Freyssenet Damien, Professeur des universités Université Jean Monnet Saint Etienne, France	Directeur de thèse

« *Goutte à goutte, l'eau est capable d'ouvrir un rocher. Et ce n'est pas en raison de sa force, mais par sa constance. C'est pour cela que les triomphes appartiennent à ceux qui ne renoncent jamais.* » Licha

REMERCIEMENTS/ACKNOWLEDGMENTS

Je tiens tout d'abord à remercier mon directeur de thèse, **Damien Freyssenet**, pour avoir accepté de me prendre en stage de L3 et de m'avoir confié ce projet, qui débutait à l'époque tout juste, alors que je n'avais que 19 ans et que je découvrais à quoi pouvait bien ressembler un laboratoire de recherche ! Je le remercie pour la bienveillance et la confiance qu'il a eu tout au long de ma thèse, son calme et surtout pour m'avoir toujours encouragée et accordé énormément de temps. J'espère que vous voudrez bien encore de moi pour ma prochaine thèse !

Je remercie les Professeurs **Amélie Rébillard** et **Jean-Paul Thissen** d'avoir accepté d'être rapporteurs de ma thèse et de prendre de leur temps pour évaluer mon travail. I would also like to thank Dr. **Maria Rohm**, Pr. **Silvia Busquets** and Pr. **Bert Blaauw** to be examinator during my defense.

Merci à **Alain Belli** de m'avoir accueillie au LPE et d'avoir contacté Damien pour me prendre en stage, puis à **Thierry Busso** par la suite de m'avoir accueillie en thèse au désormais LIBM. Un énorme merci à **Anne-Cécile Durieux** de m'avoir transmis sa science des souris, même si ce n'était pas gagné au début, pour toute l'aide au labo et la dernière relecture ! Merci à **Josiane Castells**, Josy, notre petite maman du labo, de m'avoir si bien appris à faire des PCR. Dès 2015, tu t'es occupé de « mon éducation », si j'avais une question, tu y répondais, si j'avais fait une boulette, tu trouvais toujours une solution (et si j'avais besoin d'une boîte, tu en avais forcément une qui convenait !). Tu as vraiment été un repère pour moi tout long de ma thèse (même si tu as préféré prendre ta retraite que de me supporter quand j'écrivais ma thèse…) je te remercie vraiment pour tout. Merci à **Valentine Allibert**, d'abord on a appris à faire les westerns ensemble (couler les gels à 7h du matin pour qu'ils fondent en migrant, les tic-tacs, la vaisselle, le propinel, l'activation de l'ECL à la lumière, le broyage à l'azote, tout ça…) puis tu es revenue au labo prendre la suite de Josy. Merci pour tout l'aide que tu m'as apporté, heureusement que tu étais là, speedy gonzales de la PCR ! Bonne continuation au labo et ne jette pas toutes mes manipes dès que je ne serais plus là ! Merci à **David Arnould** et **Nadir Moussaoui**, à tout jamais mes premier co-bureau, c'est aussi grâce à vous que j'ai eu envie de faire ma thèse dans ce labo. Merci pour la bonne ambiance et de m'avoir transmis votre expérience (et pour les consult western !). Merci à **Yann Gallot** pour avoir eu ce rôle de grand frère de labo tout au long de ma thèse ! Merci à **Pierre Pelliat** pour ton aide (notamment pour la récupération du fichier Word de ce manuscrit…), maintenant c'est toi le prochain à soutenir, je te souhaite le meilleur, je sais que tu seras un bon chercheur ! Merci à tous les stagiaires qui sont passés au labo pour leur aide technique et/ou psychologique : **Salma** (première co-stagiaire), **Anne-Sophie**, **Léa**, **Cindy**-**Lahcène**-**Kilian** (le trio magique), **Marie-Charlotte**, **Lisa**, **Estelle**, **Ismahane** (merci pour les souris), **Michel-Yves**, **Sarah** et **Quentin**. Merci également aux autres doctorants du laboratoire pour toutes les petites

discussions et **Anne-Cloé** pour la bonne ambiance des repas du midi ! Merci au personnel du PLEXAN, **Ghislaine**, **Coraline**, **Valentine**, pour avoir pris soin de nos petites souris et pour l'aide dans les manipes. Merci à **Christophe Hourdé** pour les journées pop-rock dans l'animalerie à mesurer les forces des souris. Merci au Dr. **Karine Abboud** pour avoir permis le développement du projet MYOCAC, même s'il n'a pas abouti de la façon dont on aurait souhaité, je la remercie pour sa bienveillance et sa rigueur à chaque test avec les patients. Merci aux secrétaires et aux infirmières du service de chirurgie thoracique pour leur accueil et leur aide. Merci à **Léonard Féasson** de m'avoir appris sa science de la biopsie musculaire et pour sa gentillesse tout au long de ma thèse. Merci à **Thomas Lapole**, **Robin Souron**, **Jérémy Rossi** pour leur expertise sur les mesures de force chez l'humain (et **Thibault** et **Loïc** pour leur aide technique avec le matériel !) et à **Sylvain**, **Marie-Charlotte** et **Michel-Yves** de m'avoir accompagné lors des tests avec les patients. Merci à **Laurent Tordella** de m'avoir aidé à décoder le questionnaire SF36. Merci à **Sylvain Grange** de m'avoir envoyé tous les scans, tu as vraiment géré, bon courage pour la fin de ta thèse ! Merci au GIMAP pour nous avoir permis d'utiliser le cryostat et à **Pauline Damien** et **Aurélie Montmartin** du Sainbiose pour nous avoir permis d'utiliser le lecteur de plaque et leur gentillesse. Merci à **Jérôme Morel** et **Julien Gondin** d'avoir participé à mes comités de suivi de thèse. Merci à **Laëtitia Mazelin** pour les souris KPZ et la visite de Berlin !

Merci aux enseignants de l'ENS de Lyon de m'avoir fait découvrir la recherche, notamment ma tutrice, **Déborah Prévôt** de m'avoir accompagnée pendant ces 3 années. Merci à **Vincent Pialoux** de m'avoir prise en stage en M2, ce n'était pas facile de gérer les 2 projets mais j'ai énormément appris, merci pour tout. Merci également à toute l'équipe du LIBM de Lyon pour leur accueil **Philippe**, **Camille**, **Cyril** et **Michel**. Merci aussi aux autres étudiants notamment **Mathilde** (toujours là pour les petites discussions sur les trajets !), **Etienne** et **Amandine** pour la super ambiance dans le bureau mais également **Chantal** (and all your assays!), **Sarah**, **Pauline**, **Ellie**, **Emmanuelle**, **Quentin**, **Elise** et **Hugo**. Merci à **Lidia** de m'avoir fait découvrir la recherche clinique, pour tout ce que tu m'as appris et pour toutes nos discussions par la suite ainsi qu'à tout le CLB pour leur accueil. Merci à **Frédéric Roche** de m'avoir prise en stage d'observation au CHU en fin de M1 et pour le temps qu'il m'a consacré et à toute l'équipe du centre Visa pour leur accueil. Ich danke **Patrick Wahl**, der mich während meines M1 für ein Praktikum bei sich aufgenommen hat. Danke, dass du es mir ermöglich hast, an allen Projekten teilzunehmen. Danke für deine große Geduld mit meiner Sprache! Ich habe dabei so viel gelernt und die Arbeit erweckte in mir die Freude an der Forschung! Ich danke allen Mitgliedern des Instituts für Trainingswissenschaft und Sportinformatik für ihr Willkommen: **Anna**, **Christian**, **Lukas**, **Prisca**, **Puni**, **Sarah**, **Theresa**, **Wiebke**, **Yvonne**, usw... Köln wird für immer in meinem Herzen bleiben! Je remercie également tous les enseignants que j'ai pu avoir durant la prépa ou avant et qui m'ont permis d'acquérir les bases de travail nécessaire pour réussir ce projet.

Je remercie tous mes amis qui ont été là pendant ces 3 années ! Les plus anciennes, les meximiardes, après Frankfort et Einsiedeln, on a fini avenue Jean Jaurès mais c'était toujours une bouffée d'air frais, rassurante et de souvenirs (et quels souvenirs xD !) de vous revoir, merci d'être toujours là, **Alix**, **Marine**, **Mégane**, **Noémie** et **Perrine**. Merci aux 2CLAMS, c'était quand même bien horrible la prépa mais sans, on ne se saurait jamais connues. Merci pour tout, les vacances, les mardis soir, le ski, les appels interminables, le shopping, vous avez et êtes toujours là pour moi, **Cécile**, **Corélie**, **Laurélène**, **Marie** et **Sandra**. Et également à tous les autres, notamment mon cocolle **Théo** et **Florian** (alias cocolito et **Elise** !). Et **Perrine** ! Merci à toute la promo Alexandre Yersin pour ces 3 années à l'école passée ensemble voire au-delà, **Amaury** (super coloc pendant 15 jours), **Arnaud** (toujours là au groupama stadium), **Charline** (binôme des vers !), **Loïc** (binôme nageur), **Noémie** (bientôt toutes les couleurs !), **Marie-Anaïs**, **Marion**… que de futurs docteurs ! Merci à l'Indépendante Stéphanoise, ma bouffée d'oxygène pendant la thèse (et à mon directeur de thèse d'avoir toujours accepté que je parte au gymnase !) merci **Cyrille** de m'avoir entraînée pendant toutes ces années et aux filles pour les heures d'entraînements passées ensemble **Juliette**, **Justine**, **Lilou**, **Louna**, **Oriane**… et L'Equipe **Charlotte**, **Louane** et **Nina**.

Merci **Papa** et **Maman** de m'avoir toujours soutenue dans mes études (et c'est pas fini !! Promis après, j'arrête…), même si je voulais retourner en CM2 et aller en STAPS, c'était pas si mal finalement ! Merci de m'avoir permis de faire mes études toujours dans les meilleures conditions et pour tout le reste, désolée d'avoir été un peu absente et pénible pendant les derniers moments de rédaction, c'est fini maintenant ! Merci pour l'éducation et tout ce que vous m'avez donné. Merci à mes sœurs, **Hélène** (grâce à qui les pages sont correctement numérotées ^^) et **Sophie** pour tout. Merci à tout le reste de la famille, et notamment les autres **Martin** pour le dernier soutien !

J'espère n'avoir oublié personne mais je remercie vraiment toutes les personnes que j'ai pu côtoyer durant ces 3 années.

TABLE OF CONTENT

LIST OF ABBREVIATIONS

ACTH: adrenocorticotropic hormone

ActRIIb: activin type IIb receptor

Alk4: activin-like kinase 4

Alk5: activin-like kinase 5

AMPK: 5'AMP-activated protein kinase

APC: adenomatous polyposis coli

BMI: body mass index

CRH: corticotropin-releasing hormone

CRP: C-reactive protein

CRTC2: CREB-regulated transcription coactivator 2

CSA: cross-sectional section

CT: computerized tomography

GC: glucocorticoid

GFR: glomerular filtration rate

GPAQ: global physical activity questionnaire

GSH: glutathione

GSK3: glycogen synthase kinase 3

GSSG: glutathione disulfide

HPA: hypothalamic-pituitary-adrenal

HU: Hounsfield unit

IGF1: insulin-like growth factor 1

JAK: janus kinase

L3: 3rd lumbar vertebrae

LLC: lewis lung carcinoma

KO: knockout

MDA: malondiadehyde

MET: metabolic equivalent of task

Mstn: myostatin

mTOR: mammalian target of rapamycin

MVC: maximal voluntary contraction

NF-κB: nuclear factor κ B

OS: oxidative stress

PARP: poly(adenosine diphosphate ribose) polymerase

QIF: *quadriceps* intermittent fatigue

ROS: reactive oxidant species

rpS6: ribosomal protein S6

S6K: S6 kinase

SMD: skeletal muscle density

SMI: skeletal muscle index

SOD: superoxide dismutase

STAT3: signal transducer and activator of transcription factor 3

TBS-T: tris buffered saline-0.1% Tween 20

TGF-ß: transforming growth factor-ß

GENERAL CONTEXT

Cachexia, from the Greek “kakos” and “hexis” meaning “bad condition”, was reported in cancer patients since the beginning of medicine [1]. Cancer cachexia is a complex systemic metabolic syndrome characterized by an involuntary body-mass loss that cannot be fully reversed by increasing conventional nutritional support. Two main definitions were proposed to clinically classify cancer patients as cachectic considering only a body mass loss greater than 5% in the past 6 months [2] or in combination with additional criteria including blood biochemistry, fatigue, anorexia, muscle force and mass [3]. Overall, cachexia is a critical determinant in cancer patient survival [4]. One of the most important phenotypic features of cancer cachexia is a pronounced loss of skeletal muscle mass. Imaging analysis of skeletal muscle from cancer patients indicates that skeletal muscle depletion varies from 5% to 89% depending on cancer type, the severity of the disease and the method of measurement [5]. Skeletal muscle mass loss is the principal cause of functional impairment, respiratory complications and fatigue that markedly reduce patients’ quality of life. Ultimately, skeletal muscle mass loss is associated with a decrease in cancer patient survival [6–15].

The research in the field has largely progressed in the past decade providing important information about the pathophysiological mechanisms involved in the regulation of skeletal muscle mass during cancer cachexia and it is also now clear that other tissues and organs, as well as tumor tissues, secrete soluble factors that act on skeletal muscle to promote wasting [16–18]. My PhD project aimed to consider the systemic effects of cancer cachexia notably on the liver. I particularly explored the biological function of the glucocorticoid pathway during cancer cachexia and its potential roles in skeletal muscle wasting and hepatic metabolism rewiring.

This manuscript is divided into three main parts. The first part deals with a review of the literature that addresses 3 main subjects. The first one concerns the phenotypic features of cancer cachexia-related loss of skeletal muscle mass and function. This work is currently submitted for review in the Journal of Cachexia, Sarcopenia and Muscle. The second one explores the molecular mechanisms of cancer cachexia-related loss of skeletal muscle mass. This chapter will be also submitted for publication. Finally, the third one focuses on the regulation of the glucocorticoid pathway during cancer cachexia. I then present my experimental work in a second part. Two studies are presented. A first study presents the data obtained in cancer patients (MYOCAC study) and a second study presents the data obtained on the *Apc*$^{Min/+}$ mouse model of cancer cachexia (*Apc* study). This mice model was used to explore the biological function of the glucocorticoid pathway during cancer cachexia. A manuscript of this second study is currently under preparation. Finally, these results are briefly discussed and the perspectives to my work are presented in the third part.

GENERAL INTRODUCTION

Chapter I: Phenotypic features of cancer cachexia-related loss of muscle mass and function: lessons from clinical and animal studies

Introduction

Cancer cachexia is a complex catabolic syndrome characterized by an involuntary body-mass loss essentially due to a severe depletion of skeletal muscle, with or without adipose tissue loss, while the non-muscle protein compartment is relatively preserved [2]. In contrast to malnutrition, cancer cachexia cannot be reversed by increasing conventional nutritional intake, thus highlighting the fact that the hypercatabolic state of cachectic patients is a critical determinant of the syndrome. The prevalence of cachexia in cancer patients is quite variable, affecting from less than 15% of prostate cancer patients to almost 70% of pancreatic cancer patients [17], with an increasing prevalence with the advanced stages of the disease. Cancer cachexia is one of the most debilitating and life-threatening aspects of cancer, profoundly affecting the patient's quality of life [4,19–24]. Cachexia increases surgical risks [25] and the susceptibility to the adverse effects of chemotherapy [23,26,27]. It also induces a progressive reduction in the body's functional capacities [28] leading to an increased sedentarization [22,29] and a loss of autonomy ultimately requiring institutional care of the people affected. Since the pioneering works of Dewys *et al.* [30], it has been consistently reported that the extent of cachexia is inversely correlated with the survival of cancer patients [4,8,13,21,22,31–35] and it is generally assumed that cachexia will be responsible for the death of approximately 20% of cancer patients, making it the leading cause of death in cancer [36].

During cancer cachexia, skeletal muscle represents the main site of protein loss [37,38]. The loss of muscle mass affects 5 to 89% of cancer patients depending on the cancer site and the method of measurement used [5]. Muscle mass loss is greater in weight-losing cancer patients when compared to weight-losing anorexia nervosa patients [39] indicating that cancer-specific factors, independently of denutrition, contribute to decrease skeletal muscle mass. As described for body mass, skeletal muscle mass loss in cancer patients is an independent factor that increases the risk of surgical complications [6,7], decreases surgical efficiency [8] and increases chemotherapy toxicity [10,11,40,41]. Skeletal muscle mass loss is therefore widely associated with a decreased survival rate of cancer patients [6–15].

Cancer cachexia is a constantly developing area of great research interest [42]. Numerous clinical and experimental studies have thus been devoted to deciphering the molecular pathways involved in cancer cachexia as well as developing strategies aimed at stopping or even reversing the loss of body mass and skeletal muscle mass loss (reviewed in [16–18,43–48]). However, what is less known are the effects of cancer cachexia on skeletal muscle structure and function. In order to fully understand the etiology of cancer cachexia, it is essential to clearly identify its effects on skeletal muscle phenotype. In this review, we will consider the effects of cancer cachexia on

skeletal muscle contractile and metabolic phenotypes both in cancer patients and in experimental animal models. Since muscle structure cannot be dissociated from muscle function, we will also consider how and to what extent cancer cachexia affects skeletal muscle function.

Skeletal muscle atrophy during cancer cachexia

When studying cancer cachexia in human patients, it is important to determine the extent of skeletal muscle atrophy since body mass loss in cancer patients does not strictly reflect skeletal muscle mass loss [49]. This is particularly true in obese cachectic patients where high body mass index may mask the extent of skeletal muscle depletion [13]. Different techniques have been used to quantify the atrophy of skeletal muscle mass during the time course of cancer cachexia (for review [50,51]). Indirect assessments of skeletal muscle mass by the analysis of whole-body composition using either neutron activation [37], dual-energy X-ray absorptiometry [52–55] or bioelectric impedance [4,56–59] indicate that lean body mass is reduced in cachectic cancer patients compared to healthy controls or non-cachectic cancer patients [35]. When specifically looking at skeletal muscle by imaging techniques, studies also clearly evidence skeletal muscle atrophy. The *quadriceps* muscle area measured by magnetic resonance is decreased by 10 to 33% in cachectic cancer patients when compared to healthy control subjects [56,60,61]. When compared to non-cachectic cancer patients, the *quadriceps* muscle area of cachectic cancer patients is either stable (female) or decreased (male) but to a lesser extent (14%) [60], indicating that even if cachexia is not clinically diagnosed (based on body mass analysis), skeletal muscle catabolism has already started. Lately, the use of computerized tomography (CT) scans has spread widely as these images may be available in the medical records of patients. CT scan analysis at the 3rd lumbar vertebrae level allows the quantification of the areas of *rectus abdominus*, *transversus abdominus*, *erector spinae*, *quadratus lumborum*, psoas minor and major, internal and external abdominal oblique muscles [62], which gives a good estimate of the whole body muscle compartment [63]. By using this technique, the atrophy of skeletal muscle is also clearly evident and increases with body mass loss in cachectic cancer patients [49]. When skeletal muscle area is normalized to the height of patients (skeletal muscle index, SMI), similar results are obtained with a 4 to 13% decrease in skeletal muscle index in cachectic cancer patients compared to non-cachectic cancer patients [4,24,58,64]. Once again, skeletal muscle mass loss increases with the severity of the disease.

Studies using different animal models of cancer cachexia also consistently report that compared to control animals a decrease is observed in lean body mass [65–68] as well as in the mass of skeletal muscle with different metabolic and contractile properties such as of *gastrocnemius* [69–94], *soleus* [68,72,76,77,79–81,85,87,89,92,95–97], *extensor digitorum longus* [68,78,79,84,87,88,92,96–100], *tibialis anterior* [68,69,72,75,78–80,83,84,87–94,96–98,100,101], *plantaris* [79,81,84,85,98], *quadriceps* [65,67,69,75,78,79,84,90,91,93,98], *triceps* [65], *epitrochlearis* [88] and diaphragm [85,95] muscles. When compared to non-cachectic cancer

animals, the muscle mass of cachectic cancer animals is also lower [70,76,78,101–105]. Similarly to human cancer patients, the extent of skeletal muscle mass loss increases with the severity of the experimental model [70,103,104,106]. When normalized to body mass, skeletal muscle mass still remains lower in cachectic cancer animals [71,78,79,84,102,107–117] indicating that other tissues, such as adipose tissue, are also depleted in these animal models. Interestingly, many studies reported no difference in *soleus* muscle mass between cachectic cancer animals and healthy animals [78,84,88,98,103,105,111,112]. The postural/anti-gravitational function of the *soleus* muscle (enriched in type I muscle fibers [118]), which involves a tonic motor nerve activity, may explain its resistance to cancer cachexia, also suggesting that skeletal muscle phenotype, function and pattern of neuronal innervation is critical in determining skeletal muscle sensitivity to cancer cachexia.

Effect of cancer cachexia on skeletal muscle fiber size and typology

Skeletal muscle mass depends on the number of muscle fibers, the cross-sectional area and the length of muscle fibers.

Skeletal muscle fiber number

Muscle atrophy during cancer cachexia does not seem to involve a decrease in the number of muscle fibers. The number of muscle fibers is similar in the *vastus lateralis* muscle of cachectic cancer patients and healthy control subjects [56], as well as the number of type I and type IIa muscle fibers in the *rectus abdominis* muscle of cachectic and non-cachectic cancer patients [119]. However, the count of muscle fibers was expressed per square millimeter [56,119], which obviously did not allow the determination of the absolute number of fibers in the muscle. In a mouse model of cancer cachexia, it has also been reported that the whole number of *tibialis anterior* muscle fibers was unchanged between control and cachectic cancer mice [98]. Therefore, the decrease in muscle mass during cancer cachexia would be mainly due to a decrease in muscle fiber volume rather than a decrease in muscle fiber number. However, if the number of muscle fibers seems to be unchanged during cancer cachexia, some myonuclear death by apoptosis may occur locally along the muscle fiber. Although not systematically observed [120], the presence of both interstitial and myonuclear apoptotic nuclei have been reported in the skeletal muscle of cachectic cancer patients [121,122] as well as in cachectic cancer mice and rats [98,103,114,115,117,123–125]. Yet, apoptosis does not seem to be high enough to decrease the whole number of muscle fibers, so that these apoptotic events may weaken the muscle fiber rather locally, rendering it more sensitive to micro-injuries (see below).

Skeletal muscle fiber size

Skeletal muscle fiber cross-sectional area is decreased in cachectic cancer patients, either when compared to healthy subjects [54,56], non-cachectic cancer patients [54,126], or arteriosclerosis patients

[127] (Table 1). A reduction in fiber cross-sectional area has also been consistently reported in cachectic cancer mice compared to control mice in the *quadriceps* [75,128], *gastrocnemius* (-28 to -62%) [68,75,91,91,129–135], *tibialis anterior* (-22 to -40%) [78,89,93,94,97,100,113,116,136–148], *soleus* (-24 to -40%) [77,145,148,149] and *extensor digitorum longus* (-28%) [150] muscles (Figure 1). Similar results have also been reported in cachectic cancer rats [86,111].

Skeletal muscle fibers are heterogeneous with respect to their expression of myosin heavy chain isoforms conferring them distinct contractile properties [151]. Based on myosin heavy chain isoform expression, it is possible to distinguish type 1, 2A, 2X and 2B (not in human) fibers. These fibers also differ in oxidative and glycolytic metabolic capacities. The distinct contractile and metabolic characteristics of skeletal muscle fiber types may affect their sensibility to cancer cachexia. The size of muscle fibers expressing type 1 myosin heavy chain (the slow contractile isoform) is decreased by about 26% in skeletal muscle of cachectic compared to non-cachectic cancer patients [119], as well as between cancer patients and healthy control subjects [53,152]. Similarly, the cross-sectional area of type 1 fibers is also decreased by about 30% in the *tibialis anterior* [96,146,153], *gastrocnemius* [117,123–125,153], diaphragm [95,117,123–125], *soleus* [148] and *extensor digitorum longus* [111] muscles of cachectic cancer mice or rats compared to control animals. However, some studies did not report any change in type 1 fiber size in cachectic cancer patients either when compared to non-cachectic cancer patients [53] or to healthy subjects [61,154]. Similar results have also been reported in cachectic cancer animals versus control animals [84,90,98,99,105,110,155,156]. These discrepancies between studies regarding the extent of the decrease in type 1 fiber cross-sectional area could be explained by the tumor localization, the severity of cachexia, the typology and function of the analyzed skeletal muscles but also by the criterion used to define cachexia. For instance, Johns *et al.* [119], showed that type 1 fiber cross-sectional area was significantly lower in cancer patients with cachexia compared to non-cachectic cancer patients only when considering low muscularity plus body mass loss as a criterion for cachexia, while no difference was observed when using either body mass loss only or low muscularity as a criterion of cachexia.

The cross-sectional area of type 2 muscle fibers (expressing either type 2A and/or type 2X myosin heavy chain isoforms) is smaller in the *quadriceps* muscle of cachectic cancer patients [53]. Similar observations have been also reported in the diaphragm [123–125] and *gastrocnemius* [123–125,155] muscles of cachectic cancer mice, as well as in the *extensor digitorum longus* [111], diaphragm [117] and *gastrocnemius* [110,117] muscles of cachectic cancer rats. If some studies show that muscle fiber atrophy is not fiber type-dependent in both patients [53,119,152] and animals [95,96,111,117,123–125,146,148,153], a preferential atrophy of type 2 muscle fibers has been reported in a biceps muscle biopsy from a cachectic cancer patient [157] and more recently in the *quadriceps* muscle of cachectic cancer patients that were compared to healthy patients [154]. Similarly, animal studies also indicate that type 2 muscle fibers are more prone to atrophy than type 1 muscle fibers [84,99,110,155,156]. Therefore, despite controversies, a preferential atrophy of type 2 muscle fibers could would occur during cancer cachexia. When specifically looking at the effect of cancer cachexia on type 2A and type 2X muscle fibers, human studies indicate that the decrease in the cross-sectional area of

type 2 muscle fibers is similar in type 2A [119,152] and type 2X [61] muscle fibers of cachectic cancer patients compared to healthy controls. Animal studies also show a similar reduction in the cross-sectional area of type 2A muscle fibers in cachectic cancer mice [79,83,95,99,103,105,146,148] and type 2B [79,83,90,95,96,99,103,153,158]. Similar results have also been reported in skeletal muscle of cachectic cancer rats [84]. However, it should be noted though that some animal studies reported a greater decrease in fiber cross-sectional area of type 2B compared to type 2A muscle fibers [90,103,105,142,147,158,159], suggesting a greater sensitivity of type 2B muscle fibers to cachexia.

Table 1. Effect of cancer cachexia on muscle fiber cross-sectional area and muscle fiber type distribution in human cancer patients. Muscle fiber types were classified as type 1, type 2A and type 2X according to the expression of myosin heavy chain isoforms.

Reference	Muscle	Cancer type	Definition of cachexia	Control	Muscle fiber CSA			Fiber type distribution		
					Type 1	Type 2A	Type 2X	Type 1	Type 2A	Type 2X
113	*Rectus abdominis*	Upper gastrointestinal or pancreatic (n=17)	Stature adjusted skeletal muscle index consistent with low muscularity and weight loss >2%	Upper gastrointestinal or pancreatic cancer age-paired patients without cachexia (n=24)	↓ (-26%)	↓ (-26%)		=	=	
55	*Vastus lateralis*	Gastric, pancreatic, colon, bronchogenic carcinoma, chronic lymphatic leukemia (n=11)	Weight loss >10% within 6 months	Age-, gender- and body weight-paired healthy controls (n=15)	=	=	↓ (-44%)	=	=	=
50	*Vastus lateralis*	Gastrointestinal (n=19)	Weight loss >10% within 6 months	Age-, gender- and body height-paired healthy controls (n=19)	↓ (-32%)					
155	*Rectus abdominis*	Pancreatic carcinoma (n=8)	Weight loss >10% within the last 6 months before operation	Pancreatic carcinoma or chronic pancreatitis age-paired patients without cachexia (n=8)				=	=	
121	Sternocleidomastoid, diaphragm, deltoid, psoas, abdominal wall, *quadriceps*, adductor of thigh and *gastrocnemius*	Esophagus, bronchial, ovarian, rectum, biliary, stomach, pancreas (n=10)	n.r.	Arteriosclerosis age-paired patients without cachexia (n=4)	↓ (n.r.)					
120	*Rectus abdominis*	Gastric (n=13)	Weight loss >5% within the last 6 months	Gastric patients with weight loss <5%	↓ (-72%)					

			before operation+SMI < cutoff values	within the last 6 months before operation+SMI > cutoff values (n=10)				
47	*Quadriceps*	Non-small cell lung (n=16)	International consensus [2]	Non-small cell lung cancer patients without cachexia age- and gender-paired (n=10)	=	=	=	=
				Healthy age- and gender paired controls (n=22)	↓ (n.r.)	↓ (n.r.)	=	=
146	*Tibialis anterior*	Small cell lung carcinoma (n=1)	n.r.	Gender-paired healthy controls (n=2)	↓ (n.r.)	↓ (n.r.)		
190	*Rectus abdominis*	Colorectal (n=10)	n.r.	Without neoplastic conditions patients (n=7)	=			
148	*Vastus lateralis*	Lung cancer (n=10)	International consensus [2]	Healthy sedentary controls (n=10)	=	↓ (-24%)	=	=
48	*Quadriceps*	Non–small cell lung cancer (n=16)	International consensus [2]	Non-small cell lung cancer patients without cachexia age- and gender-paired (n=10)	↓ (n.r.)			
				Healthy age- and gender paired controls (n=22)	↓ (-27%)			

CSA, cross-sectional area; n.r., not reported; SMI, skeletal muscle index; ↓ significantly decreased vs control.

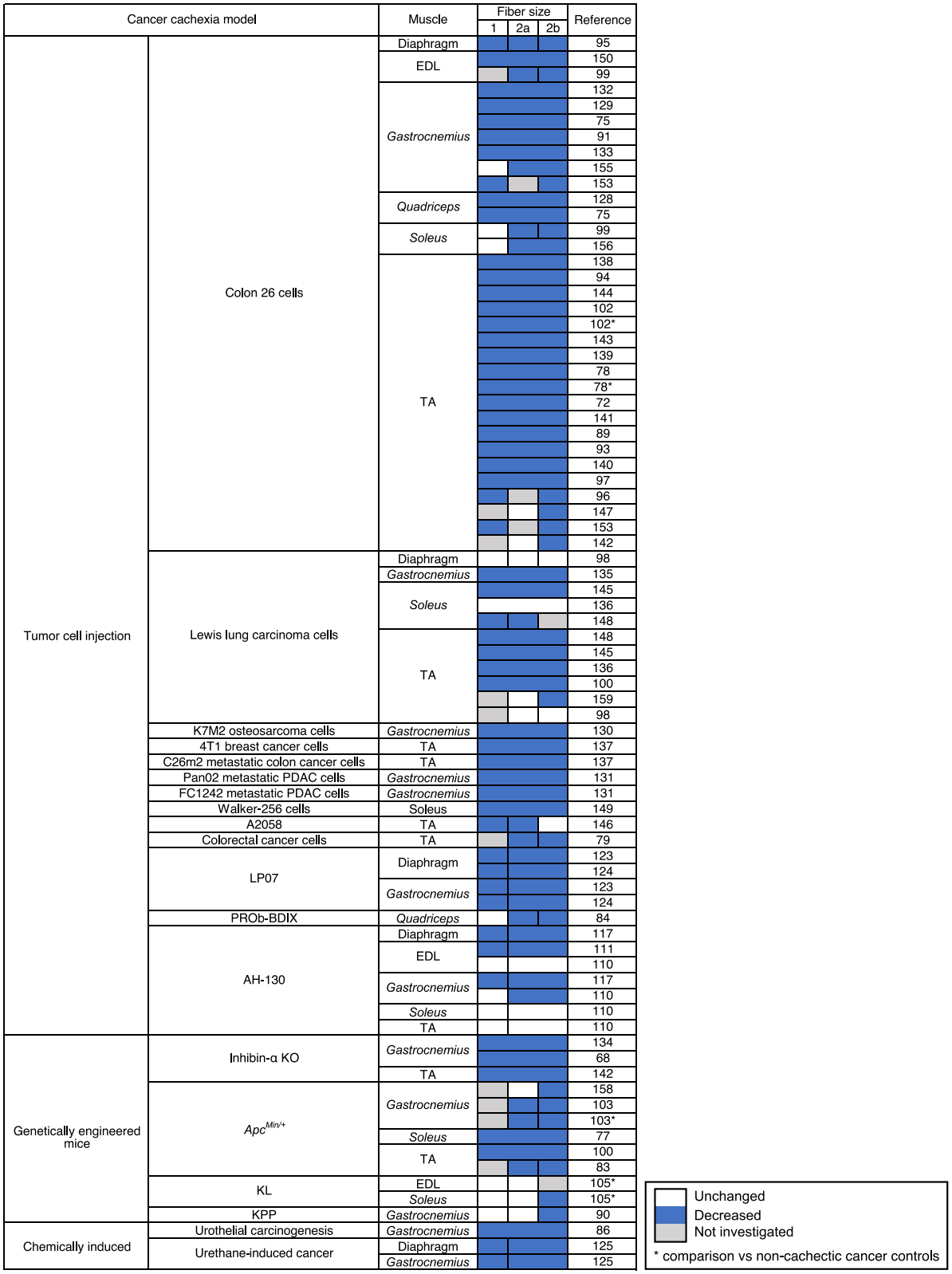

Figure 1. Muscle fiber cross-sectional area in mouse and rat models of cancer cachexia.
Unless indicated, comparisons were done with healthy control animals. *Apc*, adenomatous polyposis coli; EDL, *extensor digitorum longus*; KL, KrasG12D/+;Lkb1f/f; KPC, Kras; p53; Cre; PDAC, pancreatic ductal adenocarcinoma cancer; TA, tibialis anterior.

Skeletal muscle fiber type distribution

The relative proportion of each fiber type inside a muscle differs according to species, muscle function and innervation but also reflects dynamic adaptations to whole-body energy metabolism, neuromuscular activity and muscle repair [151]. If one study reported a shift toward an increase in the proportion of fast myosin heavy chain isoform in cachectic cancer patients [160], all other studies indicated that the distribution between type 1 and type 2 skeletal muscle fibers was unchanged in cachectic cancer patients when compared to either non-cachectic cancer patients [53,119,161] or healthy control subjects [61,154] (Table 1). Similarly, in animal models of cancer cachexia, a large majority of studies did not find any difference in fiber type distribution in the *gastrocnemius* [76,81,110,117,123–125], *plantaris* [81], *tibialis anterior* [79,98,110,147], diaphragm [95,98,117,123–125], *extensor digitorum longus* [110], *quadriceps* [162] and *soleus* [110] muscles (Figure 2). However, some animal studies reported an increase in the proportion of type 2A and 2B muscle fibers together with a concomitant decrease in the proportion of type 1 fibers in the *soleus* muscle, a slow-twitch oxidative muscle, in cachectic cancer mice compared to control mice [77,81,99]. A transition from type 2A towards type 2B has also been reported in the *soleus* [99,148] and *tibialis anterior* [142] muscles of cachectic cancer mice. Differences between studies could be explained by the physiological function of the muscle (postural/anti-gravitational such as *soleus* vs locomotor such as *gastrocnemius*) and the extent of cachexia. If the existence of a slow-to-fast fiber type shift needs to be further strengthened it is likely that such a shift would reflect an altered neuromuscular control, the innervation pattern and neuromuscular junction integrity being essential for conferring contractile and metabolic characteristics to the muscle fiber. Whether cancer cachexia is associated with alteration in innervation pattern and neuromuscular junction fragmentation of the postsynaptic membrane remains to be further explored. From a teleological point of view, a shift from slow-to-fast fiber type may lead to higher and faster force production (at the expense of greater fatigability), which may tentatively compensate for the whole decrease in muscle force due to muscle mass loss (see below).

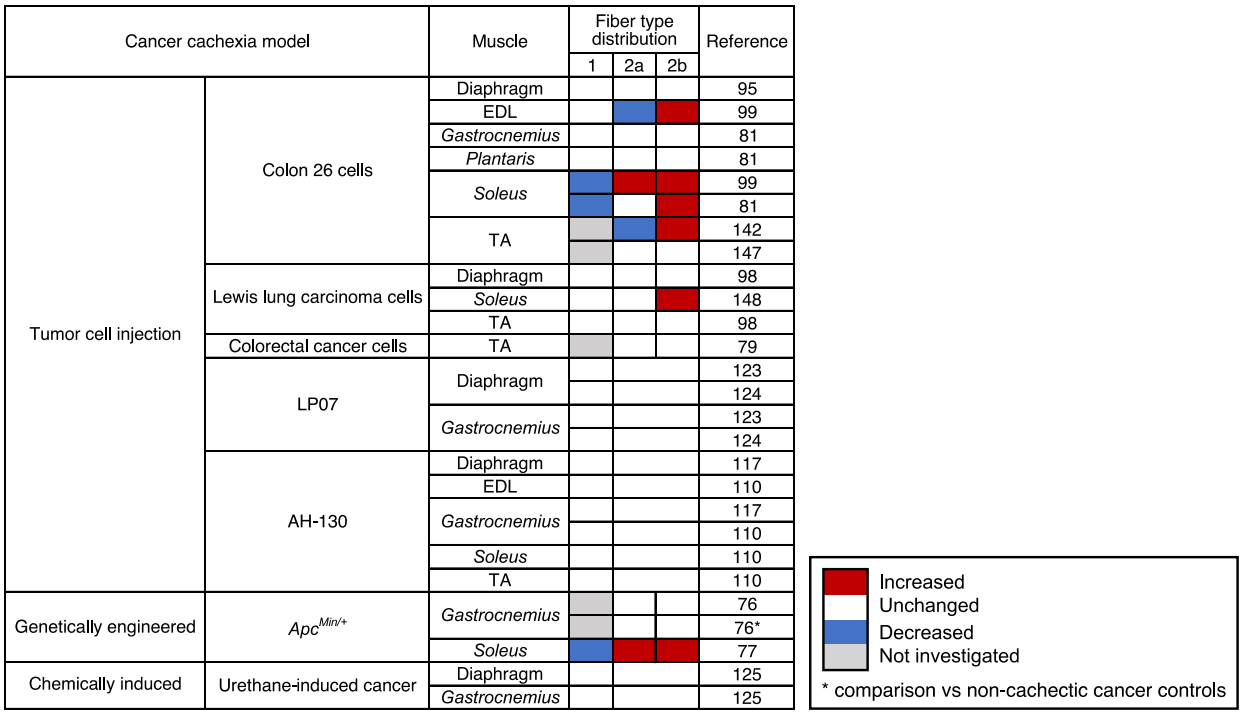

Figure 2. Muscle fiber type distribution in mouse and rat models of cancer cachexia.
Unless indicated, comparisons were done with healthy control animals. *Apc*, adenomatous polyposis coli; EDL, *extensor digitorum longus*; TA, *tibialis anterior*.

Metabolic phenotype of skeletal muscle

The diversity between muscle fibers is not restricted to the expression of myofibrillar proteins but also extends to the metabolic characteristics of the fiber. Only a limited number of studies have explored the metabolic phenotype of skeletal muscle in cancer patients. The balance between oxidative and glycolytic metabolisms seems to be maintained in skeletal muscle of cachectic cancer patients as indicated by similar ratio of oxidative-to-glycolytic enzyme activities in the *quadriceps* muscle of cachectic cancer patients compared with that of patients without cachexia and healthy subjects [53]. This is further supported by the observation that mitochondrial density is similar in skeletal muscle of cachectic cancer patients and healthy controls [154]. Similarly, the mitochondrial DNA copy number is unchanged in skeletal muscle of cachectic and non-cachectic cancer patients [122]. Only one study reported a decrease in the number of skeletal muscle mitochondria in a cachectic cancer patient [157]. By contrast, if the size of mitochondria does not seem to be affected by cancer cachexia [154], mitochondria morphology is markedly altered in skeletal muscle of cachectic cancer patients with the presence of larger intermyofibrillar mitochondrial areas [122], swollen appearance and the absence of cristae [126], suggesting an impairment in mitochondrial function. However, an in-depth analysis of mitochondrial metabolism in skeletal muscle of cachectic patients is still necessary.

Lessons from animal studies provide important supplementary information and allows us to draw a more precise picture of the regulation of energetic metabolism in skeletal muscle during cancer cachexia (Figure 3). The mitochondrial DNA-to-nuclear DNA ratio is lower in cachectic cancer mice compared to non-cachectic cancer mice [76,124,163], suggesting a decrease in mitochondrial content. This reduction was associated with body mass loss [76,163]. A lower mitochondrial content has also been reported in skeletal muscle of cachectic cancer rats compared to control rats [111]. As observed in human patients, mitochondria also present an altered morphology [163] with a swollen appearance [111,141,156,164,165], a smaller size [163] and the presence of electron-lucent areas [111,156,165], which all together clearly indicate an alteration in the mitochondrial network and function. Biochemical analyses corroborate ultrastructural information. A reduction in the metabolic flux throughout the Krebs cycle [164], which has also been confirmed by metabolomic approaches [93,166,167], as well as a decrease in the activities of complex I [168,169], II [79,98,141,168–170], III [170], IV [71,84,168,170,171] and V [71,86] have thus been consistently described. Accordingly, mitochondrial respiration rate is also reduced in isolated mitochondria from skeletal muscle of cachectic cancer mice compared to control mice [168,172,173]. Therefore, animal studies clearly indicate that the entire mitochondrial oxidative pathway is profoundly impaired by cancer cachexia. It is worth noting that a recent *in vivo* metabolomic study revealed that mitochondrial dysfunction in cachectic skeletal muscle tissue seemed to also have an influence on amino acid metabolism [162]. The oxidative activity of a muscle fiber is also tightly associated with capillary density [174], which allows oxygen supply and substrate delivery to the muscle fiber. However, cancer cachexia did not seem to impact capillary density in patients [56]. In animals, a study reported an increased number of blood vessels in skeletal muscle of cachectic cancer mice [155] but this increase could be a relative increase in capillary density because of the reduction in muscle fiber cross-sectional area in this study and thus would not reflect true angiogenesis. The decrease in oxidative activity is also associated with a decrease in ATP content [141,175], a decrease in creatine phosphate production [93], glucose concentration [91,176], glycogen store [91] and altered glycolysis [91,166,176], which together contribute to reducing the whole capacity of skeletal muscle of cachectic cancer animals to synthesize ATP [93,112,164]. Importantly, the decrease of skeletal muscle capacity to generate ATP may not only alter its contractile capacity but also its capacity to perform other cellular works involved in skeletal muscle homeostasis thus contributing in turn to skeletal muscle atrophy and dysfunction. Finally, the intense catabolism of skeletal muscle proteins during cancer cachexia [70,88,89,104,106,108,109,123,124,177–186] also raises the question of the metabolic fate of amino acids. Cancer cachexia is associated with an alteration in skeletal muscle amino-acid pattern [162], as well as with an increase in the concentration of circulating amino acids [82]. Amino acids can be released into the blood compartment to be interconverted into gluconeogenic amino acids and then recycled into glucose through hepatic gluconeogenesis thus rewiring amino acid metabolism to promote energy supply for tumor growth [18,187]. In skeletal muscle, an increased provision of

amino acids may increase the anaplerotic flux to the Krebs cycle [176]. Considering the whole decrease in mitochondrial activity that occurs during cancer cachexia, major adjustments of metabolic fluxes may occur so that the muscle fiber may adapt to this new challenging metabolic condition. The relative contribution of amino acid metabolism to the global skeletal muscle energy demand during cancer cachexia needs to be determined.

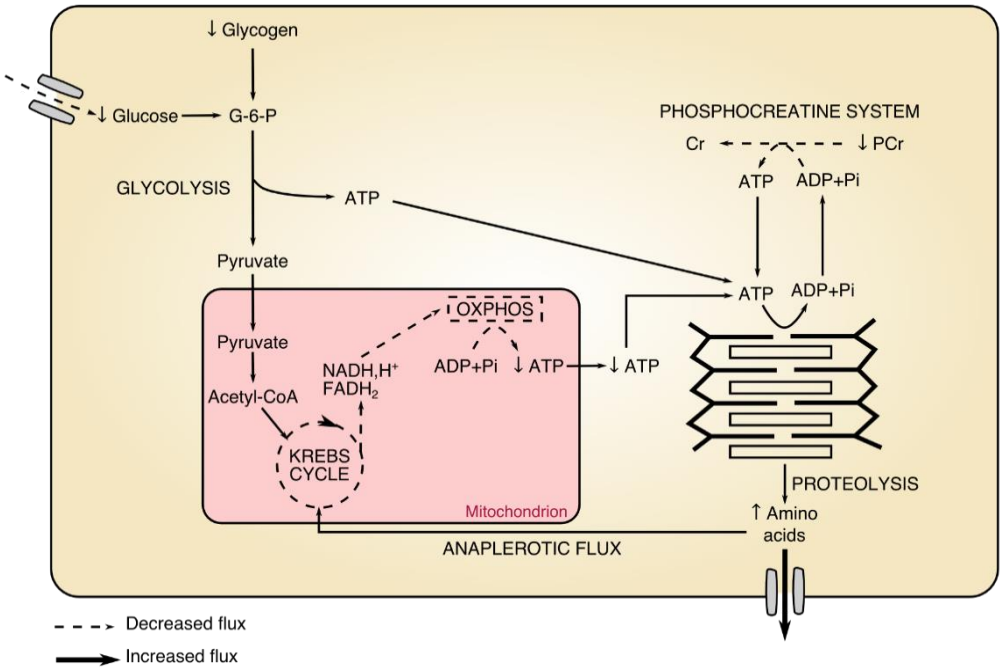

Figure 3. Main effects of cancer cachexia on skeletal muscle energetic metabolism.
This schematic representation is only based on animal studies. Reduced glycogen and glucose contents in skeletal muscle contribute to alter glycolysis flux. A decrease in mitochondrial oxidative pathway together with a decreased in ATP synthesis from phosphocreatine system lead to a reduced ATP content in skeletal muscle. Skeletal muscle proteins are degraded and subsequently processed to amino acids. Individual amino acids can be either exported or transported into the mitochondria (anaplerotic flux). Fatty acid metabolism is not represented because no study is currently available. Cr, creatine; G-6-P, glucose-6-phosphate; OXPHOS, oxidative phosphorylation; PCr, phosphocreatine.

Monucleated cell niche of skeletal muscle fiber

The microenvironment of skeletal muscle fibers contains different mononucleated cell types that are important for skeletal muscle repair and that contribute to skeletal muscle diversity. Upon muscle injury, quiescent resident satellite cells get activated, proliferate, and then fuse with preexisting damaged muscle fibers to rebuild new functional fibers [188]. The activity of these muscle progenitor cells is greatly influenced by the presence of inflammatory cells [189], fibro-adipogenic progenitors [190], fibroblasts and endothelial cells [191]. Pioneering works from Jewesbury and Topley at the beginning of the 20th century [192] and later by Marin and Denny-Brown [127] already indicated that skeletal muscle fibers from cachectic cancer patients had more nuclei in the vicinity of the sarcolemma even though the intrafiber or extrafiber localization of nuclei was not

determined in these studies. Much more recently, it was found that cancer cachexia was associated with the activation of both satellite cells and muscle progenitor cells in skeletal muscle of pancreatic cancer patients [193]. It can be noted that the extent of the activation correlated with body mass loss [193]. The presence of inflammatory cells [154], macrophages and fibro-adipogenic progenitors [194] was also reported in skeletal muscle of cachectic cancer patients. In animal models of cancer cachexia, skeletal muscle also contain a higher number of activated satellite cells [193], activated stem cells [193], undifferentiated cells [72,130] and inflammatory cells [77,117,123–125,195]. By contrast, it has also been reported that cachectic muscle of tumor-bearing mice was enriched in hematopoietic stem cells but not in inflammatory cells [138].

Alteration in the mononuclear cell profile of the cachectic muscle strongly suggests that an alteration in the properties of skeletal muscle fiber microenvironment may contribute to cancer cachexia. Indeed, a greater fragility of skeletal muscle to micro-injuries and injuries may lead to discrete episodes of degeneration/regeneration in the cachectic muscle thus allowing the chronic activation of resident myogenic precursor cells. The existence of ongoing discrete episodes of skeletal muscle regeneration in cachectic skeletal muscle is thus supported by the observation that skeletal muscle of cachectic cancer patients [194,196,197] and cachectic cancer mice or rats [77,117,123–125] display a higher number of muscle fibers with centralized nuclei, indicating the presence of regenerating muscle fibers. Interestingly, internally located nuclei were predominantly found in type 2 muscle fibers [196], which is consistent with the notion that these fibers are more prone to cachexia. Importantly, progenitor cells of cachectic cancer mice muscle were able to commit to the myogenic program but not to completely differentiate as indicated by the persistent expression of the self-renewing factor Pax7 [193]. Together with the observation of a deficiency of cancer cachectic skeletal muscle to regenerate after freeze clamping- [69,193] or cardiotoxin- [102] induced muscle injury, these data collectively indicate that an accumulation of unresolved/incomplete episodes of skeletal muscle repair could contribute to skeletal muscle mass loss during cancer cachexia. Although not mutually exclusive, these responses could also indicate the existence of a vain compensatory mechanism elicited to limit the extent of skeletal muscle mass loss during cancer cachexia.

Other histological features of cancer cachexia

Endomysial space

Skeletal muscle from cachectic cancer patients displays an increased area occupied by collagen that positively correlates with weight loss and poor survival [194]. This increase in fibrosis is in agreement with the increase in endomysial space observed in skeletal muscle of cachectic cancer patients [152,194]. A similar increase in collagen deposition was also reported in skeletal muscle of cachectic cancer mice [130,198], together with an increased area of non-contractile tissue that may reflect disrupted extracellular matrix remodeling [83]. The progressive development of fibrosis may be the long-term consequence of an increase in the expansion and differentiation of fibro-adipogenic progenitor in the cachectic muscle [194]. Although the cellular and molecular mechanisms involved in fibrosis need to be further investigated, an increase in fibrosis likely alters the mechanical properties of skeletal muscle, rendering them more susceptible to micro-injuries, thus leading to a vicious circle of chronic skeletal muscle deconditioning.

Fat depot

Computerized tomography analysis of the 3rd lumbar vertebra level has indicated an increase in fat infiltration in skeletal muscle of cachectic cancer patients [24,64,199] that was not correlated with muscle mass loss in cancer patients [200]. An increase in the size and the number of lipid droplets, which correlated with body mass loss [201] and an increase in the lipid content [194] have also been reported in skeletal muscle of cachectic cancer patients. This increase in lipid content in skeletal muscle of cachectic cancer patients is due to both an intramyocellular and an extramyocellular accumulation of triglycerides [202]. The expansion and differentiation of fibro-adipogenic progenitors that occur in skeletal muscle of cachectic cancer patients [194] may explain the accumulation of extramyocellular lipids. It has also been proposed that impaired lipid oxidation due to altered mitochondrial function may contribute to the accumulation of intramyocellular lipid droplets in skeletal muscle fibers of cachectic cancer patients [200]. It may be noted that one study reported a decreased lipid content in the slow-twitch muscle fibers of cachectic patients with late-stage non-small-cell lung cancer [203]. In animals, a lipid accumulation in the skeletal muscle fibers of cachectic cancer mice has been also reported [164]. Consequently, an increase in fat depot appears to be a common histological feature of cachectic skeletal muscle both in patients and animal models but its consequences on skeletal muscle function have to be explored.

Altered myofibrillar structure

Sarcolemmal alterations [126,154,194], which heighten with body mass loss [193], an increase in the number of damaged [194] and shrunken [152] fibers, a loss of normal cross-striation pattern [127,152,157,194], disrupted triads [122], as well as a dilated sarcoplasmic reticulum [157] has been also

observed in skeletal muscle of cachectic cancer patients. Similarly, a disorganization of the sarcolemma [75,155] and basement membrane [96,155,204], an alteration of sarcomere structure [96,156,164,165], disrupted triads [141] as well as a dilated sarcoplasmic reticulum [111] has been also reported in skeletal muscle of animal models of cancer cachexia. These structural alterations may impact membrane excitability, calcium transient between sarcoplasmic reticulum and myofibrils and cross-bridge kinetics that are major determinants of myofiber contractile performance (see below).

Figure 4 sums up the most important cellular and subcellular changes of skeletal muscle during cancer cachexia.

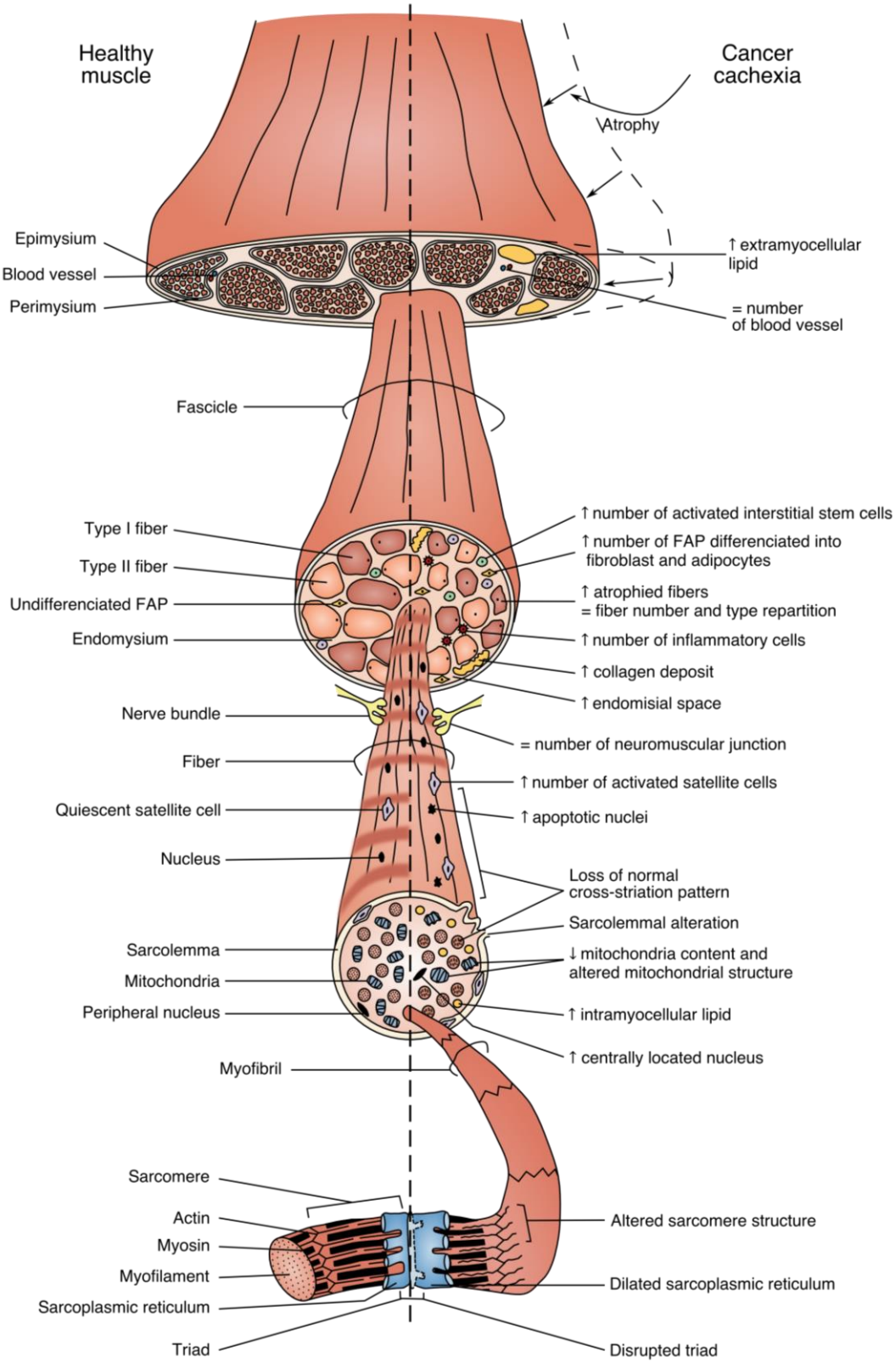

Figure 4. Schematic overview of the main cellular and subcellular phenotypic alterations in cachectic cancer skeletal muscle.

This schematic representation is based on human and animal studies. FAP, fibro-adipogenic precursor.

Skeletal muscle force

The main function of skeletal muscle is to generate force to produce movement, maintain posture and position. Any alteration in skeletal muscle mass, metabolism, structure, and organization may profoundly alter its capacity to generate force. The data reported above in human patients and in animal models of cancer cachexia that highlight marked alterations in skeletal muscle mass and metabolism indicate that skeletal muscle function must be profoundly modified in the cachectic muscle.

Cachectic cancer patients have a lower handgrip force (-7 to -31%) than cancer patients without cachexia [4,7,20,24,35,52]. Absolute isometric muscle force of knee extensors [54,56,60,154] and knee flexors [54] has also been consistently reported to be lowered in cachectic cancer patients compared to healthy subjects, as well as compared to non-cachectic cancer patients [54]. The isokinetic force of knee extensors and knee flexors is also reduced in cachectic cancer patients when compared to healthy subjects [53,56] or non-cachectic cancer patients [53]. Accordingly, the speed of contraction is also lower in men but interestingly not in women cachectic cancer patients when compared to gender-paired healthy control subjects [60]. In murine models of cancer cachexia, a decrease in grip force (-9 to -40%) has also been observed in cachectic cancer mice or rats when compared to control animals [68,72,73,78,79,91,91,93,94,100,107,131,133,137,141,147,148,150,168,173,184,205–212]. We can note that this decrease was not observed when cachectic cancer mice were compared to mild-cachectic mice [78] indicating that mild-cachectic states are already associated with functional alterations of skeletal muscle. Maximal contraction force of *the extensor digitorum longus* [66,80,90,96,99,213], *soleus* [66,96,99,169], *tibialis anterior* [78,98,101,142] and diaphragm [95] muscles are also decreased in cachectic cancer mice compared to control mice, as well as in cachectic cancer mice compared to non-cachectic cancer mice [101]. Interestingly, skeletal muscle of cachectic cancer mice with a majority of fast-fibers such as *extensor digitorum* longus are more prone to a force decrease [66], further strengthening the notion that type 2 fibers are more impacted by cachexia. Although some authors did not find any difference [78,213], the speed of muscle contraction and relaxation in response to a single twitch stimulation is also reduced in the *tibialis anterior* [101] and *extensor digitorum longus* [80,99] muscles of cachectic cancer mice when compared to control mice. Similar results have been obtained when the comparison was done with non-cachectic cancer mice [101]. Interestingly, the extent of the decrease in speed contraction correlated with body mass loss [101]. Taken together, all these data emphasize that skeletal muscle force could be an important criterion to diagnose cachexia. In this context, the knowledge of the kinetic of skeletal muscle force decrease during cancer cachexia appears to be essential. Only one study reported that isometric *quadriceps* and hamstring muscle force, as well as handgrip force were stable during eight weeks in cachectic cancer patients but skeletal muscle mass was not determined throughout

this study [214]. If the loss in muscle force occurs before the loss in muscle mass during cancer cachexia as it is observed during geriatric muscle mass loss [215], the measurement of muscle force would be an important and easily measurable predicting factor of cancer cachexia. However, longitudinal studies characterizing the kinetic of the loss in skeletal muscle mass and force loss in cancer patients are missing [216]. Finally, decreased muscle force should be associated with an increase in muscle fatigue. However, data on muscle fatigue are missing in cachectic cancer patients. If some studies reported an increase in muscle fatigue that was considered to be due to an increased central fatigue [217–219] in cancer patients, no specification about the cachectic status of the patients was reported. In animal models of cancer cachexia, muscle fatigue has been consistently reported to increase [78,79,96,99,101,147,197,213]. Importantly, muscle fatigue also correlated with body mass loss [79].

Beyond the description, remains the question of the mechanisms involved in the loss of skeletal muscle force production in the cachectic muscle. A decrease in muscle mass can obviously contribute to explain the decrease in muscle force in human cancer patients [56]. However, when muscle force is normalized to muscle cross-sectional area or body mass, differences in muscle force between cachectic cancer patients and control subjects still persist [60]. Similarly, in mice models of cancer cachexia, if a decrease in muscle force can be attributed to a loss of body mass [73] or muscle mass [213] or a decrease in skeletal muscle cross-sectional area [78,90,96,98,169], the loss in muscle force still persists even after normalization by body mass [78], muscle mass [80] or muscle fiber cross-sectional area [95,99,101] or both [66]. Collectively, these data indicate that muscle mass loss does not account entirely for the decrease in skeletal muscle force and that other factors than muscle atrophy contribute to the decrease in muscle force during cancer cachexia. Factors required for coordinated muscle contractile function involve neuromuscular junction integrity, membrane excitation, excitation-contraction coupling, calcium handling, sarcomere structure and energetic metabolism [151]. Previous studies indicate that the decrease in muscle force would not seem to involve an alteration in neuromuscular junction as cancer cachexia does not seem to affect muscular or intramuscular nerve bundles in patients [127,157], or even the number of neuromuscular junctions in muscle of cachectic cancer mice [138]. However, an in-depth analysis of skeletal muscle junction and neuromuscular coupling is clearly missing both in cancer patients and in animal models of cancer cachexia. Loss in muscle force can also result from impairment in calcium handling. Unexpectedly, isolated muscle fibers from cachectic cancer patients have an increased calcium sensitivity [160], which could be explained by a shift from slow to fast myosin isoform expression, as type 2 muscle fibers are more calcium-sensitive [220]. By contrast, muscle fiber calcium sensitivity is reduced in cachectic cancer mice compared to control mice [95]. Moreover, the calcium-activated force and cross-bridge kinetics are reduced in cachectic cancer mice compared to control mice [95] strongly suggesting that the loss of skeletal muscle force can be due

to an alteration of calcium handling. A recent study by Judge et al. also described an increase in calcium deposition in skeletal muscle of cachectic pancreatic cancer patients [194]. Calcium overload within skeletal muscle fiber may exert deleterious effects leading to muscle damage via the activation of calcium-activated proteases (calpains) and the disruption of sarcolemma integrity [221]. Furthermore, calcium overload can be also sensed by mitochondria, which may further contribute to alter mitochondrial metabolism and worsen cellular damages [221]. This may profoundly alter the capacity of the fiber to generate force. More investigations are required to determine potential alterations in muscular calcium handling during cancer cachexia. Further insights into the mechanisms involved in the loss of skeletal muscle force have been also provided by *ex vivo* analysis of the contractile properties of skeletal muscle fibers [152] or muscle fiber bundles [160] from cachectic cancer patients. The absolute [160] and specific [152] maximal force of isolated fibers is thus decreased in cachectic cancer patients. Specific maximal force correlates with myosin-to-actin ratio [152] indicating that the loss of contractile machinery is a factor contributing to decreased muscle force. Finally, the loss in muscle force and the increase in muscle fatigue in cachectic cancer skeletal muscle could also be explained by a shift from slow to fast fibers as well as by a decrease in the capacity to sustain ATP generation by mitochondrial oxidative phosphorylation.

Summary and future perspectives

The purpose of this review was to specifically focus on the structure and function of cachectic skeletal muscle. The extent of skeletal muscle mass loss has largely been described and the consequences of cachexia on skeletal muscle function are now getting more and more documented. However, the mechanisms underlying cachexia-induced loss of muscle function are complex and are far from being fully understood. The loss of muscle mass is clearly an important factor to consider when studying cancer cachexia, but qualitative factors such as changes in skeletal muscle metabolism, muscle fiber microenvironment, fibrosis, neuromuscular junction and sarcomere integrity as well as calcium handling are certainly involved in the impaired muscle function associated with cancer cachexia and need to be explored in details (Figure 5). A comparative analysis of the time-course changes of these qualitative factors and skeletal muscle mass is also necessary. Our review also underlines important methodological aspects that may explain contrasted results between studies. For instance, control subjects were quite heterogeneous between clinical studies (due to obvious constraints related to the recruitment of the subjects). Healthy control subjects, non-cachectic-cancer patients, as well as cachectic non-cancer patients have thus been used. A careful analysis of the reference group is therefore necessary to draw conclusions. Another important point is that if animal models of cancer cachexia are easily managed, they remain very different from human cancer cachexia [210]. Interspecies differences related to skeletal muscle physiology [151,222,223] must also be kept in mind.

Finally, our analysis emphasizes that measuring skeletal muscle force could be clinically fundamental to have a simple and robust mean to precociously diagnose cachexia in cancer patients. This needs to be assessed on a large epidemiologic scale that could lead to propose specific physical activity programs that may slow down the progression of cachexia and improve patient quality of life.

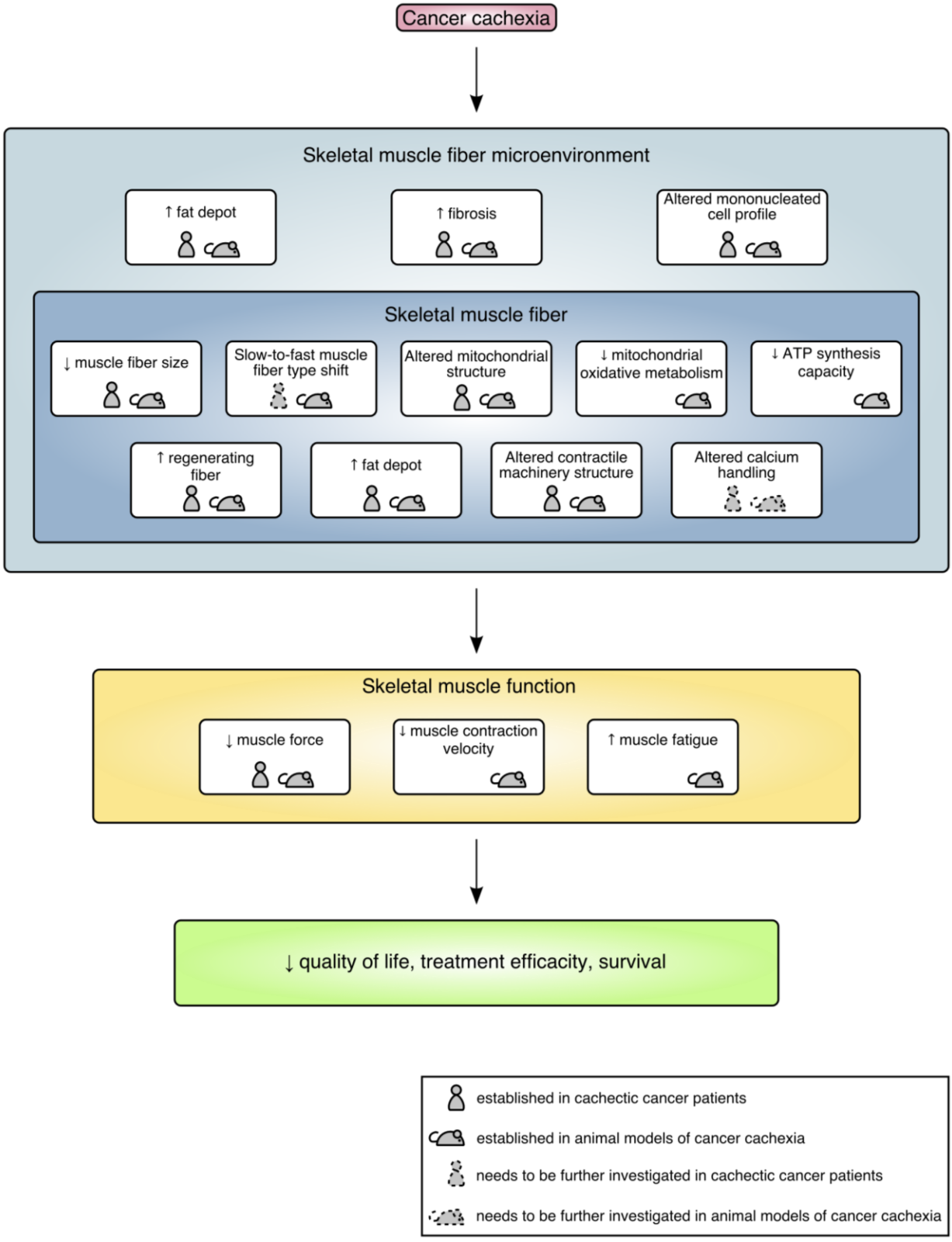

Figure 5. Factors contributing to the alteration of skeletal musclefunction during cancer cachexia.
When symbol is missing, no study is currently available.

Chapter II: Molecular mechanisms of cancer cachexia-related loss of skeletal muscle mass: lessons from clinical and animal studies

Introduction

Knowledge of the molecular pathways involved in skeletal muscle mass loss during cancer cachexia is a key issue for a comprehensive analysis purpose but also to identify molecular targets for the development of therapeutic strategies. The research in the field has largely progressed in the past decade providing important information about the pathophysiological mechanisms involved in the regulation of skeletal muscle mass during cancer cachexia. However, the identification of the molecular pathways and therapeutic targets has been impeded by the complexity of the syndrome. Indeed, it is now clear that other tissues and organs, as well as tumor tissues, secrete soluble factors (cytokines, hormones, tumor-produced factors) that act on skeletal muscle to promote wasting. In addition, skeletal muscle also releases various factors that can interact with other organs and tissues, as well as tumor tissues, during cancer cachexia. Research in the field is also largely based on experimental studies in animals and even though the number of human studies exploring the biological mechanisms of skeletal muscle wasting is increasing, human studies remain scarce and sometimes controversial due to the complexity of the clinical context compared to well-standardized animal models of cancer cachexia. This also raises the question of the translatability of animal findings to the clinical field. This is a critical point as therapeutic targets may differ between humans and animals.

In this context, the purpose of the review is to provide a comprehensive and comparative analysis of the molecular pathways involved in skeletal muscle mass loss during cancer cachexia in human and experimental models of cancer cachexia, but also to investigate to what extent findings from animal studies are relevant into clinical research in human cancer patients.

Skeletal muscle fiber proteostasis during cancer cachexia

Skeletal muscle depletion largely derives from an unbalance between protein synthesis and degradation rates. A detailed analysis of skeletal muscle protein synthesis and degradation rates in cachectic cancer patients and animal models of cancer cachexia is presented in Figure 6.

If a limited number of studies have explored the rate of skeletal muscle protein synthesis in cachectic cancer patients, they reported a reduction of around 75% in protein synthesis rate [224,225]. Similar observations were also reported in animal models of cancer cachexia [70,85,88,104,177–179,184,226–228] where protein synthesis rate was also reduced from 31% to 75%, the extent of the decreased being associated with the severity of the cachexia [70,85,104]. Importantly, protein synthesis has been sometimes reported to be higher in skeletal muscle of cachectic cancer

patients than in non-cachectic cancer patients [229,230] suggesting that a compensatory mechanism may sometimes be elicited to limit the extent of skeletal muscle mass loss during cancer cachexia. A fairly similar observation has been also reported in skeletal muscle in animal models of cancer cachexia with no modification of the protein synthesis rate [108,109,180–183,186].

Whereas only one study reports an unchanged protein degradation rate in cachectic cancer patients [225], an increase in protein degradation has been consistently reported in animal models [70,85,88,89,104,106,108,109,123,124,177–186]. As described for protein synthesis rate, the extent of the increase in proteolysis rate was associated with the severity of cachexia [70,104]. Altogether, and subject to a limited number of studies in human patients, studies indicate that a reduction in protein synthesis would be an important factor involved skeletal muscle depletion during cancer cachexia, whereas a combination of both a decrease in protein synthesis rate and an increase in protein degradation rate triggers skeletal muscle loss in animal models of cancer cachexia. Of note, decreasing protein synthesis rate is bioenergetically more interesting than increasing proteolysis as the energy cost of protein synthesis is far greater than that for proteolysis. Such a metabolic adaptation may be beneficial as it allows to spare metabolic substrates necessary for ATP production for other cellular purposes.

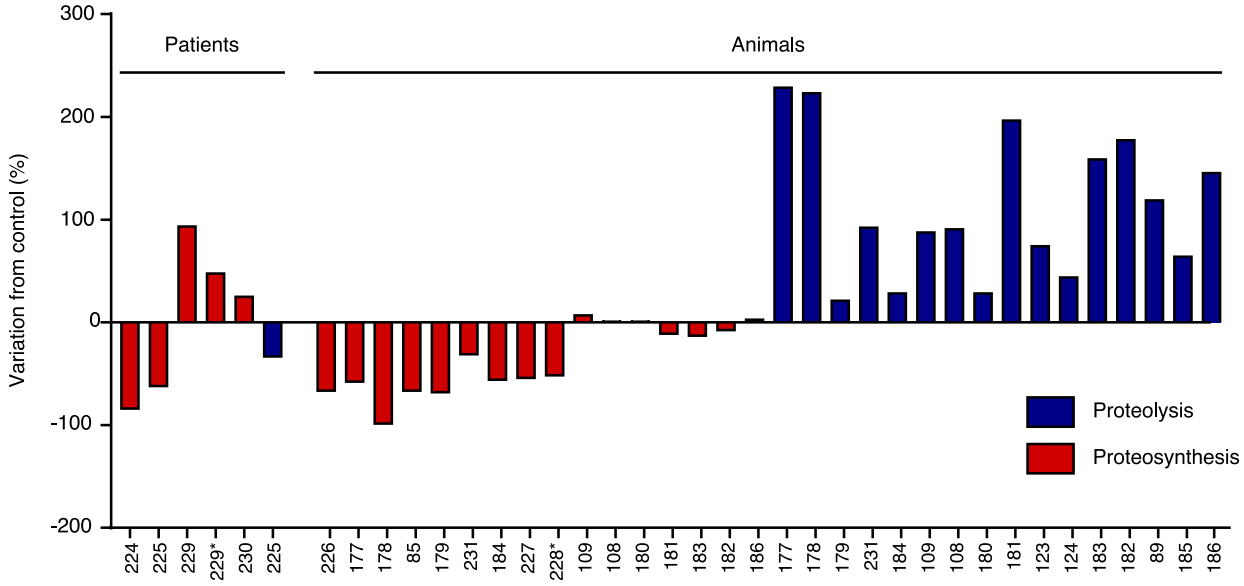

Figure 6. Proteosynthesis and proteolysis rate in human and animal models of cancer cachexia.
Data were taken from indicated references and displayed as % of corresponding controls. Unless indicated by *, comparisons were done with healthy controls.

Molecular mechanisms involved in the regulation of skeletal muscle protein synthesis during cancer cachexia

The IGF1-AKT pathway is a master regulator of protein synthesis in skeletal muscle (Figure 7) by modulating the phosphorylation of several critical translation initiation factors. A crucial regulatory knot in the pathway is the serine/threonine-protein kinase AKT. Phosphorylated AKT indirectly activates the mammalian target of rapamycin (mTOR), which then phosphorylates the ribosomal protein S6 kinase (S6K) and 4EBP1 promoting translation initiation by activating ribosomal protein S6 (rpS6) and by releasing eukaryotic initiation factor (EIF)-4E, respectively. AKT also phosphorylates and inhibits glycogen synthase kinase 3 (GSK3), thus relieving GSK3-dependent inhibition of EIF-2B. Regulation of the phosphorylation of critical intermediates of the pathway is therefore a good estimate of the activation status of the pathway.

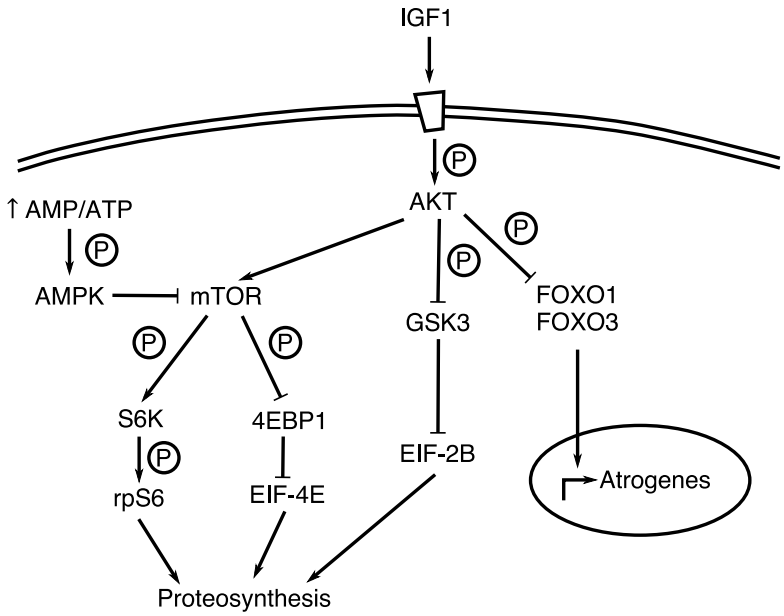

Figure 7. IGF1-AKT pathway mediates protein synthesis in skeletal muscle.

Insulin-like growth factor 1 (IGF1) is the canonical upstream regulator of the pathway. IGF1 is principally synthesized in the liver, acting as a systemic growth factor, but it is also produced by skeletal muscle. A decrease in skeletal muscle *IGF1* transcript level has been reported in cachectic cancer patients [231] and animals [70,92,112,113,133,228,232]. The circulating level of IGF1 was also decreased in cachectic cancer animals [92,133,233]. Therefore, a decrease in the triggering signal of the pathway occurs in skeletal muscle during cancer cachexia.

Level of the phosphorylated active forms of AKT, GSK3, mTOR, and S6K are decreased in skeletal muscle of cachectic cancer patients compared to non-cachectic cancer patients [161]. Similarly, a decrease in the phosphorylated inactive form of the translational repressor 4EBP1 has been also reported to decrease [203]. Thus, a reduction in AKT-dependent signaling in human skeletal muscle is probably involved in the reduction in protein synthesis rate described above and thus contributes to skeletal muscle mass loss in cancer patients. This is also reinforced by omics studies showing that expression of genes involved in protein anabolism is down-regulated [200,234] or altered [235] in skeletal muscle of cachectic cancer patients. This also indicates that both transcriptional and post-translational events are involved in the down-regulation of the pathway. However, some discrepancies exist between human studies. A number of studies reported either no change [122,154,203,236] or even an increase in the phosphorylated form of AKT [54]. Furthermore, the phosphorylation of downstream effectors of AKT such as mTOR [54,203], S6K [54,203], and 4EBP1 [54] has been also reported to be unchanged in skeletal muscle of cachectic cancer patients. Discrepancies between studies can be explained by differences in the clinical context (cancer types, the severity of the disease, and the extent of cancer cachexia), but may also reflect the existence of regulatory influence of other factors that converge to the pathway to modulate its activity. We cannot also exclude some methodological concerns, particularly regarding the stability of the phosphorylated proteins during the treatment of biological samples.

In animal models of cancer cachexia, a large majority of studies reported an inhibition of the pathway in cachectic skeletal muscle as shown by the decrease in the phosphorylation of AKT [71,117,133,237], mTOR [70,71,124,228,238,239], S6K [70,71,82,124,148,227,228,239], rpS6 [82,148,227,232], and 4EBP1 [70,82,228,232,238,239]. The decrease in the activation of AKT downstream targets was also associated with weight loss [70,228,239] indicating that the greater is the inhibition of the pathway, the greater is the extent of cachexia. The pathway is also regulated at the transcriptional level as shown by microarray analysis in skeletal muscle of cachectic cancer mice [198]. However, and as observed for human patients, some studies found that AKT phosphorylation remained unchanged [79,113,124,148,150,155] or even increased [70,73,232] in skeletal muscle of cancer cachectic animals. Similarly, some studies did not report any difference in the phosphorylation state of S6K [77], rpS6 [73], and GSK3 [94], while others even reported an increase in the phosphorylation of S6K [113,155], 4EBP1 [71], and GSK3 [113]. This could be interpreted as a vain compensatory mechanism to limit the extent of muscle mass loss, but also as a compromised ability of AKT to phosphorylate its downstream targets or the existence of regulatory influences that modulate the activity of the pathway downstream of AKT. The metabolic sensor 5' AMP-activated protein kinase (AMPK) could be one of those factors that influence the activity of the pathway. Indeed, AMPK phosphorylation [70,73,228,232] and activity [148] have been consistently reported to increase in skeletal muscle of cachectic cancer mice. Importantly, this was associated with body mass loss [70,228], suggesting that

AMPK contributes to decreasing proteosynthesis through mTOR inactivation probably via raptor phosphorylation [70]. Increased AMPK signaling has been confirmed by RNA sequencing in skeletal muscle of tumor-bearing cachectic mice [240]. Of note, AMPK activity has been shown to be unchanged in skeletal muscle of cachectic cancer patients [154].

Collectively and although some differences exist between studies, data from human cancer patients and animal models of cancer cachexia consistently indicate that a down-regulation of the IGF1-AKT would be a common molecular mechanism involved in skeletal muscle mass loss during cancer cachexia. Therefore, molecular studies in human patients and animal models of cancer cachexia agree with the decrease in skeletal muscle protein synthesis rate previously reported.

Molecular regulation of skeletal muscle protein degradation during cancer cachexia

An increase in proteolysis requires a transcription-dependent program to regulate the expression of a group of genes collectively called atrophy-related genes or atrogenes. These genes encode proteins that regulate important steps of the two main proteolytic systems, the ubiquitin-proteasome and the autophagy-lysosome systems that variably contribute to skeletal muscle mass loss [241].

Ubiquitin-proteasome system during cancer cachexia

Proteins are targeted for degradation by the 26S proteasome through an ATP-dependent ubiquitination process. The covalent attachment of a chain of ubiquitin molecules to the targeted protein involves a 3-step reaction successively performed by E1 (ubiquitin-activating enzymes), E2 (ubiquitin-conjugating enzymes), and E3 (ubiquitin-ligases enzymes). The ubiquitinated protein is then docked to the proteasome for degradation [242]. Expression of *MuRF1* (*TRIM63*) and *MAFbx* (*FBXO32*) E3-ubiquitin ligases has been consistently found to be up-regulated during multiple atrophy conditions [243]. The role of the ubiquitin-proteasome system during cancer cachexia has been thus largely inferred from the expression level (transcript and protein levels) of these E3-ubiquitin ligases. MuRF1 targets sarcomeric proteins (actin, myosin heavy chain, troponin) for degradation [244–246] while MAFbx targets MyoD and EIF3F for degradation [247,248]. As it degrades EIF3F, MAFbx is also considered as a translational repressor.

A large majority of studies in human cancer patients do not report any variation in the expression level of *MuRF1* and *MAFbx* in skeletal muscle of cachectic cancer patients compared to non-cachectic cancer patients [54,231,236,249,250] or healthy subjects [54,90,126,203,234,236,250]. Of note, only four studies reported an increase in the mRNA [126,152,251] or protein [126,154] levels of *MuRF1* and *MAFbx* in lung and gastric cachectic cancer patients compared to healthy subjects. Results on the

expression level of ubiquitin are more conflicting with some studies reporting an increase in ubiquitin mRNA level [57,252–254] and protein level [194,254] as well as an increase of ubiquitinated proteins [126,154], whereas others do not report any difference in ubiquitin mRNA level [255] and protein level [160]. A few studies also investigated the expression level of proteasome subunits, with one study reporting an increase in mRNA and protein level of proteasome subunits [256] and others no difference at the protein level [154,203]. Finally, the activity of the ubiquitin-proteasome in the skeletal muscle of cachectic cancer patients has been reported either to increase and to be inversely correlated with body mass loss [252] or to be unchanged [203]. Transcriptomics studies also reported divergent results with either increased [235], unchanged [249], or decreased [234] expression of genes related to the ubiquitin-proteasome system in skeletal muscle of cachectic cancer patients.

This clearly contrasts with the data obtained in animal models of cancer cachexia which consistently show an increase in the mRNA level of the E3-ubiquitin ligases *MAFbx* [68,70,72,75,78,79,82,84,90–92,94,95,111–113,117,129,131–133,136,137,141,142,147,148,150,153,155,158,159,164,184,190,197,204,207,208,212,227,232,237,257–270], *MuRF1* [67,68,70,75,78,79,82,84,90–92,94,95,111,117,129,131,133,136,137,141,142,145,147,148,150,155,159,173,184,190,197,204,207,212,227,237,257–259,261–264,267–271] and *Musa1* [131,137,148,227] in skeletal muscle of cachectic cancer animals compared to control animals or non-cachectic cancer animals. This was also confirmed at the protein level [70–72,96,100,124,128,134,143,158,205,267,269,270,272]. The ubiquitin mRNA level [68,92,108,109,111,115,137,180,181,184,207,257,259,269,273–278] and protein level [96] are also increased in skeletal muscle of cachectic cancer animals. Accordingly, the content of ubiquitinated proteins is increased [68,70,96,117,123,124,148,150,185,227,233,257,279]. The transcript level [70,88,106,108,109,115,137,180,184,207,274,276,278] and protein level [238,280] of several proteasome subunits are also increased in skeletal muscle of cachectic cancer animals. Transcriptomics studies also revealed an up-regulation of genes involved in the ubiquitin-proteasome system in skeletal muscle of cachectic cancer animals [105,112,137,144,198,204,205,240,259,271,281–283]. Consistent with these observations, the ubiquitin-proteasome system activity is increased in skeletal muscle of cachectic cancer animals [106,238,262,284,285].

This comparative analysis of the regulation of the ubiquitin-proteasome system components between human cancer patients and animal models of cancer cachexia (Figure 8) raises an important question: how can we explain such a contrasted picture between human and animal models of cancer cachexia? First, one may obviously consider that other proteolytic systems, such as the autophagy-lysosome system, may be involved in skeletal muscle mass loss (see below). Second, these data may simply indicate that a reduction in protein synthesis would

be the main mechanism contributing to skeletal muscle mass loss during the time course of cancer cachexia in cancer patients, which would agree with the observation that there is currently no study showing an increase in skeletal muscle proteolysis rate in cachectic cancer patients [225]. But, one may also question the timing of the proteolytic response. Some authors [231,234,253] have thus proposed that components of the ubiquitin-proteasome system are overexpressed only at an early stage of the disease before weight loss can be detected. Indeed, in animal models of cancer cachexia, the onset of tumor growth can be easily controlled either by the subcutaneous injection of cancer cells (Lewis lung carcinoma cells or C26 cells for instance) or by genetic means (*Apc*$^{Min/+}$ mice or KPC mice, for instance) allowing for a simple and accurate analysis of the kinetic of cancer cachexia. The facility to manage animal models of cancer cachexia and to detect cachexia together with the high rate of tumor growth allow to easily detect a precocious activation of the ubiquitin-proteasome system. By contrast, due to the complexity of the clinical context in cancer patients and the difficulty (impossibility) to determine the onset of tumor growth, it is readily possible that a precocious and temporally regulated increase in the ubiquitin-proteasome system has been experimentally missed in human studies. Therefore, the heterogeneity of the clinical context in human patients (even for a given cancer type) compared to well-standardized and designed experimental models of cancer cachexia may clearly be a confounding factor and may explain why no increased expression of ubiquitin-proteasome system components could be consistently reported in human cancer patients. Additionally, skeletal muscle mass loss in animal models of cancer cachexia is triggered in a couple of days/weeks, which is generally not the case for the vast majority of human cancers. Such a rapid and violent tumor growth induces a fast and important decrease in skeletal muscle compartment that strongly stimulates skeletal muscle proteolysis. This could be more difficult to observe in human cancer patients because of the chronicity of the disease and the lower rate of skeletal muscle depletion.

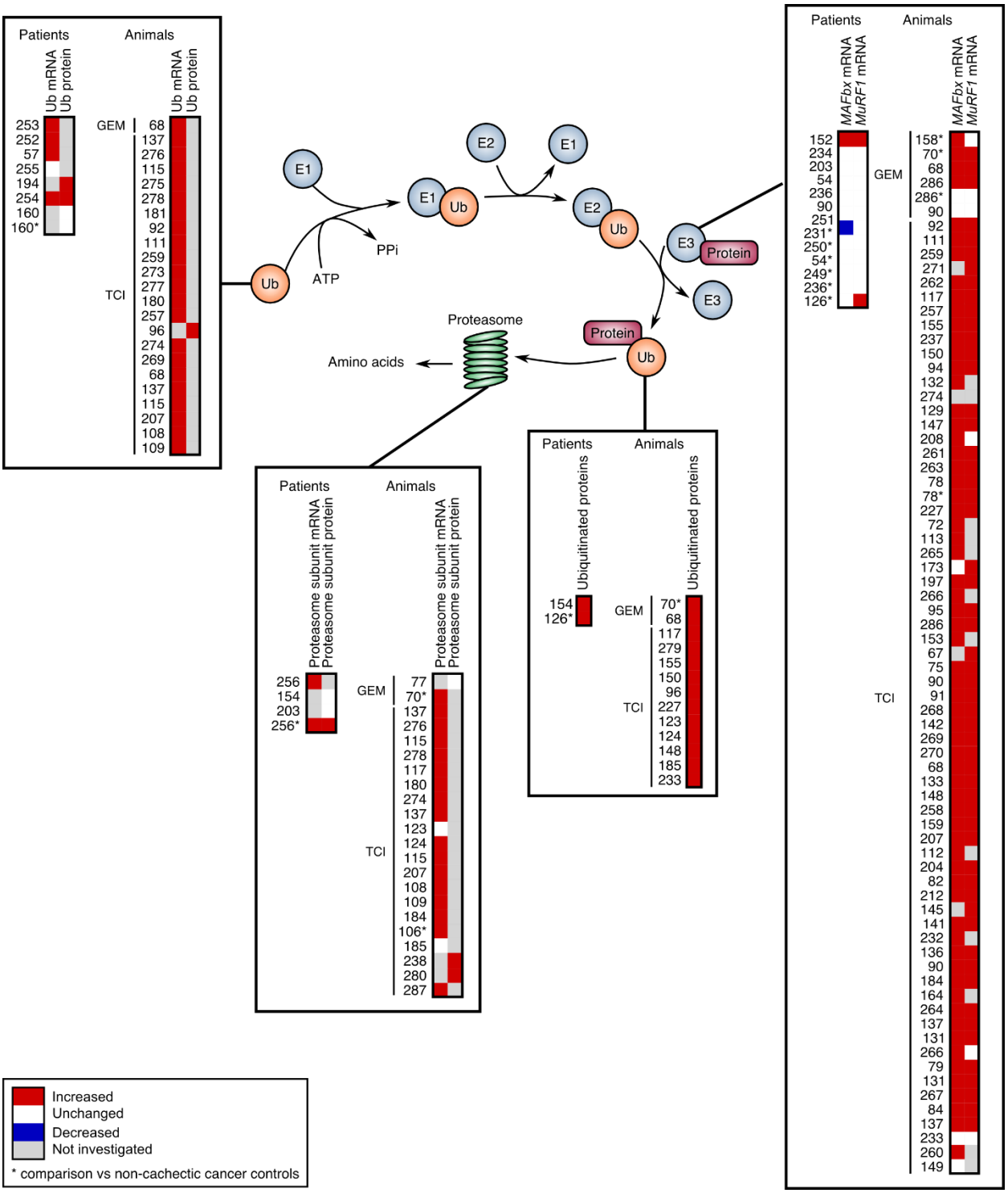

Figure 8. Transcript and protein levels of components of the ubiquitin-proteasome system in cachectic skeletal muscle of cancer patients and animals.

Data were taken from indicated references. Colors indicate when up-regulation (red), down-regulation (blue), or not significant difference was found (white). Not reported data are in grey. Unless indicated by *, comparisons were done with healthy controls. Ub, ubiquitin; GEM, genetically engineered model; TCI, tumor cell injection.

Autophagy-lysosome system during cancer cachexia

The autophagy-lysosome system is responsible for eliminating long-lived proteins, such as sarcomeric proteins and large supramolecular structures including dysfunctional mitochondria [286]. Proteins and organites to be degraded are progressively engulfed during the formation of a double-membrane structure called the autophagosome. Autophagosomes then fuse with lysosomes to form autolysosome allowing acidic proteolytic degradation of their contents by lysosomal proteases (cathepsins). Autophagy is necessary for skeletal muscle homeostasis as such a defect in autophagy will result in muscle functional impairment [287], but excessive autophagy will also contribute to skeletal muscle mass loss [288,289]. Therefore, tight regulation of the autophagy-lysosome system is necessary for proper regulation of skeletal muscle homeostasis.

The protein level of autophagosome biogenesis-related genes such as *ATG5*, *ATG7*, *Beclin1*, and *LC3B* is increased in skeletal muscle of cachectic cancer patients [54,58,119,122,126,197]. Accordingly, the number of autophagosomes increases with skeletal muscle loss in cancer patients [126], suggesting an increase in autophagosome formation. However, an accumulation of autophagosomes can be also interpreted as default in autophagosome clearance. p62 is a cargo adaptor protein involved in selectively targeting protein aggregates to autophagosomes. Since p62 is constantly removed by autophagy, an increase in p62 protein content is considered as a good marker of impairment in autophagic vesicle turnover. Human studies indicate that p62 protein content [58,126,197], as well as p62 aggregates [194], are increased in skeletal muscle of cachectic cancer patients, an observation that is consistent with an impaired autophagosome clearance. However, a defect in lysosomal biogenesis and lysosomal proteolytic capacity would not be involved in an impairment in autophagic vesicle turnover as shown by the unchanged mRNA level of *TFEB*, a master regulator of lysosome biogenesis [58] and the increase in cathepsin B mRNA level in skeletal muscle of cachectic cancer patients [255]. Of note, some studies did not report any difference in the expression of autophagy markers at the mRNA level [90,234,236] and protein level [154,251] nor in autophagosome number [154] suggesting that autophagy could be also properly balanced in skeletal muscle of cachectic cancer patients. Finally, the clearance of defective mitochondria by autophagy (mitophagy) also needs to be questioned in skeletal muscle of cachectic cancer patients [290].

In animal models of cancer cachexia, increased expression of genes involved in autophagosome biogenesis has been widely reported to increase in skeletal muscle of cachectic cancer animals [75,82,90,100,117,123,125,134,137,141,145,148,173,197,264,265,291,292]. This was also confirmed by transcriptomic analysis [105,137,144,204,259]. Accordingly, the number of autophagosomes was also increased [197]. Cathepsin expression [88,95,115,136,173,184,207,265,274,293], cathepsin activity [182,183,185,274] and lysosomal proteolysis [70,185,265,274], particularly during advanced cachexia [70], were also increased.

Therefore, there is a consensus to state that autophagy is activated in skeletal muscle of cancer cachectic mice. However, one should note that some studies reported that cathepsin activity was either unchanged [180] or even decreased [265,273]. Similarly, some studies reported no difference in lysosomal proteolysis [180,285] in skeletal muscle of cachectic cancer animals. As discussed for human patients, the increased expression of autophagosome biogenesis markers reported above can also illustrate an altered autophagosome clearance. This is supported by studies showing an accumulation of p62 in skeletal muscle of cachectic cancer animals [117,134,197,265,291,292]. Accordingly, treatment of tumor-bearing mice with either AICAR or rapamycin, two drugs that activate the autophagic flux, *i.e.* the clearance of autophagosomes, prevented the induction of autophagosome formation gene expression and improved skeletal muscle mass in cancer cachexia [197] supporting the idea that an accumulation of unprocessed autophagosomes may contribute to cachexia. Therefore, an imbalance between autophagosome biogenesis and clearance would be crucial in altering skeletal muscle homeostasis during cancer cachexia [173]. Collectively, all these data from human cancer patients and experimental models of cancer cachexia indicate that autophagy would be activated in skeletal muscle during cancer cachexia, but this would be associated with a defect in the clearance of autophagosomes, thus leading to an accumulation of unprocessed autophagosomes. This accumulation of autophagosomes may result in endoplasmic reticulum (ER) stress as indicates the increased ER stress markers in skeletal muscle of cachectic cancer patients [251] and mice [148].

Regulation of the ubiquitin-proteasome and autophagy-lysosome systems by FOXO transcription factors during cancer cachexia

Expression of *MuRF1* and *MAFbx*, as well as that of genes of the autophagy-lysosome system, is strongly controlled by the FOXO family of transcription factors (mainly FOXO1, FOXO3, and FOXO4 in skeletal muscle) [288,289,294,295]. FOXO transcriptional activity is regulated by AKT-dependent phosphorylation. Inhibition of the IGF1-AKT signaling pathway decreases FOXO phosphorylation leading to the translocation of dephosphorylated active FOXO into the nucleus and activation of target gene expression (Figure 7) [295,296].

The ratio of the phosphorylated (inactive)-to-total forms of FOXO1 [154] and FOXO3 [154,161] is decreased in skeletal muscle of cachectic cancer patients suggesting increased FOXO activity. Omic studies also indicate that genes related to the FOXO pathway are up-regulated in skeletal muscle of cachectic cancer patients [194] and that the transcript level of *FOXO1* and *FOXO3* negatively correlates with body mass loss and skeletal muscle mass [297], suggesting that transcriptional and post-translational regulations occur at the level of *FOXO* during cancer cachexia. However, in another cohort of patients, a promotor analysis revealed that the differentially regulated genes in skeletal muscle of cachectic cancer patients do not have FOXO

binding sites [249]. Only two studies concomitantly determined FOXO phosphorylation and expression of *MuRF1* and *MAFbx*. Puig-Vilanova et al. [154] reported that the reduction in FOXO1 and FOXO3 phosphorylation was accompanied by an increase in *MuRF1* and *MAFbx* expression, which is consistent the canonical view of the regulation of E3-ubiquitin ligases expression. Op den Kamp et al. [54] did not report any change in the phosphorylated-to-total forms of FOXO1 and FOXO3 in skeletal muscle of cachectic cancer patients together with no change in the transcript level of *MuRF1* and *MAFbx*. One should keep in mind when analyzing the potential role of FOXO transcription factors during cancer cachexia in human patients that expression of *MuRF1* and *MAFbx*, two canonical FOXO-responsive genes, is essentially unchanged in skeletal muscle of cachectic cancer patients (see above). Therefore, the increase in FOXO activity reported would be mainly associated with the regulation of genes involved in the autophagy-lysosome system.

In animal models of cancer cachexia, a decreased phosphorylation of FOXO3 [68,70,117,232], together with an increase in the nuclear localization of FOXO3 [233] and FOXO transcriptional activity [136] have been reported. Furthermore, motif analysis of promoter sequences allows the identification of FOXO1 as a potential key transcription factor involved in skeletal muscle atrophy during cancer cachexia [204]. This was also confirmed by genome-wide microarray analysis of the transcripts regulated by FOXO in skeletal muscle of cachectic cancer mice [282]. One should note however that some studies did not report any difference in the phosphorylation of FOXO1 [117] and FOXO3 [82], whereas others even reported a decrease in the phosphorylated form [113,123] and DNA binding activity [113] of FOXO1. Despite the existence of some divergent data, these studies essentially indicate that FOXO transcriptional activity is increased in cachectic skeletal muscle of cancer mice, which agree with the reported increase in the expression of genes related to the ubiquitin-proteasome and autophagy-lysosome systems.

Calpain during cancer cachexia

Calpains are a family of Ca^{2+}-dependent proteases. Calpain-1 and calpain-2 are ubiquitously expressed whereas calpain-3 is a muscle-specific isoform. Due to their strong cleavage activities on critical cytoskeletal proteins, calpains might be responsible for the release of myofilaments from myofibrils [298], a prerequisite step that would be necessary for the degradation of sarcomeric proteins.

To our knowledge, calpain activity has never been investigated in cachectic cancer patients. An increase in calpain activity has been reported in skeletal muscle of non-weight losing cancer patients [299], while another study did not find any difference in calpain activity in cancer patients but the cachectic status of the patients was not reported [55]. Therefore, whether or not calpain activity is increased in human cachectic cancer patients is currently an unsolved question. In

animal models of cancer cachexia, the implication of calpain has been historically determined by measuring the proteolytic flux with and without calcium-dependent protease inhibitors. These studies indicate that skeletal muscle proteolysis in cachectic cancer animals would not involve calcium-dependent proteases [88,180]. However, the results of these studies have been questioned as calcium protease inhibition likely results in the overactivation of ubiquitin-proteasome and autophagy-lysosome systems, which may obscure the potential involvement of calpain in proteolysis in skeletal muscle of cachectic cancer animals [89]. Regarding calpain activity *per se*, results are contrasted with some studies showing that calpain activity is unchanged in skeletal muscle of cachectic cancer mice [181,262], whereas others indicate that calpain activity is increased in skeletal muscle of cachectic cancer animals [238,261,284]. When increased, this could be explained by an increased expression of the different calpain isoforms [89,111,115,123,147,180,184,207,259] as well as by a decreased expression [89,261] and activity [300] of the specific inhibitor calpain inhibitor, calpastatin. Therefore, considering the major impact of cancer cachexia on skeletal muscle structure as well as the cytoskeletal remodeling function attributed to calpains, a better knowledge of calpain function during cancer cachexia would be helpful.

Upstream regulators of skeletal muscle proteostasis during cancer cachexia

A number of intracellular and extracellular regulators of skeletal muscle homeostasis have been identified in different experimental settings leading to skeletal muscle depletion [301]. Oxidative stress (OS), inflammation and TGF-ß family members appear to be the most relevant factors during cancer cachexia.

Oxidative stress in skeletal muscle during cancer cachexia

OS is characterized by a high concentration of reactive oxygen species (ROS) resulting from an imbalance between oxidant production and antioxidant defense. The main sources of ROS in skeletal muscle are mitochondria (complex I and III), NADH oxidases, but also endoplasmic reticulum, and peroxisomes where enzymatic complexes generate ROS [302]. Excessive ROS production results in an accumulation of oxidized and damaged proteins, organelles, membranes, and DNA. OS has been also shown to trigger fiber atrophy in different experimental settings by activating the ubiquitin-proteasome [303] and autophagy-lysosome [304,305] systems as well as calpains and caspases [306]. It may also inhibit the IGF1-AKT pathway [307,308] and increase FOXO activity [309].

In human, one study reported an increase in OS, as shown by an increase in malondialdehyde (MDA) [154,251,310] and carbonyl-protein adducts [154] in skeletal muscle of cachectic cancer patients. In parallel, the protein level and activity of the antioxidant enzyme superoxide dismutase were also increased [154]. This increase in antioxidant defense suggests a vain

mechanism to alleviate the increase in ROS production. However, another study reported a decrease in the mRNA level of some antioxidant genes [311] that may participate to further increase the OS.

OS is consistently increased in skeletal muscle of several animal models of cancer cachexia as indicated by the increased level of ROS [262,291] such as superoxide anion [312] and hydrogen peroxide [313] and the ratio of oxidized-to-reduced glutathione (GSSG/GSH) [147,149,170,260,262,291,292]. This increase in OS in skeletal muscle during cancer cachexia triggers oxidative damage that affects lipids [110,149,195,195,260,262,314] as well as proteins [71,110,123,124,150,169,195,260,267,314]. OS would be also more present in type 2 myofibers [110], which is in agreement with the view that type 2 muscle fibers would be more prone to atrophy during cancer cachexia [84,99,110,155,156]. Regarding the antioxidant system, studies indicate that expression of antioxidant enzymes is either decreased [112,123–125,312], or unchanged [76,110,123,125,150,291,312–314] in cachectic skeletal muscle. Accordingly, the activity of the antioxidant enzymes superoxide dismutase [262,312] and glutathione peroxidase [312], antioxidant histidine peptides [166] and total antioxidant capacity [260] have been shown to decrease in cachectic skeletal muscle. A decrease in antioxidant enzymes would thus further reinforce the effects of OS. One should note however that some studies reported an increased expression of antioxidant enzymes [110,112,125,147,150,195,291] suggesting in this case, that the main factor responsible for the increased OS would be an increase in ROS production rather than impaired induction of antioxidant enzyme expression. Transcriptomic studies in mice also identified an increased transcriptional response of genes related to OS response during cancer cachexia [112,198,271]. Therefore, current evidence indicate that cachectic skeletal muscle is subjected to OS both in cancer patients and in animal models of cancer cachexia. OS results from an increase in ROS production that can be accompanied by a decrease in antioxidant defense. The sources of ROS have not been identified yet even if an alteration in mitochondrial metabolism may significantly contribute to ROS production [168,172,173]. Importantly, OS has been shown to precede skeletal muscle mass loss [313], suggesting that an increase in OS could be a precocious event of cancer cachexia. Finally, if the capacity of OS to contribute to skeletal muscle mass loss has been demonstrated in different experimental settings [303–309], a direct molecular functional relationship between an increased ROS production and skeletal muscle mass loss during cancer cachexia still awaits experimental evidence. Finally, therapeutic strategies based on the administration of different antioxidants have displayed conflicting results showing either attenuation [260,262] or worsening [150] of cachexia in tumor-bearing animals. This suggests that OS level must be tightly balanced, too high or too low level triggering deleterious effects on skeletal muscle mass.

Inflammatory cytokines in skeletal muscle during cancer cachexia

Systemic inflammation is a common feature of cancer cachexia in human cancer patients as well as in animal models of cancer cachexia as exemplified by numerous studies. An increase in the circulating level of C-reactive protein (CRP) is thus associated with weight loss in cancer patients [4,24,54,57,315–317]. A recent systematic review reported that a systemic inflammatory response was associated with skeletal muscle mass loss in cancer patients [318]. Furthermore, the circulating levels of the pro-inflammatory cytokines such as IL-1ß [319], IL-4 [52], IL-6 [52–54,57,146,203,320–323], IL-8 [52,54,320–323], IL-10 [323], IFN-γ [52], and TNF-α [52,319,321,324] are all increased in cachectic cancer patients. Accordingly, in mice models of cancer cachexia, the circulating level of CRP [71], IL-1ß [68,71,267], IL-6 [65,68,70,72,75–77,101,112,129,134,142,156,228,267,270,283,323,325,326], IL-10 [112], IL-11 [283], IFN-γ [107,112,134] and TNF-α [68,71,109,112,134,186,267,270,283,326,327] and Tweak [71] are also increased in cancer cachectic animals. At the level of skeletal muscle, there is a large majority of studies indicating that cytokine protein content is also increased in cachectic skeletal muscle. IL-1ß [154], IL-6 [203,328], IFN-γ [154], TNF-α [328] and Tweak [71] protein levels are increased in skeletal muscle of cachectic cancer patients whereas one study reported that IL-6 and TNF-α protein levels were unchanged in the skeletal muscle of cachectic cancer patients [154]. Similarly, IL-1ß [205], IL-6 [133,270], IFN-γ [123], and TNF-α [125,133,270] protein levels are also increased in cachectic skeletal muscle of mice, whereas one study reported that IL-1ß, IL-6, and TNF-α protein level [123] was unchanged.

If the systemic inflammatory response can be largely attributed to the response of the host immune system to tumor growth, and can thus contribute to explain the increase in cytokine content of skeletal muscle described above, it is important to note that skeletal muscle is also able to synthesize and produce cytokines and thus contribute to the inflammatory response. In this context, available data are more contrasted. For instance, IL-6 [311] and TNF-α mRNA level [203,311], as well as IL-4 mRNA level [329] are unchanged whereas in another study, IL-6 mRNA level is increased [203] in skeletal muscle of cachectic cancer patients. In animal models of cancer cachexia, IL-1ß [101,205], IL-6 [65,78,79,101,147,205,227,232] and TNF-α [205] mRNA levels are increased in skeletal muscle of cachectic cancer mice, whereas other studies reported no change in the mRNA level of IL-6 [76,150,158], TNF-α [79,147,150] and Tweak [82] in skeletal muscle of cachectic cancer mice. Therefore, if an increase in skeletal muscle cytokine protein content generally occurs during cancer cachexia, it is less clear, whether or not this is supported by an increase in cytokine production by skeletal muscle itself. Furthermore, one should also question whether or not skeletal muscle contributes to the systemic inflammatory response during cancer cachexia.

Omic studies both in human patients [200,235] and animal models of cancer cachexia [112,144,198,205,281–283,330] indicate that cachectic skeletal muscle is subjected to a persistent proinflammatory cytokine signaling. Transcription factor nuclear factor kappa B (NF-κB) and signal

transducer and activator of transcription 3 (STAT3) have emerged as important transcription factors for relaying cytokine signaling in skeletal muscle. NF-κB plays a critical role in skeletal muscle mass loss induced by TNF-α. NF-κB resides in the cytosol of cells in an inactive state, tightly bound to IκB. Activation occurs when the IκB kinase (IKK) phosphorylates IκB and initiates IκB degradation via the ubiquitin-proteasome system. This leaves NF-κB free and allows it to translocate into the nucleus and binds NF-κB DNA response elements in the promoter of target genes. The phosphorylation level of NF-κBp65 is similar in skeletal muscle of cachectic cancer patients compared to non-cachectic patients [119]. However, when compared to healthy controls, NF-κB subunit 1 (p105) mRNA level is increased [203] as well as NF-κBp65 protein content [154,328], suggesting that NF-κB pathway could be precociously activated before the development of cancer cachexia in human patients. In animal models of cancer cachexia, the phosphorylated active form of NF-κB [73,101,117,123,124,142,150,155,232], the nuclear localization of NF-κB [205], as well as the DNA binding [67,135,145,205,280] and the transcriptional activity [123] of NF-κB complex are increased in cachectic skeletal muscle. Motif analysis of promoter sequences also identified the NF-κB complex as a potential key transcription factor involved in skeletal muscle atrophy during cancer cachexia [204]. A recent omic analysis also suggested that NF-κB signaling was activated in skeletal muscle of cachectic tumor-bearing mice [205]. Furthermore, the phosphorylated active form of NF-κBp65 negatively correlates with body mass loss and muscle force in cachectic cancer mice [101]. If a consensus emerges regarding the regulation of NF-κB during cancer cachexia, it is important to note that some studies failed to observe any increase in NF-κBp65 phosphorylation [82,144,262] nor in NF-κB complex DNA binding activity [115,144,277,331] in skeletal muscle of cachectic cancer animals. Similarly, ChIP-seq analysis of skeletal muscle of C26 tumor-bearing cachectic mice showed that NF-κB transcription was no required to drive skeletal muscle mass loss [144], suggesting that NF-κB-independent signaling also occurs during cancer cachexia. Therapeutic strategies invalidating TNF-α receptor [108,109,332], as well as injection of anti-TNF-α antibody [186], have also failed to provide convincing results.

STAT3 plays a critical role in muscle mass loss induced by the IL-6/Janus kinase (JAK)/STAT3 signaling pathway. Cancer mice displaying hyperactivation of STAT3 show exacerbated weight loss, reduced muscle and adipose tissue mass as well as early mortality when compared to cancer mice in which STAT3 is not hyperactivated [333]. If the phosphorylation level of STAT3 is similar in skeletal muscle of cachectic cancer patients compared to non-cachectic patients [119], an increase in STAT3 activation has been consistently reported in skeletal muscle of cachectic cancer mice [65,73,76,101,142,158,228,232,267,334]. Motif analysis of promoter sequences also identified STAT3 as a potential key transcription factor involved in skeletal muscle atrophy during cancer cachexia [204]. Accordingly, the expression of STAT3 target genes is also increased in skeletal muscle of cachectic cancer mice [283]. Finally, the phosphorylated active form of STAT3 negatively correlates with body

mass loss and muscle force in cachectic cancer mice [101]. The role that IL-6/JAK/STAT3 signaling pathway could play during cancer cachexia is also illustrated by studies showing that circulating IL-6 level in tumor-bearing mice correlates with the development of cachexia [76,325] and that cancer mice lacking IL-6 [158,333,334] do not develop cachexia. Moreover, injection of an anti-IL-6 antibody [325] or an anti-IL-6 receptor antibody [70] in tumor-bearing animals prevents cachexia progression.

Therefore, current evidence clearly indicates that cachectic skeletal muscle is subjected to inflammation both in cancer patients and in animal models of cancer cachexia (Figure 9). Skeletal muscle itself may be a source of cytokines during cancer cachexia, but the cell types responsible for the production of cytokines (skeletal muscle fiber, resident, and/or recruited mononucleated cells) have not been identified yet. Anyhow, non-muscle tissues (host immune system, tumor cells) would seem to be the main sources of cytokines during cancer cachexia. The temporal regulation of the inflammatory response in skeletal muscle is currently unknown. Finally, a direct functional relationship between increased inflammation and the regulation of proteostasis in skeletal muscle fiber during cancer cachexia still requires more experimental evidence.

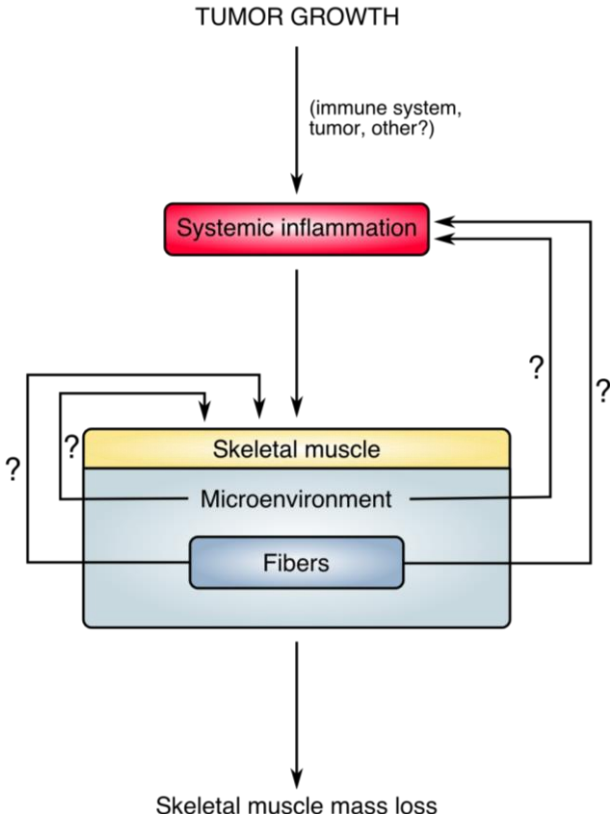

Figure 9. Integrated view of the effects of inflammation on skeletal muscle during cancer cachexia.
Tumor growth induces systemic inflammation. Inflammation is also present in skeletal muscle (increase in cytokine content, activation of NF-κB, and STAT3 signaling pathways). The contribution of skeletal muscle fibers and resident or recruited mononucleated cells to skeletal muscle inflammation is currently unknown. It is also unclear if skeletal muscle inflammation contributes to systemic inflammation. It is believed that skeletal muscle inflammation contributes to skeletal muscle mass loss during cancer cachexia.

Myostatin and activin A during cancer cachexia

Myostatin (Mstn) is a growth and differentiation factor essentially produced by skeletal muscle that belongs to the transforming growth factor-beta (TGF-ß) superfamily. MSTN acts as an autocrine/paracrine negative regulator of skeletal muscle growth during embryonic and postnatal development [335] but also in adulthood as a statin that contributes to the maintenance of skeletal muscle mass [336]. MSTN binds activin type IIB receptor (ActRIIB) leading to the recruitment and activation of TGF-ß type I receptors (either activin-like kinase 4 (Alk4) or activin-like kinase-5 (Alk5) receptors). MSTN signals through canonical SMAD2 and SMAD3 proteins, which once activated by phosphorylation will recruit SMAD4 to form an active transcriptional complex that translocates into the nucleus to regulate the transcription of target genes [337]. MSTN also inhibits the IGF1-AKT pathway [338].

Generally considered as the most powerful regulator of skeletal muscle mass, it is expected that an increase in *Mstn* expression would be a molecular signature of cancer cachexia. Surprisingly, MSTN circulating level has been shown to decrease in cachectic cancer patients compared to healthy controls [339] and to decrease [24] or to be unchanged [340] compared with non-cachectic cancer patients. *Mstn* mRNA level is also unchanged in skeletal muscle of cachectic cancer patients compared to healthy control subjects [54,203] or non-cachectic cancer patients [54,250]. Bonetto et al. even found a decrease in *Mstn* transcript level [231]. In agreement with these data, MSTN protein level [154] as well as the phosphorylation status of SMAD2 and SMAD3 has been shown to be the same in skeletal muscle of cachectic cancer patients compared to healthy control subjects [54] or non-cachectic cancer patients [54,119]. Of note, circulating level [24] and skeletal muscle transcript level [250] of follistatin, an inhibitor of MSTN and activin signaling, are unchanged in cachectic cancer patients. Finally, one should note that an omic study provides a slightly different picture as genes related to TGF-ß signaling [194] were reported to be up-regulated in skeletal muscle of cachectic cancer patients. Furthermore, the transcript level of ActRIIb negatively correlated with muscle mass in cancer patients [297]. Together, these studies do not provide clear evidence that MSTN signaling is activated in skeletal muscle of human cancer patients during cancer cachexia. Therefore, how is it possible to reconcile the fact that MSTN is a master regulator of muscle mass in humans [341] and the observation that *MSTN* expression and MSTN signaling are unchanged in skeletal muscle of cachectic cancer patients? One may first consider that as MSTN is produced by skeletal muscle, MSTN circulating level can be lowered simply as a consequence of the reduction in skeletal muscle mass during cancer cachexia. Furthermore, the data described above do not exclude the possibility that MSTN contributes to skeletal muscle mass loss earlier during the development of cancer cachexia when the skeletal

mass has not started to decrease yet. Kinetic analysis of *MSTN* expression during the time course of cachexia would allow answering this question.

In animal models of cancer cachexia, the circulating level of MSTN has been reported either to increase [71] or to be unchanged [68,87] in cachectic cancer animals compared to controls. Although some studies do not report any increase in *Mstn* expression in skeletal muscle of cachectic cancer mice or rats compared to healthy animals [82,134,227,275,342], numerous studies reported an increase in both *Mstn* mRNA level [68,87,159,190,207,343] and protein level [71,87,94,117,123,343]. Of note, the follistatin mRNA level in skeletal muscle was found to be either not modified [94] or decreased [275,342], which is also consistent with an increase in MSTN activity. Costelli et al. [87] proposed that a decrease in follistatin level would occur at the beginning of cancer cachexia, thus leading to the activation of the MSTN signaling pathway that would be then followed by an increase in follistatin expression thus allowing a subsequent down-regulation of the MSTN pathway. Downstream of the pathway, the mRNA level of ActRIIb [275], as well as the phosphorylation of SMAD2 [68,134] and SMAD3 [71,142] have been reported to increase in skeletal muscle of cachectic mice. Of note, a study by Gallot et al. [82] reported a decrease in the ActRIIb mRNA level without any modification of the transcript level of Alk4 and Alk5, as well as of the phosphorylation status of SMAD2 and SMAD3. Therefore, and even if it cannot be generalized to all animal models of cancer cachexia, MSTN signaling seems to be commonly activated during cancer cachexia. Finally, the functional role of MSTN in mice models of cancer cachexia is supported by several studies showing that cancer cachexia is blocked when MSTN signaling is inhibited, either by *Mstn* gene invalidation [82], the administration of *Mstn* antisense RNA [343], the administration of MSTN antibody [98], the administration of a soluble ActRIIb [68,184,207,227,323,344,345], the administration of Alk4/5 receptor antagonist [208], or by the administration of IMB0901, an inhibitor of MSTN signaling [128]. The beneficial actions of MSTN inhibition in these conditions have been attributed to the restoration of proteostasis in skeletal muscle, by a reduction in the ubiquitin-proteasome [68,82,128,208,345] and autophagy-lysosome [82,207] systems as well as by an increase in IGF1-AKT pathway [68].

In addition to MSTN, activin A, another TGF-ß family member, can also bind ActRIIB and activate SMAD2/3 signaling with comparable potencies and efficacy as MSTN does to trigger skeletal muscle mass loss [346]. Activin A circulating level was consistently increased in cachectic cancer patients compared to healthy control subjects [52] and non-cachectic cancer patients [24,323,340,347,348], as well as in animal models of cancer cachexia [65,68,134,142,209,323,345,349]. If activin A mRNA level in skeletal muscle during cancer cachexia has not been investigated in cancer patients, studies in animal models of cancer cachexia indicate that activin A mRNA level is either decreased [65,227,345] or unchanged [82] whereas activin A protein level has been reported to increase

[345]. Therefore, the increase in activin A circulating level may thus result from another source than skeletal muscle during cancer cachexia including tumor cells [68,227,263,345,350,351].

Together, these studies highlight discrepancies between cachectic cancer patients and animal models of cancer cachexia (Figure 10). This can be explained by methodological constraints inherent to clinical studies that for instance do not allow standardized biological analyses of cancer cachexia, but also by inter-species differences. Indeed, while MSTN circulating level is

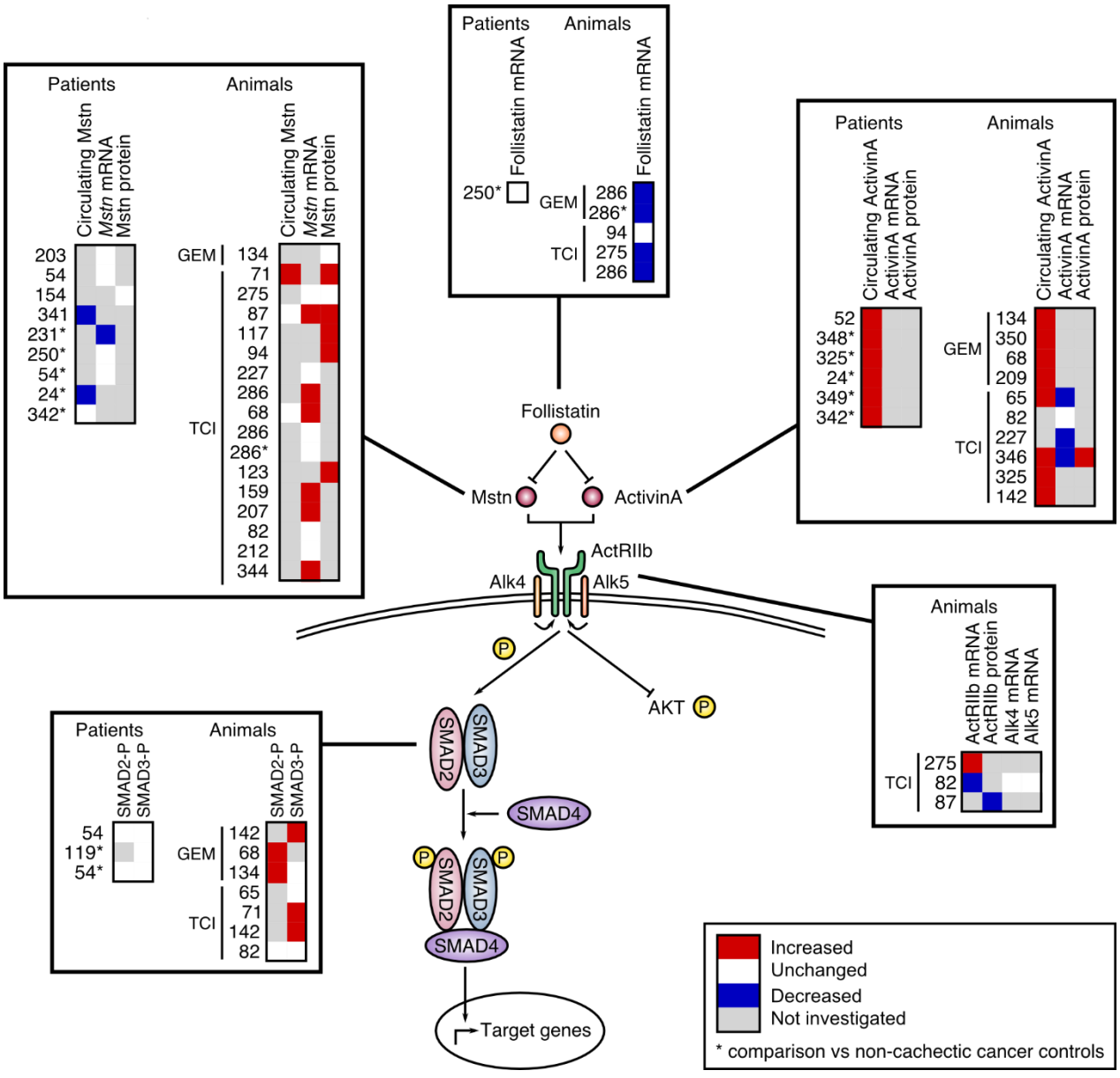

Figure 10. Regulation of myostatin signaling in cachectic skeletal muscle of cancer patients and animals.
Data were taken from indicated references. Colors indicate when up-regulation (red), down-regulation (blue), or not significant difference was found (white). Not reported data are in grey. Unless indicated by *, comparisons were done with healthy controls. ActRIIb, activin type IIb receptor; Alk4, activin-like kinase 4; Alk5, activin-like kinase 5; GEM, genetically engineered model; Mstn, myostatin; TCI, tumor cell injection.

higher and is the main negative regulator of skeletal muscle mass in mice, activin A circulating level is higher in humans than in mice [346]. Therefore, it is likely that activin A could play a more prominent role in cachectic cancer patients than MSTN does. Further investigations of ActRIIb downstream signaling are also required.

Apoptotic nuclear death during cancer cachexia

Skeletal muscle fiber is unique in that the mature fiber can contain hundreds of nuclei. The multinucleated nature of the muscle fiber is necessary to accommodate volume a lot greater than a typical mononucleated cell. Nuclei are required for the transcription of large amounts of mRNA that supports the protein synthesis required to generate and maintain the contractile apparatus. This thus raises the question of the role of apoptotic myonuclear death in skeletal muscle depletion during cancer cachexia.

Evidence that apoptosis occurs in skeletal muscle of human cancer patients has been provided by a number of studies. Cleavage of poly(adenosine diphosphate ribose) polymerase (PARP) and DNA fragmentation, hallmarks of apoptosis, have been observed in skeletal muscle of cachectic cancer patients [121] together with an increase in the mRNA level of the BAX pro-apoptotic factor [311], caspase 7 and 9 [251], phosphorylation of p53 [122] and activation of caspase-8 and -9 [122]. Although not systematically observed [120], the presence of apoptotic nuclei has been also reported in skeletal muscle of cachectic cancer patients [122]. Animal studies also consistently provided results in favor of an increase in apoptotic nuclear death in cachectic skeletal muscle. An increase in BAX pro-apoptotic-to-BCL2 anti-apoptotic protein ratio [86,261,268] and mRNA ratio [114], as well as increased expression [261,268] and cleavage [86] of caspase-3 together with increased caspase-1, -3, -6, -8 and -9 activity [115,352] have thus been reported in skeletal muscle of animal models of cancer cachexia, especially at the later stage of cachexia [103,163]. Accordingly, transcriptomic studies reported an increase in the expression of genes involved in apoptosis in skeletal muscle of cachectic cancer mice [198,282]. This was confirmed by an increase in PARP cleavage [352] and DNA fragmentation [114,115,332,353] in skeletal muscle of cachectic cancer animals. The presence of apoptotic nuclei has been also reported in muscles of cachectic cancer mice and rats [98,103,117,123–125].

However, it is important to keep in mind that skeletal muscle is a very heterogeneous tissue, where approximately half of its nuclei reside outside muscle fibers [354] including satellite cells, endothelial cells, fibroblasts, pericytes, and macrophages [355]. Therefore, it is essential to distinguish true myonuclei from those of neighboring mononuclear cells. A number of studies presented above did not specify the exact localization of apoptotic nuclei [117,122–125], so that it is difficult to determine whether apoptotic nuclear death refers to myonuclear death in these

studies. However, others studies have localized apoptotic nuclei inside (myonucleus) [103] and outside the muscle fiber (nucleus from mononucleated cells) [98,103]. Therefore, apoptotic nuclear death in cachectic cancer skeletal muscle also refers to the death of mononucleated cells present in the vicinity of the muscle fiber (muscle fiber microenvironment). The relevance of this observation in relation to the role of muscle fiber microenvironment during cancer cachexia needs to be further explored (see below). Furthermore, the multinucleated nature of skeletal muscle fibers implies that the apoptotic death of a single myonucleus does not obviously imply the destruction of the entire fiber as it occurs with apoptosis in mononucleated cells. Accordingly, the whole number of muscle fibers is maintained in cachectic skeletal muscle in human patients [61,119] and in animal models of cancer cachexia [98]. In this context, myonuclear death by apoptosis during cancer cachexia may locally trigger individual nuclei decay segmentally along the muscle fiber over an extended period of time, which may locally weaken and atrophy the muscle fiber that may render it more sensitive to micro-injuries (see below).

Muscle fiber microenvironment during cancer cachexia

The microenvironment of skeletal muscle fibers contains different mononucleated cell types that are important for skeletal muscle repair. Upon muscle injury, quiescent resident satellite cells get activated, proliferate, and then fuse with preexisting damaged muscle fibers to rebuild new functional fibers [188]. The activity of these muscle progenitor cells is greatly influenced by the presence of inflammatory cells [189], fibro-adipogenic progenitors [190], fibroblasts and endothelial cells [191]. Such a mechanism is essential for proper muscle regeneration following injury or microinjury.

The excessive presence of mononucleated cells in muscle fiber microenvironment of cachectic skeletal muscle in human patients has originally been reported at the beginning of the 20th century [192] and later by Marin and Denny-Brown [127]. They observed that skeletal muscle of cancer patients contained more nuclei in the vicinity of the sarcolemma even though the intrafiber or extrafiber localization of nuclei was not determined in these studies. More recently, inflammatory cells [154], macrophages and fibro-adipogenic progenitors cells [194] have been identified in skeletal muscle of cachectic cancer patients. Similarly, a higher number of activated satellite cells [193], activated stem cells [193], undifferentiated cells [72,130] and inflammatory cells [77,117,123–125,195] has been also reported in animal models of cancer cachexia. The myogenic properties of these cells are also altered. Progenitor cells of cachectic cancer mice muscle have thus been show to commit to the myogenic program but not to completely differentiate [193]. In addition to these observations, it has also been reported the existence of ongoing discrete episodes of skeletal muscle regeneration in cachectic skeletal muscle in cancer patients [194,196,197] and in animal models of cancer cachexia [77,117,123–125]. Together with the observation of a deficiency

of cancer cachectic skeletal muscle to regenerate after freeze clamping- [69,193] or cardiotoxin- [102] induced muscle injury, these data collectively indicate that an alteration in the properties of skeletal muscle fiber microenvironment could lead to an accumulation of unresolved/incomplete episodes of skeletal muscle repair and ultimately contribute to skeletal muscle mass loss during cancer cachexia. An important function of inflammation in skeletal muscle is to regulate the fate and function of mononucleated cells that reside in the microenvironment of the muscle fiber and that are essential for long term skeletal muscle homeostasis [191]. The data described above clearly indicate that cachectic cancer skeletal muscle is proinflammatory. As a sequential presence of proinflammatory, and then anti-inflammatory, cells is necessary for a proper and efficient regeneration process [189], a chronic inflammation state of cancer skeletal muscle would not allow a good temporal resolution of the inflammatory signals that could contribute to altering the properties of mononucleated cells. This could lead to an accumulation of unresolved/incomplete episodes of skeletal muscle repair during the chronicity of the disease, which ultimately may contribute to skeletal muscle mass loss during cancer cachexia.

Conclusion and perspectives

Our current knowledge of the mechanisms involved in skeletal muscle mass loss in human cachectic cancer patients and animal models of cancer cachexia is summarized in Figure 11. This comprehensive analysis of the literature highlights several points. First, and although this is trivial, an accurate determination of protein synthesis and degradation rates is still missing in skeletal muscle of cachectic cancer patients. If it seems quite clear that a decrease in protein synthesis rate occurs in skeletal muscle of human patients during cachexia, there are some uncertainties regarding protein degradation rate. Whether or not, protein degradation rate is increased during cancer cachexia in human patients therefore still remains a key issue. Second, our analysis also highlights that a temporal analysis of the mechanisms involved in skeletal muscle proteostasis during cancer cachexia should be performed whenever it is possible. Due to the complexity of the clinical context in cancer patients and the difficulty (impossibility) to determine the onset of tumor growth, a time-course analysis of cancer cachexia is obviously very difficult to perform, but an extensive characterization of the cachectic state of the patients would limit inherent drawbacks relative to human study. A longitudinal analysis of skeletal muscle mass and function following tumor resection would also help to understand the capacity of cachectic skeletal muscle to recover. Data from Gallagher et al. [234] suggest that skeletal muscle is able to transcriptionnally recover as changes in transcriptome are reversible following successful tumor resection. This fundamental knowledge is very important in order to develop strategies aimed at improving the recovery of skeletal muscle. Third, our analysis highlights that important differences between models exist and should be taken into account before drawing conclusions as the molecular mechanisms involved in cancer cachexia may be noticeably different depending on animal cancer

type or the severity of cachexia [90]. Inter-species differences must be also considered as important differences in skeletal muscle gene transcriptomic response exist between animal models of cancer cachexia and human patients [90,198]. Therefore, animal models of cancer cachexia should reproduce as well as possible the complexity of the clinical context (cancer type, rate of cachexia progression, existence or not of metastasis) to extend the relevance of animal findings to the human clinical context. Fourth, if most of the regulations occur at the transcriptional and post-translational level, single nucleotide polymorphism in several genes (*FOXO1*, *FOXO3*, *ActRIIb*, genes involved in glucocorticoid (GC) signaling) have been associated with weight loss and/or skeletal muscle mass loss in cancer patients [297]. Differentially alternative spliced genes involved in inflammation, protein ubiquitination, and GC signaling have been also identified in skeletal muscle of cachectic compared to non-cachectic cancer patients [64]. Therefore, gene variants may also play a role and may contribute to explaining inter-individual sensibility/variability to cancer cachexia. The functions of altered epigenetic marked in the control of gene expression also need to be explored. Finally, emerging evidence indicate that muscle fiber microenvironment is an important determinant of cancer cachexia. Whether or not this is quantitatively important in determining skeletal muscle mass loss remains to determine.

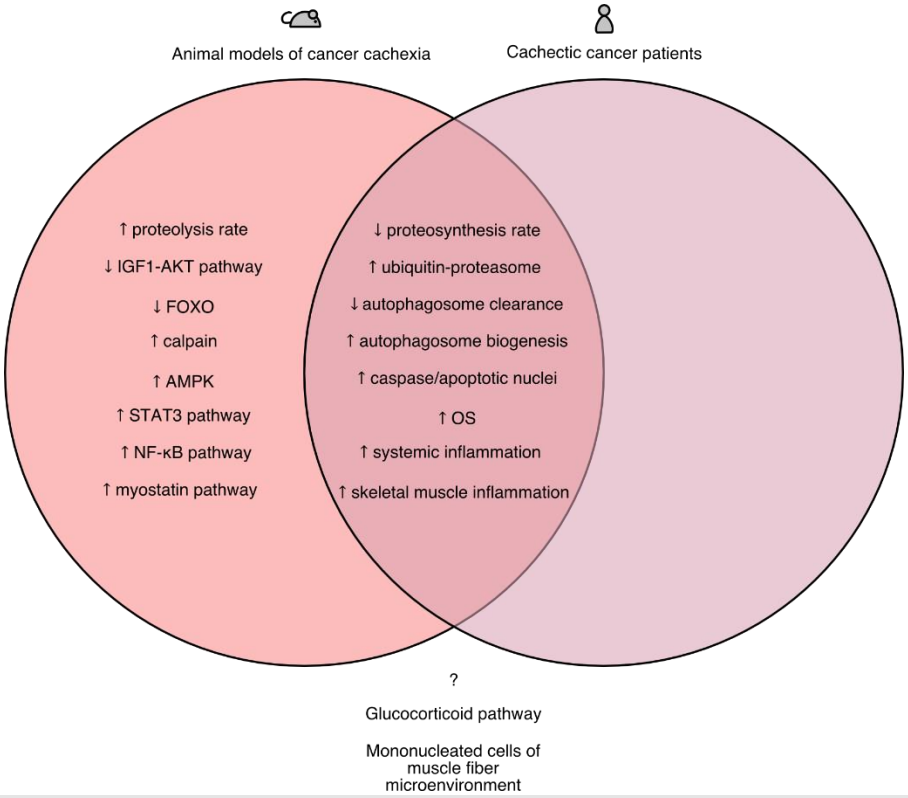

Figure 11. Venn diagram showing factors involved in skeletal muscle mass loss during cancer cachexia identified in animal models of cancer cachexia, human patients or both.

Unexplored factors in skeletal muscle of cachectic cancer patients as well as in skeletal muscle of both animal models of cancer cachexia and cachectic cancer patients are also indicated.

AMP, 5'AMP-activated protein kinase; NF-κB, nuclear factor κB; OS, oxidative stress; STAT3, signal transducer and activator of transcription factor 3.

Chapter III: Glucocorticoids and cancer cachexia

Glucocorticoids secretion during cancer cachexia

GC are steroid hormones mainly including cortisol in humans and corticosterone in rodents. GC are secreted by the adrenal cortex under the control of the hypothalamic-pituitary-adrenal (HPA) axis. In response to internal or external stimuli and circadian rhythm, the hypothalamus secretes corticotropin-releasing hormone (CRH), which stimulates the secretion of adrenocorticotropic hormone (ACTH) by the anterior pituitary gland. ACTH then binds its receptor MC2R on the adrenal cortex to activate the biosynthesis and release of GC into the blood circulation (Figure 12).

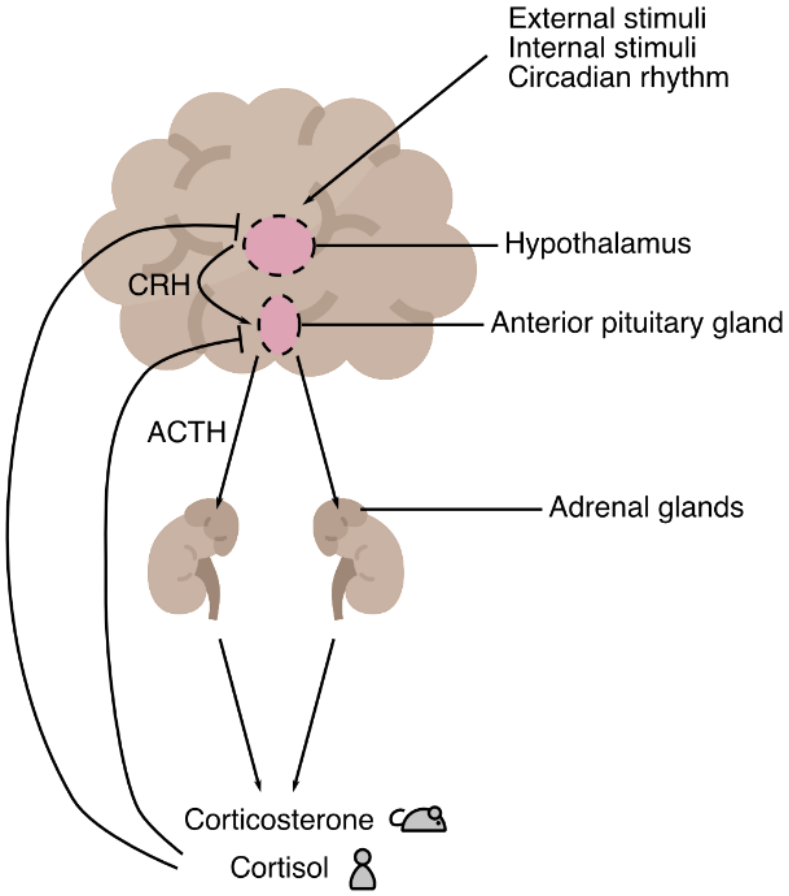

Figure 12. The HPA axis.
CRH, corticotropin-releasing hormone; ACTH, adrenocorticotropic hormone.

GC are synthesized in the *zona fasciculata*, the intermediary layer of the adrenal cortex from cholesterol through serial enzymatic reactions (Figure 13). The activity of the HPA axis is regulated by negative feedback from GC to the pituitary gland and hypothalamus.

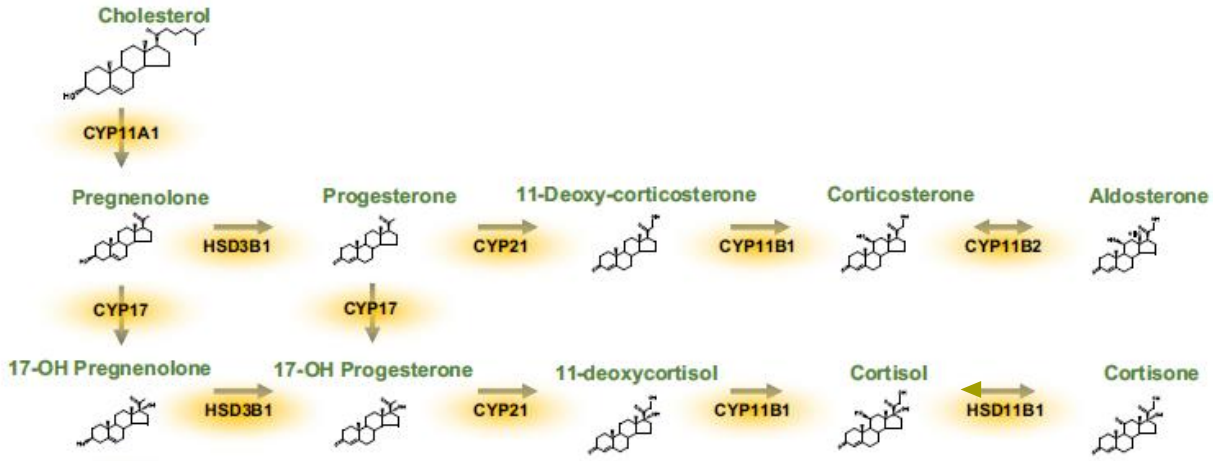

Figure 13. Biosynthesis of GC by the adrenal cortex.
CYP, cytochromes P450; HSD, hydroxysteroid dehydrogenase (from [353]).

Once GC secreted, GC action on target tissues is regulated by HSD11B1, a bidirectional enzyme, which has a reductase and dehydrogenase activity expressed in multiple tissues. HSD11B1 uses NADPH or $NADP^+$ to catalyze the interconversion of the cortisone and 11-dehydrocorticosterone (inactive form in human and mice, respectively) into cortisol and corticosterone (active form in human and mice, respectively) [356]. The flux direction depends on the ratio of oxidized and reduced NADPH [357]. GC act on multiple tissues mainly through their binding on their nuclear receptor NR3C1, which dimerizes and translocates into the nucleus to activate or inhibit the transcription of target genes [358].

The function of GC during cancer cachexia is poorly understood and essentially based on the measurement of circulating levels of GC in cancer patients and in animal models of cancer cachexia. Circulating GC level is increased in cachectic cancer patients [359–361] as well as in cachectic cancer animal models [74,105,181,182,186,278,327,361–364] suggesting that HPA axis is activated during cancer cachexia. Increased hypothalamic *CRH* transcript level [264] and an increased pituitary weight and ACTH secretion [365] have been reported in animal models of cancer cachexia. This was associated with increased adrenal activity as evidenced by their increased mass [183,365,366] and the hypertrophy of the cells in the *zona fasciculata* of the glands [365]. An increased adrenal gland mass was also found in cachectic cancer patients [367]. Together, these data suggest that the HPA axis is activated during cancer cachexia. However, additional information concerning the other components of the HPA axis is still lacking.

Action of glucocorticoids on skeletal muscle during cancer cachexia

GC administration leads to skeletal muscle atrophy by decreasing the rate of protein synthesis and increasing the rate of proteolysis [368,369]. GC binding on its receptor regulates a wide number of genes in skeletal muscle [370] affecting skeletal muscle proteostasis through several mechanisms [371,372]. In particular, GC administration increases skeletal muscle protein degradation via the activation of the transcription of genes involved in proteolytic systems such as ubiquitin-proteasome [373,374] or autophagy-lysosome systems [375] and repressing proteosynthesis via the inhibition of the IGF1-AKT pathway and its downstream effectors [373,376,377].

If it was suggested that the HPA axis activity is increased during cancer cachexia, how GC signaling is translated in skeletal muscle fibers of cachectic cancer patients is currently unknown. A role for GC during cancer cachexia is also strongly suggested by the analysis of the available transcriptomic data in skeletal muscle of cancer cachectic mice that reveals an increase in the expression of multiple GC-responsive genes [90,91,105,137,144,198,204,205,281–283] (Figure 14). However, a study exploring how GC signaling could be translated in skeletal muscle fibers of cachectic cancer patients reported that mRNA levels of NR3C1 and Hsd11ß1, an enzyme that converts inactive cortisone to active cortisol, were unchanged in skeletal muscle of cachectic cancer patients [234]. If we take into account the powerful catabolic effect of GC that has been experimentally demonstrated in skeletal muscle [372] with regard to the poverty of the available data, there is clearly a need for an in-depth analysis of the functional role of GC in cancer cachectic patients.

The studies described above suggest that GC would effectively contribute to skeletal muscle mass loss during cancer cachexia. However, strategies aimed at inhibiting the GC pathway have provided contrasting results. Adrenalectomy did not cause attenuation of cachexia [182,378] in tumor-bearing animals. The steroid hormone inhibitor RU486 has been shown either to prevent [363] or not [74,362] cachexia in cancer animals, whereas a strategy based on the utilization of muscle-specific GC receptor knockout mice, demonstrated that skeletal muscle wasting during cancer cachexia was dependent on GC signaling [159]. Therefore, if currently available data suggest that a dysregulation of the hypothalamic-pituitary-adrenal axis occurs during cancer cachexia, the involvement of the GC pathway in skeletal muscle mass loss during cancer cachexia and its potential relevance as a therapeutic target need to be further explored.

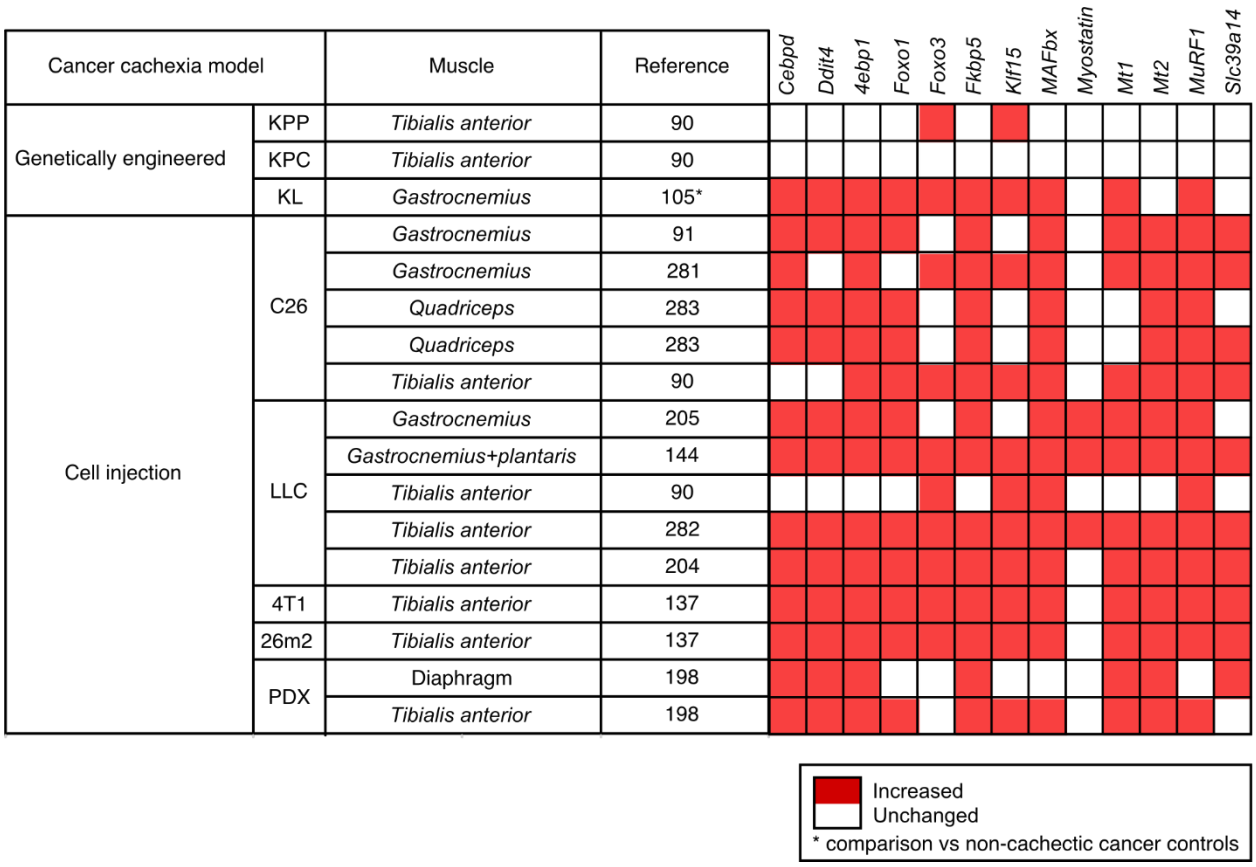

Figure 14. Skeletal muscle mRNA level of glucocorticoid-responsive genes in of animal models of cancer cachexia. Selected genes have been previously shown to be regulated in skeletal muscle by glucocorticoids in skeletal muscle [370,371,377–379].

Actions of glucocorticoids on liver during cancer cachexia

GC are since a long time known to play a role in liver metabolism promoting gluconeogenesis [379,380]. It was later determined that the GC receptor has multiple target genes in liver involved in amino acid, glucose, and lipid metabolisms [381,382]. GC-bound GC receptor induces the transcription of key enzymes involved in gluconeogenesis such as phosphoenolpyruvate carboxykinase, glucose-6-phosphatase, pyruvate carboxylase and 6-phosphofructo-2-kinase [383] and of coactivators involved in the activation of gluconeogenic genes [384–386] as well as that of genes involved in glycogen metabolism [383]. If the role of GC on hepatic lipid metabolism is less defined [387], GC administration affects the transcription of genes involved in fatty acid oxidation and in triglyceride synthesis and hydrolysis [388–390]. GC administration also contributes to enhancing the urea cycle in liver notably through the induction of Arginase I transcription [391]. GC administration was also shown to decrease the synthesis of ketone bodies by the liver [392,393]. However, further investigations are required to fully understand target genes and the involved mechanisms.

Given that liver glucose metabolism is impaired in cachectic cancer patients, notably with increased gluconeogenesis from lactate [394,395], amino acids [396–398] and glycerol [399], and that the increased hepatic gluconeogenesis in cancer patients was shown to correlate with their circulating level of the cortisol [400], it can be speculated that GC are involved in this process during cancer cachexia. However, the GC signaling pathway in the liver was never investigated in the cancer cachexia context.

AIMS OF THE THESIS

Cancer cachexia is a complex catabolic syndrome characterized by an involuntary body-mass loss essentially due to a severe depletion of skeletal muscle, with or without adipose tissue loss [2]. The prevalence of cancer cachexia increases with the severity of the disease and depends of cancer type, the highest prevalence being observed in gastric and pancreatic cancer reaching up to 80% of patients [17]. Cancer cachexia is one of the most debilitating and life-threatening aspects of cancer, profoundly affecting the patient's quality of life [4,19–24]. Cachexia decreased cancer treatment efficacy notably by increasing surgical risks [25] and the susceptibility to the adverse effects of chemotherapy [23,26,27] and it has been consistently reported that the extent of cachexia is inversely correlated with the survival of cancer patients [4,8,13,21,22,31–35]. Understanding the molecular mechanisms of cancer cachexia and developing strategies that limit and even prevent cachexia is therefore of societal relevance [401,402] to offer to cancer patients more effective clinical care, and ultimately to improve their quality of life and increase their lifespan.

Cancer cachexia is a systemic catabolic syndrome that involves a dialog between the tumor and multiple tissues and organs with important metabolic functions [16,18,44]. Pathways and mechanisms involved in the dialog between tissues and organs to trigger a coordinated response during cancer cachexia remain to be explored. GC are well known to trigger skeletal muscle in different experimental settings [271,373,403–410] however their role during cancer cachexia, which has been supported by several studies [159,258,271,363] need to be further explored. GC pathway is also known to regulate liver metabolism, but its role during cancer cachexia on liver metabolism is currently unsolved. **We thus hypothesized that GC may play a relevant role during cancer cachexia by promoting skeletal muscle mass loss and affecting hepatic metabolism.**

In a first study (MYOCAC study), we aimed to characterize the loss of skeletal muscle mass and function in patients with digestive cancer (including stomach, small intestine, appendix, colon or rectum) during a 6-month follow-up after chirurgical resection. We also aimed to explore the mechanisms involved in the skeletal muscle wasting with a particular focus on MSTN and GC pathways.

In a second study (*Apc* study), we used the *Apc*$^{Min/+}$ mouse model of intestinal cancer cachexia to explore the biological functions of the GC pathway during cancer cachexia. We first characterized hepatic metabolism during cancer cachexia in this model. We then investigated the role of the HPA axis and GC on skeletal muscle and liver during cancer cachexia. Finally, we determined the effects of the *Mstn* gene invalidation on the regulation of hepatic metabolism and GC pathway during cancer cachexia.

RESULTS

MYOCAC study

Cancer cachexia is responsible for the death of approximately 20% of patients [36]. MSTN is a master negative regulator of skeletal muscle mass [335,341]. If the role of MSTN in cancer cachexia is now well established in murine models (see Figure 9), no study has focused on muscle expression of *MSTN*n relation to the degree of cachexia. The hypothesis is that muscle *MSTN* a biological marker of cachexia in patients with digestive cancer. The primary purpose of the MYOCAC study was to determine whether skeletal muscle *MSTN* mRNA level was associated with the extent of cachexia in digestive cancer patients. The secondary purpose was to determine whether a GC dependent signature in skeletal muscle is also associated with the extent of the cachexia.

Material and methods

Study design

The MYOCAC study was a 6 month-longitudinal interventional study conducted at the Centre Hospitalier Universitaire of Saint Etienne, France. Included patients answered to questionnaires, performed physical tests and had blood sampling and an abdominal CT scan 1 month before resection surgery (T0) as well as at 1 month (M1), 3 months (M3) and 6 months (M6) postoperatively. A *vastus lateralis* muscle biopsy was performed during resection surgery under general anesthesia. A flow chart of the study is displayed below (Figure 1).

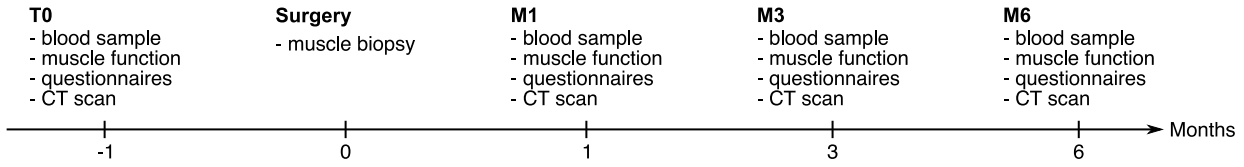

Figure 1. Patient flow chart for the MYOCAC study.

The experimental protocol was approved by the French Ethics Committee (Comité de Protection des Personnes Ile de France III) and performed in accordance with the principles of the Declaration of Helsinki. The study was reported to the National Commission for Data Protection and Liberties (CNIL; reference number: 1167710) and registered at ClinicalTrials.gov (trial number: NCT03172403).

Patients

Patients aged between 18 and 85 and diagnose for digestive cancer (including stomach, small intestine, appendix, colon or rectum) requiring resection surgery were eligible to participate in the study. Exclusion criteria were administration of corticosteroids, thyroid disease treated, severe chronic pathology during treatment (neuro-muscular pathologies, renal insufficiency

requiring dialysis, COPD under continuous oxygen therapy), psychological, familial, social or geographical conditions that could affect the participation of the subject throughout the protocol and body mass index (BMI) > 30 due to the difficulty of interpretation of BMI variations in obese patients. All patients provided written consent prior to entry into the study and were affiliate or beneficiary of social security.

Calculation of body mass loss

Body mass of patients was measured and expressed at the percentage of habitual pre-disease self-reported body mass.

CT-based analyses of muscle

CT scans used for the analysis were performed for routine patient care. The mean time between each CT scan and the corresponding visit was 4.5 days. A cross-sectional CT image at the midpoint of the third lumbar vertebrae (L3) was extracted from the abdominal CT scan of each patient using the Carestream software (NY, USA) and analyzed using the National Institutes of Health (NIH) ImageJ software [411]. All CT images were analyzed by a single trained observer. The cross-sectional area (mm^2) of the seven muscles of the L3 region (*psoas, rector spinae*, *quadratus lumborum*, *transversus abdominus*, external and internal obliques and *rectus abdominus*) was assessed by measuring the area composed by all pixels having an attenuation comprises between -29 and +150 Hounsfield units (HU) excluding those located within the internal cavity [62] and is a good indicator of the whole-body fat-free mass. SMI ($cm^2.m^{-2}$) was obtained by normalizing cross-sectional muscle area by patient stature and is known to be a good indicator of whole-body fat-free mass [63]. Skeletal muscle density (SMD) (HU) was calculated by averaging the HU of the L3 muscle cross-sectional area.

Blood parameters

All blood parameters were measured by the Laboratoire de Biologie Pathologie at the Centre Hospitalier Universitaire of Saint Etienne, France. C-reactive protein (CRP) assayed by immunoturbidimetry, creatinine with a peroxidase-antiperoxidase enzymatic method and albumin and prealbumin by immunonephelometry. Glomerular filtration rate (GFR) was estimated using the CKD-EPI formula.

Physical activity level

Physical activity was evaluated by the French version of the Global Physical Activity Questionnaire version 2 (GPAQ). The GPAQ is a validated physical activity questionnaire comprising 16 items grouped into three activity domains: activity at work, travel to and from places and recreational activities. The total level of physical activity was determined by the GPAQ total physical activity

score using the GPAP analysis guide [412] and expressed in metabolic equivalent of task (MET)-minutes per week.

Nutrition assessment

Nutritional status was evaluated by the French version of the full MNA® questionnaire, a validated screening tool to identify malnourished or at risk of malnutrition patients. The final score was calculated and interpreted following the full MNA® User Guide.

Quality of life

Quality of life was evaluated by the French version of the SF-36 questionnaire [413], a 36-item questionnaire that assessed scores of eight health domains [414]. Within a domain, lower score represents more disability.

Skeletal muscle function assessment

All force data were acquired with a PowerLab 16/30 (ADInstruments) and analyzed with LabChart Reader software 8.1.9 (ADInstruments).

Quadriceps intermittent fatigue test (QIF test)

All measurements were conducted on the dominant lower limb under isometric conditions. Patients were sat on a quadriceps chair with the knee flexed at 90° and the hip at 130°. Voluntary strength was measured with an inextensible ankle strap connected to a strain gauge (F2712-TC, Celians Meiri). Compensatory movement of the upper body was limited by two belts across thorax and abdomen. Patients were asked to keep their hands on their abdomen. Visual feedback of the force produced and the target force level was provided to the subjects.

Before starting the QIF test, patients performed ten 5-secund submaximal contractions followed by one maximal voluntary contraction (MVC) to warm up and to familiarize them with muscle force recorder set-up. After 8 min of rest, patients performed two MVC separated by 1 min of rest. Patients performed then the QIF test as previously described [415] without the femoral nerve magnetic stimulation and electromyographic recordings. Two MVC were performed at 5 min post exhaustion to assess force recovery. The MVC force was the maximum of the recorded force smoothed by a moving average of 0.5 seconds during a MVC. The maximum value of the two MVC trials was considered as the maximal. The endurance index was the total number of reached contraction.

Handgrip force test

Patients were asked to grip a grip force transducer (MLT004/ST, ADInstruments) as strong as possible during 3 seconds with their dominant hand. They performed 3 trials separated by 1

minute of rest. The recorded force was smoothed by a moving average of 0.5 second and the maximum value was considered as the maximal handgrip strength.

Statistics

Data were tested for normal distribution using a Shapiro–Wilk test. Pearson correlation was used for data with normal distribution and Spearman nonparametric correlation for data with non-normal distribution. All statistical analyses were performed using GraphPad Prism 7.0 (GraphPad Software, San Diego, CA). The significance level was set at $p<0.05$.

Results

Recruitment and follow-up

Patients were recruited between November 6, 2017 and January 1, 2020. Unfortunately, a total number of only 3 patients were included between August 2, 2018 and January 3, 2019. The 3 patients completed all assessments at the exception of the patient 2 who did not perform the skeletal muscle force assessment at M1 because of fatigue.

Patients' characteristics at baseline

The characteristics of the 3 included patients are displayed in Table 1. At inclusion, no patient elicited body mass loss as compared with their habitual body mass and thus no patient can be considered as cachectic. No patient presented abnormal blood parameters. Patient 1 was considered to achieve a moderate physical activity level while the 2 others to achieve a low physical activity level. Patient 1 had body pain and general health scores below the scores obtained from the general French population adjusted for gender and age [414] as patient 3 for role limitation due to physical and emotional health problems. All patients had a L3 skeletal muscle cross-sectional area, SMI and SMD above the cut-off between low and normal L3 skeletal muscle cross-sectional area, SMI and SMD in a healthy Caucasian population adjusted for gender, age and BMI [416].

Cancer cachexia classification

A first definition for cancer cachexia was based on body mass loss [2]. According to this criterion, patient 1 was never cachectic throughout the study. Patients 2 and 3 were both cachectic at M1 and, while patient 2 regained body mass to return to her initial body mass at M6, patient 3 remained to lose body mass to reach -16% at M6 (Figure 2A). Taking into account other factors such as blood parameters, fatigue, anorexia and skeletal muscle mass and force to define cachexia [3] is less evident given the lack of reference value for muscle force since muscle force is device-dependent. Given the low number of patient, it is of course difficult to determine, which definition of cachexia is the most pertinent in our context.

Table 1. Baseline characteristics of the patients.

	Patient 1	Patient 2	Patient 3
Anthropometrics			
Age (years)	69	71	47
Gender	M	F	M
Mass (kg)	75	63	76.5
BMI ($kg.m^{-2}$)	24	23	28
Body mass loss (%)	0	+4	+3
Cancer characteristics			
Primary location	Transverse colon	Ascending colon	Stomach
TNM stage	pT3N0M0	pT3N0M0	pT3N0M0
Pre-operative chemotherapy	no	no	yes
Pre-operative radiotherapy	no	no	no
Blood parameters			
Creatinine ($\mu mol.L^{-1}$)	84	92	53
GFR ($mL.min^{-1}.1,73m^{-2}$)	82	54	120
Albumin ($g.L^{-1}$)	41.1	40.1	39.6
Prealbumin ($g.L^{-1}$)	0.208	0.27	0.36
CRP ($mg.L^{-1}$)	0.9	2.5	4.6
Physical activity			
Total MVPA ($MET\text{-}min.wk^{-1}$)	2520	640	0
Nutrition			
Nutritional status	At risk of malnutrition	Normal nutritional status	Normal nutritional status
Quality of life			
Physical functioning	85	80	90
Role physical	100	100	0
Body pain	40	100	62
General health	47	82	67
Vitality	55	100	55
Social functioning	100	100	75
Role emotional	100	100	33
Mental health	92	100	76
Skeletal muscle characteristics			
L3 skeletal muscle cross-sectional area (cm^2)	142.82	109.81	175.75
SMI ($cm^2.m^{-2}$)	46.64	38	62.27
SDM (HU)	33	36	40
Skeletal muscle function			
Handgrip force (N)	480	261	419
Quadriceps MVC force (N.m)	139	82	208
Endurance index	46	61	54

BMI, body mass index; GFR, glomerular filtration rate; CRP, C-reactive protein; MVPA, moderate to vigorous physical activity; MVC, maximal voluntary contraction; SMI, skeletal muscle index; SMD, skeletal muscle density.

Skeletal muscle mass and function

We then compared the loss of body mass with the loss of skeletal muscle mass reflected by SMI during the follow-up of the patients (Figure 2B). Patient 1, with a constant body mass, had an increased SMI during the study suggesting that his resistance to cachexia could be due to resistance to skeletal muscle mass loss. On the contrary, patient 3, who lost body mass starkly until M3, also has a decreased SMI until M3 suggesting that the body mass loss mainly resulted from skeletal muscle mass loss. Patient 2 had a continuous decreased SMI throughout the follow-up despite her body mass increased from M1 to M6 suggesting that, once initiated, skeletal muscle mass loss persists and that her increased body mass may rather result from an increase in adipose tissue. Moreover, the SMI was not correlated with the SMD (p=0.55).

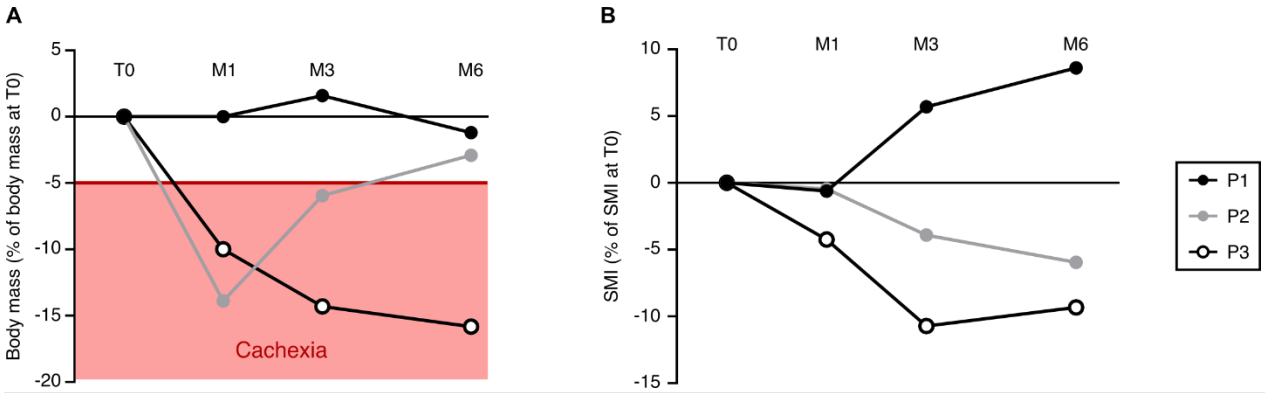

Figure 2. Evolution of the body mass (A) and SMI (B) of the three included patients.
SMI, skeletal muscle index.

For all patients, quadriceps MVC evolved similarly to SMI and was thus strongly correlated with SMI ($p<0.0001$, $r^2=0.93$) (Figure 3). Furthermore, handgrip force was also correlated with SMI ($p=0.13$, $r^2=0.51$). This highlights that the loss of skeletal muscle force reflects that of skeletal muscle mass in cancer patients. The endurance index was neither associated with SMI nor quadriceps MVC, suggesting that factors other than mass and force contribute to the variation of endurance index. Of note, this parameter was very difficult to assess because of the subjectivity of the perceived exhaustion and variable patient attrition to the QIF test.

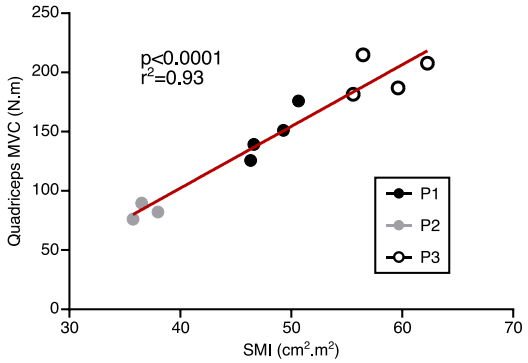

Figure 3. Pearson correlation of the quadriceps MVC with SMI in the three included patients.
MVC, maximal voluntary contraction; SMI, skeletal muscle index.

Other factors related to skeletal muscle mass and function loss

All correlations between the factors measured in the study and skeletal muscle mass and function are displayed in Figure 4. One factor known to influence skeletal muscle mass and force is physical activity. However, neither the total physical activity level nor total sitting-time correlated with SMI, quadriceps MVC or handgrip force in patients. The SMI and quadriceps MVC negatively correlated with role limitation due to physical health problems and social functioning. The quadriceps MVC and handgrip force also negatively correlated with vitality. This emphasizes the importance of skeletal muscle mass and force on the patients' quality of life. The SMI positively correlated with blood creatinine that is in range with the fact that circulating creatinine level is an accurate measure of whole-body skeletal muscle mass [417,418].

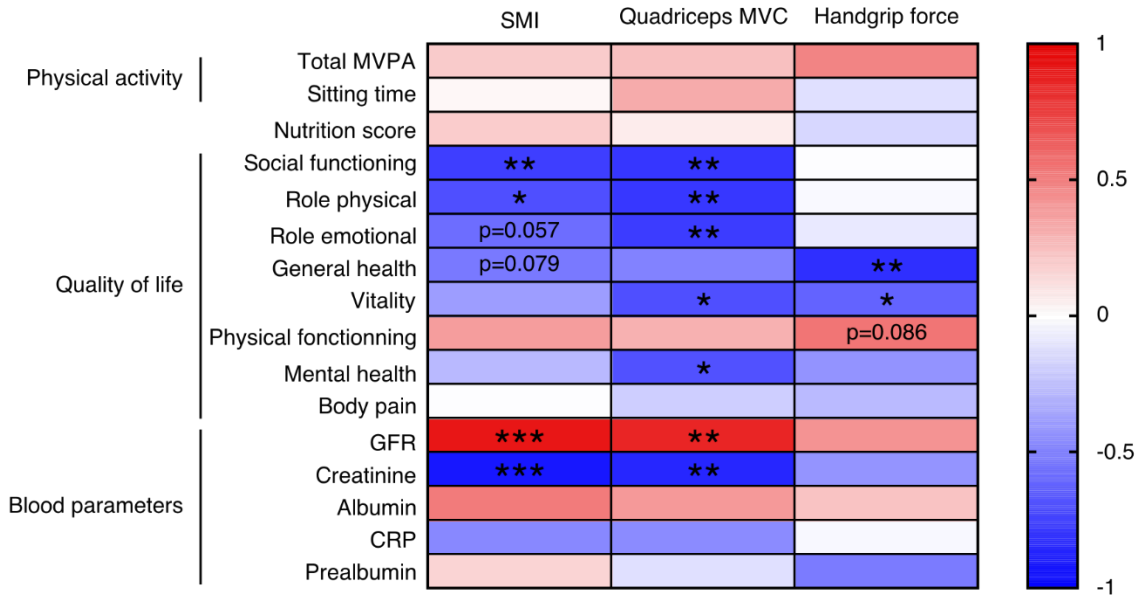

Figure 4. Visualization of correlation analysis results between skeletal muscle mass and function and other investigated parameters. Square color represents the magnitude of the correlation coefficient r. Red indicates positive correlation and blue indicates negative correlation. Significance of the correlations are indicated as: *p<0.05, **p<0.01, ***p<0.001. GFR, glomerular filtration rate; CRP, C-reactive protein; MVPA, moderate to vigorous physical activity; MVC, maximal voluntary contraction; SMI, skeletal muscle index.

Discussion

It is obviously impossible to draw conclusions given the low number of included patients however, this study allowed us to state some comments. Cachexia classification remains controversial because considering other factors than body mass loss required reference values that are currently still not clearly defined. This is a main issue as depending on the definition of cachexia, final outcomes may be different [4,20,419]. Moreover, even if only three patients were included, a great patient heterogeneity was observed. Indeed, whereas one patient never lost body mass, one lost body mass and returned to her initial body mass and one continuously lost body mass. This greater heterogeneity compared to animal studies requires a greater number of subjects and would have probably require a stratification of patient study. Finally, these preliminary data also confirmed that skeletal muscle mass largely contribute to muscle force in cancer patients affecting their quality of life. Unfortunately, recruitment of patients was far below originally expected so that we did not analyze neither patient biopsies nor plasma samples and we were unable to pursue our investigation on the mechanism leading to the skeletal muscle loss of mass and function during cancer cachexia.

Apc study

Cancer cachexia promotes a glucocorticoid-dependent response in skeletal muscle and liver of *Apc* mice inhibited by myostatin gene invalidation

Agnès Martin[1], Josiane Castells[1], Valentine Allibert[1], Cindy Zolotoff[1], Andréa Emerit[2], Yann S. Gallot[3], Victoire Cardot-Ruffino[4], Véronique Chauvet[4], Laurent Bartholin[4], Laurent Schaeffer[2], Anne-Cécile Durieux[1], Laetitia Mazelin[2], Christophe Hourdé[5], François B. Favier[6], Damien Freyssenet[1,x*]

[1]Laboratoire Interuniversitaire de Biologie de la Motricité EA 7424, Univ Lyon, Université Jean Monnet Saint-Etienne, Saint-Priest-en-Jarez, 42270, France

[2]Institut NeuroMyoGene (INMG), Univ Lyon, Université Lyon 1, CNRS UMR 5310, INSERM U 1217, Lyon, 69364, France

[3]LBEPS, Univ Evry, IRBA, Université Paris Saclay, Evry, 91025, France

[4]Centre Léon Bérard, Centre de recherche en cancérologie de Lyon (CRCL), Univ Lyon, Université Claude Bernard Lyon 1, INSERM 1052, CNRS 5286, Lyon, 69373, France

[5]Laboratoire Interuniversitaire de Biologie de la Motricité, Université Savoie Mont Blanc, Le Bourget du Lac, 73370, France

[6]Dynamique Musculaire et Métabolisme, Univ Montpellier, INRA, Montpellier, 34060, France

[x]Lead Contact

[*]Correspondence: damien.freyssenet@univ-st-etienne.fr

Summary

Cachexia affects about half of cancer patients and is characterized by a progressive body mass loss mainly resulting from skeletal muscle compartment depletion. This loss of skeletal muscle mass together with a decrease in muscle force strongly contributes to reducing cancer patient quality of life, treatment efficiency and ultimately patient survival. Glucocorticoids are steroid hormones secreted under the control of the hypothalamic-pituitary-adrenal axis that have been well described to promote skeletal muscle atrophy but also to exert systemic actions through activation or repression of gene expression in many tissues. We hypothesized that the glucocorticoid pathway could be activated during cancer cachexia in *Apc*$^{Min/+}$ mice, a mice model of intestinal cancer. Here, we report that activation of skeletal muscle catabolism was associated with a complete reprogramming of liver metabolism. Moreover, we showed an activation of the hypothalamic-pituitary-adrenal axis associated with an increase in the level of corticosterone (the main glucocorticoid in rodent) in serum, *quadriceps* muscle and liver of advanced cancer cachectic mice. The transcriptional signature in *quadriceps* muscle and liver of advanced cancer cachectic mice significantly mirrored that observed in mice treated with dexamethasone, a glucocorticoid analog. Importantly, the inhibition of cancer cachexia by myostatin gene invalidation in *Apc*$^{Min/+}$ mice restored corticosterone levels and abolished skeletal muscle and liver gene reprogramming. Together, these data indicate that glucocorticoids drive a transcriptional program to coordinately regulate skeletal muscle mass loss and hepatic metabolism rewiring. The inhibition of this response by myostatin gene invalidation highlights the existence of a molecular dialog between skeletal muscle and liver.

Keywords

Cancer cachexia, glucocorticoids, hypothalamic-pituitary-adrenal axis, liver, metabolism, myostatin, skeletal muscle

Introduction

Cancer cachexia is a devastating wasting syndrome characterized by uncontrolled catabolism of skeletal muscle with or without adipose tissue loss that cannot be reversed by conventional nutritional supports [1–3]. Cachexia is particularly prevalent in patients with lung, pancreatic or digestive cancer [4,3,5,6] and worsens with the advanced stages of the disease affecting up to 80% of patients with advanced cancers. Cachexia would account for up to 20% of cancer deaths [7].

If the reduction in skeletal muscle mass is an important determinant of cancer cachexia [8–13], cancer cachexia is also a systemic catabolic syndrome that involves a dialog between the tumor and multiple tissues and organs with important metabolic functions [14–16]. The liver is a critical regulator of glucose and lipid metabolism that orchestrates, along with skeletal muscle and adipose tissue, whole-body energy metabolism. The possibility that hepatic metabolism may be altered in cancer patients was suggested a long time ago [17]. Clinical studies in cancer patients provided support to this concept by showing a decrease in hepatic glycogen store [18], as well as an increase in hepatic gluconeogenesis from lactate [18], glycerol [19] or alanine [20], suggesting that liver metabolism is markedly impaired by cancer cachexia.

One class of hormones that play important roles in the regulation of skeletal muscle and liver metabolisms is glucocorticoids (GC). GC are steroid hormones synthesized and secreted by the adrenal cortex under the control of the hypothalamic-pituitary-adrenal (HPA) axis. GC bind to ubiquitously expressed GC receptor, which translocates to the nucleus and binds to GC response elements in the promoters of target genes to activate or inhibit their transcription. In skeletal muscle, the administration of GC induces atrophy by triggering a transcriptional program that decreases the expression of genes promoting protein synthesis and increases those promoting protein degradation [21–23]. In the liver, the administration of GC regulates the expression of numerous genes involved in amino acid metabolism, glucose metabolism as well as lipid metabolism [24,25]. The similarity between the effects triggered by GC administration on skeletal muscle and liver and those reported during cancer cachexia strongly suggests that GC could coordinately regulate skeletal muscle and hepatic metabolisms during cancer cachexia. Surprisingly, how GC could generate a functional metabolic coupling between skeletal muscle and liver during cancer cachexia remains unsolved. And yet, cancer cachexia is associated with an increase in circulating GC level in cancer cachectic patients [26–28] as well as in mice in experimental models of cancer cachexia [29–36]. Deciphering the GC-mediated regulation of skeletal muscle and liver metabolisms during cancer cachexia would be therefore important for the understanding of the systemic mechanisms involved in cancer cachexia but also for the management of cancer cachexia itself. Using a combination of *in vivo* physiological, molecular, and biochemical

approaches, we aimed to investigate the role of the HPA axis and GC on skeletal muscle and liver during cancer cachexia.

We identified GC as important determinant of cancer cachexia in the *Apc*$^{Min/+}$ (*Apc*) mouse model of intestinal cancer [37,38]. We showed that cancer cachexia elicited a hepatic metabolism reprogramming in favor of an increase in gluconeogenesis, an alteration of the urea cycle, a decrease in ketogenesis, and a decrease in lipid metabolism. We identified a GC-dependent transcriptional response both in skeletal muscle and liver of advanced cachectic mice that was completely inhibited when cachexia was blocked by myostatin (*Mstn*) gene invalidation. Our findings uncover a new role for GC in promoting skeletal muscle atrophy and hepatic metabolic reprogramming during cancer cachexia and suggest a strong metabolic relationship between skeletal muscle and liver during cancer cachexia under the control of the HPA axis.

Methods

LEAD CONTACT AND MATERIALS AVAILABILITY

Further information and requests for resources and reagents should be directed to and will be fulfilled by the Lead Contact, Damien Freyssenet (damien.freyssenet@univ-st-etienne.fr). This study did not generate new unique reagents.

EXPERIMENTAL MODELS

All animal studies were conducted in accordance with the European Community guidelines for the care and use of laboratory animals for scientific purposes, and after the authorization of the Ministère français de l'Enseignement Supérieur, de la Recherche et de l'Innovation and the Comité d'Ethique en Expérimentation Animale de la Loire (CEEAL-UJM-98, Université Jean Monnet, N° CU13N6). Male mice under the C57BL/6J genetic background were co-housed with at least one to three other mice in filter-top cages with bedding (spruce wood granulate+shavings) and nest building enrichment in a temperature-controlled (20-24°C) conventional animal facility with 12-hour light/dark cycles. Animals had free access to environmental enrichment, food, and water. Mice were checked daily by facility technicians for signs of distress and bedding changes occurred every week. Mice showing signs of distress including sores, weight loss greater than 20% of starting body weight, and frank rectal bleeding were removed from the study. No formal randomization was performed for mouse studies. Mice were used as they became available and paired with littermate controls.

Apc male mice [37,38] were purchased from the Jackson Laboratory, then breed and reproduced in the animal facility. Constitutive *Mstn* knock-out (KO) mice have been described [39] and were a gift from Anne Bonnieu (Montpellier University, France). Briefly, the third exon of the

Mstn gene flanked with a pair of loxP sites has been deleted by transiently expressed Cre recombinase at the zygote stage [39]. *Apc*$^{Min/+}$/Mstn$^{-/-}$ (ApcKO) mice were generated as previously described [40]. Briefly, *Apc* male mice were first mated to KO females. *Apc* male mice heterozygous for the *Mstn* gene from the progeny were then mated to KO females to obtain the ApcKO mice. All mice were identified after genotyping analysis.

The study consisted of two main experiments. We first used 13- (n=10) and 23-week-old (n=8) *Apc* mice. Age-matched WT littermates were used as controls (n=11 at 13 weeks and n=12 at 23 weeks). The response of *Apc* mice was also compared to that of dexamethasone-treated mice. Thirteen-week-old WT male mice received daily intraperitoneal injection of dexamethasone (3 mg/kg/day) (n= 10, WT-DEX mice) or placebo (n=10, WT-CTL mice) between 9 and 11 a.m for 5 days before tissue removal. In a second experiment, 23 week-old WT (n=10), *Apc* (n=8), KO (n=13), and ApcKo (n=10) mice used.

METHOD DETAILS

Tissue collection

Thirteen- and 23-week-old mice were anesthetized with an intraperitoneal injection of 90 mg/kg ketamine and 10 mg/kg xylazine. *Tibialis anterior*, *extensor digitorum longus*, *quadriceps*, *gastrocnemius* and *soleus* muscles, liver, adrenal glands, testis and hypothalamus were removed, weighed, rapidly frozen into liquid nitrogen and kept at -80°C until analysis. Small intestine and colon were carefully dissected, flushed with phosphate-buffered saline (PBS), opened longitudinally, and fixed in 10% paraformaldehyde before subsequent processing. For immunofluorescence microscopy, the *gastrocnemius* muscle was vertically embedded in Optimal Cutting Temperature compound (VWR), positioned on a piece of cork and frozen into isopentane chilled in liquid nitrogen, before to be stored at -80°C until analysis. Blood samples were removed from the tail under isoflurane (3%) anesthesia between 9 and 12 am in 13- and 23-week-old mice. Blood samples were left 30 minutes at room temperature and then centrifuged (10 min at 2,000 rpm, 4°C). The serum was removed and immediately frozen at -80°C until analysis.

Count of polyp number

Small and large intestines fixed in 10% paraformaldehyde were rinsed with PBS (3 × 12 hours) and stained with 0.1% methylene blue for 3 hours. The total number of polyps was then counted under a dissecting microscope.

Blood analyses

Hematocrit was measured with a Compur M1100 (Compur Werke, Munich, Germany) minicentrifuge on a 20 µL blood sample removed during tissue collection. Glycemia was

measured with a FreeStyle Optium Neo H glucometer (Abbott Diabetes Care, Witney, Oxfordshire, UK) and lactatemia with a Accutrend® Plus lactate analyzer (Roche Diagnostics GmbH, Mannheim, Germany), respectively, during tissue collection. Corticosterone concentration was measured with solid-phase enzyme-linked immunosorbent assay (MyBiosource, San Diego, USA) following the manufacturer's instructions. ß-hydroxybutyrate concentration was measured with colorimetric assay (APExBIO, Houston, USA) following the manufacturer's instructions.

Immunofluorescence analysis of myofiber cross-sectional area, image processing, and analysis

Gastrocnemius muscle transverse sections (thickness of 12 µm) were cut in a refrigerated (-20°C) microtome (Leica CM1950, Leica Biosystems, Nussloch, Germany). Muscles sections were blocked with a PBS solution containing 0.5% Tween 20, 0.1% Triton, 2% BSA, and 20% goat serum for 2 hours and then incubated overnight at 4°C with anti-mouse laminin antibody (Sigma-Aldrich, 1:200). Muscle sections were then rinsed for 10 minutes with PBS and incubated 1 hour at room temperature with a goat anti-rabbit secondary antibody Alexa Fluor 488 (Thermo Fisher Scientific, 1:500). Immunolabelled muscle sections were rinsed for 5 minutes with PBS, 5 minutes with a PBS-0.05% Tween 20 solution, and mounted with Vectashield Hard Set (Vector Laboratories). Muscle sections were examined and imaged using a Zeiss Axio Imager 2 Microscope at 5x-20x magnification. Images were stitched using the automated tile-scan tool to construct an image of the entire cross-section of the *gastrocnemius* muscle. Muscle cross-sectional area was automatically measured by ImageJ software using laminin immunostaining.

***In situ* force measurement**

A subset of 23-week-old WT (n=14) and *Apc* (n=8) mice was used for the measurement of twitch response, maximal isometric tetanic force and fatigue of *tibialis anterior* muscle by using 1300A Aurora system (Aurora Scientific, Ontario, Canada) following standardized operating procedures published by the treat-NMD network [41]. Briefly, the distal tendon of *tibialis anterior* muscle of anesthetized mice (90 mg/kg ketamine and 10 mg/kg xylazine) was attached to the force-position transducer apparatus while mice's knee was anchored and the sciatic nerve was stimulated. Force was recorded and analyzed with DMA software (Aurora Scientific, Ontario, Canada). After determination of the optimum muscle length (L_0), the response (maximum rate of force development to peak twitch ($+dP/dT_{max}$) and maximum rate of relaxation ($-dP/dT_{max}$)) to a twitch was analyzed. Maximum absolute isometric tetanic force (P_0) was determined as the maximal force recorded during stimulation of 0.5 s at 100 Hz. The maximum specific isometric tetanic (sP_0) was calculated as the maximum absolute isometric tetanic force divided by *tibialis anterior* muscle weight. Muscle fatigue was determined by recording force production during a 120-second stimulation protocol (50 Hz).

RNA isolation and RT-qPCR

Total RNA was extracted from *quadriceps* muscle, liver, adrenal glands, and hypothalamus using an RNA extraction kit (Macherey Nagel) following the manufacturer's instructions. RNA concentration and quality was determined (BioSpec-nano, Shimadzu) and 200 ng of RNA were reverse transcribed using Reverse Transcriptase Core kit (Eurogentec) following the manufacturer's instructions. qPCR was carried out on 2 µL of cDNA (1:80) using Takyon™ No Rox SYBR® MasterMix dTTP Blue (Eurogentec) and appropriate primers (Eurogentec) in a total reaction volume of 10 µL. Primer sequences and details are provided in Table S5. Fluorescence intensity was recorded using a CFX96 Real-Time PCR detection system (Bio-Rad). Data were analyzed using the ΔΔCT method of analysis. Reference genes (Ppia and Hprt for *quadriceps* muscle, Actb and Hprt for liver and adrenal glands, Actb and Tuba1 for hypothalamus) were used to normalize the expression levels of genes of interest.

Protein extraction and Western Blot analysis

Powdered *quadriceps* muscle and liver were homogenized (1:20 w:vol) in a RIPA buffer (Cell Signaling Technology) supplemented with protease and phosphatase inhibitors (Roche). Samples were centrifuged for 10 min at 12,000 g at 4°C. The protein concentration of the supernatant was determined using the DC protein assay (Bio-Rad), following the manufacturer's instructions. Thirty µg of protein (1:4 vol:vol) in reducing Laemmli buffer (Bio-Rad) were loaded into 8-16% TGX™ Stain Free SDS-PAGE precast gel (Bio-Rad) and electrophoresed at 200 V until migration front has reached the bottom of the gel. Proteins were then transferred onto a nitrocellulose membrane (Bio-Rad) using the Trans-Blot Turbo Transfer System (Bio-Rad). Total protein was visualized using stain-free technology and used for protein normalization. Membranes were blocked with a Tris Buffered Saline-0.1% Tween 20 (TBS-T) solution containing 5% non-fat dried milk for 2 hours at room temperature. Primary antibody (rpS6$^{Ser235/236}$, 1:1000; DDIT4, 1:1000; 4EBP1, 1:1000; PGC1A, 1:1000; CRTC2^{Ser171}, 1:1000; PCK1, 1:500; CREB^{Ser133}, 1:1000; CREB, 1:1000) was then applied overnight at room temperature in a 5% Bovine Serum Albumin BSA TBS-T solution. Primary antibody references are specified in the Key Resources Table. Membranes were then washed 3×5 min with a 0.1% TBS-T solution and incubated for 1 hour at room temperature with appropriate HRP-conjugated secondary antibody (Agilent, 1:2000) in a 5% non-fat dried milk TBS-T solution. After washes (3×5 min with a TBS-T solution), membranes were incubated with ECL (Bio-Rad) and imaged using ChemiDoc MP Imaging System (Bio-Rad). The protein band intensity was determined using Image Lab™ version 6.0. Stain-free technology was used for protein normalization.

Skeletal muscle and liver corticosterone content

Corticosterone content was measured from protein extracts with solid-phase enzyme-linked immunosorbent assay (MyBiosource, San Diego, USA) following the manufacturer's instructions.

QUANTIFICATION AND STATISTICAL ANALYSIS

All statistical analyses were performed using GraphPad Prism 7.0 (GraphPad Software, San Diego, CA). Grubb's test with alpha = 0.05% was systematically performed to identify potential outliers. Data were tested for normal distribution using Shapiro–Wilk test. Two-way analysis of variance (ANOVA) was used to determine differences among time (13 vs 23 weeks) and genotype (WT vs *Apc*) for polyp number, hematocrit, tissue masses, mean CSA, mRNA level in *quadriceps* muscle and liver, blood glucose, lactate, and ketone body concentration and for corticosterone concentration in serum, *quadriceps* muscle and liver. If a main effect and/or a time x genotype effect was significant, Sidak's multiple comparison test was used to identify the difference between means. A one-way ANOVA followed by Tukey's multiple comparison test in case of a significant genotype effect was used to determine differences between genotypes at 23 weeks (WT, *Apc*, KO vs ApcKO). Other data were analyzed with two-way ANOVA followed by Dunnett's and/or Sidak's multiple comparison tests (body mass evolution and muscle fatigue), a log-rank (Mantel-Cox) test (survival), Mann-Whitney or two-tailed unpaired t's test Welch's correction if necessary (P_0, protein level in muscle and liver, mRNA level in hypothalamus and adrenal glands, adrenal gland mass) and Pearson correlation. Gene expression overlapping significance, odds ratio, and Jaccard index were calculated with Fisher's exact test using GeneOverlap package (Li Shen and Mount Sinai (2019). GeneOverlap: Test and visualize gene overlaps. R package version 1.22.0. http://shenlab-sinai.github.io/shenlab-sinai/) in R (version 3.6.3). Statistical parameters are reported in the Figure legends. The significance level was set at $p<0.05$.

DATA AND CODE AVAILABILITY

Used software is available on the web sites linked in the Key Resources Table.

Results

***Apc* mice recapitulate the main features of cancer cachexia**

To investigate the mechanisms driving cancer cachexia, we used the *Apc* mouse, a mouse model of intestinal cancer that harbors a heterozygous mutation in the adenomatous polyposis coli (*APC*) gene [37,38]. Mutations in the *APC* gene in humans are responsible for familial adenomatous polyposis, an inherited colon cancer predisposition syndrome characterized by the formation of multiple colorectal adenomas, which can become malignant [42]. *Apc* mice experienced a progressive loss in body mass that began 15 weeks after birth reaching -9% of their peak body

mass at the age of 23 weeks (Figure 1A). Based on this analysis of body weight, we defined two different stages of cancer cachexia, a moderate stage of cachexia at 13 weeks and an advanced stage of cachexia at 23 weeks. *Apc* mice fed normally (Figure S1A) and had similar tibia length (Figure S1B) than wild-type (WT) age-matched littermates, suggesting that the lower body mass of *Apc* mice was not due to growth failure. *Apc* mice progressively developed polyposis (Figure 1B), as well as anemia (Figure 1C) due to intestinal bleeding. The median survival of *Apc* mice was 26 weeks (Figure 1D).

Marked reductions in adipose tissue store (Figure S1C) as well as in skeletal muscle compartment were also observed. Cachexia indifferently affected skeletal muscles with mixed contractile and metabolic phenotypes such as *quadriceps* (-24% at 13 weeks and -52% at 23 weeks) and *gastrocnemius* (-20% at 13 weeks and -53% at 23 weeks) muscles (Figure 1E) and those with a predominance of fast-twitch glycolytic fibers such as *extensor digitorum longus* (-24% at 13 weeks and -52% at 23 weeks) and *tibialis anterior* (-19% at 13 weeks and -49% at 23 weeks) muscles (Figure S1D). *Soleus* muscle, a slow-twitch oxidative postural muscle, which has not developed atrophy yet at 13 weeks (-8%), also became cachectic at 23 weeks (-30%) (Figure S1D). The reduction in *gastrocnemius* muscle mass was associated with a decrease in muscle fiber cross-sectional area both in 13- and 23-week-old *Apc* mice when compared to age-matched WT littermates (Figure 1F-H). Finally, skeletal muscle depletion significantly correlated with body mass loss (Figure S1E).

Functionally, the absolute maximal isometric tetanic force of *tibialis anterior* muscle (P_0) was significantly reduced in *Apc* mice with advanced cachexia compared to WT mice (Figure 1I). However, when normalized to muscle mass (sP_0), P_0 was not different, indicating that the loss in skeletal muscle mass strongly contributed to the loss of force (Figure 1J). The maximum rates of force development and relaxation were also reduced in the *tibialis anterior* muscle of 23-week-old *Apc* mice during a single twitch response (Figure S1F) suggesting that the decreased muscle force was also associated with an alteration of contractile properties. Finally, muscle fatigue was also increased in 23-week-old *Apc* mice compared to WT mice, as shown by the faster and greater decrease in muscle force during a fatigue protocol (Figure 1K).

Molecularly, the mRNA levels of *Trim63* (*MuRF1*) and *Fbxo32* (*MAFbx*) encoding E3-ubiquitin ligases involved in ubiquitin-proteasome dependent proteolysis were increased in the *quadriceps* muscle of 23-week-old *Apc* mice compared to WT mice (Figure 1L). This was associated with an increase in the protein content of the translational repressors, DDIT4 [43,44] and 4EBP1 [45,46] (Figure 1M). The fast migrating hypophosphorylated active form of 4EBP1 was also increased (Figure 1M). Finally, the active phosphorylated form of the translational activator, ribosomal protein S6, was decreased further indicating repression in translation initiation (Figure 1M).

Together with previous studies [47,48], these results indicate that skeletal muscle mass loss in *Apc* mice during cancer cachexia was due to an unbalance between protein synthesis and degradation.

Collectively, these results indicate that *Apc* mice recapitulate important features of cancer cachexia. Furthermore, this model attenuates the limits of large primary tumor burden models, including their extremely fast cachexia progression, their failure to form spontaneous tumors and to recapitulate the etiology of human cancers [49,50], and thus more closely mimics the progressive development of cancer cachexia in human patients.

Figure 1. *Apc* mice recapitulate the main features of cancer cachexia

(A) Relative changes in body mass in WT (n=9) and *Apc* (n=24) mice over a 23-week period after birth.

(B) Polyp number in small intestine and colon in WT and *Apc* mice at 13 (WT n=9; *Apc* n=7) and 23 (WT n=10; *Apc* n=6) weeks.

(C) Hematocrit in WT and *Apc* mice at 13 (WT n=11; *Apc* n=10) and 23 (WT n=7; *Apc* n=8) weeks.

(D) Kaplan-Meier survival curve of WT (n=31) and *Apc* (n=31) mice indicates that the half-life survival of *Apc* mice was 26 weeks.

(E) *Quadriceps* (left) and *gastrocnemius* (right) muscle mass of WT and *Apc* mice at 13 (WT n=11; *Apc* n=10) and 23 (WT n=12; *Apc* n=8) weeks.

(F) Representative laminin immunostaining of *gastrocnemius* muscle transversal sections of WT and *Apc* mice at 13 and 23 weeks. Scale bar, 100µm.

(G) Frequency distribution of fiber cross-sectional area in *gastrocnemius* muscle of WT and *Apc* mice at 13 (WT n=7; *Apc* n=6) and 23 (WT n=5; *Apc* n=4) weeks. 540 ± 247 fibers per muscle were counted. The lines represent the Gaussian regression curve fit.

(H) *Gastrocnemius* muscle mean myofiber cross-sectional area (CSA) of WT and *Apc* mice at 13 (WT n=7; *Apc* n=6) and 23 (WT n=5; *Apc* n=4) weeks. 540 ± 247 fibers per muscle were counted.

(I) Absolute maximal isometric tetanic force (P_0) of tibialis anterior muscle recorded at 100 Hz in 23-week-old WT (n=14) and *Apc* (n=8) mice.

(J) Specific maximal isometric tetanic force (sP_0) of *tibialis anterior* muscle recorded at 100 Hz in 23-week-old WT (n=14) and *Apc* (n=8) mice. Pearson correlation between *tibialis anterior* P_0 recorded at 100Hz and *tibialis anterior* muscle mass in 23-week-old WT (n=14) and *Apc* (n=8) mice.

(K) *Tibialis anterior* muscle force expressed as a percent of maximal initial force during a 120-sec fatigue protocol (50 Hz) in 23-week-old WT (n=12) and *Apc* (n=8) mice.

(L) RT-qPCR analysis of *MuRF1* and *MAFbx* mRNA level in *quadriceps* muscle of WT and *Apc* mice at 13 (WT n=11; *Apc* n=9) and 23 (WT n=12; *Apc* n=7) weeks.

(M) Representative immunoblot (left) of phosphorylated ribosomal protein S6 ($rpS6^{Ser235/236)}$, DDIT4 protein, and 4EBP1 protein content in *quadriceps* muscle of WT and *Apc* mice at 13 and 23 weeks. The hypophosphorylated active form of 4EBP1 migrates faster than the hyperphosphorylated inactive form. Quantitative analysis (right) of $rpS6^{Ser235/236}$, and 4EBP1 protein content in *quadriceps* muscle of WT and *Apc* mice at 13 (WT n=8; *Apc* n=8) and 23 (WT n=8; *Apc* n=8) weeks. DDIT4 was not quantified as expression level in WT mice was undetectable.

Data are represented as mean ± SEM. (A, B, C, E, H, K, and L) data were analyzed by a two-way ANOVA; #: significant difference with 13 weeks (Dunnett's multiple comparison test); *: significant difference between WT and *Apc* (Sidak's multiple comparison test). (D) data were analyzed by a log-rank (Mantel-Cox) test. (I, J, M) data were analyzed by a two-tailed unpaired t-test with Welch's correction when necessary. (J) Data were analyzed with a Pearson correlation test. *, #p <0.05, **p < 0.01, ***p < 0.001 and ****p < 0.0001.

See also Figure S1.

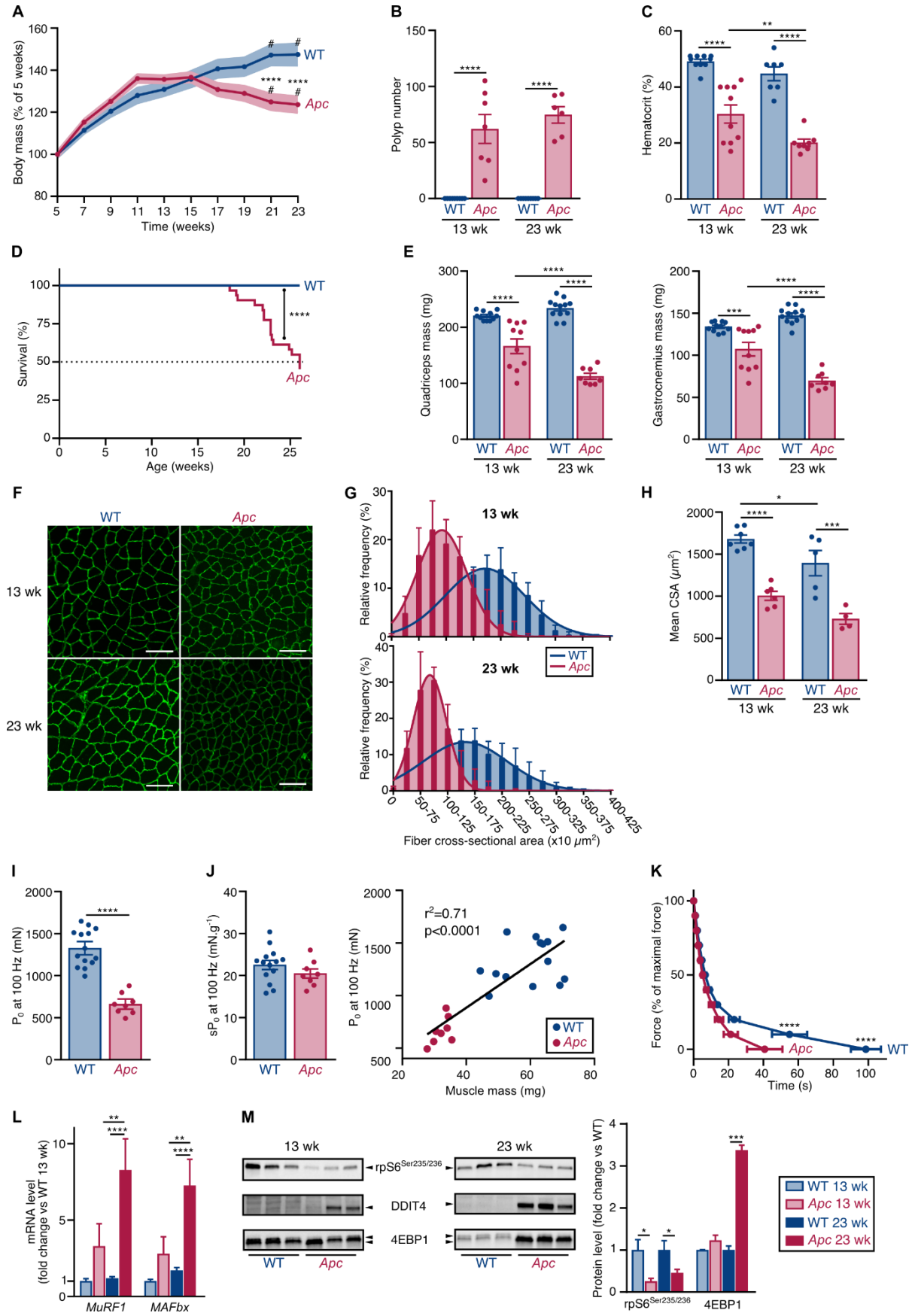
A
Body mass (% of 5 weeks)
Time (weeks)
WT
Apc
B
Polyp number
C
Hematocrit (%)
D
Survival (%)
Age (weeks)
E
Quadriceps mass (mg)
Gastrocnemius mass (mg)
13 wk
23 wk
F
WT
Apc
G
Relative frequency (%)
Fiber cross-sectional area (x10 μm²)
H
Mean CSA (μm²)
I
P0 at 100 Hz (mN)
J
sP0 at 100 Hz (mN.g-1)
r²=0.71
p<0.0001
Muscle mass (mg)
K
Force (% of maximal force)
Time (s)
L
mRNA level (fold change vs WT 13 wk)
MuRF1
MAFbx
M
rpS6Ser235/236
DDIT4
4EBP1
Protein level (fold change vs WT)
WT 13 wk
Apc 13 wk
WT 23 wk
Apc 23 wk

Advanced cancer cachexia induces rewiring of hepatic metabolism

To assess changes in liver metabolism, we first looked at gluconeogenesis. A hallmark of increased gluconeogenesis under sustained catabolic conditions, such as prolonged fasting, is a decrease in blood glucose concentration [51–53], which indicates a sustained hepatic glucose production that does not fulfill the energetic need of whole-body metabolism. During cancer cachexia, blood glucose concentration was significantly decreased in 23-week-old *Apc* mice (Figure 2A). Similar results were also reported in Lewis lung carcinoma tumor-bearing (LLC) mice, a fast tumor burden model of cancer cachexia (Figure S2A). Expression of gluconeogenic genes is classically activated by phosphorylation at Ser133 of the CREB transcription factor in response to glucagon stimulation [54,55]. Here, the active phosphorylated form of CREB was decreased in the liver of *Apc* mice and phosphorylation of the CREB-regulated transcription coactivator 2 (CRTC2) remained unchanged (Figure 2B), suggesting that this route was not activated in advanced cachectic mice. However, the expression of gluconeogenic genes is also activated by the coordinate interplay of the transcriptional co-activator PPARGC1A (PGC1A) and the transcription factor FOXO1 [56–58]. The hepatic mRNA levels of *Pgc1a* and *Foxo1*, but also *Foxo3*, were increased in 23-week-old *Apc* mice (Figure 2C-D), suggesting an activation of a PGC1A/FOXO1 axis in advanced cachectic mice. Accordingly, transcript levels of their target genes encoding key gluconeogenesis enzymes, *Pcx* and *Pck1*, were also increased in advanced cachectic mice (Figure 2C-D). The increased expression of *Pgc1a* and *Pck1* was also confirmed at the protein level (Figure 2B). Conversely, the mRNA level of *Mlxipl* (*ChREBP*), a transcription factor that drives the expression of glycolytic genes [59,60], as well as that of its target genes [61] such as the glucose transporter *Slc2a2* and glycolytic enzymes *Pklr* and *Gk* were decreased in 23-week-old *Apc* mice (Figure 2C-D). A similar result was observed for *Gpd2*, a component of the glycerol phosphate shuttle that boots glucose oxidation (Figure 2C-D). Hepatic gluconeogenesis can be fueled by lactate derived from tumoral glycolytic metabolism [18,62]. Accordingly, the blood lactate concentration was increased in 23-week-old *Apc* mice (Figure 2E), suggesting an increased provision of lactate by tumor cells. This observation was also reproduced in LLC tumor-bearing mice (Figure S2B).

This rewiring of hepatic metabolism was not limited to glucose metabolism. Amine groups originating from amino acid deamination must be recycled in the form of urea via the urea cycle to avoid the metabolic toxic effect of ammonia accumulation [63]. The expression of the enzymes of the urea cycle was also profoundly affected (Figure 2F-G). The liver also produces other energetic substrates such as ketone bodies from acetyl-CoA during excessive oxidation of non-esterified fatty acids. Serum ß-hydroxybutyrate concentration, the most prevalent circulating ketone body, was decreased in 23-week-old *Apc* mice (Figure 2H). The transcript level of *Ppara*, a master transcriptional regulator of ketogenic genes [51,64], as well as that of ketogenesis rate-

limiting enzymes *Hmgcs2* and *Bdh1*, were also decreased in 23-week-old *Apc* mice (Figure 2I). Accordingly, transcript level encoding proteins involved in lipolysis and fatty oxidation were decreased in *Apc* mice (Figure 2J). Finally, markers of lipogenesis were also consistently decreased in the liver of advanced cachectic mice (Figure 2K).

Collectively, these data indicate that the liver experiences a major metabolic rewiring during cancer cachexia that affects glucose, nitrogen, ketone body, and lipid metabolisms.

Figure 2. Cancer cachexia elicits a transcriptional rewiring of hepatic metabolism in *Apc* mice

(A) Blood glucose concentration in WT and *Apc* mice at 13 (WT n=9; *Apc* n=12) and 23 (WT n=12; *Apc* n=12) weeks.

(B) Representative immunoblot (left) and quantitative analysis (right) of PGC1A, phosphorylated CRTC2 (CRTC2^{Ser171}), PCK1, phosphorylated CREB (CREB^{Ser133}), and total CREB protein content in *quadriceps* muscle of WT and *Apc* mice at 13 (WT n=8; *Apc* n=8) and 23 (WT n=8; *Apc* n=8) weeks.

(C) Transcript level of gluconeogenic (left) and glycolytic (right) genes in liver of WT and *Apc* mice at 13 (WT n=11; *Apc* n=10) and 23 (WT n=12; *Apc* n=7) weeks.

(D) Schematic representation of glycolysis and gluconeogenesis. Indicated in red, grey, and green are the transcripts encoding enzymes that were up-, not- or down-regulated, respectively.

(E) Blood lactate concentration in WT and *Apc* mice at 13 (WT n=9; *Apc* n=12) and 23 (WT n=12; *Apc* n=12) weeks.

(F) Transcript level of genes encoding urea cycle enzymes in liver of WT and *Apc* mice at 13 (WT n=11; *Apc* n=10) and 23 (WT n=12; *Apc* n=7) weeks.

(G) Schematic representation of the urea cycle. Indicated in red, grey, and green are the transcripts encoding enzymes that were up-, not- or down-regulated, respectively.

(H) Serum ß-hydroxybutyrate concentration in WT and *Apc* mice at 13 (WT n=10; *Apc* n=13) and 23 (WT n=9; *Apc* n=12) weeks.

(I) Transcript level of ketogenic genes in the liver of WT and *Apc* mice at 13 (WT n=11; *Apc* n=10) and 23 (WT n=12; *Apc* n=7) weeks. Schematic representation of ketogenesis in the liver. Indicated in green are the transcripts encoding enzymes that were up-regulated.

(J) Transcript level of genes encoding lipolytic and fatty oxidation enzymes in liver of WT and *Apc* mice at 13 (WT n=11; *Apc* n=10) and 23 (WT n=12; *Apc* n=7) weeks. Schematic representation of triglyceride hydrolysis and fatty acid oxidation. Indicated in red, grey, and green are the transcripts encoding enzymes that were up-, not- or down-regulated, respectively.

(K) Transcript level of genes encoding lipogenic enzymes in the liver of WT and *Apc* mice at 13 (WT n=11; *Apc* n=10) and 23 (WT n=12; *Apc* n=7) weeks. Schematic representation of lipogenesis. Indicated in green are the transcripts encoding enzymes that were up-regulated.

Data are represented as mean ± SEM. (A, C, E, F, H, I, J, and K) data were analyzed by two-way ANOVA. (B) data were analyzed by a two-tailed unpaired t-test with Welch's correction when necessary. * represents a significant difference after Sidak's multiple comparison test and § represents a main genotype effect. * or §p <0.05, ** or §§p < 0.01, ***p < 0.001, or ****p < 0.0001.

See also Figure S2.

DG, diglyceride; DHAP, dihydroxyacetone phosphate; F1,6 BP, fructose 1,6 bisphosphate; F6P, fructose 6 phosphate; FFA, free fatty acid; G6P, glucose 6 phosphate; GA3P, glyceraldehyde 3 phopshate; MG, monoglyceride; MUFA, monounsaturated fatty acid; OAA, oxaloacetic acid; PEP, phosphoenolpyruvate; TG, triglyceride

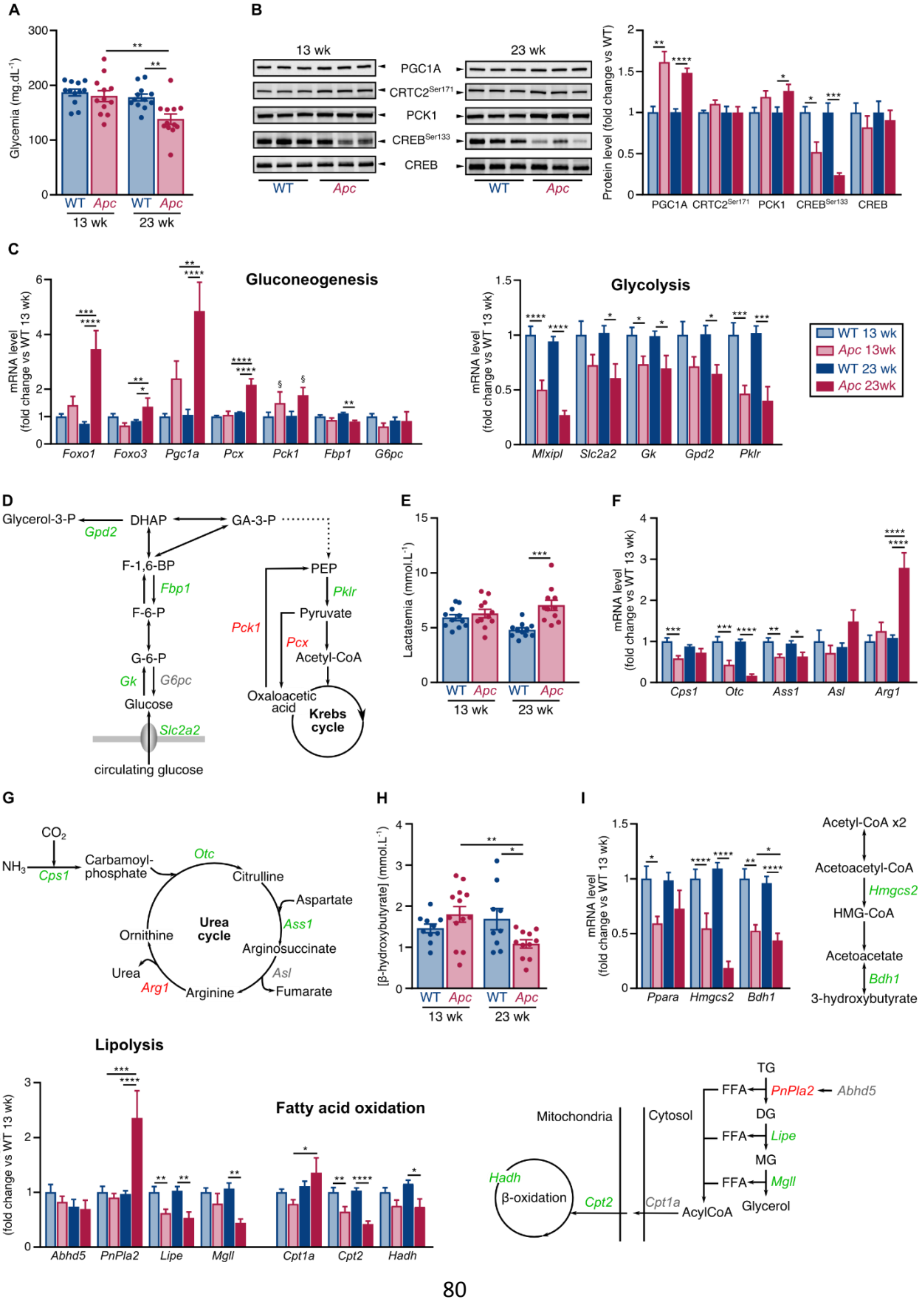
A
Glycemia (mg.dL-1)
WT Apc WT Apc
13 wk 23 wk
B
13 wk
23 wk
PGC1A
CRTC2Ser171
PCK1
CREBSer133
CREB
WT Apc WT Apc
Protein level (fold change vs WT)
PGC1A CRTC2Ser171 PCK1 CREBSer133 CREB
C
Gluconeogenesis
mRNA level (fold change vs WT 13 wk)
Foxo1 Foxo3 Pgc1a Pcx Pck1 Fbp1 G6pc
Glycolysis
Mlxipl Slc2a2 Gk Gpd2 Pklr
WT 13 wk
Apc 13wk
WT 23 wk
Apc 23wk
D
Glycerol-3-P
Gpd2
DHAP
GA-3-P
F-1,6-BP
Fbp1
F-6-P
G-6-P
Gk
G6pc
Glucose
Slc2a2
circulating glucose
PEP
Pklr
Pyruvate
Pck1
Pcx
Acetyl-CoA
Oxaloacetic acid
Krebs cycle
E
Lactatemia (mmol.L-1)
WT Apc WT Apc
13 wk 23 wk
F
mRNA level (fold change vs WT 13 wk)
Cps1 Otc Ass1 Asl Arg1
G
CO2
NH3
Cps1
Carbamoyl-phosphate
Otc
Citrulline
Aspartate
Ass1
Arginosuccinate
Asl
Fumarate
Arginine
Arg1
Urea
Ornithine
Urea cycle
H
[β-hydroxybutyrate] (mmol.L-1)
WT Apc WT Apc
13 wk 23 wk
I
mRNA level (fold change vs WT 13 wk)
Ppara Hmgcs2 Bdh1
Acetyl-CoA x2
Acetoacetyl-CoA
Hmgcs2
HMG-CoA
Acetoacetate
Bdh1
3-hydroxybutyrate
J
Lipolysis
mRNA level (fold change vs WT 13 wk)
Abhd5 PnPla2 Lipe Mgll
Fatty acid oxidation
Cpt1a Cpt2 Hadh
TG
FFA
PnPla2
Abhd5
DG
FFA
Lipe
MG
FFA
Mgll
Glycerol
Mitochondria
Cytosol
Hadh
β-oxidation
Cpt2
Cpt1a
AcylCoA

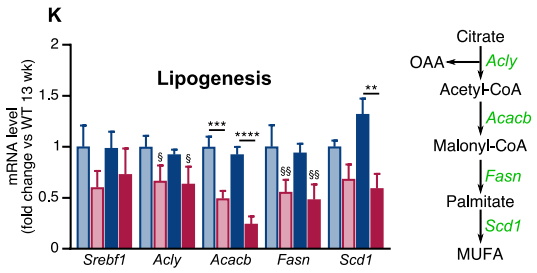

Advanced cancer cachexia activates the hypothalamic-pituitary-adrenal axis

We then asked whether a common molecular mechanism could coordinate these molecular adaptations in skeletal muscle and liver during advanced cancer cachexia. GC are steroids secreted by the adrenal cortex under the control of the HPA axis. Hypothalamic mRNA level of corticotropin-releasing hormone (*Crh*) that activates the pituitary secretion of adrenocorticotropic hormone (ACTH), was increased in 23-week-old *Apc* mice (Figure 3A). Hypothalamic expression of *Fkbp5*, indicative of the hyperactive function of the hypothalamus [65], was also increased (Figure 3A). ACTH then stimulates the release of GC by adrenal glands. The adrenal glands were hyperactivated as indicated by their increased mass [66] in 23-week-old *Apc* mice (Figure 3B), confirming previous studies in rat models of cancer cachexia [67–69] and cachectic cancer patients [70]. The mRNA levels of *Mc2r* (ACTH receptor), as well as those of *Cyp21a1* and *Cyp11b1*, which encode enzymes involved in adrenal corticosterone biosynthesis [71], were also increased in 23-week-old *Apc* mice (Figure 3C). Furthermore, hepatic transcript levels of GC detoxifying enzymes such as *Papss2*, *Srd5a1*, *Ugt2b35*, and *Ugt2b36* [72] were all decreased in 23-week-old *Apc* mice compared to WT mice (Figure 3D). In agreement with all these data, the circulating level of corticosterone, the predominant GC in mice, was higher in both 13- and 23-week-old *Apc* mice than in age-matched WT littermates (Figure 3E). Of note, circulating corticosterone level positively correlated with *Crh* mRNA level ($p=0.045$, $r^2=0.51$) (Figure 3F) further illustrating activation of the HPA axis. Finally, and in agreement with a hypercortisolemia state [73], testis mass was significantly decreased in 23-week-old *Apc* mice (Figure 3G). Together, these data indicate that activation of the HPA axis and a lower capacity of hepatic GC detoxification contribute to increasing the circulating corticosterone level during cancer cachexia.

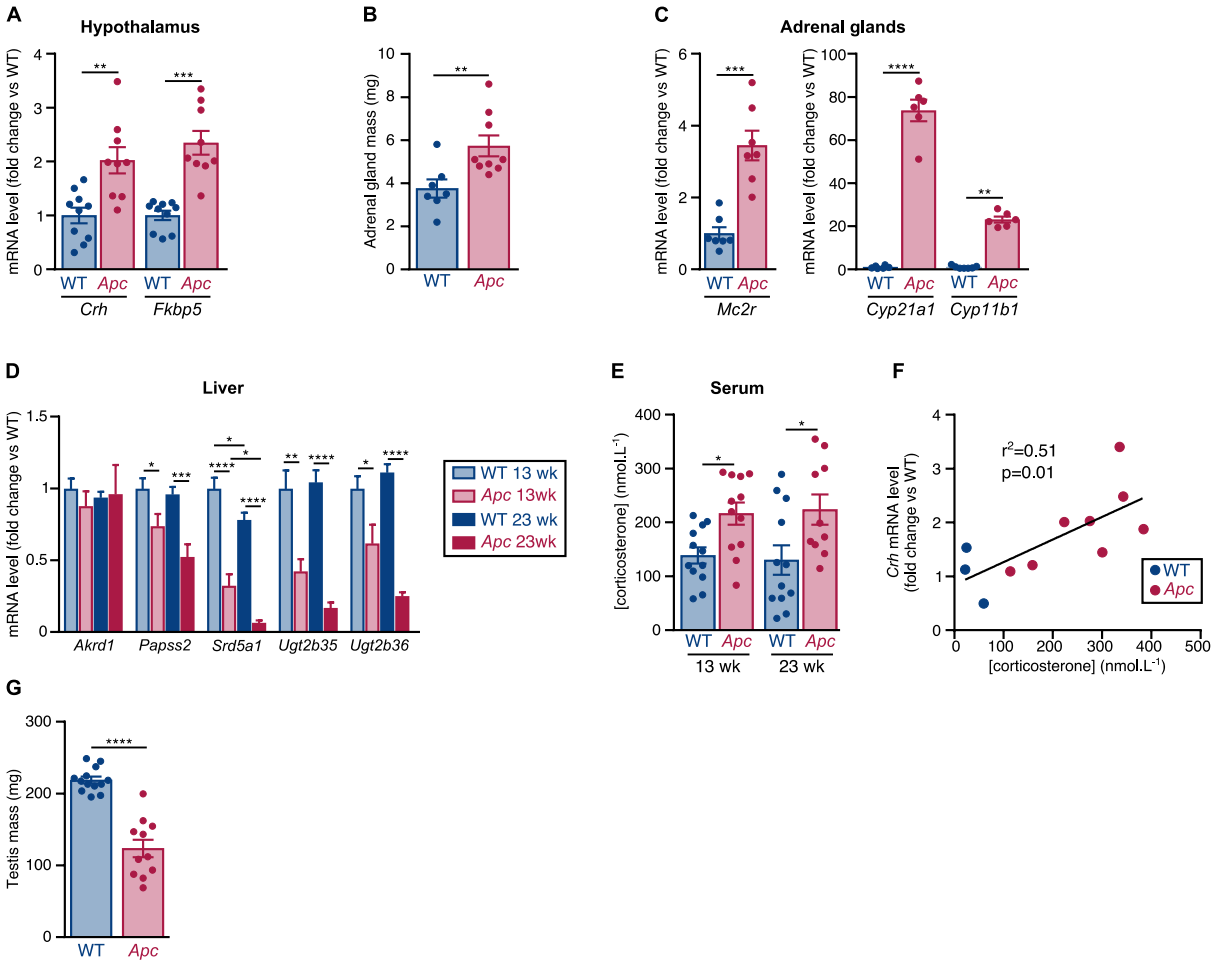

Figure 3. The hypothalamic-pituitary-adrenal axis is activated during cancer cachexia

(A) RT-qPCR analysis of *Crh* and *Fkbp5* mRNA levels in hypothalamus in 23-week-old WT (n=10) and *Apc* (n=9) mice.

(B) Mass of adrenal glands in 23-week-old WT (n=7) and *Apc* (n=9) mice.

(C) RT-qPCR analysis of *Mc2r*, *Cyp11b1*, and *Cyp21a1* mRNA levels in adrenal glands of 23-week-old WT (n=7) and *Apc* (n=7) mice.

(D) RT-qPCR analysis of transcripts encoding steroid detoxification enzymes in the liver of WT and *Apc* mice at 13 (WT n=11; *Apc* n=10) and 23 (WT n=12; *Apc* n=7) weeks.

(E) Serum corticosterone concentration in WT and *Apc* mice at 13 (WT n=12; *Apc* n=12) and 23 (WT n=12; *Apc* n=10) weeks.

(F) Pearson correlation between serum corticosterone concentration and Crh transcript level in 13- and 23-week-old WT (n=3) and *Apc* (n=8) mice.

(G) Testis mass in 23-week-old WT (n=13) and *Apc* (n=11) mice.

Data are represented as means ± SEM. (A, B, C, G) data were analyzed by Mann-Whitney test or two-tailed unpaired t-test with Welch's correction when necessary. (D, E) data were analyzed by two-way ANOVA. * represents a significant difference after Sidak's multiple comparison test. (F) data were analyzed with a Pearson correlation test. *p <0.05, **p < 0.01, ***p < 0.001, or ****p < 0.0001.

A glucocorticoid-dependent transcriptional response occurs in the *quadriceps* muscle and liver of *Apc* mice during cancer cachexia

To identify the existence of a GC-dependent transcriptional response in skeletal muscle of Apc mice, we reasoned that the transcriptional signature of genes that classically respond to the administration of a synthetic GC such as dexamethasone should be also significantly reproduced in skeletal muscle of Apc mice. Administration of dexamethasone triggers a typical transcriptional response in skeletal muscle characterized by an increase in the expression of Bnip3 [53], *Ddit4* [22,53], *Fkbp5* [22,53], *Klf15* [22,53], *Foxo1*[22,23,53], *Foxo3* [22,53], *MuRF1*[22,23,53], *MAFbx*, [22,23,53], *Mstn* [22,74], *4ebp1* [23], *Cebpd* [75], *Mt1* [76], *Mt2* [23,76], and *Lc3b* [53], whereas others transcripts such as *Nr3c1* (GC receptor) [22,53], *Foxo4* [22,53], and *Bcat2* [22] remained unchanged. This transcriptional response thus signs the GC/GC receptor transcriptional function in skeletal muscle. In the present study, intraperitoneal administration of dexamethasone for 5 days in WT mice reproduced this transcriptomic signature (Figure 4A, Table S1). We also identified *Slc39a14* as a GC-responsive gene. Skeletal muscle from 23-week-old *Apc* mice also displayed an increase in the expression of these GC-responsive genes as evidenced by the marked increase in the transcript level of *Cebpd* (x9), *Ddit4* (x23), *4ebp1* (x7), *Fkbp5* (x6), *Foxo1* (x7), *Foxo3* (x3), *Klf15* (x4), *MAFbx* (x4), *Mt1* (x56), *Mt2* (x83), *MuRF1* (x7), and *Slc39a14* (x8) (Figure 4A, Table S1). DDIT4 and 4EBP1 were also increased at the protein level (Figure 1M). Overall, the transcriptional signature in skeletal muscle of dexamethasone-treated mice was significantly reproduced in 23-week-old *Apc* mice (Figure 4B). Out of 15 genes differentially expressed in dexamethasone-treated mice, 13 behaved similarly in 23-week-old *Apc* mice. Importantly, this transcriptional response was partly reproduced (insignificant) in 13-week-old *Apc* mice (p=0.96, Figure 4A), indicating that the response was specifically associated with advanced cancer cachexia. To determine whether this signature was specific to *Apc* mice or common to other models of cancer cachexia, we also performed our analysis on LLC-tumor bearing mice. The transcriptional response of *Apc* mice was also reproduced in skeletal muscle of LLC mice (Figure S2C). Collectively, these data suggest that a GC-dependent transcriptional response is a common signature of advanced cancer cachexia in mice. In multiple tissues, including skeletal muscle, conversion of the inactive 11-dehydrocorticosterone to the active form corticosterone is performed by HSD11B1 [77] and requires NADPH provided by the enzyme H6PD. Although the *H6pd* transcript level and *Nr3c1* remained unchanged, the *Hsd11b1* mRNA level was increased in *quadriceps* muscle of advanced cachexic *Apc* mice (Figure 4C) suggesting an increased conversion of inactive 11-dehydrocorticosterone into active corticosterone in skeletal muscle. This was further corroborated by an increased corticosterone content in the *quadriceps* muscle of 23-week-old *Apc* mice (Figure 4D). Of note, skeletal muscle corticosterone content negatively correlated with body mass (Figure 4E).

To determine if the transcriptional response observed in the liver of Apc mice (Figure 2) signed a GC action, we determine the expression levels of these genes in the liver of dexamethasone-treated mice. Additionally, GC-responsive (*Mt1*, *Mt2*, *Slc39a14*, *Ddit4*, *Fkbp5*, and *Cebpd*) and non-responsive (*Klf15*, *Foxo4*) genes identified in skeletal muscle were also selected and analyzed by RT-qPCR analysis. When carried out, this analysis indicated that 19 out of 27 genes differentially expressed in dexamethasone-treated mice were also similarly regulated in 23-week-old *Apc* mice (Figure 4F, see also Table S2). The overlap of gene transcription profiles between dexamethasone-treated WT mice and 23 week-old *Apc* mice was significant both for up- ($p=2\times10^{-4}$) and down-regulated ($p=3.7\times10^{-3}$) transcripts (Figure 4G). Of note, only 7 genes in 13-week-old *Apc* mice were similarly expressed in dexamethasone-treated mice (p=0.61 for down-regulated genes and p=0.064 for up-regulated genes) (Figure 4F), further emphasizing that the GC-dependent transcriptional response progressively takes place during the development of cancer cachexia. As observed for skeletal muscle, liver corticosterone content was also increased in 23-week-old *Apc* mice when compared to age-matched WT mice (Figure 4H). Collectively, these data demonstrate that a GC-dependent transcriptional response occurs in skeletal muscle and liver during advanced cancer cachexia in *Apc* mice.

Figure 4. A glucocorticoid-dependent transcriptional response occurs in *quadriceps* muscle and liver of *Apc* mice during cancer cachexia

(A) Heatmap displaying the glucocorticoid-dependent transcriptional signature in *quadriceps* muscle of *Apc* mice at 13 weeks (WT n=11, *Apc*=10) and 23 weeks (WT n=12, *Apc*=7) and dexamethasone-treated WT mice (WT-CTL n=10; WT-DEX n=10). mRNA level was determined by RT-qPCR analysis and expressed as Log_2(fold change vs age-paired WT mice). For Log_2(fold change)>5, cells are set by default in the most intense red.

(B) Venn diagram of differentially expressed genes in quadriceps muscle of 23-week-old *Apc* (WT n=12; *Apc* n=7) and WT-DEX (WT n=10; WT-DEX n=10) mice.

(C) RT-qPCR analysis of *H6pd*, *Hsd11b1* and *Nr3c1* mRNA level in *quadriceps* muscle of WT and *Apc* mice at 13 (WT n=11; *Apc* n=10) and 23 (WT n=12; *Apc* n=7) weeks.

(D) Corticosterone level in the *quadriceps* muscle in WT and *Apc* mice at 13 (WT n=11; *Apc* n=10) and 23 (WT n=11; *Apc* n=7) weeks (left).

(E) Pearson correlation between corticosterone level in *quadriceps* muscle and body mass in WT and *Apc* mice at 13 (WT n=11; *Apc* n=10) and 23 (WT n=11; *Apc* n=7) weeks.

(F) Heatmap displaying the glucocorticoid-dependent transcriptional signature in the liver of *Apc* mice at 13 (WT n=11, *Apc*=10) and 23 weeks (WT n=17, *Apc*=7) and dexamethasone-treated WT mice (WT n=10; WT-DEX n=10). mRNA level was measured by RT-qPCR and expressed in Log_2(fold change vs age-paired WT mice). For Log_2(fold change)>6, cells are set by default in the most intense red.

(G) Venn diagram of differentially expressed up-regulated (left) and down-regulated (right) genes in liver of 23-week-old *Apc* (WT n=12; *Apc* n=7) and WT-DEX (WT n=10; WT-DEX n=10) mice.

(H) Corticosterone level in liver of WT and *Apc* mice at 13 (WT n=11; *Apc* n=10) and 23 (WT n=12; *Apc* n=7) weeks.

Data are represented as mean ± SEM. (B and G), differentially expressed genes were identified after Mann-Whitney test or two-tailed unpaired t-test with Welch's correction if necessary. Overlapping significance, odds ratio, and Jaccard index were calculated with Fisher's exact test. (C, D, H) data were analyzed by two-way ANOVA. * represents a significant difference after Sidak's multiple comparison test and + represents a main genotype effect. (E) data were analyzed with a Pearson correlation test. * or +p <0.05, **p < 0.01, ***p < 0.001, or ****p < 0.0001.

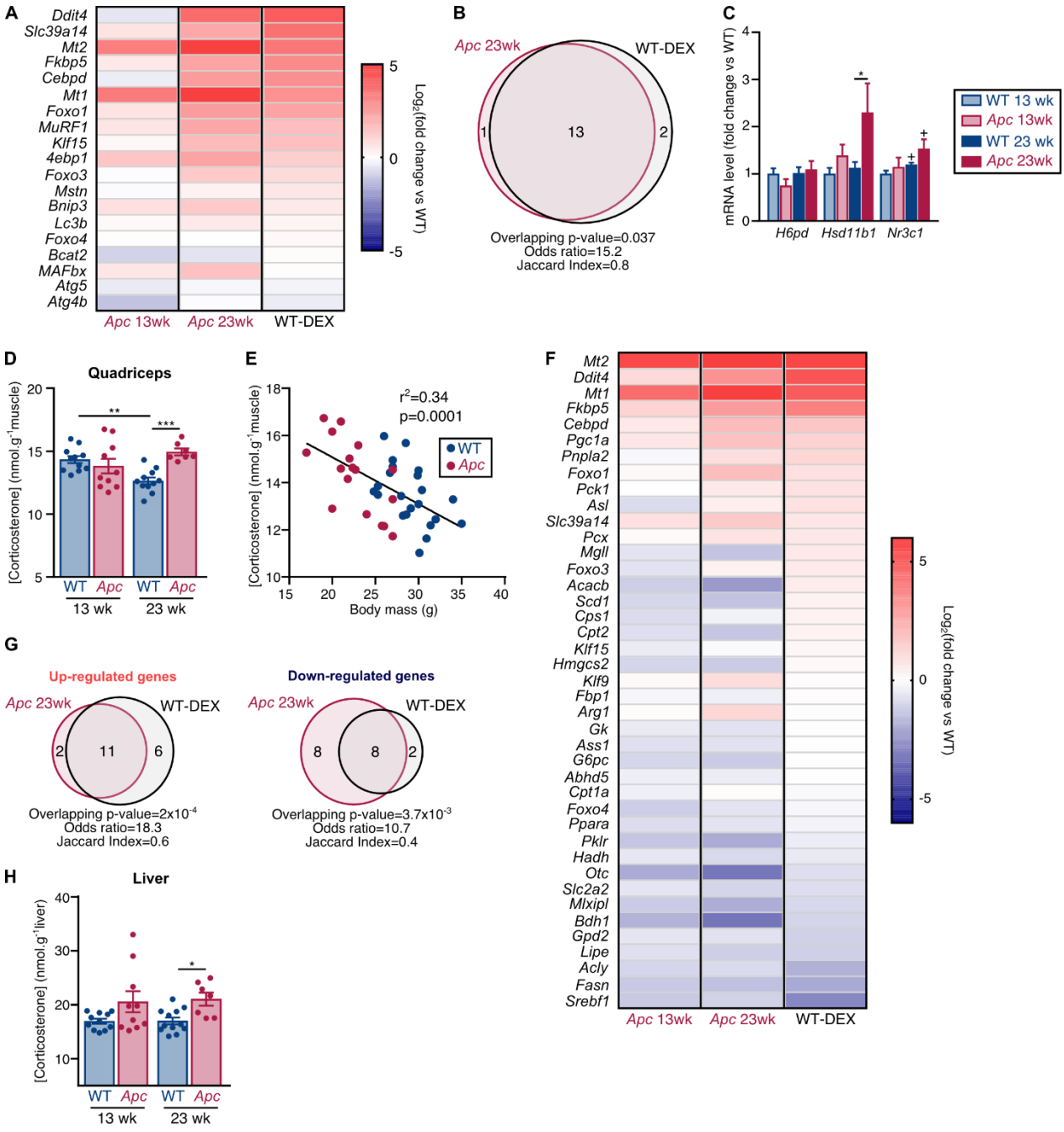
A
Ddit4
Slc39a14
Mt2
Fkbp5
Cebpd
Mt1
Foxo1
MuRF1
Klf15
4ebp1
Foxo3
Mstn
Bnip3
Lc3b
Foxo4
Bcat2
MAFbx
Atg5
Atg4b
Apc 13wk
Apc 23wk
WT-DEX
5
0
-5
Log2(fold change vs WT)
B
Apc 23wk
WT-DEX
1
13
2
Overlapping p-value=0.037
Odds ratio=15.2
Jaccard Index=0.8
C
mRNA level (fold change vs WT)
H6pd
Hsd11b1
Nr3c1
WT 13 wk
Apc 13wk
WT 23 wk
Apc 23wk
D
Quadriceps
[Corticosterone] (nmol.g-1muscle)
WT
Apc
13 wk
23 wk
E
r2=0.34
p=0.0001
[Corticosterone] (nmol.g-1muscle)
Body mass (g)
F
Mt2
Ddit4
Mt1
Fkbp5
Cebpd
Pgc1a
Pnpla2
Foxo1
Pck1
Asl
Slc39a14
Pcx
Mgll
Foxo3
Acacb
Scd1
Cps1
Cpt2
Klf15
Hmgcs2
Klf9
Fbp1
Arg1
Gk
Ass1
G6pc
Abhd5
Cpt1a
Foxo4
Ppara
Pklr
Hadh
Otc
Slc2a2
Mlxipl
Bdh1
Gpd2
Lipe
Acly
Fasn
Srebf1
Apc 13wk
Apc 23wk
WT-DEX
Log2(fold change vs WT)
G
Up-regulated genes
Apc 23wk
WT-DEX
2
11
6
Overlapping p-value=2x10-4
Odds ratio=18.3
Jaccard Index=0.6
Down-regulated genes
Apc 23wk
WT-DEX
8
8
2
Overlapping p-value=3.7x10-3
Odds ratio=10.7
Jaccard Index=0.4
H
Liver
[Corticosterone] (nmol.g-1liver)
WT
Apc
13 wk
23 wk

Prevention of cancer cachexia by myostatin gene invalidation prevents hepatic metabolism transcriptional reprogramming in *Apc* mice and reduces corticosterone level

MSTN is a TGF-ß family member that functions as a master negative regulator of skeletal muscle mass during skeletal muscle development [78] and in adulthood [79,80]. In the present study, the *Mstn* mRNA level was negatively correlated with *quadriceps* muscle mass ($p=0.011$, $r^2=0.16$, Figure S3A) and positively correlated with circulating corticosterone level ($p=0.048$, $r^2=0.14$, Figure S3B), illustrating the regulatory function of myostatin in this situation. We, therefore, reasoned that inhibiting skeletal muscle wasting by *Mstn* gene invalidation would restore hepatic metabolic function together with a restoration of corticosterone levels. In this second experiment, we thus generated *Mstn* knockout (KO), *Apc* mice knockout for the *Mstn* gene (ApcKO mice), as well as a new set of 23-week-old WT and *Apc* mice. *Mstn* gene invalidation completely prevented body mass loss (Figure 5A), polyposis (Figure 5B), anemia (Figure 5C), and adipose tissue loss (Figure S3C) of ApcKO mice. The hypermuscular phenotype of KO mice was clearly evident as shown by the marked increase in skeletal muscle mass when compared to WT mice (Figure 5D and S3D). Furthermore, *Mstn* gene invalidation completely prevented skeletal muscle mass loss under the *Apc* genetic background. The mass of *quadriceps*, *gastrocnemius*, *soleus*, *tibialis anterior*, and *extensor digitorum longus* skeletal muscles (Figure 5D and S3D) remained unchanged in ApcKO mice compared to KO mice. Accordingly, *gastrocnemius* muscle fiber cross-sectional area that was markedly reduced in *Apc* mice remained unchanged in ApcKO mice compared to KO mice (Figure 5E-F). Molecularly, the increase in the mRNA level of the E3-ubiquitin ligases *MuRF1* and *MAFbx* observed in *Apc* mice was completely prevented in the *quadriceps* muscle of ApcKO mice (Figure 5G). Similarly, this was also associated with a restoration of DDIT4 and total and hypophosphorylated active forms of 4EBP1 to control levels (Figure 5H). Therefore, *Mstn* gene invalidation in ApcKO mice completely prevented cancer cachexia by reestablishing the balance between protein synthesis and degradation.

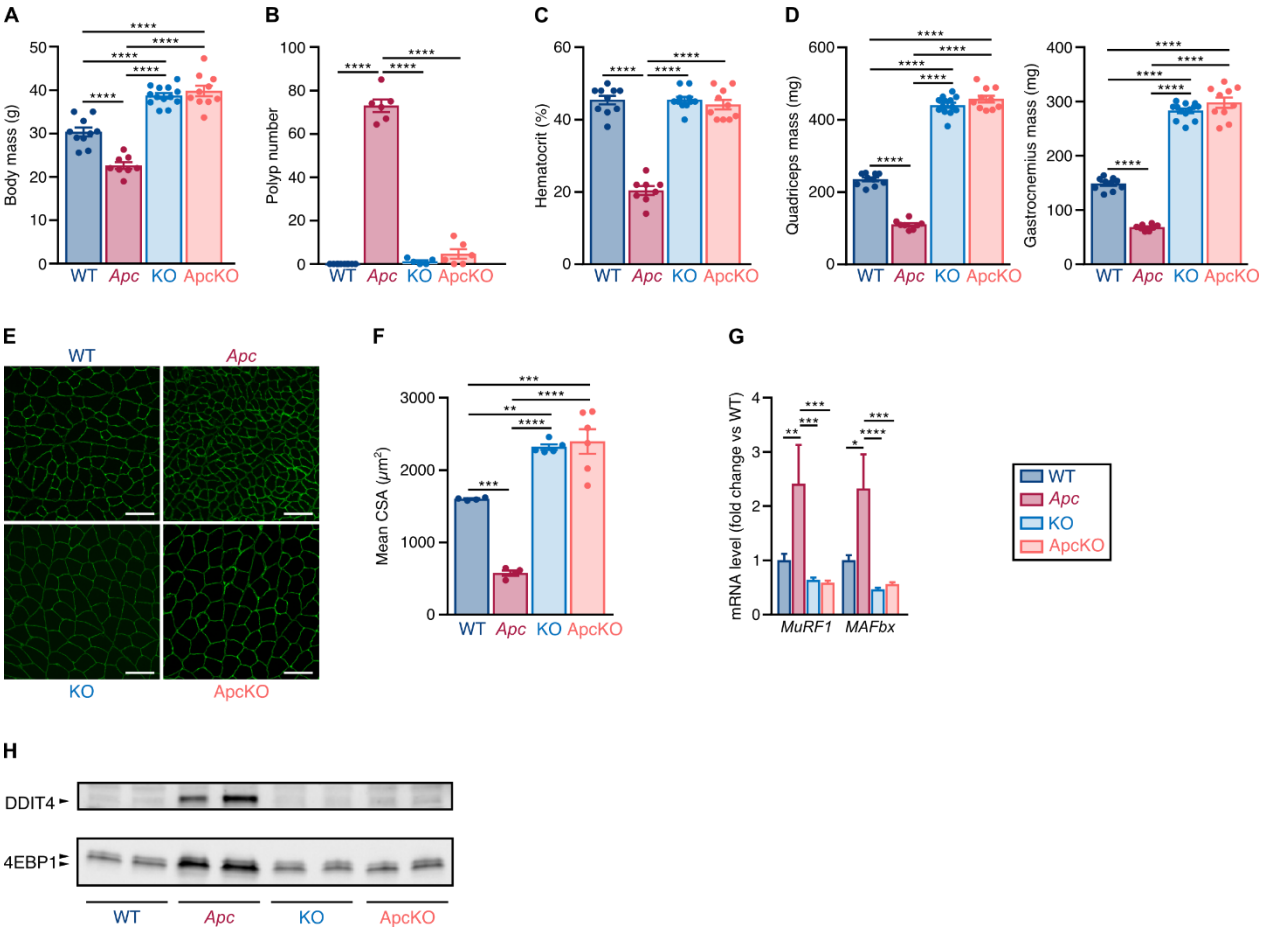

Figure 5. Myostatin gene invalidation prevents cancer cachexia in 23-week-old ApcKO mice

(A) Body mass of WT (n=10), *Apc* (n=8), KO (n=13), and ApcKO (n=10) mice at 23 weeks.

(B) Polyp number in small intestine and colon of WT (n=10), *Apc* (n=6), KO (n=5), and ApcKO (n=6) mice at 23 weeks.

(C) Hematocrit in WT (n=10), *Apc* (n=8), KO (n=11), and ApcKO (n=10) mice at 23 weeks.

(D) *Quadriceps* (left) and *gastrocnemius* (right) muscle mass in WT (n=10), *Apc* (n=8), KO (n=13), and ApcKO (n=10) mice at 23 weeks.

(E) Representative laminin immunostaining of *gastrocnemius* muscle fiber cross-sectional (CSA) area in WT, *Apc*, KO, and ApcKO mice at 23 weeks. Scale bar, 100 µm.

(F) Myofiber CSA of *gastrocnemius* muscle in WT (n=4), *Apc* (n=4), KO (n=6), and ApcKO (n=6) mice at 23 weeks. 475 ± 306 fibers per muscle were counted.

(G) RT-qPCR analysis *MuRF1* and *MAFbx* mRNA level in the *quadriceps* muscle of WT (n=10), *Apc* (n=8), KO (n=13), and ApcKO (n=10) mice at 23 weeks.

(H) Representative immunoblot of DDIT4 and 4EBP1 protein level in the *quadriceps* muscle of WT, *Apc*, KO, and ApcKO mice at 23 weeks. The hypophosphorylated active form of 4EBP1 migrates faster than the hyperphosphorylated inactive form.

Data are represented as mean ± SEM. (A, B, C, D, F, and G) data were analyzed by one-way ANOVA. * represents a significant difference after Tukey's multiple comparison test. *p <0.05, **p < 0.01, ***p < 0.001, or ****p < 0.0001. See also Figure S3.

We next determined whether inhibiting skeletal muscle wasting prevents or limits the GC-dependent response in skeletal muscle and liver of ApcKO mice. We first should note that the GC-dependent transcriptional signature in *quadriceps* muscle and liver first described in 23-week-old *Apc* mice (Figure 4A and 4F, Tables S1 and S2) was almost identically reproduced in this second set of *Apc* mice (Figure 6A-B, Tables S3 and S4). Nine out of 12 genes that were found to be upregulated in the *quadriceps* muscle of 23-week-old *Apc* mice were restored to KO level in ApcKO mice (Figure 6A, Table S3). The 3 transcripts that were not restored to control levels (*Cebpd*, *4ebp1*, *Mt1*) were however markedly down-regulated. Similarly, the GC-dependent transcriptional signature in the liver was not observed anymore in ApcKO mice (Figure 6B, Table S4). Twenty-three out of 25 transcript levels that were regulated 23-week-old *Apc* mice were restored to KO level in ApcKO mice. Accordingly, the protein level of PGC1A, PCK1, and DDIT4 were also restored to the KO level (Figure 6C). In agreement with these data, the corticosterone level in serum (Figure 6D), skeletal muscle (Figure 6E), and liver (Figure 6F) of *Apc*KO mice remained unchanged when compared to WT or KO mice indicating a restoration of HPA axis activity in *Apc*KO mice. Therefore, preventing skeletal muscle mass loss by *Mstn* gene invalidation prevented a systemic increase in corticosterone level and the associated GC-dependent transcriptional response in skeletal muscle and liver.

Figure 6. Prevention of cancer cachexia by myostatin gene invalidation prevents hepatic metabolism transcriptional reprogramming in *Apc* mice and reduces corticosterone level

(A) Heatmap displaying the restoration of the glucocorticoid-dependent transcriptional signature measured by RT-qPCR in the *quadriceps* muscle of *Apc* (WT=10, Apc=8) and ApcKO (KO=13, ApcKO=10) mice at 23 weeks. mRNA level was expressed in mean of Log2(fold change vs 23-week-old WT mice for *Apc* mice and vs 23-week-old KO mice for ApcKO mice). For Log2(fold change)>5, cells are set by default in the most intense red.

(B) Heatmap displaying the restoration of glucocorticoid-dependent transcriptional signature measured by RT-qPCR in the liver of *Apc* (WT=10, Apc=6) and ApcKO (KO=10, ApcKO=10) mice at 23 weeks. mRNA level was expressed in mean of Log2(fold change vs 23-week-old WT mice and vs 23-week-old KO mice for ApcKO mice). For Log2(fold change)>6, cells are set by default in the most intense red.

(C) Representative immunoblot of PGC1A, PCK1, and DDIT4 protein level in liver of WT, *Apc*, KO, and ApcKO mice at 23 weeks.

(D) Serum corticosterone concentration in WT (n=11), *Apc* (n=6), KO (n=11), and ApcKO (n=11) mice at 23 weeks.

(E) Corticosterone level in the *quadriceps* muscle of WT (n=9), *Apc* (n=8), KO (n=12), and ApcKO (n=11) mice at 23 weeks.

(F) Corticosterone level in the liver of WT (n=11), *Apc* (n=5), KO (n=10), and ApcKO (n=11) mice at 23 weeks.

Data are represented as mean ± SEM. (D, E, and F) data were analyzed by one-way ANOVA. * represents a significant difference after Tukey's multiple comparison test. *p <0.05, **p < 0.01, and ***p < 0.001.

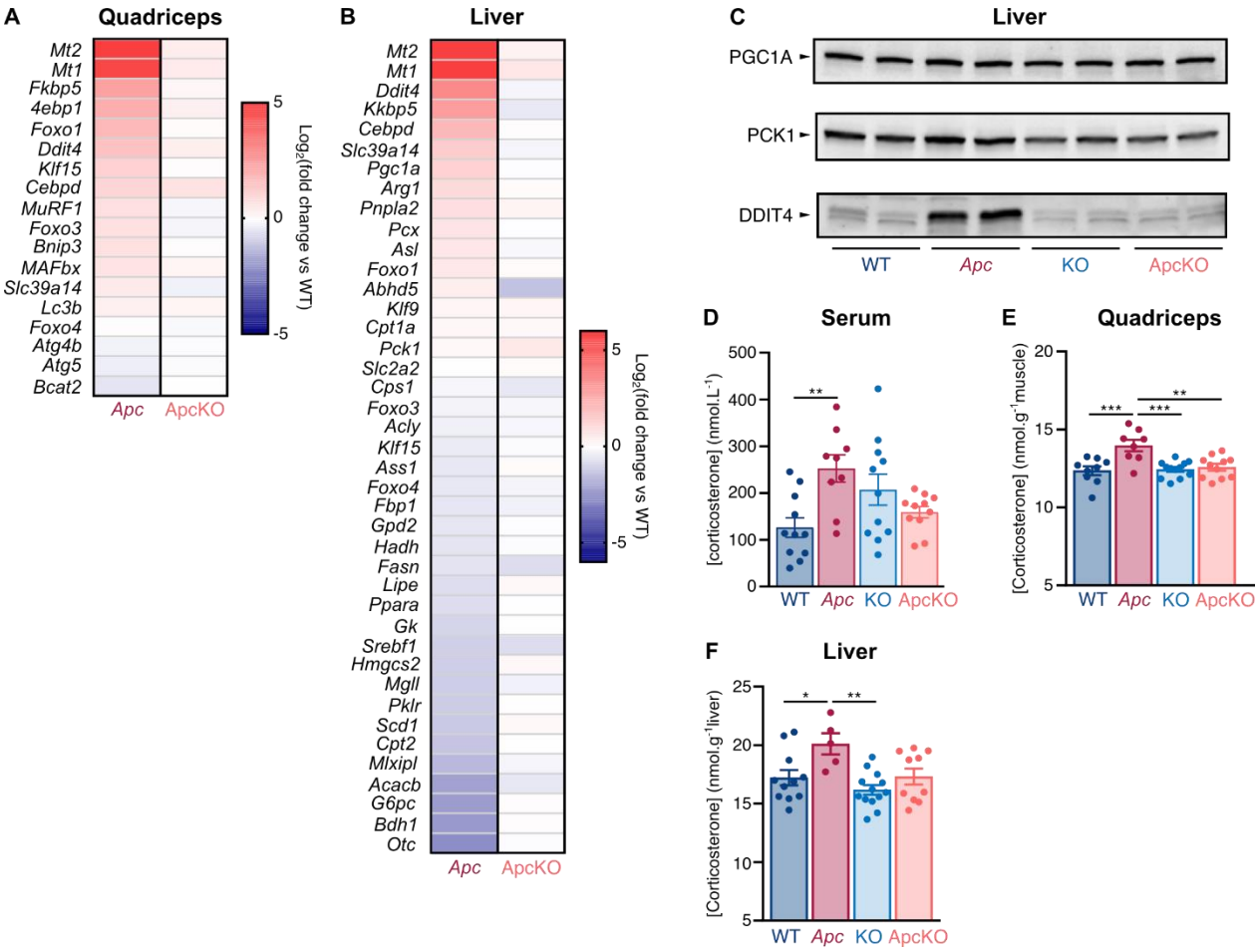

Discussion

Cancer cachexia results in major adaptations in skeletal muscle that profoundly impact patient's quality of life and ultimately patients' survival [4,81,3,82]. Research in the field has traditionally focused on the molecular mechanisms involved in skeletal muscle wasting during cancer cachexia. However, a systemic approach is now necessary to shed a different light on the mechanisms involved in cancer cachexia and to understand as a whole the diversity and complexity of cancer cachexia [14–16]. Our findings showing that cancer cachexia elicits skeletal muscle wasting and liver metabolism rewiring in a GC-dependent manner strongly indicate that systemic energy redistribution during cancer cachexia is, at least partly, regulated by the HPA axis. Our study also, indicates that the capacity of skeletal muscle to resist the wasting syndrome is a key element in the regulation of this GC-dependent response.

In this study, we used the *Apc* mice as a model of cancer cachexia. The *APC* tumor suppressor gene encodes a protein that down-regulates the transcriptional activation mediated by ß-catenin and T cell transcription factor 4 (Tcf4) [83]. Disruption of *APC*-mediated regulation of ß-catenin-Tcf4-regulated transcription is critical for colorectal tumorigenesis. In carriers of *APC*

inactivating mutation, the risk of colorectal cancer by the age of 40 is almost 100% [42] and the *APC* gene is mutated in more than half of colorectal cancer patients [84]. Importantly, about 50% of patients with intestinal cancer will develop cachexia [4,3,5,6]. Similarly to human patients, *Apc* mice accumulated intestinal polyps [85] leading to intestinal bleeding and progressively developed cachexia. We could also clearly identify a moderate cachectic stage at 13 weeks of age and an advanced cachectic stage at 23 weeks of age. In agreement with previous studies, we also found that skeletal muscle wasting during cancer cachexia in *Apc* mice was also characterized by a decrease in myofiber size [86,87] and muscle force [88]. This was associated with an imbalance in skeletal muscle proteostasis towards an increase in proteolysis and a decrease in proteosynthesis [47,48,86]. Together, these data indicate that *Apc* mice recapitulate some very important features of cancer cachexia and more closely model the kinetic of cancer cachexia encountered in human patients compared to other fast tumor burden models of cancer cachexia.

We provide for the first-time evidence that hepatic metabolism was entirely rewired during advanced cancer cachexia. We thus determined that 23-week-old *Apc* mice have increased gluconeogenesis and reduced glycolysis. Our data also suggest that a GC-dependent FOXO1/PGC1A pathway [56,89] is predominantly involved in this regulation. The rewiring of hepatic metabolism towards glucose production in advanced cachectic *Apc* mice together with the changes in glycemia and lactatemia is consistent with a metabolic schema in which end-products of skeletal muscle and adipose tissue catabolism (amino acids and glycerol, respectively), together with the lactate produced by tumoral metabolism [62], are recycled as substrates for hepatic gluconeogenesis to produce glucose for tumor growth [18,90]. Liver nitrogen metabolism was also profoundly affected. The urea cycle converts highly toxic ammonia resulting from amino acid deamination into urea for urinary excretion. Out of the 5 enzymes involved in the urea cycle, 3 transcripts were down-regulated, one remained unchanged and one was up-regulated, suggesting that the transcriptional regulatory mechanisms governing the expression of these enzymes were probably different [91–93]. Previous studies indicated an increase in urea cycle enzyme activity in tumor-bearing mice [94] as well as an increase in urea concentration in tumor-bearing rats [95]. Even if the circulating concentrations of urea and ammonia were not determined in the present study, our data strongly suggest that the capacity of the liver to manage the flux of amine groups resulting from the deamination of amino acids originating from skeletal muscle catabolism would be modified during cancer cachexia. The consequences of altered circulating levels of ammonia and urea during cancer cachexia have to deserve further investigations. Advanced cachectic *Apc* mice also displayed a hypoketonemic phenotype that was associated with a reduction in the expression of hepatic fatty acid oxidation genes. The liver produces ketone bodies from acetyl CoA when a strong stimulation of fatty acid oxidation leads to a high rate of acetyl-CoA production that exceeds the capacity of citrate to be incorporated into the

tricarboxylic acid cycle. In the present study, the almost complete exhaustion of adipose tissue store in 23-week-old *Apc* mice cannot obviously sustain ketogenesis, and may also explain why the expression of lipid metabolism markers were all decreased in 23-week-old *Apc* mice. Conversely, the high rate of lipolysis that led to the depletion of adipose tissue store earlier during the development of cachexia may have transitory increase ketone body production. Hypoketonemia thus signs here the existence of an advanced cachectic state. Ketone bodies are mitochondrially oxidized to produce ATP by most tissues but not by tumor cells [96,97]. Therefore, maintaining ketone production is probably favorable to limit the progression of cancer cachexia [31,98].

Our biomolecular analyses at the level of the hypothalamus and adrenal glands, together with the increased corticosterone concentration in serum, skeletal muscle and liver, clearly demonstrate that the HPA axis is activated during cancer cachexia in 23-week-old *Apc* mice. Of note, the transcript level of liver GC detoxifying enzymes was also down-regulated in 23-week-old *Apc* mice suggesting that the whole GC metabolism was regulated to sustain an enhanced biodisponibility of GC during cancer cachexia. Our data thus raise an important question concerning the upstream regulatory mechanisms involved in the regulation of the HPA axis during cancer cachexia. An increase in the circulating level of GC is classically expected to exert negative feedback on their own secretion by inhibiting the stimulatory influence of the hypothalamus and pituitary on adrenal glands. In the present study, the high level of circulating corticosterone associated with a high level of *Crh* transcript in the hypothalamus rather indicates a resistance to the negative feedback action of GC. The HPA axis can be stimulated by pro-inflammatory cytokines. For instance, the intracerebroventricular injection of IL-1ß induces the activation of the HPA axis together with the expression of GC-responsive genes in skeletal muscle and skeletal muscle atrophy [99]. Hypothalamic inflammation has been consistently reported in animal models of cancer cachexia [99–102]. If the existence of a central inflammation is currently unknown in cancer cachectic patients, a chronic systemic inflammation state has been associated with skeletal muscle mass loss in human cancer patients [103]. Similar observations have been reported in experimental models of cancer cachexia [29,104,105]. Moreover, intravenous injection of cytokines in cancer patients increases circulating cortisol level through HPA axis activation [106–110]. Therefore, the systemic inflammatory host response to tumor growth could be centrally sensed and relayed within the hypothalamus to trigger cancer cachexia via the regulation of the HPA axis.

Our comparative analysis of cachectic muscles and dexamethasone-treated mice statistically demonstrated the existence of a GC-dependent transcriptional signature in skeletal muscle and liver of 23-week-old *Apc* mice. Our molecular analysis indicates that this signature is involved in the negative regulation of proteostasis in skeletal muscle, in the activation of gluconeogenesis,

regulation of ureogenesis, inhibition of ketogenesis and lipid metabolism in the liver. Thus, our data identify GC as a critical regulating factor that systematically coordinately regulate skeletal muscle and liver metabolisms during cancer cachexia. It should be noted however that some genes were not commonly regulated between *Apc* mice and dexamethasone-treated mice, indicating that GC-independent mechanisms are also involved in the regulation of skeletal muscle and liver metabolism during cancer cachexia. The transcriptomic signature was also largely reproduced in skeletal muscle of LLC-tumor bearing mice. The use of different mice models of cancer cachexia with different tumor types and distinct oncogenic drivers (tumor-bearing mice and genetically engineered mouse models) further extends the scope and the biological relevance of our findings. Furthermore, the analysis of the available lists of differentially expressed genes obtained by transcriptomic analysis in skeletal muscle of several animal models of cancer cachexia shows that this GC-dependent transcriptional signature is, at least partially, shared by several studies [105,111,112,31,113,50,114–118], further illustrating the importance of this response. Finally, it is also necessary to confirm the relevance of our findings in skeletal muscle samples from digestive cancer patients with or without cachexia. In the liver, omics data are lacking and require further investigations to confirm the existence of a GC-dependent transcriptional response.

These data obviously question the relevance of GC-inhibiting strategies to combat cancer cachexia. Some pioneering studies had proposed to inhibit GC signaling to combat cancer cachexia. Adrenalectomy of tumor-bearing animals did not attenuate cancer cachexia [36,119]. The steroid hormone inhibitor RU486 has been historically used to inhibit GC transcriptional activity [120]. However, due to its wide spectrum of action (RU486 is also an antiprogestogen and antiandrogen) and its short half-life in rodents [121], the use of RU486 have provided contrasting results, some studies providing convincing effects [34] on cancer cachexia, others not [32,33]. Together with the difficulty to biologically assess the efficiency of this drug [122], the use of RU486 remains a controversial issue. The relevance of GC-based therapy has been most convincingly provided by GC receptor muscle-specific knock-out mice. Muscle-specific invalidation of GC receptor abrogates skeletal muscle mass loss in LLC-tumor bearing cachectic mice [123]. Finally, one may also question the efficiency of single target-based therapy. Considering the systemic nature of the cachectic syndrome that involves multiple circulating factors that are coordinately regulated with a specific time frame during the progression of the disease, we believe that the GC-dependent response is part of a more generalized response involving other blood-borne factors.

In agreement with previous studies [40,124–133], we confirm that targeting Mstn is an efficient strategy to prevent cancer cachexia, an action that has been mainly attributed to the restoration of proteostasis in skeletal muscle [40,125–129,131–133]. What is new in the present study is the finding that the prevention of cancer cachexia by *Mstn* gene invalidation also suppressed hepatic

metabolism reprogramming while restoring GC levels, thus providing evidence a functional relationship between Mstn, skeletal muscle, liver and the regulation of the HPA axis during cancer cachexia. Therefore, the capacity of skeletal muscle to resist to cachexia is a key element in the regulation of the GC-dependent response. Non-mutually exclusive mechanisms can be considered to explain our findings. First, the resistance conferred by *Mstn* gene invalidation to skeletal muscle catabolism may have a strong impact on liver metabolism. The rupture in the amino acid provision due to this Mstn-dependent muscle wasting sparing effect should considerably reduce the provision of gluconeogenic substrates to the liver. In this scheme, skeletal muscle would govern hepatic metabolic reprogramming and could be viewed as a metabolic rheostat that provides clues to regulate hepatic metabolic function. Second, one may also consider that MSTN could directly regulate hepatic metabolism [134,135]. Constitutive *Mstn* gene invalidation may thus confer other advantages that may protect the liver from the adverse effects of cancer cachexia. Importantly, this protective effect of *Mstn* invalidation would only be expressed under catabolic conditions as the vast majority of hepatic metabolic genes in the present study were not differentially expressed between WT and KO mice. Third, MSTN could also directly trigger central effects that contribute to the regulation of the HPA axis. In support of this hypothesis, MSTN has been immunochemically detected in several brain regions including the hypothalamus [136] and also regulates pituitary development [137]. Furthermore, our unpublished observations indicate that MSTN receptors (Activin type IIB receptor and activin-like kinase 4 and 5 receptors) are transcriptionally expressed in the hypothalamus. Therefore, Mstn could exert a central action by directly stimulating the HPA axis during cancer cachexia, an effect that would be inhibited in ApcKO mice. Fourth, *Mstn* expression is known to be transitory activated early after GC administration [74,138] and *Mstn* gene invalidation prevents GC-induced skeletal muscle wasting [139]. In the present study, *Mstn* expression was non-significantly increased in *Apc* mice and correlated with muscle mass and circulating corticosterone content, thus illustrating the functional relationship between GC, *Mstn* expression and muscle mass. Finally, we cannot also exclude that *Mstn* gene invalidation may exert an anti-tumoral effect. Indeed, one striking observation of the present study, which we also previously observed [40], was the reduction in polyp number in ApcKO mice. This clearly questions whether *Mstn* gene invalidation prevents HPA activation and cancer cachexia by reducing intestinal polyp development in ApcKO mice. Although a reduction in tumor growth has not been systematically observed [124,129,130,133], our observations are consistent with a previous study demonstrating that administration of a soluble MSTN and activin inhibitor slowed tumor growth [125,132] and lung metastases [131] in mice. Other studies have also reported that reducing/inhibiting MSTN and activin signaling slowed tumor development in gonads [140–143]. An association between the reduction in tumor growth and the prevention of cachexia does not prove causality, but obviously mechanistic links involving MSTN must exist. Therefore, *Mstn* gene invalidation in *Apc* mice may contribute to preventing HPA axis

activation and cancer cachexia by collectively inhibiting tumor development and conferring resistance to skeletal muscle wasting.

Since the discovery of GC in the 1940s and the recognition of their anti-inflammatory effects, GC have been amongst the most widely used and effective treatments to control inflammatory processes. GC are also used as a curative treatment for some cancers or as palliative use against adverse effects of other cancer treatments [144]. However, administration of GC has also many pleiotropic adverse effects, which include skeletal muscle and adipose tissue catabolism, osteoporosis, hypertension, and insulin resistance, so that their clinical benefits, depending on the dose and frequency of administration, may be compromised during long-term treatment [145]. Furthermore, endogenous GC production can be stimulated by chemotherapy [146,147] or opioids [148]. In the present study, it is important to remind that the role of GC is only considered through the endogenous regulation of the HPA axis. In this context, our data provide information about the mechanisms by which GC exert their metabolic actions and will help to further discriminate between the beneficial and adverse effects of GC in cancer.

In summary, our findings point to GC as important regulators of skeletal muscle catabolism and hepatic metabolism rewiring during advanced cancer cachexia. Understanding to what extent skeletal muscle regulates hepatic metabolism, the impact of hepatic metabolism rewiring on tumor growth as well as how is HPA axis regulated during cancer cachexia clearly need to be further explored. Our study thus provides important pieces of information on the comprehensive analysis of the systemic nature of cancer cachexia.

Acknowledgments

A.M. is financially supported by the Ministère de l'Enseignement Supérieur de la Recherche et de l'Innovation. This work was supported by the Fondation ARC pour la Recherche sur le Cancer (PJA 2018 1207841). We thank all the PLEXAN personnel for animal care. We thank Ismahane Benhamane for her help in muscle force measurement. Gimap laboratory is gratefully acknowledged for giving us the opportunity to gain access to cryostat microtome. We also thank Aurélie Montmartin and Pauline Damien from Sainbiose for the use of the microplate reader. Rémi Mounier is gratefully acknowledged for helpful and stimulating discussions at the beginning of the project.

Author contributions

Conceptualization, A.M. and D.F., Methodology, A.C.D., A.M., C.H., D.F., F.F., and J.C.; Validation, A.M. and D.F.; Formal Analysis, A.M., C.Z., D.F., J.C. and V.A., Investigation, A.C.D., A.M., C.Z., C.H.,

D.F., F.F., J.C., V.A., and Y.S.G.; Writing – Original Draft, A.M. and D.F., Writing – Review & Editing, all authors, Visualization, A.M.; Supervision, D.F., Funding Acquisition, D.F.

Declaration of interests

The authors declare no competing interest.

References

1. Evans WJ, Morley JE, Argilés J, Bales C, Baracos V, Guttridge D *et al.* Cachexia: A new definition. *Clinical Nutrition* 2008;**27**:793–799.

2. Fearon K, Strasser F, Anker SD, Bosaeus I, Bruera E, Fainsinger RL *et al.* Definition and classification of cancer cachexia: an international consensus. *The Lancet Oncology* 2011;**12**:489–495.

3. Vanhoutte G, van de Wiel M, Wouters K, Sels M, Bartolomeeussen L, De Keersmaecker S *et al.* Cachexia in cancer: what is in the definition? *BMJ Open Gastroenterol* 2016;**3**:e000097.

4. Blum D, Stene GB, Solheim TS, Fayers P, Hjermstad MJ, Baracos VE *et al.* Validation of the Consensus-Definition for Cancer Cachexia and evaluation of a classification model--a study based on data from an international multicentre project (EPCRC-CSA). *Ann Oncol* 2014;**25**:1635–1642.

5. Rier HN, Jager A, Sleijfer S, Maier AB, Levin M-D. The Prevalence and Prognostic Value of Low Muscle Mass in Cancer Patients: A Review of the Literature. *Oncologist* 2016;**21**:1396.

6. Baracos VE, Martin L, Korc M, Guttridge DC, Fearon KCH. Cancer-associated cachexia. *Nature Reviews Disease Primers* 2018;**4**:17105.

7. Warren S. The immediate causes of death in cancer. *The American Journal of the Medical Sciences* 1932;**148**:610–615.

8. Basile D, Parnofiello A, Vitale MG, Cortiula F, Gerratana L, Fanotto V *et al.* The IMPACT study: early loss of skeletal muscle mass in advanced pancreatic cancer patients. *J Cachexia Sarcopenia Muscle* 2019;**10**:368–377.

9. Bozzetti F. Forcing the vicious circle: sarcopenia increases toxicity, decreases response to chemotherapy and worsens with chemotherapy. *Ann Oncol* 2017;**28**:2107–2118.

10. Loumaye A, de Barsy M, Nachit M, Lause P, van Maanen A, Trefois P *et al.* Circulating Activin A predicts survival in cancer patients: Circulating ActivinA. *Journal of Cachexia, Sarcopenia and Muscle* 2017;**8**:768–777.

11. Martin L, Birdsell L, MacDonald N, Reiman T, Clandinin MT, McCargar LJ *et al.* Cancer Cachexia in the Age of Obesity: Skeletal Muscle Depletion Is a Powerful Prognostic Factor, Independent of Body Mass Index. *Journal of Clinical Oncology* 2013;**31**:1539–1547.

12. Naumann P, Eberlein J, Farnia B, Liermann J, Hackert T, Debus J *et al.* Cachectic Body Composition and Inflammatory Markers Portend a Poor Prognosis in Patients with Locally Advanced Pancreatic Cancer Treated with Chemoradiation. *Cancers* 2019;**11**:1655.

13. Prado CM, Sawyer MB, Ghosh S, Lieffers JR, Esfandiari N, Antoun S *et al.* Central tenet of cancer cachexia therapy: do patients with advanced cancer have exploitable anabolic potential? *Am J Clin Nutr* 2013;**98**:1012–1019.

14. Argilés JM, Busquets S, Stemmler B, López-Soriano FJ. Cancer cachexia: understanding the molecular basis. *Nature Reviews Cancer* 2014;**14**:754–762.

15. Argilés JM, Stemmler B, López-Soriano FJ, Busquets S. Inter-tissue communication in cancer cachexia. *Nat Rev Endocrinol* 2018;**15**:9–20.

16. Rohm M, Zeigerer A, Machado J, Herzig S. Energy metabolism in cachexia. *EMBO Rep* 2019;**20**:e47258.

17. Glicksman AS, Rawson RW. Diabetes and altered carbohydrate metabolism in patients with cancer. *Cancer* 1956;**9**:1127–1134.

18. Holroyde CP, Skutches CL, Boden G, Reichard GA. Glucose Metabolism in Cachectic Patients with Colorectal Cancer. *Cancer Res* 1984;**44**:5910–5913.

19. Lundholm K, Edström S, Karlberg I, Ekman L, Scherstén T. Glucose turnover, gluconeogenesis from glycerol, and estimation of net glucose cycling in cancer patients. *Cancer* 1982;**50**:1142–1150.

20. Waterhouse C, Jeanpretre N, Keilson J. Gluconeogenesis from Alanine in Patients with Progressive Malignant Disease. *Cancer Res* 1979;**39**:1968–1972.

21. Kuo T, Lew MJ, Mayba O, Harris CA, Speed TP, Wang J-C. Genome-wide Analysis of Glucocorticoid Receptor-Binding Sites in Myotubes Identifies Gene Networks Modulating Insulin Signaling. *Proc Natl Acad Sci U S A* 2012;**109**:11160–11165.

22. Shimizu N, Yoshikawa N, Ito N, Maruyama T, Suzuki Y, Takeda S *et al.* Crosstalk between Glucocorticoid Receptor and Nutritional Sensor mTOR in Skeletal Muscle. *Cell Metabolism* 2011;**13**:170–182.

23. Watson ML, Baehr LM, Reichardt HM, Tuckermann JP, Bodine SC, Furlow JD. A cell-autonomous role for the glucocorticoid receptor in skeletal muscle atrophy induced by systemic glucocorticoid exposure. *Am J Physiol Endocrinol Metab* 2012;**302**:E1210–E1220.

24. Malkawi AK, Masood A, Shinwari Z, Jacob M, Benabdelkamel H, Matic G *et al.* Proteomic Analysis of Morphologically Changed Tissues after Prolonged Dexamethasone Treatment. *International Journal of Molecular Sciences* 2019;**20**:3122.

25. Phuc Le P, Friedman JR, Schug J, Brestelli JE, Parker JB, Bochkis IM *et al.* Glucocorticoid Receptor-Dependent Gene Regulatory Networks. *PLoS Genet* 2005;**1**.

26. Knapp ML, Al-Sheibani S, Riches PG, Hanham IWF, Phillips RH. Hormonal Factors Associated with Weight Loss in Patients with Advanced Breast Cancer. *Ann Clin Biochem* 1991;**28**:480–486.

27. Cala MP, Agulló-Ortuño MT, Prieto-García E, González-Riano C, Parrilla-Rubio L, Barbas C *et al.* Multiplatform plasma fingerprinting in cancer cachexia: a pilot observational and translational study. *J Cachexia Sarcopenia Muscle* 2018;**9**:348–357.

28. Flint TR, Janowitz T, Connell CM, Roberts EW, Denton AE, Coll AP *et al.* Tumor-Induced IL-6 Reprograms Host Metabolism to Suppress Anti-tumor Immunity. *Cell Metabolism* 2016;**24**:672–684.

29. Costelli P, Carbó N, Tessitore L, Bagby GJ, Lopez-Soriano FJ, Argilés JM *et al.* Tumor necrosis factor-alpha mediates changes in tissue protein turnover in a rat cancer cachexia model. *J Clin Invest* 1993;**92**:2783–2789.

30. Costelli P, García-Martínez C, Llovera M, Carbó N, López-Soriano FJ, Agell N *et al.* Muscle protein waste in tumor-bearing rats is effectively antagonized by a beta 2-adrenergic agonist (clenbuterol). Role of the ATP-ubiquitin-dependent proteolytic pathway. *J Clin Invest* 1995;**95**:2367–2372.

31. Goncalves MD, Hwang S-K, Pauli C, Murphy CJ, Cheng Z, Hopkins BD *et al.* Fenofibrate prevents skeletal muscle loss in mice with lung cancer. *Proc Natl Acad Sci USA* 2018;**115**:E743–E752.

32. Llovera M, García-Martínez C, Costelli P, Agell N, Carbo N, Lopez-Soriano FJ *et al.* Muscle hypercatabolism during cancer cachexia is not reversed by the glucocorticoid receptor antagonist RU38486. *Cancer Letters* 1996;**99**:7–14.

33. Rivadeneira DE, Naama HA, McCarter MD, Fujita J, Evoy D, Mackrell P *et al.* Glucocorticoid Blockade Does Not Abrogate Tumor-Induced Cachexia. *Nutrition and Cancer* 1999;**35**:202–206.

34. Russell ST, Tisdale MJ. The role of glucocorticoids in the induction of zinc- α 2 -glycoprotein expression in adipose tissue in cancer cachexia. *British Journal of Cancer* 2005;**92**:876–881.

35. Tanaka Y, Eda H, Tanaka T, Udagawa T, Ishikawa T, Horii I *et al.* Experimental Cancer Cachexia Induced by Transplantable Colon 26 Adenocarcinoma in Mice. *Cancer Res* 1990;**50**:2290–2295.

36. Tessitore L, Costelli P, Baccino FM. Pharmacological interference with tissue hypercatabolism in tumour-bearing rats. *Biochem J* 1994;**299**:71–78.

37. Moser AR, Pitot HC, Dove WF. A dominant mutation that predisposes to multiple intestinal neoplasia in the mouse. *Science* 1990;**247**:322–324.

38. Su LK, Kinzler KW, Vogelstein B, Preisinger AC, Moser AR, Luongo C *et al.* Multiple intestinal neoplasia caused by a mutation in the murine homolog of the APC gene. *Science* 1992;**256**:668–670.

39. Grobet L, Pirottin D, Farnir F, Poncelet D, Royo LJ, Brouwers B *et al.* Modulating skeletal muscle mass by postnatal, muscle-specific inactivation of the myostatin gene. *genesis* 2003;**35**:227–238.

40. Gallot YS, Durieux A-C, Castells J, Desgeorges MM, Vernus B, Plantureux L *et al.* Myostatin Gene Inactivation Prevents Skeletal Muscle Wasting in Cancer. *Cancer Research* 2014;**74**:7344–7356.

41. Barton ER, Lynch G, Khurana TS. Measuring isometric force of isolated mouse muscles in vitro. 2008;15.

42. Markowitz SD. Molecular Basis of Colorectal Cancer. *The New England Journal of Medicine* 2009;**361**(25):2449-2460.

43. Britto FA, Begue G, Rossano B, Docquier A, Vernus B, Sar C *et al.* REDD1 deletion prevents dexamethasone-induced skeletal muscle atrophy. *American Journal of Physiology-Endocrinology and Metabolism* 2014;**307**:E983–E993.

44. Brugarolas J, Lei K, Hurley RL, Manning BD, Reiling JH, Hafen E *et al.* Regulation of mTOR function in response to hypoxia by REDD1 and the TSC1/TSC2 tumor suppressor complex. *Genes Dev* 2004;**18**:2893–2904.

45. Lin T-A, Kong X, Haystead TAJ, Pause A, Belsham G, Sonenberg N *et al.* PHAS-I as a Link Between Mitogen-Activated Protein Kinase and Translation Initiation. *Science* 1994;**266**:653–656.

46. Pause A, Belsham GJ, Gingras A-C, Donzé O, Lin T-A, Lawrence JC *et al.* Insulin-dependent stimulation of protein synthesis by phosphorylation of a regulator of 5'-cap function. *Nature* 1994;**371**:762–767.

47. Lima M, Sato S, Enos RT, Baynes JW, Carson JA. Development of an UPLC mass spectrometry method for measurement of myofibrillar protein synthesis: application to analysis of murine muscles during cancer cachexia. *J Appl Physiol (1985)* 2013;**114**:824–828.

48. White JP, Baynes JW, Welle SL, Kostek MC, Matesic LE, Sato S *et al.* The Regulation of Skeletal Muscle Protein Turnover during the Progression of Cancer Cachexia in the ApcMin/+ Mouse. *PLOS ONE* 2011;**6**:e24650.

49. Penna F, Busquets S, Argilés JM. Experimental cancer cachexia: Evolving strategies for getting closer to the human scenario. *Seminars in Cell & Developmental Biology* 2016;**54**:20–27.

50. Talbert EE, Cuitiño MC, Ladner KJ, Rajasekerea PV, Siebert M, Shakya R *et al.* Modeling Human Cancer-induced Cachexia. *Cell Rep* 2019;**28**:1612–16224.

51. Kersten S, Seydoux J, Peters JM, Gonzalez FJ, Desvergne B, Wahli W. Peroxisome proliferator–activated receptor α mediates the adaptive response to fasting. *J Clin Invest* 1999;**103**:1489–1498.

52. Renquist BJ, Murphy JG, Larson EA, Olsen D, Klein RF, Ellacott KLJ *et al.* Melanocortin-3 receptor regulates the normal fasting response. *Proc Natl Acad Sci U S A* 2012;**109**:E1489–E1498.

53. Shimizu N, Maruyama T, Yoshikawa N, Matsumiya R, Ma Y, Ito N *et al.* A muscle-liver-fat signalling axis is essential for central control of adaptive adipose remodelling. *Nat Commun* 2015;**6**:6693.

54. Altarejos JY, Montminy M. CREB and the CRTC co-activators: sensors for hormonal and metabolic signals. *Nat Rev Mol Cell Biol* 2011;**12**:141–151.

55. Herzig S, Long F, Jhala US, Hedrick S, Quinn R, Bauer A *et al.* CREB regulates hepatic gluconeogenesis through the coactivator PGC-1. *Nature* 2001;**413**:179–183.

56. Puigserver P, Rhee J, Donovan J, Walkey CJ, Yoon JC, Oriente F *et al.* Insulin-regulated hepatic gluconeogenesis through FOXO1–PGC-1α interaction. *Nature* 2003;**423**:550–555.

57. Liang H, Ward WF. PGC-1α: a key regulator of energy metabolism. *Advances in Physiology Education* 2006;**30**:145–151.

58. Unterman TG. Regulation of Hepatic Glucose Metabolism by FoxO Proteins, an Integrated Approach. In: *Current Topics in Developmental Biology*. Elsevier; 2018. pp. 119–147.

59. Yamashita H, Takenoshita M, Sakurai M, Bruick RK, Henzel WJ, Shillinglaw W *et al.* A glucose-responsive transcription factor that regulates carbohydrate metabolism in the liver. *PNAS* 2001;**98**:9116–9121.

60. Abdul-Wahed A, Guilmeau S, Postic C. Sweet Sixteenth for ChREBP: Established Roles and Future Goals. *Cell Metabolism* 2017;**26**:324–341.

61. Poungvarin N, Chang B, Imamura M, Chen J, Moolsuwan K, Sae-Lee C *et al.* Genome-Wide Analysis of ChREBP Binding Sites on Male Mouse Liver and White Adipose Chromatin. *Endocrinology* 2015;**156**:1982–1994.

62. Warburg O. Über den Stoffwechsel der Carcinomzelle. *Naturwissenschaften* 1924;**12**:1131–1137.

63. Blanco A, Blanco G. Chapter 16 - Amino Acid Metabolism. In: Blanco A, Blanco G, editors. *Medical Biochemistry*. Academic Press; 2017. pp. 367–399.

64. Grabacka M, Pierzchalska M, Dean M, Reiss K. Regulation of Ketone Body Metabolism and the Role of PPARα. *IJMS* 2016;**17**:2093.

65. Häusl AS, Hartmann J, Pöhlmann ML, Brix LM, Lopez J-P, Brivio E *et al.* The co-chaperone Fkbp5 shapes the acute stress response in the paraventricular nucleus of the hypothalamus. *bioRxiv* 2019;824664.

66. Ferreira JG, Cruz CD, Neves D, Pignatelli D. Increased extracellular signal regulated kinases phosphorylation in the adrenal gland in response to chronic ACTH treatment. *Journal of Endocrinology* 2007;**192**:647–658.

67. Ball HA, Samuels LT. Adrenal Weights in Tumor-Bearing Rats. *Proceedings of the Society for Experimental Biology and Medicine* 1938;**38**:441–443.

68. Crespigio J, Weidmann R, Macioszek MA, de Oliveira JF, de Souza M, Pignatelli D *et al.* Impaired Glucocorticoid Synthesis in Cancer Cachexia-Anorexia Syndrome in an Experimental Model. *Annals of Clinical & Experimental Metabolism* 2016;**1**:1008.

69. Tessitore L, Costelli P, Bonetti G, Baccino FM. Cancer Cachexia, Malnutrition, and Tissue Protein Turnover in Experimental Animals. *Archives of Biochemistry and Biophysics* 1993;**306**:52–58.

70. Sarason EL. Adrenal cortex in systemic disease: a morphologic study. *Arch Intern Med (Chic)* 1943;**71**:702–712.

71. Nicolaides NC, Chrousos GP. Adrenal Cortex Hormones. In: *Hormonal Signaling in Biology and Medicine*. Elsevier; 2020. pp. 619–633.

72. Agarwal MK, Mirshahi M. General overview of mineralocorticoid hormone action. *Pharmacology & Therapeutics* 1999;**84**:273–326.

73. Luton JP, Thieblot P, Valcke JC, Mahoudeau JA, Bricaire H. Reversible gonadotropin deficiency in male Cushing's disease. *J Clin Endocrinol Metab* 1977;**45**:488–495.

74. Ma K, Mallidis C, Bhasin S, Mahabadi V, Artaza J, Gonzalez-Cadavid N *et al.* Glucocorticoid-induced skeletal muscle atrophy is associated with upregulation of myostatin gene expression. *Am J Physiol Endocrinol Metab* 2003;**285**:E363-371.

75. Yang H, Mammen J, Wei W, Menconi M, Evenson A, Fareed M *et al.* Expression and activity of C/EBPβ and δ are upregulated by dexamethasone in skeletal muscle. *Journal of Cellular Physiology* 2005;**204**:219–226.

76. Summermatter S, Bouzan A, Pierrel E, Melly S, Stauffer D, Gutzwiller S *et al.* Blockade of Metallothioneins 1 and 2 Increases Skeletal Muscle Mass and Strength. *Mol Cell Biol* 2017;**37**.

77. Morgan SA, McCabe EL, Gathercole LL, Hassan-Smith ZK, Larner DP, Bujalska IJ *et al.* 11 -HSD1 is the major regulator of the tissue-specific effects of circulating glucocorticoid excess. *Proceedings of the National Academy of Sciences* 2014;**111**:E2482–E2491.

78. McPherron AC, Lawler AM, Lee S-J. Regulation of skeletal muscle mass in mice by a new TGF-p superfamily member. *Nature* 1997;**387**:83–90.

79. Durieux A-C, Amirouche A, Banzet S, Koulmann N, Bonnefoy R, Pasdeloup M *et al.* Ectopic Expression of Myostatin Induces Atrophy of Adult Skeletal Muscle by Decreasing Muscle Gene Expression. *Endocrinology* 2007;**148**:3140–3147.

80. Amirouche A, Durieux A-C, Banzet S, Koulmann N, Bonnefoy R, Mouret C *et al.* Down-Regulation of Akt/Mammalian Target of Rapamycin Signaling Pathway in Response to Myostatin Overexpression in Skeletal Muscle. *Endocrinology* 2009;**150**:286–294.

81. Loumaye A, de Barsy M, Nachit M, Lause P, Frateur L, van Maanen A *et al.* Role of Activin A and Myostatin in Human Cancer Cachexia. *J Clin Endocrinol Metab* 2015;**100**:2030–2038.

82. Vagnildhaug OM, Blum D, Wilcock A, Fayers P, Strasser F, Baracos VE *et al.* The applicability of a weight loss grading system in cancer cachexia: a longitudinal analysis. *Journal of Cachexia, Sarcopenia and Muscle* 2017;**8**:789–797.

83. Morin PJ, Sparks AB, Korinek V, Barker N, Clevers H, Vogelstein B *et al.* Activation of β-Catenin-Tcf Signaling in Colon Cancer by Mutations in β-Catenin or APC. *Science* 1997;**275**:1787–1790.

84. The Cancer Genome Atlas Network. Comprehensive molecular characterization of human colon and rectal cancer. *Nature* 2012;**487**:330–337.

85. Luongo C, Moser AR, Gledhill S, Dove WF. Loss of Apc+ in intestinal adenomas from Min mice. *Cancer research* 1994;**54**:5947–5952.

86. Baltgalvis KA, Berger FG, Peña MMO, Davis JM, White JP, Carson JA. Muscle wasting and interleukin-6-induced atrogin-I expression in the cachectic Apc Min/+ mouse. *Pflügers Archiv - European Journal of Physiology* 2009;**457**:989–1001.

87. Mehl KA, Davis JM, Berger FG, Carson JA. Myofiber degeneration/regeneration is induced in the cachectic ApcMin/+ mouse. *Journal of Applied Physiology* 2005;**99**:2379–2387.

88. VanderVeen BN, Fix DK, Carson JA. Disrupted Skeletal Muscle Mitochondrial Dynamics, Mitophagy, and Biogenesis during Cancer Cachexia: A Role for Inflammation. *Oxid Med Cell Longev* 2017;**2017**:3292087.

89. Yoon JC, Puigserver P, Chen G, Donovan J, Wu Z, Rhee J *et al.* Control of hepatic gluconeogenesis through the transcriptional coactivator PGC-1. *Nature* 2001;**413**:131–138.

90. Argiles JM, Azcon-Bieto J. The metabolic environment of cancer. *Mol Cell Biochem* 1988;**81**.

91. Caldovic L. Data Mining Approaches for Understanding of Regulation of Expression of the Urea Cycle Genes. *Gene Expression and Control* 2018.

92. Morris SM, Moncman CL, Rand KD, Dizikes GJ, Cederbaum SD, O'Brien WE. Regulation of mRNA levels for five urea cycle enzymes in rat liver by diet, cyclic AMP, and glucocorticoids. *Arch Biochem Biophys* 1987;**256**:343–353.

93. Ulbright C, Snodgrass PJ. Coordinate Induction of the Urea Cycle Enzymes by Glucagon and Dexamethasone Is Accomplished by Three Different Mechanisms. *Archives of Biochemistry and Biophysics* 1993;**301**:237–243.

94. Sano M. Activities of urea cycle enzymes in tumor-bearing mice. *Nagoya J Med Sci* 1971;**33**:315–328.

95. Corbello Pereira SR, Darronqui E, Constantin J, da Silva MH da RA, Yamamoto NS, Bracht A. The urea cycle and related pathways in the liver of Walker-256 tumor-bearing rats. *Biochim Biophys Acta* 2004;**1688**:187–196.

96. Kaya ZZ, Yilmaz AM, Yalçin AS. Effect of ketone bodies on viability of human breast cancer cells (MCF-7). *Marmara Medical Journal* 2018;**31**:1–4.

97. Skinner R, Trujillo A, Ma X, Beierle EA. Ketone bodies inhibit the viability of human neuroblastoma cells. *J Pediatr Surg* 2009;**44**:212–216.

98. Koutnik AP, Poff AM, Ward NP, DeBlasi JM, Soliven MA, Romero MA *et al.* Ketone Bodies Attenuate Wasting in Models of Atrophy. *Journal of Cachexia, Sarcopenia and Muscle* 2020;11(4):**973**-996.

99. Braun TP, Zhu X, Szumowski M, Scott GD, Grossberg AJ, Levasseur PR *et al.* Central nervous system inflammation induces muscle atrophy via activation of the hypothalamic–pituitary–adrenal axis. *J Exp Med* 2011;**208**:2449–2463.

100. Lira FS, Yamashita AS, Rosa JC, Tavares FL, Caperuto E, Carnevali LC *et al.* Hypothalamic inflammation is reversed by endurance training in anorectic-cachectic rats. *Nutr Metab (Lond)* 2011;**8**:60.

101. Michaelis KA, Zhu X, Burfeind KG, Krasnow SM, Levasseur PR, Morgan TK *et al.* Establishment and characterization of a novel murine model of pancreatic cancer cachexia. *Journal of Cachexia, Sarcopenia and Muscle* 2017;**8**:824–838.

102. Plata-Salamán CR, Ilyin SE, Gayle D. Brain cytokine mRNAs in anorectic rats bearing prostate adenocarcinoma tumor cells. *American Journal of Physiology-Regulatory, Integrative and Comparative Physiology* 1998;**275**:R566–R573.

103. Abbass T, Dolan RD, Laird BJ, McMillan DC. The Relationship between Imaging-Based Body Composition Analysis and the Systemic Inflammatory Response in Patients with Cancer: A Systematic Review. *Cancers* 2019;**11**:1304.

104. Baltgalvis KA, Berger FG, Pena MMO, Davis JM, Muga SJ, Carson JA. Interleukin-6 and cachexia in ApcMin/+ mice. *American Journal of Physiology-Regulatory, Integrative and Comparative Physiology* 2008;**294**:R393–R401.

105. Bonetto A, Aydogdu T, Kunzevitzky N, Guttridge DC, Khuri S, Koniaris LG *et al.* STAT3 Activation in Skeletal Muscle Links Muscle Wasting and the Acute Phase Response in Cancer Cachexia. *PLoS ONE* 2011;**6**:e22538.

106. Curti BD, Urba WJ, Longo DL, Janik JE, Sharfman WH, Miller LL *et al.* Endocrine effects of IL-1 alpha and beta administered in a phase I trial to patients with advanced cancer. *J Immunother Emphasis Tumor Immunol* 1996;**19**:142–148.

107. Gisslinger H, Svoboda T, Clodi M, Gilly B, Ludwig H, Havelec L *et al.* Interferon-alpha stimulates the hypothalamic-pituitary-adrenal axis in vivo and in vitro. *Neuroendocrinology* 1993;**57**:489–495.

108. Mastorakos G, Chrousos GP, Weber JS. Recombinant interleukin-6 activates the hypothalamic-pituitary-adrenal axis in humans. *J Clin Endocrinol Metab* 1993;**77**:1690–1694.

109. Mastorakos G, Weber JS, Magiakou MA, Gunn H, Chrousos GP. Hypothalamic-pituitary-adrenal axis activation and stimulation of systemic vasopressin secretion by recombinant interleukin-6 in humans: potential implications for the syndrome of inappropriate vasopressin secretion. *J Clin Endocrinol Metab* 1994;**79**:934–939.

110. Nolten W e., Goldstein D, Lindstrom M, McKENNA M v., Carlson I h., Trump D l. *et al.* Effects of Cytokines on the Pituitary–Adrenal Axis in Cancer Patients. *Journal of Interferon Research* 1993;**13**:349–357.

111. Cornwell EW, Mirbod A, Wu C-L, Kandarian SC, Jackman RW. C26 Cancer-Induced Muscle Wasting Is IKKβ-Dependent and NF-kappaB-Independent. *PLoS ONE* 2014;**9**:e87776.

112. Shum AMY, Fung DCY, Corley SM, McGill MC, Bentley NL, Tan TC *et al.* Cardiac and skeletal muscles show molecularly distinct responses to cancer cachexia. *Physiological Genomics* 2015;**47**:588–599.

113. Wang G, Biswas AK, Ma W, Kandpal M, Coker C, Grandgenett PM *et al.* Metastatic cancers promote cachexia through ZIP14 upregulation in skeletal muscle. *Nature Medicine* 2018;**24**:770–781.

114. Nosacka RL, Delitto AE, Delitto D, Patel R, Judge SM, Trevino JG *et al.* Distinct cachexia profiles in response to human pancreatic tumours in mouse limb and respiratory muscle. *Journal of Cachexia, Sarcopenia and Muscle* 2020;**11**:820–837.

115. Tseng YC, Kulp SK, Lai IL, Hsu EC, He WA, Frankhouser DE *et al.* Preclinical Investigation of the Novel Histone Deacetylase Inhibitor AR-42 in the Treatment of Cancer-Induced Cachexia. *J Natl Cancer Inst* 2015;**107**:djv274–djv274.

116. Fernandez GJ, Ferreira JH, Vechetti IJJ, de Moraes LN, Cury SS, Freire PP *et al.* MicroRNA-mRNA Co-sequencing Identifies Transcriptional and Post-transcriptional Regulatory Networks Underlying Muscle Wasting in Cancer Cachexia. *Front Genet* 2020;**11**:541.

117. Judge SM, Wu C-L, Beharry AW, Roberts BM, Ferreira LF, Kandarian SC *et al.* Genome-wide identification of FoxO-dependent gene networks in skeletal muscle during C26 cancer cachexia. *BMC Cancer* 2014;**14**:997.

118. Bae T, Jang J, Lee H, Song J, Chae S, Park M *et al.* Paeonia lactiflora root extract suppresses cancer cachexia by down-regulating muscular NF-κB signalling and muscle-specific E3 ubiquitin ligases in cancer-bearing mice. *Journal of Ethnopharmacology* 2020;**246**:112222.

119. Svaninger G, Gelin J, Lundholm K. Tumor-host wasting not explained by adrenal hyperfunction in tumor-bearing animals. *J Natl Cancer Inst* 1987;**79**:1135–1141.

120. Gagne D, Pons M, Philibert D. RU 38486: a potent antiglucocorticoid in vitro and in vivo. *J Steroid Biochem* 1985;**23**:247–251.

121. Heikinheimo O, Pesonen U, Huupponen R, Koulu M, Lähteenmäki P. Hepatic metabolism and distribution of mifepristone and its metabolites in rats. *Hum Reprod* 1994;**9 Suppl 1**:40–46.

122. Kumari R, Willing L, Jefferson LS, Simpson IA, Kimball SR. REDD1 (Regulated in DNA Damage and Development 1) Expression in Skeletal Muscle as a Surrogate Biomarker of the Efficiency of Glucocorticoid Receptor Blockade. *Biochem Biophys Res Commun* 2011;**412**:644–647.

123. Braun TP, Grossberg AJ, Krasnow SM, Levasseur PR, Szumowski M, Zhu XX *et al.* Cancer- and endotoxin-induced cachexia require intact glucocorticoid signaling in skeletal muscle. *The FASEB Journal* 2013;**27**:3572–3582.

124. Benny Klimek ME, Aydogdu T, Link MJ, Pons M, Koniaris LG, Zimmers TA. Acute inhibition of myostatin-family proteins preserves skeletal muscle in mouse models of cancer cachexia. *Biochemical and Biophysical Research Communications* 2010;**391**:1548–1554.

125. Busquets S, Toledo M, Orpí M, Massa D, Porta M, Capdevila E *et al.* Myostatin blockage using actRIIB antagonism in mice bearing the Lewis lung carcinoma results in the improvement of muscle wasting and physical performance. *Journal of Cachexia, Sarcopenia and Muscle* 2012;**3**:37–43.

126. Levolger S, Wiemer E a. C, van Vugt JLA, Huisman SA, van Vledder MG, van Damme-van Engel S *et al.* Inhibition of activin-like kinase 4/5 attenuates cancer cachexia associated muscle wasting. *Scientific Reports* 2019;**9**:1–11.

127. Liu CM, Yang Z, Liu CW, Wang R, Tien P, Dale R *et al.* Myostatin antisense RNA-mediated muscle growth in normal and cancer cachexia mice. *Gene therapy* 2008;**15**:155.

128. Liu D, Qiao X, Ge Z, Shang Y, Li Y, Wang W *et al.* IMB0901 inhibits muscle atrophy induced by cancer cachexia through MSTN signaling pathway. *Skeletal Muscle* 2019;**9**:8.

129. Murphy KT, Chee A, Gleeson BG, Naim T, Swiderski K, Koopman R *et al.* Antibody-directed myostatin inhibition enhances muscle mass and function in tumor-bearing mice. *American Journal of Physiology-Regulatory, Integrative and Comparative Physiology* 2011;**301**:R716–R726.

130. Nissinen TA, Hentilä J, Penna F, Lampinen A, Lautaoja JH, Fachada V *et al.* Treating cachexia using soluble ACVR2B improves survival, alters mTOR localization, and attenuates liver and spleen responses: Treating cachexia using soluble ACVR2B. *Journal of Cachexia, Sarcopenia and Muscle* 2018;**9**:514–529.

131. Toledo M, Busquets S, Penna F, Zhou X, Marmonti E, Betancourt A *et al.* Complete reversal of muscle wasting in experimental cancer cachexia: Additive effects of activin type II receptor inhibition and β-2 agonist. *International Journal of Cancer* 2016;**138**:2021–2029.

132. Zhong X, Pons M, Poirier C, Jiang Y, Liu J, Sandusky GE *et al.* The systemic activin response to pancreatic cancer: implications for effective cancer cachexia therapy. *Journal of Cachexia, Sarcopenia and Muscle* 2019;**10**:1083–1101.

133. Zhou X, Wang JL, Lu J, Song Y, Kwak KS, Jiao Q *et al.* Reversal of Cancer Cachexia and Muscle Wasting by ActRIIB Antagonism Leads to Prolonged Survival. *Cell* 2010;**142**:531–543.

134. Guo T, Bond ND, Jou W, Gavrilova O, Portas J, McPherron AC. Myostatin Inhibition Prevents Diabetes and Hyperphagia in a Mouse Model of Lipodystrophy. *Diabetes* 2012;**61**:2414–2423.

135. Guo W, Wong S, Bhasin S. AAV-Mediated Administration of Myostatin Pro-Peptide Mutant in Adult Ldlr Null Mice Reduces Diet-Induced Hepatosteatosis and Arteriosclerosis. *PLOS ONE* 2013;**8**:e71017.

136. Hayashi Y, Mikawa S, Ogawa C, Masumoto K, Katou F, Sato K. Myostatin expression in the adult rat central nervous system. *Journal of Chemical Neuroanatomy* 2018;**94**:125–138.

137. Czaja W, Nakamura YK, Li N, Eldridge JA, DeAvila DM, Thompson TB *et al.* Myostatin regulates pituitary development and hepatic IGF1. *American Journal of Physiology-Endocrinology and Metabolism* 2019;**316**:E1036–E1049.

138. Wang R, Jiao H, Zhao J, Wang X, Lin H. Glucocorticoids Enhance Muscle Proteolysis through a Myostatin-Dependent Pathway at the Early Stage. *PLOS ONE* 2016;**11**:e0156225.

139. Gilson H, Schakman O, Combaret L, Lause P, Grobet L, Attaix D *et al.* Myostatin gene deletion prevents glucocorticoid-induced muscle atrophy. *Endocrinology* 2007;**148**:452–460.

140. Cipriano SC, Chen L, Kumar TR, Matzuk MM. Follistatin is a modulator of gonadal tumor progression and the activin-induced wasting syndrome in inhibin-deficient mice. *Endocrinology* 2000;**141**:2319–2327.

141. Coerver KA, Woodruff TK, Finegold MJ, Mather J, Bradley A, Matzuk MM. Activin signaling through activin receptor type II causes the cachexia-like symptoms in inhibin-deficient mice. *Mol Endocrinol* 1996;**10**:534–543.

142. Kumar TR, Palapattu G, Wang P, Woodruff TK, Boime I, Byrne MC *et al.* Transgenic models to study gonadotropin function: the role of follicle-stimulating hormone in gonadal growth and tumorigenesis. *Mol Endocrinol* 1999;**13**:851–865.

143. Li Q, Kumar R, Underwood K, O'Connor AE, Loveland KL, Seehra JS *et al.* Prevention of cachexia-like syndrome development and reduction of tumor progression in inhibin-deficient mice following administration of a chimeric activin receptor type II-murine Fc protein. *Mol Hum Reprod* 2007;**13**:675–683.

144. Pufall MA. Glucocorticoids and Cancer. *Adv Exp Med Biol* 2015;**872**:315–333.

145. Oray M, Samra KA, Ebrahimiadib N, Meese H, Foster CS. Long-term side effects of glucocorticoids. *Expert Opinion on Drug Safety* 2016;**15**:457–465.

146. Braun TP, Szumowski M, Levasseur PR, Grossberg AJ, Zhu X, Agarwal A *et al.* Muscle Atrophy in Response to Cytotoxic Chemotherapy Is Dependent on Intact Glucocorticoid Signaling in Skeletal Muscle. *PLOS ONE* 2014;**9**:e106489.

147. Limberaki E, Eleftheriou P, Gasparis G, Karalekos E, Kostoglou V, Petrou C. Cortisol levels and serum antioxidant status following chemotherapy. *Health* 2012.

148. Dev R, Hui D, Dalal S, Nooruddin ZI, Yennurajalingam S, Del Fabbro E *et al.* Association Between Serum Cortisol and Testosterone Levels, Opioid Therapy, and Symptom Distress in Patients with Advanced Cancer. *Journal of Pain and Symptom Management* 2011;**41**:788–795.

Supplemental information

SUPPLEMENTAL METHODS

LLC tumor-bearing mice used here were previously generated [41]. Briefly, 15-week-old mice were subcutaneously inoculated with LLC cells (n=12) or DPBS (n=8). Tissues were removed 35 days thereafter.

KEY RESOURCES TABLE

REAGENT or RESOURCE	SOURCE	IDENTIFIER
Antibodies		
Rabbit Anti-Mouse Laminine	Sigma-Aldrich	Cat#L9393; RRID:AB_477163
Goat anti-Rabbit IgG (H+L) Cross-Adsorbed Secondary polyclonal antibody, Alexa Fluor 488	Thermo Fisher Scientific	Cat# A-11008, RRID:AB_143165
Rabbit Anti-phospho-S6 Ribosomal Protein (Ser235/236) monoclonal antibody	Cell Signaling	Cat#4856; RRID:AB_2181037
Rabbit Anti-4EBP1 polyclonal antibody	Cell Signaling	Cat#9452; RRID:AB_331692
Rabbit Anti-DDIT4 polyclonal antibody	Proteintech	Cat# 10638-1-AP; RRID:AB_2245711
Rabbit Anti-PGC1A, C-Terminal (777-797) polyclonal antibody	Millipore	Cat#516557; RRID:AB_2268432
Rabbit Anti-Phospho-TORC2/CRTC2(Ser171) Polyclonal Antibody	Bioss	Cat# bs-3415R; RRID:AB_10856186
Rabbit Anti-PCK1 polyclonal antibody	Cayman Chemical	Cat#10004943; RRID:AB_10141789
Rabbit Anti-CREB (48H2) monoclonal antibody	Cell Signaling	Cat# 9197; RRID:AB_331277
Rabbit Phospho-CREB (Ser133) (87G3) monoclonal antibody	Cell Signaling	Cat# 9198, RRID:AB_2561044
Goat Anti-Rabbit Immunoglobulins/HRP polyclonal antibody	Agilent	Cat# P0448, RRID:AB_2617138
Chemicals, Peptides, and Recombinant Proteins		
Dexamethasone	Sigma	Cat#50-02-2
Paraformaldehyde	Sigma	Cat#158-127
Methyle blue	Sigma	Cat#M9140
Q Path® OCT	VWR	Cat#00411243
Vectashield Hard Set Mounting Medium	Vector Laboratories	Cat# H-1400, RRID:AB_2336787
RIPA buffer	Cell Signaling	Cat#9806
cOmplete™, Mini Protease Inhibitor Cocktail	Roche	Cat#11836153001
Phosphatase inhibitor PhosSTOP™	Roche	Cat#4906837001
8-16% TGX™ Stain Free SDS-PAGE precast gel	Bio-Rad	Cat#456-8103
Electrophoresis buffer	Bio-Rad	Cat#1610732
Laemmli Buffer	Bio-Rad	Cat#161-0747
Regilait	Casino	
BSA	Affymetrix	Cat#9048-46-8

Clarity Max Western ECL Substrate	Bio-Rad	Cat#1705062
Critical Commercial Assays		
Corticosterone enzyme immunoassay	MyBiosource	Cat#MBS494312
ß-hydroxybutyrate colorimetric assay kit	APExBIO	Cat#K2136
RNA extraction kit	Macherey Nagel	Cat#740406.50
Reverse Transcriptase Core kit	Eurogentec	Cat#RT-RTCK-03
Takyon™ No Rox SYBR® MasterMix dTTP Blue	Eurogentec	Cat#UF-NSMT-B0701
DC protein assay	Bio-Rad	Cat#5000113 and 5000114
Trans-Blot® Turbo™ RTA Mini Nitrocellulose Transfer Kit	Bio-Rad	Cat#1704270
Experimental Models: Organisms/Strains		
Mouse: WT C57Bl/6J		RRID:IMSR_JAX:000664
Mouse: *Apc*$^{Min/+}$ (*Apc*)	The Jackson Laboratory	RRID:IMSR_JAX:002020
Mouse: *Myostatin* knock-out (KO)	Gift (Anne Bonnieu, Montpellier University, France)	
Mouse: ApcKO	This publication	N/A
Oligonucleotides		
Primers, see TableS5	Eurogentec	N/A
Software and Algorithms		
ImageJ		https://imagej.nih.gov/ij/; RRID:SCR_003070
DMC	Aurora Scientific	N/A
DMA	Aurora Scientific	N/A
Image Lab™ version 6.0	Bio-Rad	https://www.bio-rad.com/fr-fr/product/image-lab-software?ID=KRE6P5E8Z; RRID:SCR_014210
GraphPad Prism version 7.0	GraphPad	https://www.graphpad.com/; RRID:SCR_002798
R version 3.6.3		https://www.r-project.org/; RRID:SCR_001905
GeneOverlap R package		RRID:SCR_018419
Other		
FreeStyle Optium Neo H glucometer	Abbott	Cat#71355-80
Accutrend® Plus	Roche	Cat#05050499016
Leica CM1950 cryostat	Leica Biosystems	N/A
Zeiss Axio Imager 2 Microscope	Zeiss	RRID:SCR_018876
Aurora 1300A	Aurora Scientific	N/A
BioSpec-Nano	Shiladzu	N/A
CFX96 Real-Time System	Bio-Rad	N/A
Trans-Blot® Turbo™ Transfer System	Bio-Rad	Cat#1704150
ChemiDoc MP Imaging System	Bio-Rad	Cat#17001402

SUPPLEMENTAL FIGURES

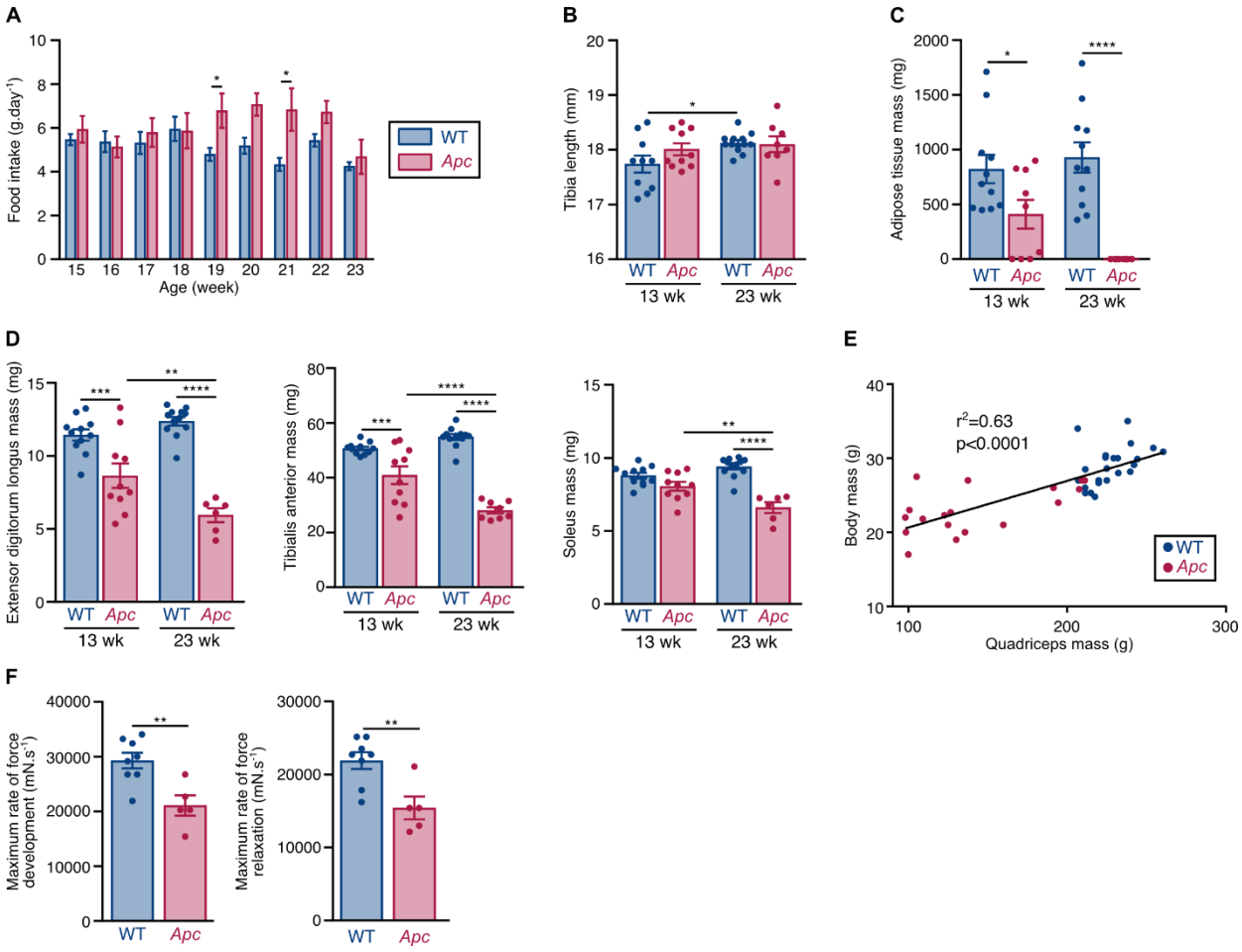

Figure S1. *Apc* mice recapitulate the main features of cancer cachexia

(A) Food intake in WT (n=14) and *Apc* (n=14) mice.

(B) Tibia length of WT and *Apc* mice at 13 (WT n=10; *Apc* n=10) and 23 (WT n=12; *Apc* n=8) weeks.

(C) Adipose tissue mass of WT and *Apc* mice at 13 (WT n=11; *Apc* n=10) and 23 weeks (WT n=11; *Apc* n=8).

(D) *Extensor digitorum longus* (left), *tibialis anterior* (center) and *soleus* (right) muscle mass of WT and *Apc* mice at 13 (WT n=11; *Apc* n=10) and 23 (WT n=12; *Apc* n=8) weeks.

(E) Pearson correlation between body mass and *quadriceps* muscle mass in 13WT (n=23) and *Apc* (n=18) mice aged at 13 and 23 weeks.

(F) The maximum rate of force development (+dP/dTmax) and maximum rate of relaxation (-dP/dTmax) during a twitch of *tibialis anterior* muscle in 23-week-old WT (n=8) and *Apc* (n=5) mice.

Data are represented as mean ± SEM. (A, B, C, and D) data were analyzed by a two-way ANOVA followed by a Sidak's multiple comparison test. (E) Data were analyzed with a Pearson correlation test. (F) data were analyzed by a two-tailed unpaired t-test.*p <0.05, **p < 0.01, ***p < 0.001 and ****p < 0.0001.

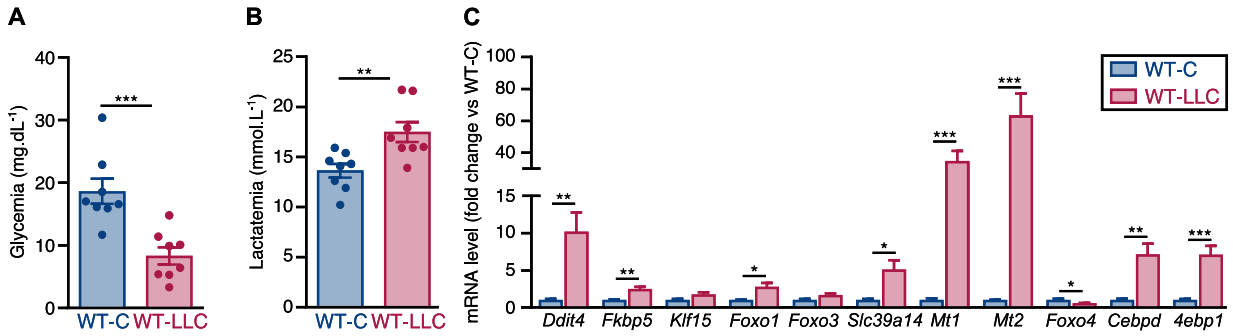

Figure S2. Alteration of circulating glucose and lactate and GC-dependent transcriptional response in *gastrocnemius* muscle in LLC mice

(A) Glucose blood level in 15-week-old mice 35 days after DPBS (WT-C, n=8) or LLC cells (WT-LLC, n=8) inoculation.
(B) Lactate blood level in 15-week-old mice 35 days after DPBS (n=8) or LLC cells (n=8) inoculation.
(C) RT-qPCR analysis of glucocorticoid-responsive gene mRNA level in *gastrocnemius* muscle of WT-C (n=8) and WT-LLC (n=12) mice.

Data are represented as mean ± SEM. Data were analyzed by a two-tailed unpaired t-test with Welch's correction when necessary. *p<0.05, **p < 0.01 and ***p < 0.001.

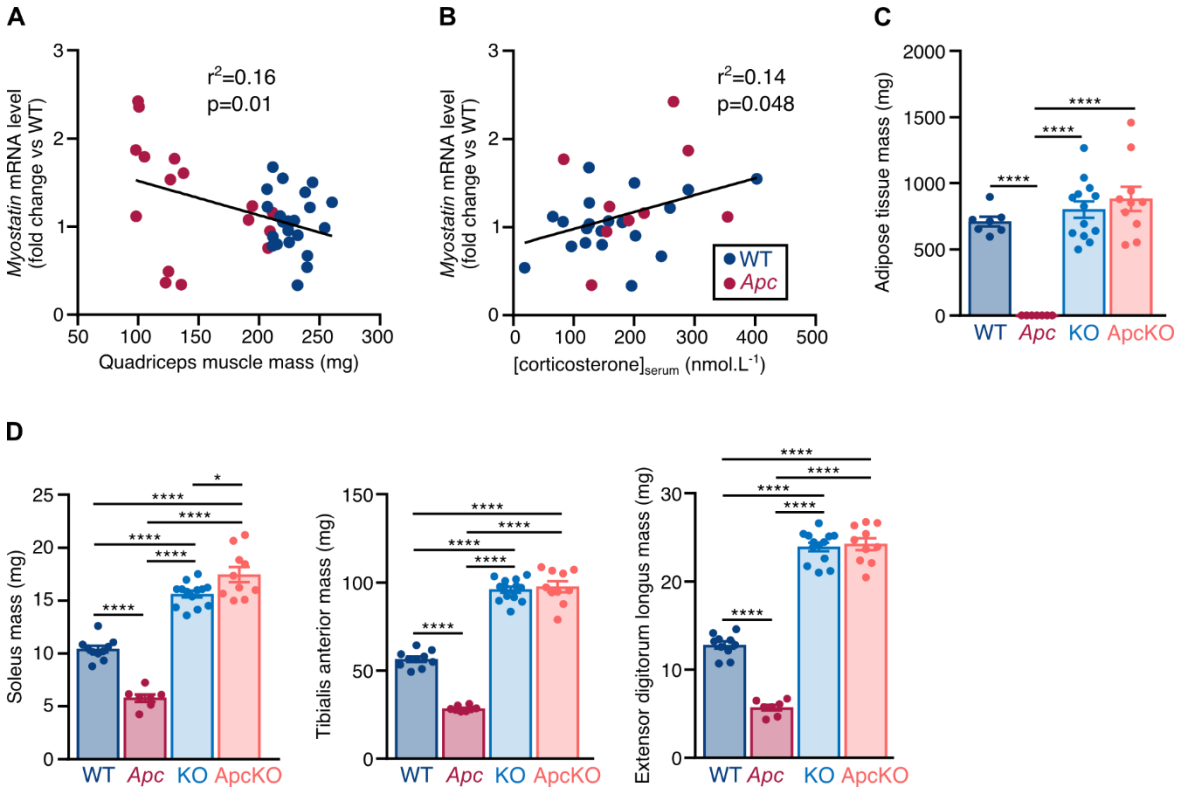

Figure S3. Myostatin gene invalidation prevents loss of muscle and adipose tissue mass in *Apc* mice during cancer cachexia

(A) Pearson correlation between circulating *Mstn* mRNA level and quadriceps muscle mass in 13- and 23-week-old WT (n=23) and *Apc* (n=16) mice.

(B) Pearson correlation between circulating *Mstn* mRNA level and circulating corticosterone in 13- and 23-week-old WT (n=20) and *Apc* (n=9) mice.

(C) Adipose tissue mass of WT (n=7), *Apc* (n=7), KO (n=13) and ApcKO (n=10) mice at 23 weeks.

(D) *Soleus* (left), *tibialis anterior*, (middle) and *extensor digitorum longus* (right) muscle mass of WT (n=10), *Apc* (n=7 or 8), KO (n=13) and ApcKO (n=10) mice at 23 weeks.

Data are represented as mean ± SEM. (A and B) data were analyzed with a Pearson correlation test. (C and D) data were analyzed by one-way ANOVA. * represents a significant difference after Tukey's multiple comparison test. *p <0.05 or ****p < 0.0001.

SUPPLEMENTAL TABLES

Table S1. qPCR primer details.

Genes	Sequence accession number	Sequence (5'-3')	Amplicon length (bp)	Concentration (nM)	Annealing temperature (°C)	Sample
Abhd5	NM_026179.2	Fwd: GGCTTCGAGGTGTGTCCC	130	400	62	Liver *Apc*
		Rev: GACACCAGGTAGGAAGCCAC		400	62	Liver DEX
Acacb	NM_133904.2	Fwd: GCTCAAGATCGAGGAGTCGG	148	400	63.2	Liver *Apc*
		Rev: GTTGGTGATGAAGAGGCGGA		400	60	Liver DEX
Acly	NM_134037.3	Fwd: CAGCCAAGGCAATTTCAGAGC	195 on 2 exons	400	60	Liver *Apc*
		Rev: CTCGACGTTTGATTAACTGGTCT		400	60	Liver DEX
Actb	NM_007393.3	Fwd: AGCAAGCAGGAGTACGATGAG	80	400	60	Liver *Apc*
				400	60	Liver DEX
		Rev: AACGCAGCTCAGTAACAGTC		400	60	Adrenal glands *Apc*
				400	60	Hypothalamus *Apc*
Akr1d1	NM_145364.2	Fwd: AAGACAGCTATTGATGAGGGGT	114	400	60	Liver *Apc*
		Rev: CCTCTTTACCTTCCCTTCTGCTA				
Arg1	NM_007482.3	Fwd: GTACATTGGCTTGCGAGACG	103	400	62	Liver *Apc*
		Rev: GCCAATCCCCAGCTTGTCTA		400	62	Liver DEX
Asl	NM_133768.5	Fwd: TGGGCTGGGGGATTTGTTG	93	400	60	Liver *Apc*
		Rev: TCCTGTCTCTCTTTGCATTGGC		400	60	Liver DEX
Ass1	NM_007494.3	Fwd: CGTGAAGGGGCCAAGTATGT	89	400	60	Liver *Apc*
		Rev: GGTGCCAGTGAATAGCAGGT		400	60	Liver DEX
Atg4b	NM_174874.3	Fwd: ACAGATGATCTTTGCCCAGG	179	400	62	*Quadriceps Apc*
		Rev: TAGACTTGCCTTCGCCAACT		300	62	*Quadriceps* DEX
Atg5	NM_053069.5	Fwd: TGAAAGAGTGTGTCCTCCTC	91	500	60	*Quadriceps Apc*
		Rev: GCCTCCACTGAACTTGACTG		500	62	*Quadriceps* DEX
Bcat2	NM_009737.3	Fwd: CCTGCTCTGGTCTGCACTAC	116 on 2 exons	400	55	*Quadriceps Apc*
		Rev: ACGTAGCATCCTGTCCATGTT		400	62	*Quadriceps* DEX
Bdh1	NM_001122683.1	Fwd: GGTGGAACCTGGCAACTTCAT	151	400	60	Liver *Apc*

		Rev: GGTCATCCCACATCTTCTTGG		400	60	Liver DEX
Bnip3	NM_009760.4	Fwd: AGATTGGATATGGGATTGGTCAAG	121	400	60	*Quadriceps Apc*
		Rev: CCCTTTCTTCATAACGCTTGTG		500	62	*Quadriceps* DEX
Cebpd	NM_007678.3	Fwd: TACCGAGTAGGGGGAGCAAA Rev: TCATTTTTCTCACGGGGCCA	93	500	64	*Quadriceps Apc*
				500	64	*Quadriceps* DEX
				400	63	Liver *Apc*
				400	63	Liver DEX
				500	64	*Gastrocnemius* LLC
Cps1	NM_001080809.2	Fwd: ACAGCTTTCTTTCACACTGGTT	148	400	60	Liver *Apc*
		Rev: CCAAAGCCACTCTTCAGGGTC		400	60	Liver DEX
Cpt1a	NM_013495.2	Fwd: CTCCGCCTGAGCCATGAAG	100	400	58	Liver *Apc*
		Rev: CACCAGTGATGATGCCATTCT		400	58	Liver DEX
Cpt2	NM_009949.2	Fwd: TGTGAGCGGAAGATCCCAAC	80	400	62	Liver *Apc*
		Rev: GCTTTCCAACCCGATCTCCT		600	62	Liver DEX
Crh	NM_205769.3	Fwd: TCTCACCTTCCACCTTCTGC	118	400	58	Hypothalamus *Apc*
		Rev: AAGCGCAACATTTCATTTCC		400	58	Hypothalamus DEX
Cyp11b1	NM_001033229.3	Fwd: CTGAACCCAAATGTTCTGTCACC Rev: CAAAGTCCCTTGCTATCCCATC	76	400	60	Adrenal glands *Apc*
Cyp21a1	NM_009995.2	Fwd: GCAAAGGGATGGCAAAGACG Rev: GGATCTCAGGGTGGTGAAGC	143	400	63	Adrenal glands *Apc*
Ddit4	NM_029083.2	Fwd: GTGCTGCGTCTGGACTCTC Rev: CCGGTACTTAGCGTCAGGG	107 on 3 exons	200	60	*Quadriceps Apc*
				200	60	*Quadriceps* DEX
				200	60	Liver *Apc*
				200	60	Liver DEX
				200	60	*Gastrocnemius* LLC
Fasn	NM_007988.3	Fwd: GGAGGTGGTGATAGCCGGTAT	140 on 2 exons	400	58	Liver *Apc*
		Rev: TGGGTAATCCATAGAGCCCAG		400	58	Liver DEX
Fbp1	NM_019395.3	Fwd: AGGAAGCACAAAGCCAAGTGAAGG	164	400	60	Liver *Apc*
		Rev: TGAGGATGAAGTGACCTTGGGCAT		400	60	Liver DEX
Fkbp5	NM_010220.4	Fwd: TGAGGGCACCAGTAACAATGG	172 on 2 exons	400	60	*Quadriceps Apc*
		Rev: CAACATCCCTTTGTAGTGGACAT		400	60	*Quadriceps* DEX

				300	60	Liver *Apc*
				400	60	Liver DEX
				500	60	Hypothalamus *Apc*
				400	60	*Gastrocnemius* LLC
Foxo1	NM_019739.3	Fwd: TACGAGTGGATGGTGAAGAG Rev: TCTTGCCTCCCTCTGGATTG	178	400	60	*Quadriceps Apc*
				400	60	*Quadriceps* DEX
				300	60	Liver *Apc*
				400	60	Liver DEX
				400	60	*Gastrocnemius* LLC
Foxo3	NM_019740.2	Fwd: GGAAATGGGCAAAGCAGA Rev: AAACGGATCACTGTCCACTTG	94 on 2 exons	400	60	*Quadriceps Apc*
				400	60	*Quadriceps* DEX
				400	60	*Gastrocnemius* LLC
				400	60	Liver *Apc*
				400	60	Liver DEX
Foxo4	NM_018789.2	Fwd: CGGAGTGAAAGGGACAGTTTAG Rev: CCCTGTGGCTGACTTCTTATTC	195	400	58	*Quadriceps Apc*
				400	58	*Quadriceps* DEX
				300	60	Liver *Apc*
				400	58	Liver DEX
				400	60	*Gastrocnemius* LLC
Gk	NM_008194.3	Fwd: TGAACCTGAGGATTTGTCAGC Rev: CCATGTGGAGTAACGGATTTCG	88	400	60	Liver *Apc*
				250	60	Liver DEX
Gpd2	NM_001145820.2	Fwd: GACTCTCTCCGTTTGCTCATTAC Rev: GGATGTCAAATTCGGGTGTGT	150 on 2 exons	400	60	Liver *Apc*
				400	60	Liver DEX
G6pc	NM_008061.4	Fwd: ACTGTGGGCATCAATCTCCT Rev: CGTTGTCCAAACAGAATCCA	83 on 2 exons	400	60	Liver *Apc*
				400	60	Liver DEX
Hadh	NM_008212.4	Fwd: TGGAGTGGTGGGCAAATACC Rev: GAAGGACGGACAGTGATGGT	93	400	62	Liver *Apc*
				400	62	Liver DEX
Hmgcs2	NM_008256.4	Fwd: TATGGGCTTCTGTTCAGTCCA Rev: AGCACTGTTTTGACAGCCTTG	159	400	60	Liver *Apc*
				400	60	Liver DEX
Hprt	NM_013556.2	Fwd: CAGGCCAGACTTTGTTGGAT Rev: TTGCGCTCATCTTAGGCTTT	147 on 3 exons	400	60	*Quadriceps Apc*
				400	60	*Quadriceps* DEX

				400	60	Liver *Apc*
				400	60	Liver DEX
				400	60	Adrenal glands *Apc*
Hsd11b1	NM_008288.2	Fwd: GGAGCCCATGTGGTATTGACT Rev: CCGCAAATGTCATGTCTTCCAT	127	400	60	*Quadriceps Apc*
H6pd	NM_173371.4	Fwd: AGTGGAGGACTATCAGACCCT Rev: GGCGGCACACTGAAGTAGAAG	99	400	60	*Quadriceps Apc*
Klf9	NM_010638.5	Fwd: TGGAGAGTCCCGATGAGGATA Rev: GAGGCGTGTTTCCCCTTCG	160	400	60	Liver *Apc*
				400	60	Liver DEX
Klf15	NM_023184.3	Fwd: GAGACCTTCTCGTCACCGAAA Rev: GCTGGAGACATCGCTGTCAT	117	400	60	*Quadriceps Apc*
				400	59	*Quadriceps* DEX
				400	60	Liver *Apc*
				400	60	Liver DEX
				400	60	*Gastrocnemius* LLC
Lc3b	NM_026160.4	Fwd: CACTGCTCTGTCTTGTGTAGGTTG Rev: TCGTTGTGCCTTTATTAGTGCATC	170	400	62	*Quadriceps Apc*
				400	62	*Quadriceps* DEX
Lipe	NM_010719.5	Fwd: CCAGCCTGAGGGCTTACTG Rev: CTCCATTGACTGTGACATCTCG	106	400	58	Liver *Apc*
				400	58	Liver DEX
MAFbx	NM_026346.2	Fwd: GTTTTCAGCAGGCCAAGAAG Rev: TTGCCAGAGAACACGCTATG	115	400	60	*Quadriceps Apc*
				400	60	*Quadriceps* DEX
				400	60	*Gastrocnemius* LLC
Mc2r	NM_008560.3	Fwd: TATGTTCCGGCCTTTCCTGC Rev: CCTCTCCTTGGCTTTGTCACT	150	500	60	Adrenal glands *Apc*
Mlxipl	NM_021455.4	Fwd: AGATGGAGAACCGACGTATCA Rev: ACTGAGCGTGCTGACAAGTC	104 on 2 exons	400	60	Liver *Apc*
				400	60	Liver DEX
Mgll	NM_011844.4	Fwd: GTGCTCGGGGAACGTGAC Rev: ACTGTCCGTCTGCATTGACC	142	300	60	Liver *Apc*
				300	60	Liver DEX
Mstn	NM_010834.3	Fwd: TTGGGCTTGACTGCGATGAG Rev: GGCTTCAAAATCGACCGTGAG	74 on 3 exon	400	60	*Quadriceps Apc*
				400	60	*Quadriceps* DEX
Mt1	NM_013602.3	Fwd: AGATCTCGGAATGGACCCCA Rev: AGGAGCAGCAGCTCTTCTTG	116	400	62	*Quadriceps Apc*
				400	62	*Quadriceps* DEX

				400	62	Liver *Apc*
				600	60	Liver DEX
				400	62	*Gastrocnemius* LLC
Mt2	NM_008630.2	Fwd: CTGCAAAGAGGCTTCCGACA Rev: GTGGAGAACGAGTCAGGGTT	125	400	62	*Quadriceps Apc*
				400	62	*Quadriceps* DEX
				400	62	Liver *Apc*
				400	62	Liver DEX
				400	62	*Gastrocnemius* LLC
MuRF1	NM_001039048.2	Fwd: ACCTGCTGGTGGAAAACATC Rev: AGGAGCAAGTAGGCACCTCA	147	300	60	*Quadriceps Apc*
				300	60	*Quadriceps* DEX
				300	60	*Gastrocnemius* LLC
Nr3c1	NM_008173.3	Fwd: CAAAGATTGCAGGTATCCTATGAA Rev: TGGCTCTTCAGACCTTCCTT	89 on 2 exons	400	58	*Quadriceps Apc*
				400	58	*Gastrocnemius* LLC
Otc	NM_008769.4	Fwd: TTAGTGTTCCCAGAGGCAGAG Rev: GGAGCACAGGTGAGTAGTCTG	85	500	60	Liver *Apc*
				500	60	Liver DEX
Papss2	NM_001201470.1	Fwd: GACCAGCAAAAATCCACCAATG Rev: CACACGGTACATCCTCGGAAT	107	500	60	Liver *Apc*
Pck1	NM_011044.2	Fwd: GTGCTGGAGTGGATGTTCGG Rev: CTGGCTGATTCTCTGTTTCAGG	258	400	60	Liver *Apc*
				400	60	Liver DEX
Pcx	NM_001162946.1	Fwd: AATGTCCGGCGTCTGGAGTA Rev: ACGCACGAAACACTCGGAT	85 on 2 exons	400	60	Liver *Apc*
				400	60	Liver DEX
Pklr	NM_013631.2	Fwd: CCCGAGATACGCACTGGAG Rev: CGACCTGGGTGATATTGTGGT	154 on 2 exons	400	60	Liver *Apc*
				400	60	Liver DEX
PnPla2	NM_001163689.1	Fwd: TGTGCAAACAGGGCTACAG Rev: AAGGGTTGGGTTGGTTCAG	72	300	60	Liver *Apc*
				200	60	Liver DEX
Ppara	NM_011144.6	Fwd: TACTGCCGTTTTCACAAGTGC Rev: AGGTCGTGTTCACAGGTAAGA	122 on 2 exons	400	60	Liver *Apc*
				400	60	Liver DEX
Pgc1a	NM_008904.2	Fwd: TATGGAGTGACATAGAGTGTGCT Rev: CCACTTCAATCCACCCAGAAAG	134 on 2 exons	400	60	Liver *Apc*
				400	60	Liver DEX
Ppia	NM_008907.1	Fwd: AGCATACAGGTCCTGGCA TC Rev: TTCACCTTCCCAAAGACCAC	127 on 2 exon	500	60	*Quadriceps Apc*
				500	60	*Quadriceps* DEX

Scd1	NM_009127.4	Fwd: TGGAGCCACAGAACTTACAAG	93 on 2 exons	400	60	Liver *Apc*
		Rev: CCATTCGTACACGTCATTCTG		400	60	Liver DEX
Slc2a2	NM_031197.2	Fwd: TGTGCTGCTGGATAAATTCGCCTG	109 on 2 exons	500	60	Liver *Apc*
		Rev: AACCATGAACCAAGGGATTGGACC		500	60	Liver DEX
Srebf1	NM_001358315.1	Fwd: TGACCCGGCTATTCCGTGA	61	400	60	Liver *Apc*
		Rev: CTGGGCTGAGCAATACAGTTC		300	60	Liver DEX
Srd5a1	NM_175283.3	Fwd: CTGTTCACCTTTGTCTTGGCC	83	400	60	Liver *Apc*
		Rev: TACACCGCAAACTGGCTCAAG				
Tuba1	NM_011653.2	Fwd: TGAGGAGGTTGGTGTGGATTC	99	400	60	Hypothalamus *Apc*
		Rev: AAACATCCCTGTGGAAGCAG				
Ugt2b35	NM_172881.3	Fwd: CCTGCTAAGCCCTTGCCTAAG	124 on 2 exons	400	60	Liver *Apc*
		Rev: AAATTGCGTTGGCCCTTTCTT				
Ugt2b36	NM_001029867.1	Fwd: GTATGGCCGGTGGACTACAG	213	500	60	Liver *Apc*
		Rev: AGTCCATCTTTCCACAGCCTT				
Slc39a14	NM_144808.4	Fwd: CCTCAGGACAATTACGTCTCCA	111 on 2 exon	400	60	*Quadriceps Apc*
				400	60	*Quadriceps* DEX
		Rev: ATGGTGCTCGTTTTTCTGCTT		500	60	Liver *Apc*
				500	60	Liver DEX
				400	55	*Gastrocnemius* LLC
4ebp1	NM_007918.4	Fwd: GGGGACTACAGCACCACTC	171	400	62	*Quadriceps Apc*
		Rev: CTCATCGCTGGTAGGGCTA		400	60	*Quadriceps* DEX

Fwd, forward; Rev, reverse.

Table S2. Differentially expressed genes in *quadriceps* muscle of 13- and 23-week-old *Apc* mice and WT-DEX mice.

Gene	*Apc* 13 wk vs WT 13wk		*Apc* 23 wk vs WT 23wk		WT-DEX vs WT-CTL	
	p	Difference between means	p	Difference between means	p	Difference between means
Atg4b	**0.0002**	-0.5117 ± 0.1198	0.9573	0.01606 ± 0.2955	0.1418	-0.2058 ± 0.1339
Atg5	**0.0471**	-0.2159 ± 0.1017	0.5993	-0.08255 ± 0.1542	**0.0425**	0.8525 ± 0.02693
Bcat2	0.4262	-0.2914 ± 0.2514	0.5132	-0.1846 ± 0.2764	0.4239	0.0781 ± 0.1134
Bnip3	0.1734	1.671 ± 0.8811	**0.0235**	2.279 ± 0.7642	**0.0001**	0.4901 ± 0.0734
Cebpd	0.6275	-0.1046 ± 0.2113	**0.0146**	8.039 ± 2.383	**0.0001**	6.768 ± 0.5376
Ddit4	0.4678	-0.2047 ± 0.2752	**0.0123**	21.54 ± 6.103	**0.0001**	17.8 ± 0.9272
4ebp1	**0.0355**	3.822 ± 1.549	**0.0175**	6.488 ± 2.009	**0.0003**	1.551 ± 0.2967
Fkbp5	0.1135	0.8433 ± 0.4688	**0.0053**	5.11 ± 1.205	**0.0001**	7.3 ± 0.3204
Foxo1	0.1119	2.616 ± 1.69	**0.0041**	6.237 ± 1.389	**0.0001**	4.272 ± 0.2011
Foxo3	0.5447	0.152 ± 0.2426	**0.0051**	1.842 ± 0.4576	**0.0001**	0.9325 ± 0.1293
Foxo4	0.2476	0.3345 ± 0.2725	0.6715	0.08066 ± 0.1869	0.1271	0.1218 ± 0.07591
Klf15	0.4561	1.065 ± 0.6526	**0.0084**	3.22 ± 0.8484	**0.0001**	2.163 ± 0.185
Lc3b	0.2828	0.3173 ± 0.287	**0.0194**	0.6627 ± 0.3102	**0.0004**	0.2209 ± 0.05058
MAFbx	0.6027	1.789 ± 1.122	**0.0176**	3.265 ± 1.016	0.97	-0.0053 ± 0.139
Mstn	0.6117	0.1204 ± 0.2331	0.111	0.3903 ± 0.217	**0.0001**	0.572 ± 0.1035
Mt1	**0.0028**	37.17 ± 13.48	**0.0101**	54.86 ± 14.82	**0.0001**	6.717 ± 1.022
Mt2	**0.0068**	33.31 ± 11.38	**0.0001**	76.36 ± 23.23	**0.0001**	11.49 ± 1.626
MuRF1	0.4561	2.285 ± 1.49	**0.0131**	6.053 ± 1.745	**0.0001**	2.257 ± 0.1443
Slc39a14	0.2014	2.493 ± 1.677	**0.0259**	7.293 ± 2.484	**0.0001**	12.27 ± 0.7318

Table S3. Differentially expressed genes in liver of 13- and 23-week-old *Apc* mice and WT-DEX mice.

Gene	*Apc* 13 wk vs WT 13wk		*Apc* 23 wk vs WT23wk		WT-DEX vs WT-CTL	
	p	Difference between means	p	Difference between means	p	Difference between means
Abhd5	0.3342	-0.1782 ± 0.1799	0.8411	-0.06006 ± 0.295	0.9094	0.0144 ± 0.1241
Acacb	**0.0008**	-0.5062 ± 0.1265	**0.0001**	-0.7355 ± 0.1214	**0.0178**	0.6254 ± 0.2238
Acly	0.0853	-0.3354 ± 0.1848	0.1469	-0.3128 ± 0.1917	**0.0002**	-0.694 ± 0.125
Arg1	0.4561	0.2472 ± 0.2601	**0.0034**	1.57 ± 0.3481	0.5650	0.0603 ± 0.1029
Asl	0.4421	-0.2866 ± 0.3653	0.0779	0.7183 ± 0.3515	**0.0001**	0.9286 ± 0.1298
Ass1	**0.0041**	-0.3791 ± 0.1153	**0.0226**	-0.3367 ± 0.1343	0.6688	0.0373 ± 0.08575
Bdh1	**0.0112**	-0.4549 ± 0.162	**0.0001**	-0.8303 ± 0.07848	**0.0001**	-0.4858 ± 0.08533
Cebpd	0.1519	1.08 ± 0.4841	**0.0026**	3.72 ± 0.7895	**0.0001**	2.487 ± 0.2671
Cps1	**0.0014**	-0.4156 ± 0.1111	0.1276	-0.1727 ± 0.1078	**0.0004**	0.3628 ± 0.08429
Cpt1a	**0.0397**	-0.213 ± 0.09564	0.4143	0.2227 ± 0.2576	0.6044	-0.0769 ± 0.1458

Cpt2	**0.0132**	-0.3543 ± 0.1295	**0.0001**	-0.5917 ± 0.07532	**0.0067**	0.3336 ± 0.1088
Ddit4	0.0882	6.809 ± 3.51	**0.0410**	22.79 ± 8.785	**0.0001**	40.78 ± 3.537
Fasn	0.0924	-0.4432 ± 0.2501	**0.0114**	-0.4864 ± 0.1714	**0.0022**	-0.748 ± 0.1781
Fbp1	0.1820	-0.1307 ± 0.09438	**0.0001**	-0.2318 ± 0.0462	0.1831	0.06 ± 0.04334
Fkbp5	**0.0233**	3.286 ± 1.208	**0.0039**	8.976 ± 1.976	**0.0001**	14.28 ± 0.5006
Foxo1	0.2446	0.4148 ± 0.3371	**0.0069**	3.721 ± 0.934	**0.0001**	0.9722 ± 0.1458
Foxo3	**0.0389**	-0.3324 ± 0.1492	0.1516	0.6327 ± 0.3883	**0.0003**	0.5966 ± 0.1316
Foxo4	**0.0009**	-0.537 ± 0.1264	0.0711	-0.3221 ± 0.1673	0.4505	-0.0984 ± 0.1276
G6pc	**0.0390**	-0.3647 ± 0.1639	0.2256	-0.3052 ± 0.2421	0.7595	0.0663 ± 0.2133
Gk	**0.0162**	-0.267 ± 0.1012	0.0567	-0.2999 ± 0.134	0.6292	0.0381 ± 0.07755
Gpd2	0.0766	-0.2865 ± 0.1525	**0.0107**	-0.358 ± 0.1248	**0.0001**	-0.5166 ± 0.06027
Hadh	0.0789	-0.2503 ± 0.1348	**0.0085**	-0.3668 ± 0.1234	**0.0005**	-0.2963 ± 0.06858
Hmgcs2	**0.0003**	-0.4754 ± 0.1082	**0.0001**	-0.5463 ± 0.09794	0.0890	0.169 ± 0.094
Klf9	0.3522	0.2459 ± 0.2571	**0.0287**	1.443 ± 0.5141	0.3527	0.0745 ± 0.1403
Klf15	0.2893	-0.1891 ± 0.1735	0.6698	0.1054 ± 0.2429	0.0640	0.1773 ± 0.08514
Lipe	**0.0093**	-0.3795 ± 0.1312	**0.0017**	-0.4821 ± 0.1286	**0.0004**	-0.4989 ± 0.1145
Mgll	0.3304	-0.2102 ± 0.2073	**0.0007**	-0.5872 ± 0.1415	**0.0001**	0.6788 ± 0.1401
Mlxipl	**0.0004**	-0.499 ± 0.1176	**0.0001**	-0.7142 ± 0.07503	**0.0001**	-0.4692 ± 0.0761
Mt1	**0.0001**	84.89 ± 35.6	**0.0019**	392.3 ± 74.57	**0.0001**	34.91 ± 3.436
Mt2	**0.0250**	182.5 ± 66.35	**0.0001**	558.1 ± 108.8	**0.0001**	55.34 ± 3.359
Otc	**0.0021**	-0.5708 ± 0.1617	**0.0001**	-0.8398 ± 0.0928	**0.0001**	-0.4113 ± 0.06573
Pck1	0.2989	0.4853 ± 0.4462	**0.0261**	0.7437 ± 0.3051	**0.0021**	0.9814 ± 0.2495
Pcx	0.3113	0.2398 ± 0.2228	**0.0042**	0.8739 ± 0.1956	**0.0001**	0.6987 ± 0.1139
Pgc1a	0.0618	1.384 ± 0.654	**0.0018**	3.036 ± 0.619	**0.0001**	1.684 ± 0.1621
Pklr	**0.0010**	-0.5365 ± 0.1361	**0.0002**	-0.6082 ± 0.1299	0.3948	-0.1658 ± 0.1902
PnPla2	0.5286	-0.09886 ± 0.1535	**0.0321**	1.441 ± 0.5241	**0.0001**	1.519 ± 0.2615
Ppara	**0.0067**	-0.4094 ± 0.1347	0.1034	-0.2672 ± 0.1552	0.1260	-0.1632 ± 0.1017
Scd1	0.0644	-0.317 ± 0.156	**0.0054**	-0.5508 ± 0.1726	0.0632	0.4929 ± 0.2389
Slc2a2	0.1051	-0.2763 ± 0.1623	**0.0061**	-0.4041 ± 0.1292	**0.0006**	-0.4018 ± 0.09593
Srebf1	0.1542	-0.3993 ± 0.2691	0.2268	-0.2609 ± 0.2905	**0.0001**	-0.8404 ± 0.05443
Slc39a14	0.0610	1.864 ± 0.8741	**0.0035**	2.408 ± 0.5271	**0.0001**	0.7144 ± 0.1367

Table S4. Differentially expressed genes in *Quadriceps* muscle of 23-week-old *Apc* and ApcKO mice.

Gene	*Apc* 23 wk vs WT 23 wk		ApcKO 23 wk vs KO 23 wk	
	p	Difference between means	*p*	Difference between means
4ebp1	**0.0099**	4.59 ± 1.318	**0.0099**	0.3299 ± 0.1302
Atg4b	0.5420	-0.1157 ± 0.1857	0.7717	0.05872 ± 0.1998
Atg5	0.2868	-0.1863 ± 0.1691	0.7767	-0.03512 ± 0.1222

Bcat2	0.1959	-0.2553 ± 0.1891	0.4754	0.1526 ± 0.21
Bnip3	**0.0385**	0.9688 ± 0.4018	0.3547	0.07422 ± 0.07842
Cebpd	**0.0266**	2.09 ± 0.8758	**0.021**	0.8396 ± 0.3398
Ddit4	**0.0003**	2.109 ± 0.4275	0.2543	0.8663 ± 0.4867
Fkbp5	**0.0010**	4.761 ± 0.8241	0.3533	0.1702 ± 0.1793
Foxo1	**0.0070**	2.89 ± 0.7221	0.4112	0.1055 ± 0.1258
Foxo3	**0.0050**	0.8083 ± 0.2462	0.6008	-0.07085 ± 0.1334
Foxo4	0.4029	0.1823 ± 0.2121	0.8330	-0.04629 ± 0.2169
Klf15	**0.0009**	1.353 ± 0.3294	0.9999	0.1441 ± 0.2436
Lc3b	0.1189	0.5024 ± 0.3049	**0.0483**	0.2154 ± 0.1028
MAFbx	**0.0445**	1.323 ± 0.6034	0.0712	0.2091 ± 0.1097
Mt1	**0.0074**	33.48 ± 8.437	**0.0067**	0.485 ± 0.147
Mt2	**0.0063**	53.3 ± 13	0.0715	0.6219 ± 0.3148
MuRF1	**0.0474**	1.407 ± 0.6473	0.4442	-0.08556 ± 0.1097
Slc39a14	0.0920	0.7821 ± 0.499	0.6926	-0.0984 ± 0.1977

Table S5. Differentially expressed genes in liver of 23-week-old *Apc* and ApcKO mice.

Gene	*Apc* 23 wk vs WT 23 wk		ApcKO23 wk vs KO 23 wk	
	p	Difference between means	*p*	Difference between means
Abhd5	0.0988	0.6291 ± 0.4127	**0.0210**	-0.4005 ± 0.1584
Acacb	**0.0001**	-0.6951 ± 0.1209	0.2556	-0.2277 ± 0.1939
Acly	0.3964	-0.1745 ± 0.1995	0.6315	-0.0891 ± 0.1826
Arg1	**0.0088**	1.279 ± 0.3403	0.3022	0.0978 ± 0.09208
Asl	**0.0188**	0.8107 ± 0.3642	0.5415	-0.0892 ± 0.1433
Ass1	0.1198	-0.2435 ± 0.147	0.3548	0.1186 ± 0.1249
Bdh1	**0.0001**	-0.7089 ± 0.1257	0.4372	0.06666 ± 0.08378
Cebpd	**0.0223**	4.36 ± 1.349	0.3370	-0.2451 to 0.6789
Cps1	0.7925	-0.0713 ± 0.1922	0.0565	-0.2658 ± 0.1304
Cpt1a	0.3106	0.3328 ± 0.3003	0.1477	0.2063 ± 0.1364
Cpt2	**0.0001**	-0.6118 ± 0.0588	0.7659	0.0283 ± 0.09363
Ddit4	**0.0093**	20.8 ± 9.134	0.6698	-0.065 ± 0.1913
Fasn	0.1752	-0.3117 ± 0.2183	0.1435	-0.2922 ± 0.1869
Fbp1	**0.0011**	-0.3072 ± 0.07327	**0.0326**	-0.1962 ± 0.08474
Fkbp5	**0.0072**	8.5 ± 1.952	**0.0031**	-0.4493 ± 0.1192
Foxo1	**0.0009**	0.6218 ± 0.1458	0.3975	0.1682 ± 0.1941
Foxo3	0.8985	-0.0284 ± 0.2187	0.9208	-0.0207 ± 0.2054
Foxo4	0.0606	-0.3097 ± 0.1498	0.3401	-0.1299 ± 0.1325
G6pc	**0.0001**	-0.7714 ± 0.08449	0.2938	0.311 ± 0.2876

Gk	**0.0010**	-0.4628 ± 0.09343	0.9682	0.08211 ± 0.1632
Gpd2	0.8611	-0.06 ± 0.3279	0.9471	-0.008 ± 0.119
Hadh	**0.0157**	-0.3018 ± 0.1098	0.8812	-0.0158 ± 0.1043
Hmgcs2	**0.0001**	-0.5257 ± 0.08963	0.0952	0.1514 ± 0.08597
Klf9	0.1598	0.2725 ± 0.1827	0.1448	0.2222 ± 0.1454
Klf15	0.2601	-0.2497 ± 0.2121	0.6305	0.019 ± 0.1748
Lipe	0.2891	-0.2708 ± 0.2335	0.2616	0.269 ± 0.2317
Mgll	**0.0348**	-0.5093 ± 0.2179	0.6305	-0.0292 ± 0.2678
Mlxipl	**0.0002**	-0.6708 ± 0.1249	0.2560	-0.1228 ± 0.1047
Mt1	**0.0004**	434 ± 38.68	**0.0298**	0.8949 ± 0.3541
Mt2	**0.0117**	847.7 ± 192.7	0.4598	1.172 ± 0.7187
Otc	**0.0001**	-0.8135 ± 0.08476	0.6577	-0.0426 ± 0.09456
Pck1	0.3736	0.1928 ± 0.2092	**0.0158**	0.7291 ± 0.2737
Pcx	**0.0029**	0.8057 ± 0.2206	0.9389	0.0102 ± 0.1312
Pgc1a	**0.0434**	2.08 ± 0.7833	0.8631	0.0318 ± 0.1818
Pklr	**0.0106**	-0.5353 ± 0.1815	0.6425	-0.05154 ± 0.1091
Pnpla2	**0.0101**	1.241 ± 0.5329	0.0809	0.3326 ± 0.1799
Ppara	0.0601	-0.3676 ± 0.1797	0.9027	0.01989 ± 0.1603
Scd1	**0.0200**	-0.5323 ± 0.2028	0.3783	0.1761 ± 0.195
Slc2a2	0.8711	0.03297 ± 0.1995	0.3914	0.1097 ± 0.1249
Srebf1	0.3420	-0.3747 ± 0.3809	**0.0271**	-0.3941 ± 0.158
Slc39a14	**0.0116**	2.15 ± 0.5621	0.2117	-0.1293 ± 0.09985

Complementary results

Confirmation of our results in another mouse model of cancer cachexia

To verify that the GC-dependent transcriptional response we observed in our study was not specific to the *Apc* mice model but a common feature of cancer cachexia, we collaborated with Laetitia Mazelin from the Institut NeuroMyoGène (CNRS UMR 5310 – INSERM U1217, Team Nerve-Muscle Interaction) who worked on the KPZ (*Kras*$^{+/LSL\text{-}G12D}$, *Trp53*$^{+/R270H}$, *Pdx1*$^{+/Cre}$) mice. KPZ mouse is a genetically engineered mouse model of pancreatic cancer [420] described to develop cachexia [90,209,342]. Tissues were removed from KPZ mice before body mass loss had occurred (between 84 and 89 days, KPZ non-cachectic) or when endpoints (high body mass loss or sign of sufferance) were reached (KPZ cachectic) as well as from age-matched WT littermates (WT-C). The transcript level of the GC-dependent responsive genes previously identified in *Apc* mice were determined by RT-qPCR in the *tibialis anterior* muscle and liver. The transcriptional response was reproduced in skeletal muscle of KPZ mice and was associated with the severity of the cachectic syndrome (Figure 1A). When performed on the liver, the transcript level of genes was similarly regulated in cachectic KPZ mice and in advanced cachectic *Apc* mice (Figure 1B-C). Of note, the transcript level of most of genes encoding gluconeogenic proteins remained unchanged (Figure 1C). This may rely on the tumor site as KPZ mice develop ductal pancreatic tumors, which may alter the regulation of insulin and glucagon production.

Collectively, these data demonstrate that the GC-dependent transcriptional response occurring in skeletal muscle and liver during advanced cancer cachexia in *Apc* also occurs in KPZ mice, another genetically engineered model of cancer cachexia. Further data analysis is currently ongoing.

Figure 1. A glucocorticoid-dependent transcriptional response occurs in *tibialis anterior* muscle and liver of KPZ mice during cancer cachexia

(A) RT-qPCR analysis of glucocorticoid-responsive gene mRNA level in *tibialis anterior* muscle of WT-C (n=17), non-cachectic KPZ (n=11), and cachectic KPZ (n=15) mice.

(B) RT-qPCR analysis of glucocorticoid-responsive gene mRNA level in liver of WT-C (n=19), non-cachectic KPZ (n=9), and cachectic KPZ (n=15) mice.

(C) RT-qPCR analysis of metabolic gene mRNA level in liver of WT-C (n=19), non-cachectic KPZ (n=9), and cachectic KPZ (n=15) mice.

Data are represented as mean ± SEM. Data were analyzed by a Kruskal-Wallis test. * represents a significant difference after Dunn's multiple comparisons test. *p<0.05, **p < 0.01 and ***p < 0.001.

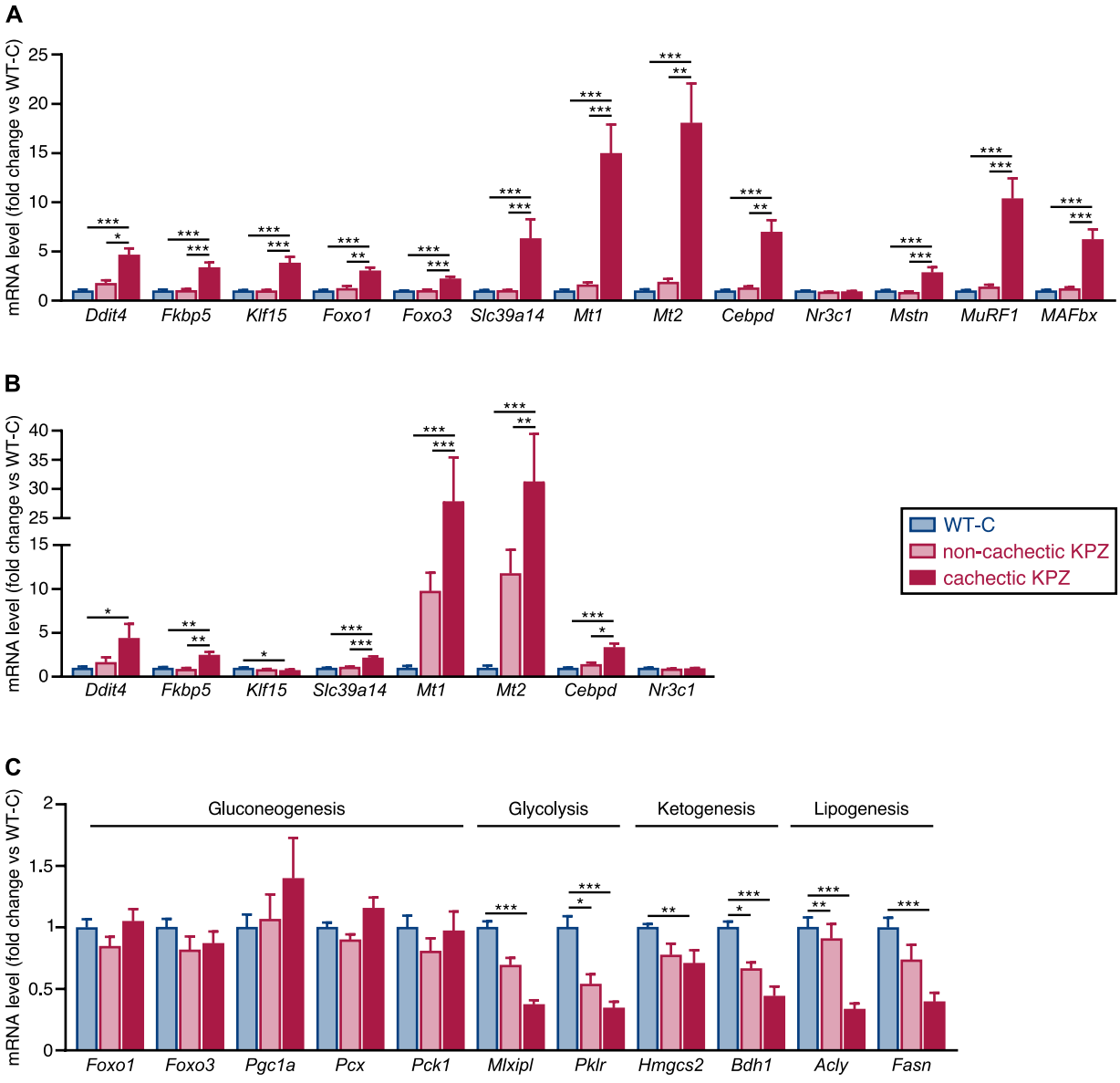
A
mRNA level (fold change vs WT-C)
Ddit4
Fkbp5
Klf15
Foxo1
Foxo3
Slc39a14
Mt1
Mt2
Cebpd
Nr3c1
Mstn
MuRF1
MAFbx
B
mRNA level (fold change vs WT-C)
Ddit4
Fkbp5
Klf15
Slc39a14
Mt1
Mt2
Cebpd
Nr3c1
WT-C
non-cachectic KPZ
cachectic KPZ
C
mRNA level (fold change vs WT-C)
Gluconeogenesis
Glycolysis
Ketogenesis
Lipogenesis
Foxo1
Foxo3
Pgc1a
Pcx
Pck1
Mlxipl
Pklr
Hmgcs2
Bdh1
Acly
Fasn

Targeting GC to prevent cancer cachexia in Apc mice

As we showed that GC are critical determinants of skeletal muscle catabolism and hepatic metabolism rewiring during advanced cancer cachexia, we thus aimed to de determine whether blocking GC by RU486 in Apc mice would limit/prevent skeletal muscle mass loss and hepatic metabolism rewiring. The steroid hormone inhibitor RU486 has been historically used to inhibit GC transcriptional activity in skeletal muscle [421]. We decided to implant a slow-releasing pellet containing RU486 (Innovative Research of America, Sarasota, FL). The pellets were designed to release a continuous flow of 33 mg of RU486 during 60 days corresponding to a rate of 10 mg/kg/day. One pellet containing RU486 was subcutaneously implanted according to the manufacturer's instructions (see Figure 1) in 13-week-old *Apc* mice under general anesthesia (isoflurane 3%) (Apc-RU, n=7). Placebo pellets were also implanted in 13-week-old WT (WT-P, n=10) and Apc (Apc-P, n=6) mice. Tissues were removed at 23 weeks of age for analysis.

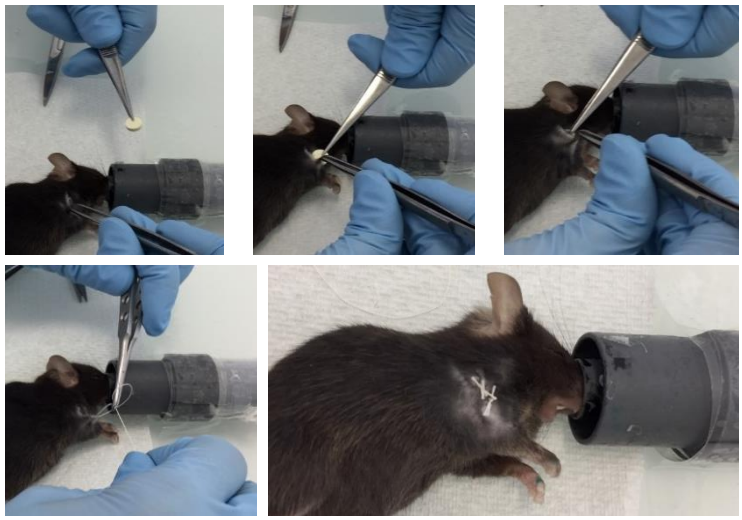

Figure 1. Implantation of a RU486 and placebo pellet in mice.
Pellets were implanted according to the manufacturer's instructions between the shoulder and the ear of the mice under general anesthesia (Isoflurane 3%). The skin was then stitched with 4-5 stitches.

As we previously observed, *Apc*-P mice progressively lost body mass from 15 weeks. *Apc*-RU mice similarly lost body mass and even displayed significantly lower body mass than *Apc*-P mice at 20, 21 and, 23 weeks of age (Figure 2A). Tibia length (Figure 2B) was similar between all groups showing that implantation of RU486 pellet did not affect overall growth. Hematocrit was lower in both *Apc*-P and *Apc*-RU mice compared to WT-P (Figure 2C) suggesting that implantation of RU486 pellet did not attenuate polyp development. Muscle weight loss of quadriceps, gastrocnemius, extensor digitorum longus, tibialis anterior and soleus muscle was similar in *Apc*-RU and *Apc*-P mice (Figure 2D). These data suggest that implantation of RU486 pellet did not prevent the loss of body and muscle mass during cancer cachexia in *Apc* mice. *Apc*-P mice displayed decreased glycemia and increased lactatemia. However, once again there was no

difference between *Apc*-P and *Apc*-RU mice (Figure 2E) suggesting that implantation of RU486 pellet did not prevent the hepatic metabolism rewiring during cancer cachexia in *Apc* mice. Biomolecular analyses of hepatic metabolism have not been performed yet. The adrenal gland mass was similarly increased in *Apc*-P and *Apc*-RU (Figure 2F). Finally, to further determine whether implantation of RU486 pellet exerted biological effects, we then decided to check the efficiency of implantation of RU486 pellet by analyzing the serum corticosterone concentration at implantation, 12 days after and at 23 weeks. Since GC exert negative feedback on their own production, we expected that trapping GC with RU486 will increase serum corticosterone level in mice implanted with RU486 pellets [422]. However, serum corticosterone level was statistically unchanged between *Apc*-P and *Apc*-RU mice at implantation (T0) 12 weeks and 23 weeks (Figure 2G), suggesting similar over-activation of the HPA in response to implantation of RU486 pellet. Therefore, our analyses so far did not provide any evidence of a beneficial effect of implantation of RU486 pellet. Of note, it was also shown that RU486 administration was not always associated with increased serum corticosterone and that *Ddit4* expression is a better marker for the efficacy of RU486 treatment [423]. We thus have to measure the *Ddit4* mRNA level in skeletal muscle of our mice. Therefore, we do not have definitive biological evidence that implantation of RU486 pellet was efficient in releasing RU486. The short half-life of RU486 in rodents [424] may have limited its biological action. However, the use of slow-releasing pellets should have normally overcome this drawback. Analysis of blood samples for the presence of RU486 would provide an answer to this question. Furthermore, RU486 is also an antiprogestogen and antiandrogen. Due to its wide spectrum of action, one may hypothesize that implantation of RU486 pellet could have also exerted effects that may interfere with those expected on skeletal muscle and liver. This may also explain why the use of RU486 have provided contrasting results, some studies providing convincing effects [363] on cancer cachexia, other not [74,362].

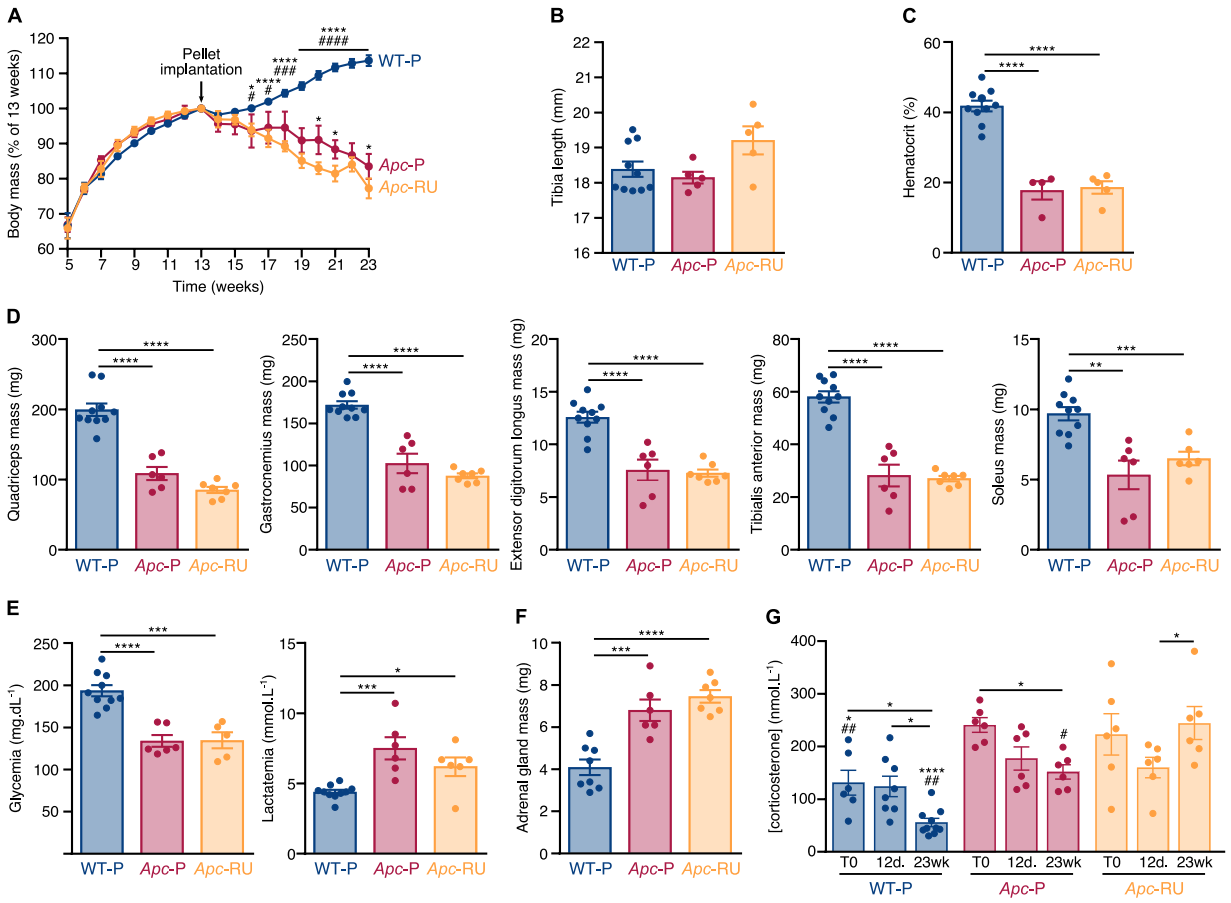

Figure 2. Effect of the implantation of RU486 pellet in *Apc* mice.

(A) Relative changes in body mass in WT-P (n=10), *Apc*-P (n=6), and *Apc*-RU (n=7) mice over a 23-week period after birth.

(B) Tibia length of WT-P (n=10), *Apc*-P (n=6), and *Apc*-RU (n=7) mice at 23 weeks.

(C) Hematocrit in WT-P (n=10), *Apc*-P (n=6), and *Apc*-RU (n=7) mice at 23 weeks.

(D) Quadriceps, gastrocnemius, extensor digitorum longus, tibialis anterior, and soleus muscle mass of WT-P (n=10), *Apc*-P (n=6) and *Apc*-RU (n=7) mice at 23 weeks.

(E) Blood glucose (left) and lactate (right) concentration in WT-P (n=10), *Apc*-P (n=6), and *Apc*-RU (n=7) mice at 23 weeks.

(F) Mass of adrenal glands in WT-P (n=10), *Apc*-P (n=6), and *Apc*-RU (n=7) mice at 23 weeks.

(G) Serum corticosterone concentration in WT-P (n=10), *Apc*-P (n=6), and *Apc*-RU (n=7) mice at pellet implantation (T0), 12 days after pellet implantation (12d.), and 23 weeks (23wk).

Data are represented as mean ± SEM. (A and G) data were analyzed by a two-way ANOVA; #: significant difference with *Apc*-P; *: significant difference with *Apc*-RU (Sidak's multiple comparison test). (B, C, D, E, F, G) data were analyzed by a one-way ANOVA. * represents a significant difference after Tukey's multiple comparison test. *, #p <0.05, **,##p < 0.01, ***, ###p < 0.001 and ****,####p < 0.0001.

CONCLUSION AND PERSPECTIVES

Main results of the work

In this work, we gave evidence that cancer cachexia elicits a complete reprogramming of hepatic metabolism in favor of an increase in gluconeogenesis, alteration of the urea cycle, a decrease in ketogenesis, and a decrease in lipid metabolism. Moreover, we demonstrated that the HPA axis was activated during cancer cachexia in *Apc* mice leading to an increased systemic level of corticosterone. This was associated with a GC-dependent transcriptional response in skeletal muscle and liver of advanced cachectic *Apc* mice. Prevention of skeletal muscle mass loss by *Mstn* gene invalidation abolished this response (Figure 15).

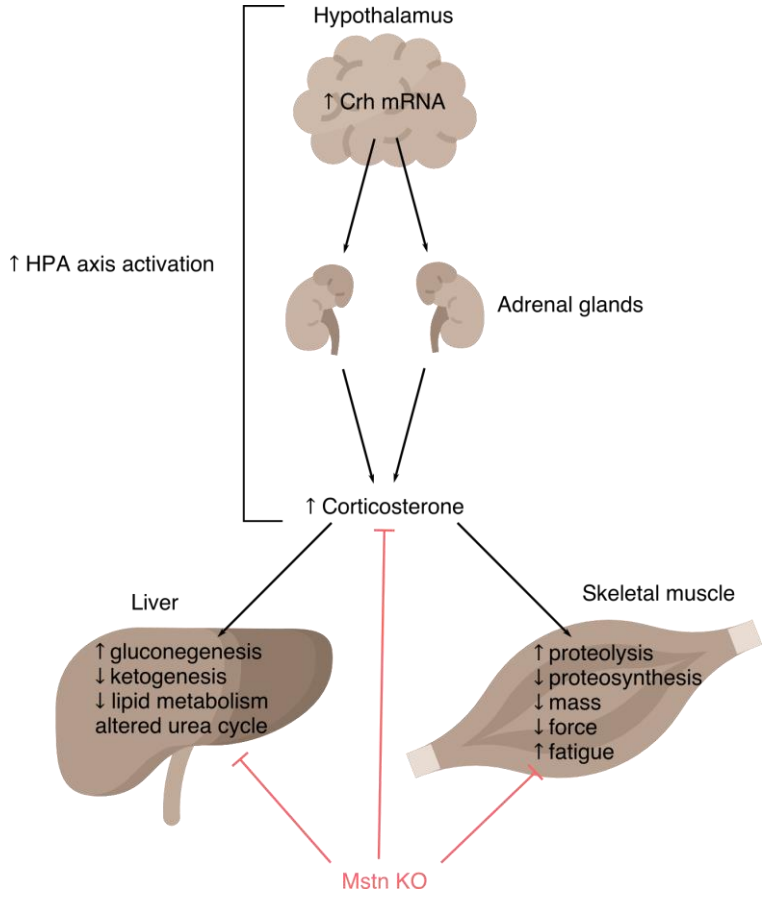

Figure 15. Schematic view of the main findings of our study.

Clinical translation

It is now essential to clinically confirm the biological relevance of our observations in cachectic cancer patients. As illustrated by Talbert et al. [90] who showed differences in skeletal muscle gene transcriptomic response between animal models of cancer cachexia and human patients, interspecies differences may sensibly modify the clinical impact of findings obtained from animal studies. We have the opportunity to work with clinicians on this topic. Biological samples (*vastus*

lateralis muscle biopsies and blood) from patients of the MYOCAC study could be used to determine the circulating level of cortisol, the existence of a GC-dependent transcriptional signature in skeletal muscle and whether this could be associated with the extent of the loss of skeletal muscle mass and function. Additionally, it would be of great interest to perform a ChIP-seq analysis of GC receptor binding in skeletal muscle biopsies to further confirm the action of GC during cancer cachexia and identified other target genes. Moreover, we demonstrated a potential role for MSTN in the regulation of hepatic metabolism rewiring and HPA axis regulation. A completed investigation of the MSTN pathway in skeletal muscle of cachectic cancer patients is still lacking and it would be one of our planned purposes. Unfortunately, we have not included as many patients as we initially hoped but the project is still open for inclusion.

Research prospects

Figure 16 summarizes important questions that could be experimentally addressed in the future. Each of these questions is developed below.

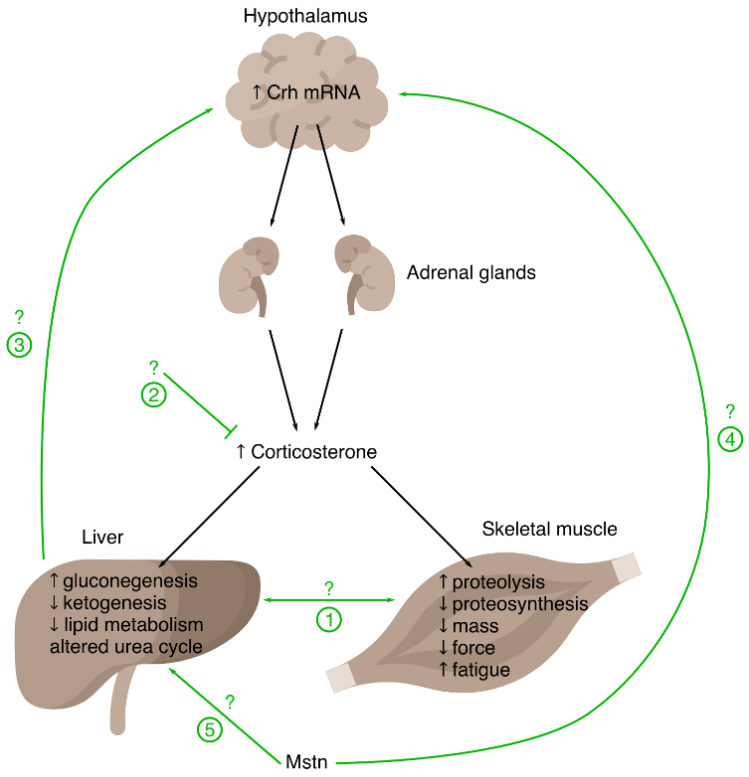

Figure 16. Schematic view of remaining questions that could be experimentally tested.

Inter-tissue temporal regulation during cancer cachexia

Our work raised an important question regarding the temporality of the dialog between skeletal muscle and liver during cancer cachexia (question mark n°1 Figure 16). It has been already reported that blocking adipose tissue loss inhibited the loss of skeletal muscle mass during cancer cachexia [425] indicating the existence of a dialog between adipose tissue and skeletal muscle that would control the depletion of skeletal muscle compartment. Our data in *Apc* mice also indicate that adipose tissue store is largely depleted before the major decrease in skeletal muscle mass had occurred. We also showed that blocking skeletal muscle mass loss by *Mstn* gene invalidation completely prevented hepatic metabolism rewiring. Together these data would suggest that cancer cachexia would first affect adipose tissue, then skeletal muscle and liver (Figure 17). This hypothesis obviously needs to be strengthened but it suggests that the temporality of these events responds to distinct metabolic needs during the progression through the disease. This also provides a conceptual framework to define windows for interventional therapeutics.

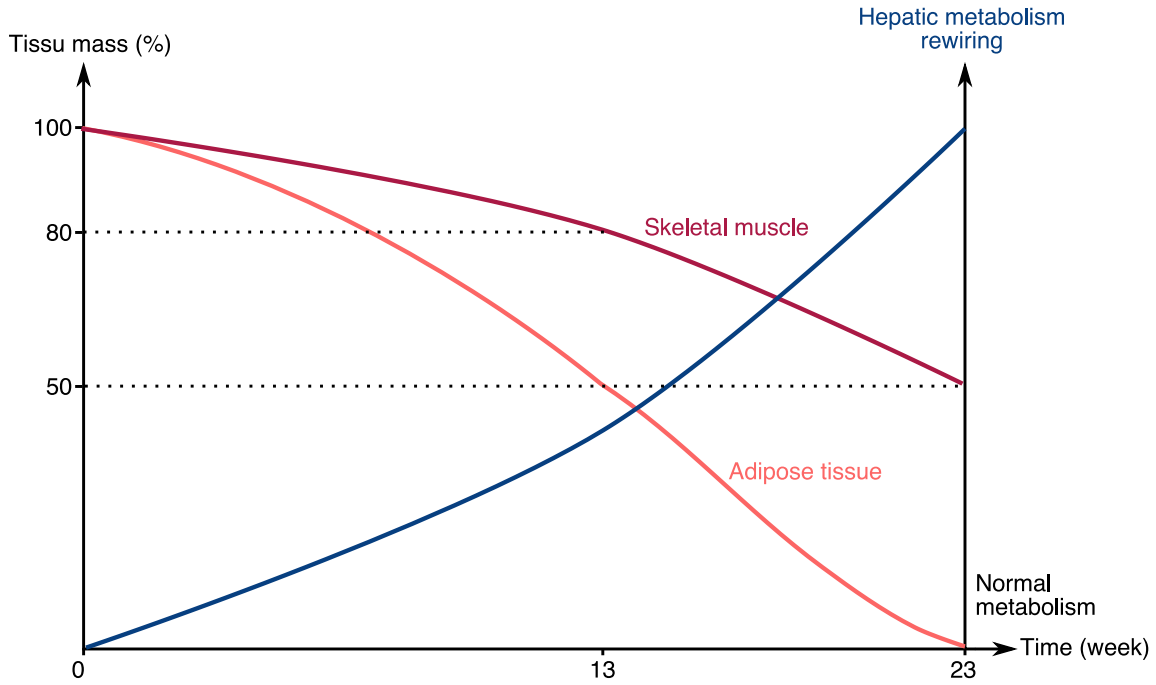

Figure 17. Conceptual view of the timing of skeletal muscle and adipose tissue loss and liver metabolism rewiring.

Exploring liver metabolism during the time course of skeletal muscle atrophy would be also particularly interesting. An inducible mice model of skeletal muscle atrophy (inducible expression of a constitutively active TGF-βI receptor, TGFβ-RI-CA (abstract 6-08 in [426]) is currently hosted and used by our collaborators (Laurent Schaeffer and Laetitia Mazelin, INMG). Studying liver metabolism in this condition would provide important information about the dialog between

skeletal muscle and liver and the interdependence of skeletal muscle and liver metabolisms. This could provide important clues about the systemic nature of the cachectic syndrome.

Anti-GC-based therapeutic strategy

As reported in the complementary results, we failed to accurately inhibit the GC action in *Apc* mice by implanting pellets releasing RU486. Actually, we currently do not have biological evidence that the drug was effectively administered and biologically efficient. To alleviate this major drawback, but also to overcome the potential undesirable effects of RU486 due to its wide spectrum of actionwe have developed a collaboration with Corcept Therapeutics (Menlo Park, California, USA) to test Relacorilant (CORT125134), a non-steroidal selective GC receptor antagonist that does not bind to the androgen receptor or the progesterone receptor in *Apc* mice. Relacorilant is currently assessed in a phase III clinical trial in pancreatic cancer patients in combination with Abraxane (Paclitaxel). The use of this specific GC receptor antagonist will be useful to better characterize the systemic role of GC on both skeletal muscle and liver during cancer cachexia (question mark n°2 Figure 16). We plan to inject Relacorilant in *Apc* mice once weight loss is detected in order to determine whether it can counteract skeletal muscle wasting and liver metabolism rewiring and reestablish the balance of the HPA axis (curative treatment).

Regulation of the HAP axis – metabolic blood-borne factors

Our data clearly show that the HPA axis is strongly activated during cancer cachexia. However, the mechanisms that could regulate the HPA axis are currently unknown. If cytokines have already been shown to activate the HPA axis and induce skeletal muscle atrophy [258], other molecules such as glucose, lipids, ketone bodies, or hormones are known to reach the hypothalamus via non-neuronal cells [427]. In the present study, we detected variations in the concentration of blood-borne metabolic factors such as lactate, ketone bodies, or glucose. Whether or not the variations in the circulating concentrations of these factors can be sensed at the hypothalamic level to regulate the HPA axis during cancer cachexia is currently unknown, but this remains an attractive possibility (question mark n°3 Figure 16). Variations in the concentrations of blood-borne factors may also modulate the permeability of the blood-brain barrier rendering hypothalamus more sensible to activating molecules. For instance, a low blood glucose concentration was shown to increase the blood-brain-barrier plasticity through the reorganization of tight junctions of the tanycytes and increased the permeability of the median eminence microvessels [428]. The decrease in glycemia observed in our study could thus increase the accessibility of other circulating factors such as cytokines to the hypothalamus, thus potentiating the central action of cytokines which could in turn activate the HPA axis. This hypothesis could be tested by intracerebroventricular injection of 2-deoxy-D-glucose in mice. 2-deoxy-D-glucose is a glucose analog that increases blood-brain-barrier plasticity as it occurred during low glycemia [428]. We could then determine

whether this increased permeability of the blood-brain-barrier in response to low glycemia would reinforce the GC-dependent transcriptomic signature occurring in response to an intravenous injection of cytokines [258]. A chronic HPA axis activation could thus be explained by a vicious circle in which altered concentrations of blood-borne factors triggered either directly or indirectly HPA axis activation, which in turn acts on the liver to trigger hepatic metabolism rewiring.

Regulation of the HPA axis – myostatin

We also showed that the circulating corticosterone level was restored to control level in ApcKO mice, suggesting that variations in MSTN concentrations could either directly or indirectly modulate the activity of the HPA axis during cancer cachexia. This is an interesting possibility that is supported by recent studies [429,430] and our observations that activin type I and type IIB receptors are expressed in the hypothalamus. This hypothesis could be experimentally tested by determining whether intracerebroventricular injection of MSTN can regulate a GC-dependent transcriptional signature in skeletal muscle and liver thus mimicking the response we observed during cancer cachexia (question mark n°4 Figure 16). Of note, *Mstn* expression is also induced by GC administration [431,432] (see also Figure 4A of study *Apc*). Therefore, we could hypothesize that activation of the HPA axis would increase *Mstn* expression which in turn would reinforce HPA axis activation.

To better characterize the role of MSTN on the HPA axis during cancer cachexia and to overcome the effects of constitutive *Mstn* gene invalidation of our KO model, we develop a collaboration with Dr. Olli Ritvos from the University of Helsinki (Finland) who provided us purified hActRIIB-hFc(IgG1)-6His (sActRIIb) protein, which is a dimeric activin receptor ectodomain Fc fusion trap molecule that blocks or traps activin A, B and AB, MSTN and GDF11 produced as previously described [433]. The injection of this sActRIIb has been shown to prevent skeletal muscle mass loss in C26 tumor-bearing mice [227]. However, its effects on hepatic metabolism and the regulation of the HPA axis in the context of cancer cachexia remain unknown (question mark n°4 and 5 Figure 16). We intraperitoneally injected 13-week-old WT (WT-sActRIIb) and *Apc* (*Apc*-sActRIIb) mice with 10 mg/kg of sActRIIb twice a week for 10 weeks. Control 13-week-old WT (WT-P) and *Apc* (*Apc*-P) littermates were injected with a corresponding volume of DPBS. Tissues were removed from 23-week-old mice. To date, we collected the tissues for 10 WT-P, 4 *Apc*-P, 4 WT-sActRIIb and 2 *Apc*-sActRIIb. For this preliminary set of mice, injections began at 14 weeks because of lock-down due to Coronavirus. Our preliminary results suggest that the injection of sActRIIb would not affect the growth of the animals as shown by unchanged tibia length (Figure 18A). Hematocrit was similarly lowered in *Apc*-P and *Apc*-sActRIIb mice (Figure 18B) indicating that sActRIIb would probably not affect polyp development. Importantly, body mass would be maintained in *Apc*-sActRIIb mice when compared to WT-P (Figure 18C). As expected, skeletal muscle mass was dramatically increased in WT-sActRIIb (x1.5 for *quadriceps*, x1.6 for

gastrocnemius, x1.6 for *extensor digitorum longus*, x1.6 for *tibialis anterior* and x1.3 for *soleus* muscle, Figure 18D) illustrating the biological efficiency of the drug. The injection of sActRIIb in *Apc* mice seems to reestablish skeletal muscle mass to level very closed to those of WT-P (Figure 18D). The completion of this animal study is currently undergoing. Our objectives will be then to explore whether pharmacological inhibition of MSTN regulates the HPA axis, as well as skeletal muscle and liver metabolisms.

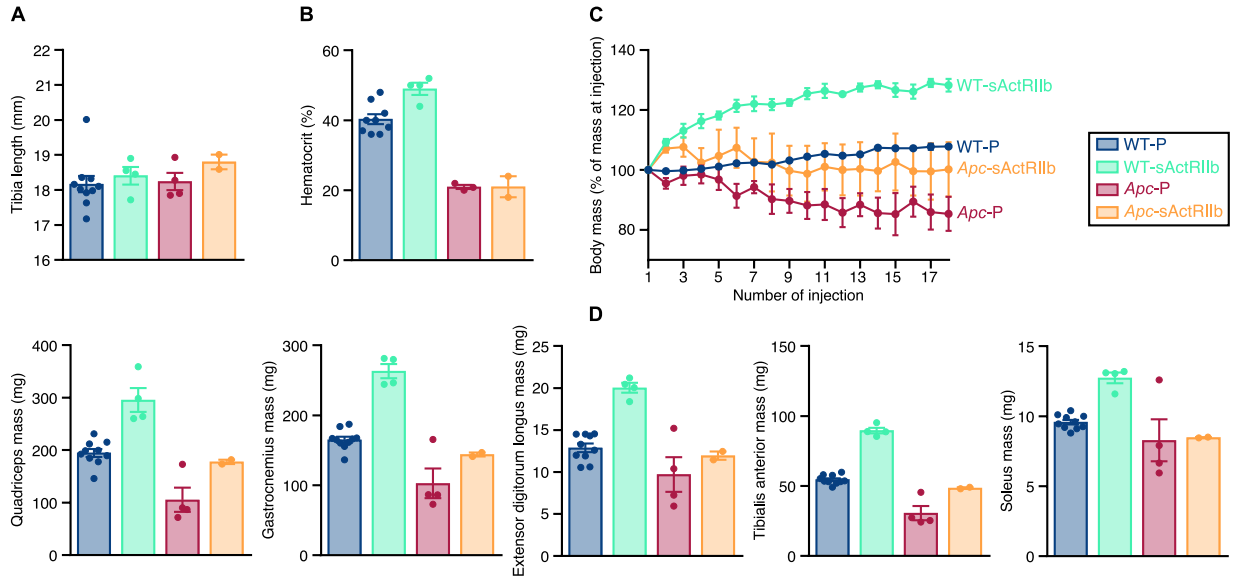

Figure 18. Effect of the injection of sActRIIb in *Apc* mice.

(A) Tibia length of WT-P (n=10), WT-sActRIIb (n=4), *Apc*-P (n=4) and *Apc*-sActRIIb (n=2) mice at 23 weeks.

(B) Hematocrit in WT-P (n=10), WT-sActRIIb (n=4), *Apc*-P (n=4) and *Apc*-sActRIIb (n=2) mice at 23 weeks.

(C) Relative changes in body mass in WT-P (n=10), WT-sActRIIb (n=4), *Apc*-P (n=4) and *Apc*-sActRIIb (n=2) mice over a 23-week period after birth.

(D) *Quadriceps*, *gastrocnemius*, *extensor digitorum longus*, *tibialis anterior* and *soleus* muscle mass of WT-P (n=10), WT-sActRIIb (n=4), *Apc*-P (n=4) and *Apc*-sActRIIb (n=2) mice at 23 weeks.

Data are represented as mean ± SEM. Given the low number of mice, we did not perform statistical analysis.

Together, my PhD work highlights the role of GC during cancer cachexia but a lot still remains to be investigated.

PUBLICATIONS AND COMMUNICATIONS

Publications

PhD Thesis

Martin, A., and Freyssenet, D. Phenotypic features of cancer cachexia-related loss of muscle mass and function: lessons from clinical and animal studies. (Under review in Journal of Cachexia, Sarcopenia and Muscle)

MS Sc Research 2nd year

Febvey-Combes, O., Jobard, E., Rossary, A., Pialoux, V., Foucaut, A.M., Morelle, M., Delrieu, L., **Martin, A.**, Caldefie-Chézet, F., Touillaud, M., Berthouze, S.E., Boumaza, H., Elena-Herrmann, B., Bachmann, P., Trédan, O., Vasson, M.P., Fervers, B. Effects of an exercise intervention on circulating biomarkers and metabolomic profiling during adjuvant treatment for localized breast cancer. (Under review in Integrative Cancer Therapies)

Delrieu, L., Touillaud, M,. Pérol, O., Morelle, M., **Martin, A.**, Friedenreich, C., Mury, P., Dufresne, A., Bachelot, T., Heudel, P.E., Fervers, B., Trédan, O., Pialoux, V. Pro-oxidant/antioxidant during a personalized six-month physical activity program in metastatic breast cancer patients. (Under review in Oxidative Medicine and Cellular Longetivity)

Martin, A., Millet, G., Osredkar, D., Mramor, M., Faes, C., Gouraud, E., Debevec, T., and Pialoux, V. (2020). Effect of pre-term birth on oxidative stress responses to normoxic and hypoxic exercise. Redox Biology 32, 101497.

Rytz, C.L., Pialoux, V., Mura, M., **Martin, A.**, Hogan, D.B., Hill, M.D., and Poulin, M.J. (2020). Impact of Aerobic Exercise, Sex and Metabolic Syndrome on Markers of Oxidative Stress: Results from the Brain in Motion Study. Journal of Applied Physiology.

Debevec, T., Pialoux, V., Poussel, M., Willis, S.J., **Martin, A.**, Osredkar, D., and Millet, G.P. (2020). Cardio-respiratory, oxidative stress and acute mountain sickness responses to normobaric and hypobaric hypoxia in prematurely born adults. Eur. J. Appl. Physiol.

Delrieu, L., Pialoux, V., Pérol, O., Morelle, M., **Martin, A.**, Friedenreich, C., Febvey-Combes, O., Pérol, D., Belladame, E., Clémençon, M., et al. (2020). Feasibility and Health Benefits of an Individualized Physical Activity Intervention in Women With Metastatic Breast Cancer: Intervention Study. JMIR Mhealth Uhealth 8, e12306.

Debevec, T., Pialoux, V., Millet, G.P., **Martin, A.**, Mramor, M., and Osredkar, D. (2019). Exercise Overrides Blunted Hypoxic Ventilatory Response in Prematurely Born Men. Frontiers in Physiology 10, 437.

Martin, A., Faes, C., Debevec, T., Rytz, C., Millet, G., and Pialoux, V. (2018). Preterm birth and oxidative stress: Effects of acute physical exercise and hypoxia physiological responses. Redox Biology 17, 315–322.

MS Sc Research 1st year

Zwingmann, L., Strütt, S., **Martin, A.**, Volmary, P., Bloch, W., and Wahl, P. (2019). Modifications of the Dmax method in comparison to the maximal lactate steady state in young male athletes. Phys Sportsmed 47, 174–181.

Publication associated to a congress

Martin A, Castells J, Favier F, Zolotoff C, Allibert V, Gallot Y, Durieux A, Hourde C, Freyssenet D. Skeletal muscle and liver gene reprogramming during cancer cachexia in *Apc*$^{Min/+}$ mice: potential role of glucocorticoids. (2019). Abstract. Journal of Cachexia, Sarcopenia and Muscle *10*, 1378–1435.

Poster communications

Martin A, Castells J, Favier F, Zolotoff C, Allibert V, Gallot Y, Durieux A, Hourde C, Freyssenet D. Skeletal muscle and liver gene reprogramming during cancer cachexia in *Apc*$^{Min/+}$ mice: potential role of glucocorticoids. 12th International Conference on Cachexia, Sarcopenia & Muscle Wasting, Berlin, Germany, December 6-8th 2019.

Martin A, Castells J, Favier F, Zolotoff C, Allibert V, Gallot Y, Durieux A, Hourde C, Freyssenet D. *Myostatin* gene invalidation inhibits a glucocorticoid-like response involved in skeletal muscle wasting in advanced cancer cachexia. 17èmes Journées de la Société Française de Myologie, Marseille, France, November 20-22th 2019.

REFERENCES

1. Bennani-Baiti N, Walsh D. What is cancer anorexia-cachexia syndrome? A historical perspective. 2009;**39**:257–262.

2. Fearon K, Strasser F, Anker SD, Bosaeus I, Bruera E, Fainsinger RL *et al.* Definition and classification of cancer cachexia: an international consensus. *The Lancet Oncology* 2011;**12**:489–495.

3. Evans WJ, Morley JE, Argilés J, Bales C, Baracos V, Guttridge D *et al.* Cachexia: A new definition. *Clinical Nutrition* 2008;**27**:793–799.

4. Vanhoutte G, van de Wiel M, Wouters K, Sels M, Bartolomeeussen L, De Keersmaecker S *et al.* Cachexia in cancer: what is in the definition? *BMJ Open Gastroenterol* 2016;**3**:e000097.

5. Rier HN, Jager A, Sleijfer S, Maier AB, Levin M-D. The Prevalence and Prognostic Value of Low Muscle Mass in Cancer Patients: A Review of the Literature. *Oncologist* 2016;**21**:1396.

6. Weerink LBM, Hoorn A van der, Leeuwen BL van, Bock GH de. Low skeletal muscle mass and postoperative morbidity in surgical oncology: a systematic review and meta-analysis. *Journal of Cachexia, Sarcopenia and Muscle* 2020;**11**.

7. Huang D-D, Wang S-L, Zhuang C-L, Zheng B-S, Lu J-X, Chen F-F *et al.* Sarcopenia, as defined by low muscle mass, strength and physical performance, predicts complications after surgery for colorectal cancer. *Colorectal Dis* 2015;**17**:O256–O264.

8. Naumann P, Eberlein J, Farnia B, Liermann J, Hackert T, Debus J *et al.* Cachectic Body Composition and Inflammatory Markers Portend a Poor Prognosis in Patients with Locally Advanced Pancreatic Cancer Treated with Chemoradiation. *Cancers* 2019;**11**:1655.

9. Prado CM, Sawyer MB, Ghosh S, Lieffers JR, Esfandiari N, Antoun S *et al.* Central tenet of cancer cachexia therapy: do patients with advanced cancer have exploitable anabolic potential? *Am J Clin Nutr* 2013;**98**:1012–1019.

10. Jung H-W, Kim JW, Kim J-Y, Kim S-W, Yang HK, Lee JW *et al.* Effect of muscle mass on toxicity and survival in patients with colon cancer undergoing adjuvant chemotherapy. *Support Care Cancer* 2015;**23**:687–694.

11. Tan BHL, Brammer K, Randhawa N, Welch NT, Parsons SL, James EJ *et al.* Sarcopenia is associated with toxicity in patients undergoing neo-adjuvant chemotherapy for oesophago-gastric cancer. *Eur J Surg Oncol* 2015;**41**:333–338.

12. Choi MH, Oh SN, Lee IK, Oh ST, Won DD. Sarcopenia is negatively associated with long-term outcomes in locally advanced rectal cancer. *J Cachexia Sarcopenia Muscle* 2018;**9**:53–59.

13. Martin L, Birdsell L, MacDonald N, Reiman T, Clandinin MT, McCargar LJ *et al.* Cancer Cachexia in the Age of Obesity: Skeletal Muscle Depletion Is a Powerful Prognostic Factor, Independent of Body Mass Index. *Journal of Clinical Oncology* 2013;**31**:1539–1547.

14. Basile D, Parnofiello A, Vitale MG, Cortiula F, Gerratana L, Fanotto V *et al.* The IMPACT study: early loss of skeletal muscle mass in advanced pancreatic cancer patients. *J Cachexia Sarcopenia Muscle* 2019;**10**:368–377.

15. da Cunha LP, Silveira MN, Mendes MCS, Costa FO, Macedo LT, de Siqueira NS *et al.* Sarcopenia as an independent prognostic factor in patients with metastatic colorectal cancer: A retrospective evaluation. *Clinical Nutrition ESPEN* 2019;**32**:107–112.

16. Argilés JM, Busquets S, Stemmler B, López-Soriano FJ. Cancer cachexia: understanding the molecular basis. *Nature Reviews Cancer* 2014;**14**:754–762.

17. Baracos VE, Martin L, Korc M, Guttridge DC, Fearon KCH. Cancer-associated cachexia. *Nature Reviews Disease Primers* 2018;**4**:17105.

18. Rohm M, Zeigerer A, Machado J, Herzig S. Energy metabolism in cachexia. *EMBO Rep* 2019;**20**:e47258.

19. Takayama K, Atagi S, Imamura F, Tanaka H, Minato K, Harada T *et al.* Quality of life and survival survey of cancer cachexia in advanced non-small cell lung cancer patients—Japan nutrition and QOL survey in patients with advanced non-small cell lung cancer study. *Support Care Cancer* 2016;**24**:3473–3480.

20. Fearon KC, Voss AC, Hustead DS. Definition of cancer cachexia: effect of weight loss, reduced food intake, and systemic inflammation on functional status and prognosis. *Am J Clin Nutr* 2006;**83**:1345–1350.

21. Blum D, Stene GB, Solheim TS, Fayers P, Hjermstad MJ, Baracos VE *et al.* Validation of the Consensus-Definition for Cancer Cachexia and evaluation of a classification model--a study based on data from an international multicentre project (EPCRC-CSA). *Ann Oncol* 2014;**25**:1635–1642.

22. Wallengren O, Lundholm K, Bosaeus I. Diagnostic criteria of cancer cachexia: relation to quality of life, exercise capacity and survival in unselected palliative care patients. *Support Care Cancer* 2013;**21**:1569–1577.

23. Andreyev HJN, Norman AR, Oates J, Cunningham D. Why do patients with weight loss have a worse outcome when undergoing chemotherapy for gastrointestinal malignancies? *European Journal of Cancer* 1998;**34**:503–509.

24. Loumaye A, de Barsy M, Nachit M, Lause P, Frateur L, van Maanen A *et al.* Role of Activin A and Myostatin in Human Cancer Cachexia. *J Clin Endocrinol Metab* 2015;**100**:2030–2038.

25. Mason MC, Garcia JM, Sansgiry S, Walder A, Berger DH, Anaya DA. Preoperative cancer cachexia and short-term outcomes following surgery. *J Surg Res* 2016;**205**:398–406.

26. Ross PJ, Ashley S, Norton A, Priest K, Waters JS, Eisen T *et al.* Do patients with weight loss have a worse outcome when undergoing chemotherapy for lung cancers? *Br J Cancer* 2004;**90**:1905–1911.

27. da Rocha IMG, Marcadenti A, de Medeiros GOC, Bezerra RA, Rego JF de M, Gonzalez MC *et al.* Is cachexia associated with chemotherapy toxicities in gastrointestinal cancer patients? A prospective study. *J Cachexia Sarcopenia Muscle* 2019;**10**:445–454.

28. Schwarz S, Prokopchuk O, Esefeld K, Gröschel S, Bachmann J, Lorenzen S *et al.* The clinical picture of cachexia: a mosaic of different parameters (experience of 503 patients). *BMC Cancer* 2017;**17**.

29. Fouladiun M, Korner U, Gunnebo L, Sixt-Ammilon P, Bosaeus I, Lundholm K. Daily Physical-Rest Activities in Relation to Nutritional State, Metabolism, and Quality of Life in Cancer Patients with Progressive Cachexia. *Clinical Cancer Research* 2007;**13**:6379–6385.

30. Dewys WD, Begg C, Lavin PT, Band PR, Bennett JM, Bertino JR *et al.* Prognostic effect of weight loss prior tochemotherapy in cancer patients. *The American journal of medicine* 1980;**69**:491–497.

31. Martin L. Diagnostic criteria for cancer cachexia: data versus dogma. *Curr Opin Clin Nutr Metab Care* 2016;**19**:188–198.

32. Martin L, Senesse P, Gioulbasanis I, Antoun S, Bozzetti F, Deans C *et al.* Diagnostic Criteria for the Classification of Cancer-Associated Weight Loss. *Journal of Clinical Oncology* 2015;**33**:90–99.

33. Bachmann J, Heiligensetzer M, Krakowski-Roosen H, Büchler MW, Friess H, Martignoni ME. Cachexia Worsens Prognosis in Patients with Resectable Pancreatic Cancer. *J Gastrointest Surg* 2008;**12**:1193–1201.

34. Vagnildhaug OM, Blum D, Wilcock A, Fayers P, Strasser F, Baracos VE *et al.* The applicability of a weight loss grading system in cancer cachexia: a longitudinal analysis. *Journal of Cachexia, Sarcopenia and Muscle* 2017;**8**:789–797.

35. Chen X, Zeng Y, Huang Y, Xu J, Meng W, Wang X *et al.* Preoperative Cachexia predicts poor outcomes in young rather than elderly gastric cancer patients: a prospective study. *Cancer Manag Res* 2019;**11**:8101–8110.

36. Warren S. The immediate causes of death in cancer. *The American Journal of the Medical Sciences* 1932;**148**:610–615.

37. Fearon KCH, Preston T. Body Composition in Cancer Cachexia. *TMH* 1990;**17**:63–66.

38. Cohn SH, Gartenhaus W, Sawitsky A, Rai K, Zanzi I, Vaswani A *et al.* Compartmental body composition of cancer patients by measurement of total body nitrogen, potassium, and water. *Metabolism* 1981;**30**:222–229.

39. Moley JF, Aamodt R, Rumble W, Kaye W, Norton JA. Body Cell Mass in Cancer-Bearing and Anorexic Patients. *Journal of Parenteral and Enteral Nutrition* 1987;**11**:219–222.

40. Mir O, Coriat R, Blanchet B, Durand J-P, Boudou-Rouquette P, Michels J *et al.* Sarcopenia predicts early dose-limiting toxicities and pharmacokinetics of sorafenib in patients with hepatocellular carcinoma. *PLoS ONE* 2012;**7**:e37563.

41. Wendrich AW, Swartz JE, Bril SI, Wegner I, de Graeff A, Smid EJ *et al.* Low skeletal muscle mass is a predictive factor for chemotherapy dose-limiting toxicity in patients with locally advanced head and neck cancer. *Oral Oncol* 2017;**71**:26–33.

42. Ebner N, Anker SD, Haehling S von. Recent developments in the field of cachexia, sarcopenia, and muscle wasting: highlights from the 12th Cachexia Conference. *Journal of Cachexia, Sarcopenia and Muscle* 2020;**11**:274–285.

43. Argilés JM, López-Soriano FJ, Busquets S. Mechanisms and treatment of cancer cachexia. *Nutrition, Metabolism and Cardiovascular Diseases* 2013;**23**:S19–S24.

44. Argilés JM, Stemmler B, López-Soriano FJ, Busquets S. Inter-tissue communication in cancer cachexia. *Nat Rev Endocrinol* 2018;**15**:9–20.

45. Fearon K, Arends J, Baracos V. Understanding the mechanisms and treatment options in cancer cachexia. *Nature Reviews Clinical Oncology* 2012;**10**:90–99.

46. Johns N, Stephens NA, Fearon KCH. Muscle wasting in cancer. *The International Journal of Biochemistry & Cell Biology* 2013;**45**:2215–2229.

47. Schmidt SF, Rohm M, Herzig S, Berriel Diaz M. Cancer Cachexia: More Than Skeletal Muscle Wasting. *Trends in Cancer* 2018;**4**:849–860.

48. Tisdale MJ. Mechanisms of cancer cachexia. *Physiol Rev* 2009;**89**:381–410.

49. Roeland EJ, Ma JD, Nelson SH, Seibert T, Heavey S, Revta C *et al.* Weight loss versus muscle loss: re-evaluating inclusion criteria for future cancer cachexia interventional trials. *Support Care Cancer* 2017;**25**:365–369.

50. Blauwhoff-Buskermolen S, Langius JAE, Becker A, Verheul HMW, de van der Schueren MAE. The influence of different muscle mass measurements on the diagnosis of cancer cachexia: Muscle measurements in the diagnosis of cachexia. *Journal of Cachexia, Sarcopenia and Muscle* 2017;**8**:615–622.

51. Heymsfield SB, Gonzalez MC, Lu J, Jia G, Zheng J. Skeletal muscle mass and quality: evolution of modern measurement concepts in the context of sarcopenia. *Proceedings of the Nutrition Society* 2015;**74**:355–366.

52. Lerner L, Hayes TG, Tao N, Krieger B, Feng B, Wu Z *et al.* Plasma growth differentiation factor 15 is associated with weight loss and mortality in cancer patients. *J Cachexia Sarcopenia Muscle* 2015;**6**:317–324.

53. Op den Kamp C, Gosker HR, Lagarde S, Tan DY, Snepvangers FJ, Dingemans A-MC *et al.* Preserved muscle oxidative metabolic phenotype in newly diagnosed non-small cell lung cancer cachexia. *Journal of Cachexia, Sarcopenia and Muscle* 2015;**6**:164–173.

54. Op den Kamp CM, Langen RC, Snepvangers FJ, de Theije CC, Schellekens JM, Laugs F *et al.* Nuclear transcription factor κ B activation and protein turnover adaptations in skeletal muscle of patients with progressive stages of lung cancer cachexia. *Am J Clin Nutr* 2013;**98**:738–748.

55. Tardif N, Klaude M, Lundell L, Thorell A, Rooyackers O. Autophagic-lysosomal pathway is the main proteolytic system modified in the skeletal muscle of esophageal cancer patients. *Am J Clin Nutr* 2013;**98**:1485–1492.

56. Weber M-A, Krakowski-Roosen H, Schröder L, Kinscherf R, Krix M, Kopp-Schneider A *et al.* Morphology, metabolism, microcirculation, and strength of skeletal muscles in cancer-related cachexia. *Acta Oncol* 2009;**48**:116–124.

57. Dejong CHC, Busquets S, Moses AGW, Schrauwen P, Ross JA, Argiles JM *et al.* Systemic inflammation correlates with increased expression of skeletal muscle ubiquitin but not uncoupling proteins in cancer cachexia. *Oncology Reports* 2005;**14**:257–263.

58. Aversa Z, Pin F, Lucia S, Penna F, Verzaro R, Fazi M *et al.* Autophagy is induced in the skeletal muscle of cachectic cancer patients. *Sci Rep* 2016;**6**:30340.

59. Falconer JS, Fearon KC, Plester CE, Ross JA, Carter DC. Cytokines, the acute-phase response, and resting energy expenditure in cachectic patients with pancreatic cancer. *Ann Surg* 1994;**219**:325–331.

60. Stephens NA, Gray C, MacDonald AJ, Tan BH, Gallagher IJ, Skipworth RJE *et al.* Sexual dimorphism modulates the impact of cancer cachexia on lower limb muscle mass and function. *Clinical Nutrition* 2012;**31**:499–505.

61. Weber M-A, Kinscherf R, Krakowski-Roosen H, Aulmann M, Renk H, Künkele A *et al.* Myoglobin plasma level related to muscle mass and fiber composition: a clinical marker of muscle wasting? *J Mol Med* 2007;**85**:887–896.

62. Gomez-Perez SL, Haus JM, Sheean P, Patel B, Mar W, Chaudhry V *et al.* Measuring Abdominal Circumference and Skeletal Muscle From a Single Cross-Sectional Computed Tomography Image: A Step-by-Step Guide for Clinicians Using National Institutes of Health ImageJ. *Journal of Parenteral and Enteral Nutrition* 2016;**40**:308–318.

63. Mourtzakis M, Prado CMM, Lieffers JR, Reiman T, McCargar LJ, Baracos VE. A practical and precise approach to quantification of body composition in cancer patients using computed tomography images acquired during routine care. *Appl Physiol Nutr Metab* 2008;**33**:997–1006.

64. Narasimhan A, Greiner R, Bathe OF, Baracos V, Damaraju S. Differentially expressed alternatively spliced genes in skeletal muscle from cancer patients with cachexia: Alternatively spliced genes in cancer cachexia. *Journal of Cachexia, Sarcopenia and Muscle* 2018;**9**:60–70.

65. Chen JL, Walton KL, Qian H, Colgan TD, Hagg A, Watt MJ *et al.* Differential Effects of IL6 and Activin A in the Development of Cancer-Associated Cachexia. *Cancer Res* 2016;**76**:5372–5382.

66. Choi E, Carruthers K, Zhang L, Thomas N, Battaglino RA, Morse LR *et al.* Concurrent muscle and bone deterioration in a murine model of cancer cachexia. *Physiol Rep* 2013;**1**:e00144.

67. Shadfar S, Couch ME, McKinney KA, Weinstein LJ, Yin X, Rodríguez JE *et al.* Oral Resveratrol Therapy Inhibits Cancer-Induced Skeletal Muscle and Cardiac Atrophy In Vivo. *Nutrition and Cancer* 2011;**63**:749–762.

68. Zhou X, Wang JL, Lu J, Song Y, Kwak KS, Jiao Q *et al.* Reversal of Cancer Cachexia and Muscle Wasting by ActRIIB Antagonism Leads to Prolonged Survival. *Cell* 2010;**142**:531–543.

69. Coletti D, Aulino P, Pigna E, Barteri F, Moresi V, Annibali D *et al.* Spontaneous Physical Activity Downregulates Pax7 in Cancer Cachexia. *Stem Cells Int* 2016;**2016**:6729268.

70. White JP, Baynes JW, Welle SL, Kostek MC, Matesic LE, Sato S *et al.* The Regulation of Skeletal Muscle Protein Turnover during the Progression of Cancer Cachexia in the ApcMin/+ Mouse. *PLOS ONE* 2011;**6**:e24650.

71. Padrão AI, Oliveira P, Vitorino R, Colaço B, Pires MJ, Márquez M *et al.* Bladder cancer-induced skeletal muscle wasting: Disclosing the role of mitochondria plasticity. *The International Journal of Biochemistry & Cell Biology* 2013;**45**:1399–1409.

72. Penna F, Costamagna D, Fanzani A, Bonelli G, Baccino FM, Costelli P. Muscle Wasting and Impaired Myogenesis in Tumor Bearing Mice Are Prevented by ERK Inhibition. *PLOS ONE* 2010;**5**:e13604.

73. Puppa MJ, Murphy EA, Fayad R, Hand GA, Carson JA. Cachectic skeletal muscle response to a novel bout of low-frequency stimulation. *Journal of Applied Physiology* 2014;**116**:1078–1087.

74. Rivadeneira DE, Naama HA, McCarter MD, Fujita J, Evoy D, Mackrell P *et al.* Glucocorticoid Blockade Does Not Abrogate Tumor-Induced Cachexia. *Nutrition and Cancer* 1999;**35**:202–206.

75. Talbert EE, Metzger GA, He WA, Guttridge DC. Modeling human cancer cachexia in colon 26 tumor-bearing adult mice. *J Cachexia Sarcopenia Muscle* 2014;**5**:321–328.

76. White JP, Baltgalvis KA, Puppa MJ, Sato S, Baynes JW, Carson JA. Muscle oxidative capacity during IL-6-dependent cancer cachexia. *American Journal of Physiology-Regulatory, Integrative and Comparative Physiology* 2010;**300**:R201–R211.

77. Mehl KA, Davis JM, Berger FG, Carson JA. Myofiber degeneration/regeneration is induced in the cachectic ApcMin/+ mouse. *Journal of Applied Physiology* 2005;**99**:2379–2387.

78. Murphy KT, Chee A, Trieu J, Naim T, Lynch GS. Importance of functional and metabolic impairments in the characterization of the C-26 murine model of cancer cachexia. *Disease Models & Mechanisms* 2012;**5**:533–545.

79. Murphy KT, Struk A, Malcontenti-Wilson C, Christophi C, Lynch GS. Physiological characterization of a mouse model of cachexia in colorectal liver metastases. *American Journal of Physiology-Regulatory, Integrative and Comparative Physiology* 2013;**304**:R854–R864.

80. Norren K van, Kegler D, Argilés JM, Luiking Y, Gorselink M, Laviano A *et al.* Dietary supplementation with a specific combination of high protein, leucine, and fish oil improves muscle function and daily activity in tumour-bearing cachectic mice. *British Journal of Cancer* 2009;**100**:713–722.

81. Diffee GM, Kalfas K, Al-Majid S, McCarthy DO. Altered expression of skeletal muscle myosin isoforms in cancer cachexia. *American Journal of Physiology-Cell Physiology* 2002;**283**:C1376–C1382.

82. Gallot YS, Durieux A-C, Castells J, Desgeorges MM, Vernus B, Plantureux L *et al.* Myostatin Gene Inactivation Prevents Skeletal Muscle Wasting in Cancer. *Cancer Research* 2014;**74**:7344–7356.

83. Hardee JP, Mangum JE, Gao S, Sato S, Hetzler KL, Puppa MJ *et al.* Eccentric contraction-induced myofiber growth in tumor-bearing mice. *Journal of Applied Physiology* 2015;**120**:29–37.

84. Julienne CM, Dumas J-F, Goupille C, Pinault M, Berri C, Collin A *et al.* Cancer cachexia is associated with a decrease in skeletal muscle mitochondrial oxidative capacities without alteration of ATP production efficiency. *J Cachexia Sarcopenia Muscle* 2012;**3**:265–275.

85. Lima M, Sato S, Enos RT, Baynes JW, Carson JA. Development of an UPLC mass spectrometry method for measurement of myofibrillar protein synthesis: application to analysis of murine muscles during cancer cachexia. *J Appl Physiol (1985)* 2013;**114**:824–828.

86. Antunes D, Padrão AI, Maciel E, Santinha D, Oliveira P, Vitorino R *et al.* Molecular insights into mitochondrial dysfunction in cancer-related muscle wasting. *Biochimica et Biophysica Acta (BBA) - Molecular and Cell Biology of Lipids* 2014;**1841**:896–905.

87. Costelli P, Muscaritoli M, Bonetto A, Penna F, Reffo P, Bossola M *et al.* Muscle myostatin signalling is enhanced in experimental cancer cachexia. *European Journal of Clinical Investigation* 2008;**38**:531–538.

88. Baracos VE, DeVivo C, Hoyle DH, Goldberg AL. Activation of the ATP-ubiquitin-proteasome pathway in skeletal muscle of cachectic rats bearing a hepatoma. *American Journal of Physiology-Endocrinology and Metabolism* 1995;**268**:E996–E1006.

89. Pin F, Minero VG, Penna F, Muscaritoli M, De Tullio R, Baccino FM *et al.* Interference with Ca2+-Dependent Proteolysis Does Not Alter the Course of Muscle Wasting in Experimental Cancer Cachexia. *Front Physiol* 2017;**8**:213.

90. Talbert EE, Cuitiño MC, Ladner KJ, Rajasekerea PV, Siebert M, Shakya R *et al.* Modeling Human Cancer-induced Cachexia. *Cell Rep* 2019;**28**:1612–16224.

91. Tseng YC, Kulp SK, Lai IL, Hsu EC, He WA, Frankhouser DE *et al.* Preclinical Investigation of the Novel Histone Deacetylase Inhibitor AR-42 in the Treatment of Cancer-Induced Cachexia. *J Natl Cancer Inst* 2015;**107**:djv274–djv274.

92. Costelli P, Muscaritoli M, Bossola M, Penna F, Reffo P, Bonetto A *et al.* IGF-1 is downregulated in experimental cancer cachexia. *American Journal of Physiology-Regulatory, Integrative and Comparative Physiology* 2006;**291**:R674–R683.

93. Pin F, Barreto R, Couch ME, Bonetto A, O'Connell TM. Cachexia induced by cancer and chemotherapy yield distinct perturbations to energy metabolism. *Journal of Cachexia, Sarcopenia and Muscle* 2019;**10**:140–154.

94. Bonetto A, Penna F, Minero VG, Reffo P, Bonelli G, Baccino FM *et al.* Deacetylase inhibitors modulate the myostatin/follistatin axis without improving cachexia in tumor-bearing mice. *Curr Cancer Drug Targets* 2009;**9**:608–616.

95. Roberts BM, Ahn B, Smuder AJ, Al-Rajhi M, Gill LC, Beharry AW *et al.* Diaphragm and ventilatory dysfunction during cancer cachexia. *The FASEB Journal* 2013;**27**:2600–2610.

96. Aulino P, Berardi E, Cardillo VM, Rizzuto E, Perniconi B, Ramina C *et al.* Molecular, cellular and physiological characterization of the cancer cachexia-inducing C26 colon carcinoma in mouse. *BMC cancer* 2010;**10**:363.

97. Segatto M, Fittipaldi R, Pin F, Sartori R, Dae Ko K, Zare H *et al.* Epigenetic targeting of bromodomain protein BRD4 counteracts cancer cachexia and prolongs survival. *Nat Commun* 2017;**8**:1–16.

98. Murphy KT, Chee A, Gleeson BG, Naim T, Swiderski K, Koopman R *et al.* Antibody-directed myostatin inhibition enhances muscle mass and function in tumor-bearing mice. *American Journal of Physiology-Regulatory, Integrative and Comparative Physiology* 2011;**301**:R716–R726.

99. Roberts BM, Frye GS, Ahn B, Ferreira LF, Judge AR. Cancer cachexia decreases specific force and accelerates fatigue in limb muscle. *Biochemical and Biophysical Research Communications* 2013;**435**:488–492.

100. Zhang G, Liu Z, Ding H, Zhou Y, Doan HA, Sin KWT *et al.* Tumor induces muscle wasting in mice through releasing extracellular Hsp70 and Hsp90. *Nature Communications* 2017;**8**:1–16.

101. VanderVeen BN, Hardee JP, Fix DK, Carson JA. Skeletal muscle function during the progression of cancer cachexia in the male ApcMin/+ mouse. *Journal of Applied Physiology* 2017;**124**:684–695.

102. Inaba S, Hinohara A, Tachibana M, Tsujikawa K, Fukada S. Muscle regeneration is disrupted by cancer cachexia without loss of muscle stem cell potential. *PLoS One* 2018;**13**:e0205467.

103. Baltgalvis KA, Berger FG, Peña MMO, Mark Davis J, White JP, Carson JA. Activity level, apoptosis, and development of cachexia in ApcMin/+ mice. *Journal of Applied Physiology* 2010;**109**:1155–1161.

104. Smith KL, Tisdale MJ. Increased protein degradation and decreased protein synthesis in skeletal muscle during cancer cachexia. *British Journal of Cancer* 1993;**67**:680–685.

105. Goncalves MD, Hwang S-K, Pauli C, Murphy CJ, Cheng Z, Hopkins BD *et al.* Fenofibrate prevents skeletal muscle loss in mice with lung cancer. *Proc Natl Acad Sci USA* 2018;**115**:E743–E752.

106. Khal J, Wyke SM, Russell ST, Hine AV, Tisdale MJ. Expression of the ubiquitin-proteasome pathway and muscle loss in experimental cancer cachexia. *British Journal of Cancer* 2005;**93**:774–780.

107. Penna F, Busquets S, Pin F, Toledo M, Baccino FM, López-Soriano FJ *et al.* Combined approach to counteract experimental cancer cachexia: eicosapentaenoic acid and training exercise. *Journal of Cachexia, Sarcopenia and Muscle* 2011;**2**:95–104.

108. Llovera M, García-Martínez C, López-Soriano J, Agell N, López-Soriano FJ, Garcia I *et al.* Protein turnover in skeletal muscle of tumour-bearing transgenic mice overexpressing the soluble TNF receptor-1. *Cancer Letters* 1998;**130**:19–27.

109. Llovera M, García-Martínez C, López-Soriano J, Carbó N, Agell N, López-Soriano FJ *et al.* Role of TNF receptor 1 in protein turnover during cancer cachexia using gene knockout mice. *Molecular and Cellular Endocrinology* 1998;**142**:183–189.

110. Marin-Corral J, Fontes CC, Pascual-Guardia S, Sanchez F, Olivan M, Argilés JM *et al.* Redox Balance and Carbonylated Proteins in Limb and Heart Muscles of Cachectic Rats. *Antioxidants & Redox Signaling* 2009;**12**:365–380.

111. Fontes-Oliveira CC, Busquets S, Toledo M, Penna F, Aylwin MP, Sirisi S *et al.* Mitochondrial and sarcoplasmic reticulum abnormalities in cancer cachexia: Altered energetic efficiency? *Biochimica et Biophysica Acta (BBA) - General Subjects* 2013;**1830**:2770–2778.

112. Constantinou C, Constantinou C, Oliveira F de, Cristine C, Oliveira F de, Cristine C *et al.* Nuclear magnetic resonance in conjunction with functional genomics suggests mitochondrial dysfunction in a murine model of cancer cachexia. *International Journal of Molecular Medicine* 2011;**27**:15–24.

113. Penna F, Bonetto A, Muscaritoli M, Costamagna D, Minero VG, Bonelli G *et al.* Muscle atrophy in experimental cancer cachexia: is the IGF-1 signaling pathway involved? *Int J Cancer* 2010;**127**:1706–1717.

114. Figueras M, Busquets S, Carbó N, Barreiro E, Almendro V, Argilés JM *et al.* Interleukin-15 is able to suppress the increased DNA fragmentation associated with muscle wasting in tumour-bearing rats. *FEBS Lett* 2004;**569**:201–206.

115. Busquets S, Figueras MT, Fuster G, Almendro V, Moore-Carrasco R, Ametller E *et al.* Anticachectic effects of formoterol: a drug for potential treatment of muscle wasting. *Cancer Res* 2004;**64**:6725–6731.

116. Bonetto A, Rupert JE, Barreto R, Zimmers TA. The Colon-26 Carcinoma Tumor-bearing Mouse as a Model for the Study of Cancer Cachexia. *J Vis Exp* 2016;e54893.

117. Salazar-Degracia A, Busquets S, Argilés JM, Bargalló-Gispert N, López-Soriano FJ, Barreiro E. Effects of the beta2 agonist formoterol on atrophy signaling, autophagy, and muscle phenotype in respiratory and limb muscles of rats with cancer-induced cachexia. *Biochimie* 2018;**149**:79–91.

118. Augusto V, Padovani CR, Campos GR. Skeletal muscle fiber types in C57BL6J mice. *Braz J Morphol Sci* 2004;**21**:89–94.

119. Johns N, Hatakeyama S, Stephens NA, Degen M, Degen S, Frieauff W *et al.* Clinical Classification of Cancer Cachexia: Phenotypic Correlates in Human Skeletal Muscle. *PLOS ONE* 2014;**9**:e83618.

120. Bossola M, Mirabella M, Ricci E, Costelli P, Pacelli F, Tortorelli AP *et al.* Skeletal muscle apoptosis is not increased in gastric cancer patients with mild–moderate weight loss. *The International Journal of Biochemistry & Cell Biology* 2006;**38**:1561–1570.

121. Busquets S, Deans C, Figueras M, Moore-Carrasco R, López-Soriano FJ, Fearon KCH *et al.* Apoptosis is present in skeletal muscle of cachectic gastro-intestinal cancer patients. *Clinical Nutrition* 2007;**26**:614–618.

122. de Castro GS, Simoes E, Lima JDCC, Ortiz-Silva M, Festuccia WT, Tokeshi F *et al.* Human Cachexia Induces Changes in Mitochondria, Autophagy and Apoptosis in the Skeletal Muscle. *Cancers (Basel)* 2019;**11**:1264.

123. Chacon-Cabrera A, Fermoselle C, Urtreger AJ, Mateu-Jimenez M, Diament MJ, de Kier Joffé EDB *et al.* Pharmacological strategies in lung cancer-induced cachexia: effects on muscle proteolysis, autophagy, structure, and weakness. *J Cell Physiol* 2014;**229**:1660–1672.

124. Chacon-Cabrera A, Mateu-Jimenez M, Langohr K, Fermoselle C, García-Arumí E, Andreu AL *et al.* Role of PARP activity in lung cancer-induced cachexia: Effects on muscle oxidative stress, proteolysis, anabolic markers, and phenotype. *J Cell Physiol* 2017;**232**:3744–3761.

125. Salazar-Degracia A, Blanco D, Vilà-Ubach M, de Biurrun G, de Solórzano CO, Montuenga LM *et al.* Phenotypic and metabolic features of mouse diaphragm and gastrocnemius muscles in chronic lung carcinogenesis: influence of underlying emphysema. *J Transl Med* 2016;**14**:244.

126. Zhang Y, Wang J, Wang X, Gao T, Tian H, Zhou D *et al.* The autophagic-lysosomal and ubiquitin proteasome systems are simultaneously activated in the skeletal muscle of gastric cancer patients with cachexia. *Am J Clin Nutr* 2020;**111**:570–579.

127. Marin O, Denny-Brown D. Changes in skeletal muscle associated with cachexia., Changes in Skeletal Muscle Associated with Cachexia. *Am J Pathol* 1962;**41, 41**:23, 23–39.

128. Liu D, Qiao X, Ge Z, Shang Y, Li Y, Wang W *et al.* IMB0901 inhibits muscle atrophy induced by cancer cachexia through MSTN signaling pathway. *Skeletal Muscle* 2019;**9**:8.

129. Hall DT, Griss T, Ma JF, Sanchez BJ, Sadek J, Tremblay AMK *et al.* The AMPK agonist 5-aminoimidazole-4-carboxamide ribonucleotide (AICAR), but not metformin, prevents inflammation-associated cachectic muscle wasting. *EMBO Molecular Medicine* 2018;**10**:e8307.

130. Mu X, Agarwal R, March D, Rothenberg A, Voigt C, Tebbets J *et al.* Notch Signaling Mediates Skeletal Muscle Atrophy in Cancer Cachexia Caused by Osteosarcoma. *Sarcoma* 2016;**2016**.

131. Shakri AR, Zhong TJ, Ma W, Coker C, Kim S, Calluori S *et al.* Upregulation of ZIP14 and Altered Zinc Homeostasis in Muscles in Pancreatic Cancer Cachexia. *Cancers* 2020;**12**:3.

132. Damrauer JS, Stadler ME, Acharyya S, Baldwin AS, Couch ME, Guttridge DC. Chemotherapy-induced muscle wasting: association with NF-κB and cancer cachexia. *European journal of translational myology* 2018;**28**:7590.

133. Zhuang P, Zhang J, Wang Y, Zhang M, Song L, Lu Z *et al.* Reversal of muscle atrophy by Zhimu and Huangbai herb pair via activation of IGF-1/Akt and autophagy signal in cancer cachexia. *Support Care Cancer* 2016;**24**:1189–1198.

134. Marino FE, Risbridger G, Gold E. Activin-βC modulates cachexia by repressing the ubiquitin-proteasome and autophagic degradation pathways. *Journal of Cachexia, Sarcopenia and Muscle* 2015;**6**:365–380.

135. Cai D, Frantz JD, Tawa NE, Melendez PA, Oh B-C, Lidov HGW *et al.* IKKβ/NF-κB Activation Causes Severe Muscle Wasting in Mice. *Cell* 2004;**119**:285–298.

136. Reed SA, Sandesara PB, Senf SM, Judge AR. Inhibition of FoxO transcriptional activity prevents muscle fiber atrophy during cachexia and induces hypertrophy. *The FASEB Journal* 2011;**26**:987–1000.

137. Wang G, Biswas AK, Ma W, Kandpal M, Coker C, Grandgenett PM *et al.* Metastatic cancers promote cachexia through ZIP14 upregulation in skeletal muscle. *Nature Medicine* 2018;**24**:770–781.

138. Berardi E, Aulino P, Murfuni I, Toschi A, Padula F, Scicchitano BM *et al.* Skeletal muscle is enriched in hematopoietic stem cells and not inflammatory cells in cachectic mice. *Neurological Research* 2008;**30**:160–169.

139. Molinari F, Pin F, Gorini S, Chiandotto S, Pontecorvo L, Penna F *et al.* The mitochondrial metabolic reprogramming agent trimetazidine as an 'exercise mimetic' in cachectic C26-bearing mice. *J Cachexia Sarcopenia Muscle* 2017;**8**:954–973.

140. Sciorati C, Touvier T, Buono R, Pessina P, François S, Perrotta C *et al.* Necdin is expressed in cachectic skeletal muscle to protect fibers from tumor-induced wasting. *Journal of Cell Science* 2009;**122**:1119–1125.

141. Pin F, Busquets S, Toledo M, Camperi A, Lopez-Soriano FJ, Costelli P *et al.* Combination of exercise training and erythropoietin prevents cancer-induced muscle alterations. *Oncotarget* 2015;**6**:43202–43215.

142. Winbanks CE, Murphy KT, Bernardo BC, Qian H, Liu Y, Sepulveda PV *et al.* Smad7 gene delivery prevents muscle wasting associated with cancer cachexia in mice. *Science Translational Medicine* 2016;**8**:348ra98.

143. Martinelli GB, Olivari D, Re Cecconi AD, Talamini L, Ottoboni L, Lecker SH *et al.* Activation of the SDF1/CXCR4 pathway retards muscle atrophy during cancer cachexia. *Oncogene* 2016;**35**:6212–6222.

144. Cornwell EW, Mirbod A, Wu C-L, Kandarian SC, Jackman RW. C26 Cancer-Induced Muscle Wasting Is IKKβ-Dependent and NF-kappaB-Independent. *PLoS ONE* 2014;**9**:e87776.

145. Paul PK, Gupta SK, Bhatnagar S, Panguluri SK, Darnay BG, Choi Y *et al.* Targeted ablation of TRAF6 inhibits skeletal muscle wasting in mice. *J Cell Biol* 2010;**191**:1395–1411.

146. Pettersen K, Andersen S, Degen S, Tadini V, Grosjean J, Hatakeyama S *et al.* Cancer cachexia associates with a systemic autophagy-inducing activity mimicked by cancer cell-derived IL-6 trans-signaling. *Scientific Reports* 2017;**7**:1–16.

147. Ham DJ, Murphy KT, Chee A, Lynch GS, Koopman R. Glycine administration attenuates skeletal muscle wasting in a mouse model of cancer cachexia. *Clinical Nutrition* 2014;**33**:448–458.

148. Bohnert KR, Gallot YS, Sato S, Xiong G, Hindi SM, Kumar A. Inhibition of ER stress and unfolding protein response pathways causes skeletal muscle wasting during cancer cachexia. *FASEB J* 2016;**30**:3053–3068.

149. Padilha CS, Borges FH, Costa Mendes da Silva LE, Frajacomo FTT, Jordao AA, Duarte JA *et al.* Resistance exercise attenuates skeletal muscle oxidative stress, systemic pro-inflammatory state, and cachexia in Walker-256 tumor-bearing rats. *Appl Physiol Nutr Metab* 2017;**42**:916–923.

150. Assi M, Derbré F, Lefeuvre-Orfila L, Rébillard A. Antioxidant supplementation accelerates cachexia development by promoting tumor growth in C26 tumor-bearing mice. *Free Radic Biol Med* 2016;**91**:204–214.

151. Schiaffino S, Reggiani C. Fiber Types in Mammalian Skeletal Muscles. *Physiological Reviews* 2011;**91**:1447–1531.

152. Banduseela V, Ochala J, Lamberg K, Kalimo H, Larsson L. Muscle paralysis and myosin loss in a patient with cancer cachexia. *Acta Myol* 2007;**26**:136–144.

153. Schwarzkopf M, Coletti D, Sassoon D, Marazzi G. Muscle cachexia is regulated by a p53–PW1/Peg3-dependent pathway. *Genes Dev* 2006;**20**:3440–3452.

154. Puig-Vilanova E, Rodriguez DA, Lloreta J, Ausin P, Pascual-Guardia S, Broquetas J *et al.* Oxidative stress, redox signaling pathways, and autophagy in cachectic muscles of male patients with advanced COPD and lung cancer. *Free Radic Biol Med* 2015;**79**:91–108.

155. Acharyya S, Butchbach MER, Sahenk Z, Wang H, Saji M, Carathers M *et al.* Dystrophin glycoprotein complex dysfunction: a regulatory link between muscular dystrophy and cancer cachexia. *Cancer Cell* 2005;**8**:421–432.

156. Shum AMY, Mahendradatta T, Taylor RJ, Painter AB, Moore MM, Tsoli M *et al.* Disruption of MEF2C signaling and loss of sarcomeric and mitochondrial integrity in cancer-induced skeletal muscle wasting. *Aging (Albany NY)* 2012;**4**:133–143.

157. Mendell JR, Engel WK. The fine structure of type II muscle fiber atrophy. *Neurology* 1971;**21**:358–365.

158. Baltgalvis KA, Berger FG, Peña MMO, Davis JM, White JP, Carson JA. Muscle wasting and interleukin-6-induced atrogin-I expression in the cachectic Apc Min/+ mouse. *Pflügers Archiv - European Journal of Physiology* 2009;**457**:989–1001.

159. Braun TP, Grossberg AJ, Krasnow SM, Levasseur PR, Szumowski M, Zhu XX *et al.* Cancer- and endotoxin-induced cachexia require intact glucocorticoid signaling in skeletal muscle. *The FASEB Journal* 2013;**27**:3572–3582.

160. Taskin S, Stumpf VI, Bachmann J, Weber C, Martignoni ME, Friedrich O. Motor protein function in skeletal abdominal muscle of cachectic cancer patients. *J Cell Mol Med* 2014;**18**:69–79.

161. Schmitt TL, Martignoni ME, Bachmann J, Fechtner K, Friess H, Kinscherf R *et al.* Activity of the Akt-dependent anabolic and catabolic pathways in muscle and liver samples in cancer-related cachexia. *Journal of Molecular Medicine* 2007;**85**:647–654.

162. Kunzke T, Buck A, Prade VM, Feuchtinger A, Prokopchuk O, Martignoni ME *et al.* Derangements of amino acids in cachectic skeletal muscle are caused by mitochondrial dysfunction. *Journal of Cachexia, Sarcopenia and Muscle* 2020;**11**:226–240.

163. White JP, Puppa MJ, Sato S, Gao S, Price RL, Baynes JW *et al.* IL-6 regulation on skeletal muscle mitochondrial remodeling during cancer cachexia in the ApcMin/+ mouse. *Skeletal Muscle* 2012;**2**:14.

164. Tzika AA, Tzika AA, Fontes-Oliveira CC, Fontes-Oliveira CC, Shestov AA, Shestov AA *et al.* Skeletal muscle mitochondrial uncoupling in a murine cancer cachexia model. *International Journal of Oncology* 2013;**43**:886–894.

165. Shum AMY, Poljak A, Bentley NL, Turner N, Tan TC, Polly P. Proteomic profiling of skeletal and cardiac muscle in cancer cachexia: alterations in sarcomeric and mitochondrial protein expression. *Oncotarget* 2018;**9**:22001–22022.

166. Der-Torossian H, Wysong A, Shadfar S, Willis MS, McDunn J, Couch ME. Metabolic derangements in the gastrocnemius and the effect of Compound A therapy in a murine model of cancer cachexia. *Journal of Cachexia, Sarcopenia and Muscle* 2013;**4**:145–155.

167. Lautaoja JH, Lalowski M, Nissinen TA, Hentilä J, Shi Y, Ritvos O *et al.* Muscle and serum metabolomes are dysregulated in colon-26 tumor-bearing mice despite amelioration of cachexia with activin receptor type 2B ligand blockade. *American Journal of Physiology-Endocrinology and Metabolism* 2019;**316**:E852–E865.

168. Fermoselle C, García-Arumí E, Puig-Vilanova E, Andreu AL, Urtreger AJ, De EKJ *et al.* Mitochondrial dysfunction and therapeutic approaches in respiratory and limb muscles of cancer cachectic mice. *Exp Physiol* 2013;**98**:1349–1365.

169. Gilliam LAA, Lark DS, Reese LR, Torres MJ, Ryan TE, Lin C-T *et al.* Targeted overexpression of mitochondrial catalase protects against cancer chemotherapy-induced skeletal muscle dysfunction. *American Journal of Physiology-Endocrinology and Metabolism* 2016;**311**:E293–E301.

170. Ushmorov A, Hack V, Dröge W. Differential Reconstitution of Mitochondrial Respiratory Chain Activity and Plasma Redox State by Cysteine and Ornithine in a Model of Cancer Cachexia. *Cancer Res* 1999;**59**:3527–3534.

171. VanderVeen BN, Fix DK, Carson JA. Disrupted Skeletal Muscle Mitochondrial Dynamics, Mitophagy, and Biogenesis during Cancer Cachexia: A Role for Inflammation. *Oxid Med Cell Longev* 2017;**2017**:3292087.

172. Neyroud D, Nosacka RL, Judge AR, Hepple RT. Colon 26 adenocarcinoma (C26)-induced cancer cachexia impairs skeletal muscle mitochondrial function and content. *J Muscle Res Cell Motil* 2019;**40**:59–65.

173. Penna F, Ballarò R, Martinez-Cristobal P, Sala D, Sebastian D, Busquets S *et al.* Autophagy Exacerbates Muscle Wasting in Cancer Cachexia and Impairs Mitochondrial Function. *J Mol Biol* 2019;**431**:2674–2686.

174. Romanul FCA. Distribution of Capillaries in Relation to Oxidative Metabolism of Skeletal Muscle Fibres. *Nature* 1964;**201**:307–308.

175. Hochwald SN, Harrison LE, Port JL, Blumberg D, Brennan MF, Burt M. Depletion of high energy phosphate compounds in the tumor-bearing state and reversal after tumor resection. *Surgery* 1996;**120**:534–541.

176. Cui P, Huang C, Guo J, Wang Q, Liu Z, Zhuo H *et al.* Metabolic Profiling of Tumors, Sera, and Skeletal Muscles from an Orthotopic Murine Model of Gastric Cancer Associated-Cachexia. *J Proteome Res* 2019;**18**:1880–1892.

177. Beck SA, Smith KL, Tisdale MJ. Anticachectic and Antitumor Effect of Eicosapentaenoic Acid and Its Effect on Protein Turnover. *Cancer Res* 1991;**51**:6089–6093.

178. Smith HJ, Greenberg NA, Tisdale MJ. Effect of eicosapentaenoic acid, protein and amino acids on protein synthesis and degradation in skeletal muscle of cachectic mice. *British Journal of Cancer* 2004;**91**:408–412.

179. Samuels SE, Knowles AL, Tilignac T, Debiton E, Madelmont JC, Attaix D. Higher skeletal muscle protein synthesis and lower breakdown after chemotherapy in cachectic mice. *American Journal of Physiology-Regulatory, Integrative and Comparative Physiology* 2001;**281**:R133–R139.

180. Temparis S, Asensi M, Taillandier D, Aurousseau E, Larbaud D, Obled A *et al.* Increased ATP-Ubiquitin-dependent Proteolysis in Skeletal Muscles of Tumor-bearing Rats. *Cancer Res* 1994;**54**:5568–5573.

181. Costelli P, García-Martínez C, Llovera M, Carbó N, López-Soriano FJ, Agell N *et al.* Muscle protein waste in tumor-bearing rats is effectively antagonized by a beta 2-adrenergic agonist (clenbuterol). Role of the ATP-ubiquitin-dependent proteolytic pathway. *J Clin Invest* 1995;**95**:2367–2372.

182. Tessitore L, Costelli P, Baccino FM. Pharmacological interference with tissue hypercatabolism in tumour-bearing rats. *Biochem J* 1994;**299**:71–78.

183. Tessitore L, Costelli P, Bonetti G, Baccino FM. Cancer Cachexia, Malnutrition, and Tissue Protein Turnover in Experimental Animals. *Archives of Biochemistry and Biophysics* 1993;**306**:52–58.

184. Toledo M, Busquets S, Penna F, Zhou X, Marmonti E, Betancourt A *et al.* Complete reversal of muscle wasting in experimental cancer cachexia: Additive effects of activin type II receptor inhibition and β-2 agonist. *International Journal of Cancer* 2016;**138**:2021–2029.

185. Lorite MJ, Thompson MG, Drake JL, Carling G, Tisdale MJ. Mechanism of muscle protein degradation induced by a cancer cachectic factor. *Br J Cancer* 1998;**78**:850–856.

186. Costelli P, Carbó N, Tessitore L, Bagby GJ, Lopez-Soriano FJ, Argilés JM *et al.* Tumor necrosis factor-alpha mediates changes in tissue protein turnover in a rat cancer cachexia model. *J Clin Invest* 1993;**92**:2783–2789.

187. Argilés JM, Stemmler B, López-Soriano FJ, Busquets S. Nonmuscle Tissues Contribution to Cancer Cachexia. *Mediators of Inflammation* 2015;**2015**:1–9.

188. Chargé SBP, Rudnicki MA. Cellular and Molecular Regulation of Muscle Regeneration. *Physiological Reviews* 2004;**84**:209–238.

189. Mounier R, Théret M, Arnold L, Cuvellier S, Bultot L, Göransson O *et al.* AMPKα1 Regulates Macrophage Skewing at the Time of Resolution of Inflammation during Skeletal Muscle Regeneration. *Cell Metabolism* 2013;**18**:251–264.

190. Roberts EW, Deonarine A, Jones JO, Denton AE, Feig C, Lyons SK *et al.* Depletion of stromal cells expressing fibroblast activation protein-α from skeletal muscle and bone marrow results in cachexia and anemia. *The Journal of Experimental Medicine* 2013;**210**:1137–1151.

191. Bentzinger CF, Wang YX, Dumont NA, Rudnicki MA. Cellular dynamics in the muscle satellite cell niche. *EMBO reports* 2013;**14**:1062–1072.

192. Jewesbury RC, Topley WWC. On certain changes occurring in the voluntary muscles in general diseases. *J Pathol* 1912;**17**:432–453.

193. He WA, Berardi E, Cardillo VM, Acharyya S, Aulino P, Thomas-Ahner J *et al.* NF-κB–mediated Pax7 dysregulation in the muscle microenvironment promotes cancer cachexia. *J Clin Invest* 2013;**123**:4821–4835.

194. Judge SM, Nosacka RL, Delitto D, Gerber MH, Cameron ME, Trevino JG *et al.* Skeletal Muscle Fibrosis in Pancreatic Cancer Patients with Respect to Survival. *JNCI Cancer Spectr* 2018;**2**.

195. Salazar-Degracia A, Busquets S, Argilés JM, López-Soriano FJ, Barreiro E. Formoterol attenuates increased oxidative stress and myosin protein loss in respiratory and limb muscles of cancer cachectic rats. *PeerJ* 2017;**5**:e4109.

196. Zampieri S, Doria A, Adami N, Biral D, Vecchiato M, Savastano S *et al.* Subclinical myopathy in patients affected with newly diagnosed colorectal cancer at clinical onset of disease: evidence from skeletal muscle biopsies. *Neurological Research* 2010;**32**:20–25.

197. Pigna E, Berardi E, Aulino P, Rizzuto E, Zampieri S, Carraro U *et al.* Aerobic Exercise and Pharmacological Treatments Counteract Cachexia by Modulating Autophagy in Colon Cancer. *Sci Rep* 2016;**6**:26991.

198. Nosacka RL, Delitto AE, Delitto D, Patel R, Judge SM, Trevino JG *et al.* Distinct cachexia profiles in response to human pancreatic tumours in mouse limb and respiratory muscle. *Journal of Cachexia, Sarcopenia and Muscle* 2020;**11**:820–837.

199. Gabiatti CTB, Martins MCL, Miyazaki DL, Silva LP, Lascala F, Macedo LT *et al.* Myosteatosis in a systemic inflammation-dependent manner predicts favorable survival outcomes in locally advanced esophageal cancer. *Cancer Med* 2019;**8**:6967–6976.

200. Stretch C, Aubin J-M, Mickiewicz B, Leugner D, Al-manasra T, Tobola E *et al.* Sarcopenia and myosteatosis are accompanied by distinct biological profiles in patients with pancreatic and periampullary adenocarcinomas. *PLOS ONE* 2018;**13**:e0196235.

201. Stephens NA, Skipworth RJ, Macdonald AJ, Greig CA, Ross JA, Fearon KC. Intramyocellular lipid droplets increase with progression of cachexia in cancer patients., Intramyocellular lipid droplets increase with progression of cachexia in cancer patients. *J Cachexia Sarcopenia Muscle* 2011;**2, 2**:111, 111–117.

202. Bhullar AS, Anoveros-Barrera A, Dunichand-Hoedl A, Martins K, Bigam D, Khadaroo RG *et al.* Lipid is heterogeneously distributed in muscle and associates with low radiodensity in cancer patients. *Journal of Cachexia, Sarcopenia and Muscle* 2020;**11**:735–747.

203. Murton AJ, Maddocks M, Stephens FB, Marimuthu K, England R, Wilcock A. Consequences of Late-Stage Non–Small-Cell Lung Cancer Cachexia on Muscle Metabolic Processes. *Clinical Lung Cancer* 2017;**18**:e1–e11.

204. Fernandez GJ, Ferreira JH, Vechetti IJJ, de Moraes LN, Cury SS, Freire PP *et al.* MicroRNA-mRNA Co-sequencing Identifies Transcriptional and Post-transcriptional Regulatory Networks Underlying Muscle Wasting in Cancer Cachexia. *Front Genet* 2020;**11**:541.

205. Bae T, Jang J, Lee H, Song J, Chae S, Park M *et al.* Paeonia lactiflora root extract suppresses cancer cachexia by down-regulating muscular NF-κB signalling and muscle-specific E3 ubiquitin ligases in cancer-bearing mice. *Journal of Ethnopharmacology* 2020;**246**:112222.

206. Busquets S, Toledo M, Sirisi S, Orpí M, Serpe R, COUTINHO J *et al.* Formoterol and cancer muscle wasting in rats: Effects on muscle force and total physical activity. *Exp Ther Med* 2011;**2**:731–735.

207. Busquets S, Toledo M, Orpí M, Massa D, Porta M, Capdevila E *et al.* Myostatin blockage using actRIIB antagonism in mice bearing the Lewis lung carcinoma results in the improvement of muscle wasting and physical performance. *Journal of Cachexia, Sarcopenia and Muscle* 2012;**3**:37–43.

208. Levolger S, Wiemer E a. C, van Vugt JLA, Huisman SA, van Vledder MG, van Damme-van Engel S *et al.* Inhibition of activin-like kinase 4/5 attenuates cancer cachexia associated muscle wasting. *Scientific Reports* 2019;**9**:1–11.

209. Parajuli P, Kumar S, Loumaye A, Singh P, Eragamreddy S, Nguyen TL *et al.* Twist1 Activation in Muscle Progenitor Cells Causes Muscle Loss Akin to Cancer Cachexia. *Dev Cell* 2018;**45**:712–725.

210. Penna F, Busquets S, Argilés JM. Experimental cancer cachexia: Evolving strategies for getting closer to the human scenario. *Seminars in Cell & Developmental Biology* 2016;**54**:20–27.

211. Toledo M, Busquets S, Sirisi S, Serpe R, Orpí M, Coutinho J *et al.* Cancer cachexia: Physical activity and muscle force in tumour-bearing rats. *Oncology Reports* 2011;**25**:189–193.

212. Kir S, Komaba H, Garcia AP, Economopoulos KP, Liu W, Lanske B *et al.* PTH/PTHrP Receptor Mediates Cachexia in Models of Kidney Failure and Cancer. *Cell Metabolism* 2016;**23**:315–323.

213. Gorselink Marchel, Vaessen Stefan F.C., van der Flier Laurens G., Leenders Inge, Kegler Diane, Caldenhoven Eric *et al.* Mass-dependent decline of skeletal muscle function in cancer cachexia. *Muscle & Nerve* 2006;**33**:691–693.

214. Gale N, Wasley D, Roberts S, Backx K, Nelson A, van Deursen R *et al.* A longitudinal study of muscle strength and function in patients with cancer cachexia. *Support Care Cancer* 2019;**27**:131–137.

215. Goodpaster BH, Park SW, Harris TB, Kritchevsky SB, Nevitt M, Schwartz AV *et al.* The Loss of Skeletal Muscle Strength, Mass, and Quality in Older Adults: The Health, Aging and Body Composition Study. *J Gerontol A Biol Sci Med Sci* 2006;**61**:1059–1064.

216. Williams GR, Muss HB, Shachar SS. Cachexia in patients with cancer. *The Lancet Oncology* 2016;**17**:e220.

217. Cai B, Allexandre D, Rajagopalan V, Jiang Z, Siemionow V, Ranganathan VK *et al.* Evidence of Significant Central Fatigue in Patients with Cancer-Related Fatigue during Repetitive Elbow Flexions till Perceived Exhaustion. *PLOS ONE* 2014;**9**:e115370.

218. Yavuzsen T, Davis MP, Ranganathan VK, Walsh D, Siemionow V, Kirkova J *et al.* Cancer-Related Fatigue: Central or Peripheral? *Journal of Pain and Symptom Management* 2009;**38**:587–596.

219. Kisiel-Sajewicz K, Siemionow V, Seyidova-Khoshknabi D, Davis MP, Wyant A, Ranganathan VK *et al.* Myoelectrical Manifestation of Fatigue Less Prominent in Patients with Cancer Related Fatigue. *PLOS ONE* 2013;**8**:e83636.

220. Bottinelli R, Pellegrino MA, Canepari M, Rossi R, Reggiani C. Specific contributions of various muscle fibre types to human muscle performance: an in vitro study. *J Electromyogr Kinesiol* 1999;**9**:87–95.

221. Gissel H. The Role of Ca2+ in Muscle Cell Damage. *Annals of the New York Academy of Sciences* 2005;**1066**:166–180.

222. Jones RA, Harrison C, Eaton SL, Hurtado ML, Graham LC, Alkhammash L *et al.* Cellular and Molecular Anatomy of the Human Neuromuscular Junction. *Cell Reports* 2017;**21**:2348–2356.

223. Mierzejewski B, Archacka K, Grabowska I, Florkowska A, Ciemerych MA, Brzoska E. Human and mouse skeletal muscle stem and progenitor cells in health and disease. *Seminars in Cell & Developmental Biology* 2020;**104**:93–104.

224. Emery PW, Edwards RH, Rennie MJ, Souhami RL, Halliday D. Protein synthesis in muscle measured in vivo in cachectic patients with cancer. *Br Med J (Clin Res Ed)* 1984;**289**:584–586.

225. Dworzak F, Ferrari P, Gavazzi C, Maiorana C, Bozzetti F. Effects of cachexia due to cancer on whole body and skeletal muscle protein turnover. *Cancer* 1998;**82**:42–48.

226. Emery PW, Lovell L, Rennie MJ. Protein Synthesis Measured in Vivo in Muscle and Liver of Cachectic Tumor-bearing Mice. *Cancer Res* 1984;**44**:2779–2784.

227. Nissinen TA, Hentilä J, Penna F, Lampinen A, Lautaoja JH, Fachada V *et al.* Treating cachexia using soluble ACVR2B improves survival, alters mTOR localization, and attenuates liver and spleen responses: Treating cachexia using soluble ACVR2B. *Journal of Cachexia, Sarcopenia and Muscle* 2018;**9**:514–529.

228. White JP, Puppa MJ, Gao S, Sato S, Welle SL, Carson JA. Muscle mTORC1 suppression by IL-6 during cancer cachexia: a role for AMPK. *American Journal of Physiology-Endocrinology and Metabolism* 2013;**304**:E1042–E1052.

229. Shaw JH, Humberstone DA, Douglas RG, Koea J. Leucine kinetics in patients with benign disease, non-weight-losing cancer, and cancer cachexia: studies at the whole-body and tissue level and the response to nutritional support. *Surgery* 1991;**109**:37–50.

230. MacDonald AJ, Johns N, Stephens N, Greig C, Ross JA, Small AC *et al.* Habitual Myofibrillar Protein Synthesis Is Normal in Patients with Upper GI Cancer Cachexia. *Clin Cancer Res* 2015;**21**:1734–1740.

231. Bonetto A, Penna F, Aversa Z, Mercantini P, Baccino FM, Costelli P *et al.* Early changes of muscle insulin-like growth factor-1 and myostatin gene expression in gastric cancer patients. *Muscle Nerve* 2013;**48**:387–392.

232. Puppa MJ, Gao S, Narsale AA, Carson JA. Skeletal muscle glycoprotein 130's role in Lewis lung carcinoma-induced cachexia. *FASEB J* 2014;**28**:998–1009.

233. Koutnik AP, Poff AM, Ward NP, DeBlasi JM, Soliven MA, Romero MA *et al.* Ketone Bodies Attenuate Wasting in Models of Atrophy. *Journal of Cachexia, Sarcopenia and Muscle* 2020 doi:10.1002/jcsm.12554.

234. Gallagher IJ, Stephens NA, MacDonald AJ, Skipworth RJE, Husi H, Greig CA *et al.* Suppression of Skeletal Muscle Turnover in Cancer Cachexia: Evidence from the Transcriptome in Sequential Human Muscle Biopsies. *Clin Cancer Res* 2012;**18**:2817–2827.

235. Skorokhod A, Bachmann J, Giese NA, Martignoni ME, Krakowski-Roosen H. Real-imaging cDNA-AFLP transcript profiling of pancreatic cancer patients: Egr-1 as a potential key regulator of muscle cachexia. *BMC Cancer* 2012;**12**:265.

236. Stephens NA, Skipworth RJE, Gallagher IJ, Greig CA, Guttridge DC, Ross JA *et al.* Evaluating potential biomarkers of cachexia and survival in skeletal muscle of upper gastrointestinal cancer patients. *Journal of Cachexia, Sarcopenia and Muscle* 2015;**6**:53.

237. Asp ML, Tian M, Wendel AA, Belury MA. Evidence for the contribution of insulin resistance to the development of cachexia in tumor-bearing mice. *International Journal of Cancer* 2010;**126**:756–763.

238. Russell ST, Siren PMA, Siren MJ, Tisdale MJ. Attenuation of skeletal muscle atrophy in cancer cachexia by d-myo-inositol 1,2,6-triphosphate. *Cancer Chemother Pharmacol* 2009;**64**:517–527.

239. Eley HL, Russell ST, Tisdale MJ. Effect of branched-chain amino acids on muscle atrophy in cancer cachexia. *Biochem J* 2007;**407**:113–120.

240. Blackwell TA, Cervenka I, Khatri B, Brown JL, Rosa-Caldwell ME, Lee DE *et al.* Transcriptomic analysis of the development of skeletal muscle atrophy in cancer-cachexia in tumor-bearing mice. *Physiol Genomics* 2018;**50**:1071–1082.

241. Sandri M. Protein breakdown in muscle wasting: Role of autophagy-lysosome and ubiquitin-proteasome. *The International Journal of Biochemistry & Cell Biology* 2013;**45**:2121–2129.

242. Hershko A. The ubiquitin system for protein degradation and some of its roles in the control of the cell division cycle*. *Cell Death and Differentiation* 2005;**12**:1191–1197.

243. Bodine SC, Baehr LM. Skeletal muscle atrophy and the E3 ubiquitin ligases MuRF1 and MAFbx/atrogin-1. *American Journal of Physiology-Endocrinology and Metabolism* 2014;**307**:E469–E484.

244. Kedar V, McDonough H, Arya R, Li H-H, Rockman HA, Patterson C. Muscle-specific RING finger 1 is a bona fide ubiquitin ligase that degrades cardiac troponin I. *PNAS* 2004;**101**:18135–18140.

245. Clarke BA, Drujan D, Willis MS, Murphy LO, Corpina RA, Burova E *et al.* The E3 Ligase MuRF1 Degrades Myosin Heavy Chain Protein in Dexamethasone-Treated Skeletal Muscle. *Cell Metabolism* 2007;**6**:376–385.

246. Polge C, Heng A-E, Jarzaguet M, Ventadour S, Claustre A, Combaret L *et al.* Muscle actin is polyubiquitinylated in vitro and in vivo and targeted for breakdown by the E3 ligase MuRF1. *The FASEB Journal* 2011;**25**:3790–3802.

247. Tintignac LA, Lagirand J, Batonnet S, Sirri V, Leibovitch MP, Leibovitch SA. Degradation of MyoD mediated by the SCF (MAFbx) ubiquitin ligase. *J Biol Chem* 2005;**280**:2847–2856.

248. Csibi A, Cornille K, Leibovitch M-P, Poupon A, Tintignac LA, Sanchez AMJ *et al.* The Translation Regulatory Subunit eIF3f Controls the Kinase-Dependent mTOR Signaling Required for Muscle Differentiation and Hypertrophy in Mouse. *PLOS ONE* 2010;**5**:e8994.

249. Stephens NA, Gallagher IJ, Rooyackers O, Skipworth RJ, Tan BH, Marstrand T *et al.* Using transcriptomics to identify and validate novel biomarkers of human skeletal muscle cancer cachexia. *Genome Medicine* 2010;**2**:1.

250. D'Orlando C, Marzetti E, François S, Lorenzi M, Conti V, Stasio E di *et al.* Gastric cancer does not affect the expression of atrophy-related genes in human skeletal muscle. *Muscle & Nerve* 2014;**49**:528–533.

251. Barreiro E, Salazar-Degracia A, Sancho-Muñoz A, Gea J. Endoplasmic reticulum stress and unfolded protein response profile in quadriceps of sarcopenic patients with respiratory diseases. *Journal of Cellular Physiology* 2019;**234**:11315–11329.

252. Bossola M, Muscaritoli M, Costelli P, Grieco G, Bonelli G, Pacelli F *et al.* Increased Muscle Proteasome Activity Correlates With Disease Severity in Gastric Cancer Patients. *Ann Surg* 2003;**237**:384–389.

253. Bossola M, Muscaritoli M, Costelli P, Bellantone R, Pacelli F, Busquets S *et al.* Increased muscle ubiquitin mRNA levels in gastric cancer patients. *American Journal of Physiology-Regulatory, Integrative and Comparative Physiology* 2001;**280**:R1518–R1523.

254. Sun Y-S, Ye Z-Y, Qian Z-Y, Xu X-D, Hu J-F. Expression of TRAF6 and ubiquitin mRNA in skeletal muscle of gastric cancer patients. *Journal of Experimental & Clinical Cancer Research* 2012;**31**:81.

255. Jagoe RT, Redfern CPF, Roberts RG, Gibson GJ, Goodship THJ. Skeletal muscle mRNA levels for cathepsin B, but not components of the ubiquitin-proteasome pathway, are increased in patients with lung cancer referred for thoracotomy. *Clin Sci* 2002;**102**:353–361.

256. Khal J, Hine AV, Fearon KCH, Dejong CHC, Tisdale MJ. Increased expression of proteasome subunits in skeletal muscle of cancer patients with weight loss. *The International Journal of Biochemistry & Cell Biology* 2005;**37**:2196–2206.

257. Acharyya S, Ladner KJ, Nelsen LL, Damrauer J, Reiser PJ, Swoap S *et al.* Cancer cachexia is regulated by selective targeting of skeletal muscle gene products. *J Clin Invest* 2004;**114**:370–378.

258. Braun TP, Zhu X, Szumowski M, Scott GD, Grossberg AJ, Levasseur PR *et al.* Central nervous system inflammation induces muscle atrophy via activation of the hypothalamic–pituitary–adrenal axis. *J Exp Med* 2011;**208**:2449–2463.

259. Fontes-Oliveira CC, Busquets S, Fuster G, Ametller E, Figueras M, Olivan M *et al.* A differential pattern of gene expression in skeletal muscle of tumor-bearing rats reveals dysregulation of excitation–contraction coupling together with additional muscle alterations. *Muscle Nerve* 2014;**49**:233–248.

260. Guarnier FA, Cecchini AL, Suzukawa AA, Maragno ALGC, Simão ANC, Gomes MD *et al.* Time course of skeletal muscle loss and oxidative stress in rats with walker 256 solid tumor. *Muscle & Nerve* 2010;**42**:950–958.

261. Lin X-Y, Chen S-Z. Calpain inhibitors ameliorate muscle wasting in a cachectic mouse model bearing CT26 colorectal adenocarcinoma. *Oncology Reports* 2017;**37**:1601–1610.

262. Mastrocola R, Reffo P, Penna F, Tomasinelli CE, Boccuzzi G, Baccino FM *et al.* Muscle wasting in diabetic and in tumor-bearing rats: role of oxidative stress. *Free Radic Biol Med* 2008;**44**:584–593.

263. Matsuyama T, Ishikawa T, Okayama T, Oka K, Adachi S, Mizushima K *et al.* Tumor inoculation site affects the development of cancer cachexia and muscle wasting. *International Journal of Cancer* 2015;**137**:2558–2565.

264. Michaelis KA, Zhu X, Burfeind KG, Krasnow SM, Levasseur PR, Morgan TK *et al.* Establishment and characterization of a novel murine model of pancreatic cancer cachexia. *Journal of Cachexia, Sarcopenia and Muscle* 2017;**8**:824–838.

265. Penna F, Costamagna D, Pin F, Camperi A, Fanzani A, Chiarpotto EM *et al.* Autophagic Degradation Contributes to Muscle Wasting in Cancer Cachexia. *The American Journal of Pathology* 2013;**182**:1367–1378.

266. Re Cecconi AD, Forti M, Chiappa M, Zhu Z, Zingman LV, Cervo L *et al.* Musclin, A Myokine Induced by Aerobic Exercise, Retards Muscle Atrophy During Cancer Cachexia in Mice. *Cancers* 2019;**11**:1541.

267. Shukla SK, Markov SD, Attri KS, Vernucci E, King RJ, Dasgupta A *et al.* Macrophages potentiate STAT3 signaling in skeletal muscles and regulate pancreatic cancer cachexia. *Cancer Letters* 2020;**484**:29–39.

268. Wang Q, Li C, Peng X, Kang Q, Deng D, Zhang L *et al.* Combined treatment of carfilzomib and z-VAD-fmk inhibits skeletal proteolysis and apoptosis and ameliorates cancer cachexia. *Med Oncol* 2015;**32**:100.

269. Yuan L, Han J, Meng Q, Xi Q, Zhuang Q, Jiang Y *et al.* Muscle-specific E3 ubiquitin ligases are involved in muscle atrophy of cancer cachexia: An in vitro and in vivo study. *Oncology Reports* 2015;**33**:2261–2268.

270. Zhang L, Tang H, Kou Y, Li R, Zheng Y, Wang Q *et al.* MG132-mediated inhibition of the ubiquitin–proteasome pathway ameliorates cancer cachexia. *J Cancer Res Clin Oncol* 2013;**139**:1105–1115.

271. Lecker SH, Jagoe RT, Gilbert A, Gomes M, Baracos V, Bailey J *et al.* Multiple types of skeletal muscle atrophy involve a common program of changes in gene expression. *FASEB j* 2004;**18**:39–51.

272. QuanJun Y, GenJin Y, LiLi W, Yan H, YongLong H, Jin L *et al.* Integrated analysis of serum and intact muscle metabonomics identify metabolic profiles of cancer cachexia in a dynamic mouse model. *RSC Adv* 2015;**5**:92438–92448.

273. Llovera M, García-Martínez C, Agell N, Marzábal M, López-Soriano FJ, Argilés JM. Ubiquitin gene expression is increased in skeletal muscle of tumour-bearing rats. *FEBS Lett* 1994;**338**:311–318.

274. Fujita J, Tsujinaka T, Jano M, Ebisui C, Saito H, Katsume A *et al.* Anti-interleukin-6 receptor antibody prevents muscle atrophy in colon-26 adenocarcinoma-bearing mice with modulation of lysosomal and ATP-ubiquitin-dependent proteolytic pathways. *International Journal of Cancer* 1996;**68**:637–643.

275. Busquets S, Toledo M, Marmonti E, Orpí M, Capdevila E, Betancourt A *et al.* Formoterol treatment downregulates the myostatin system in skeletal muscle of cachectic tumour-bearing rats. *Oncol Lett* 2012;**3**:185–189.

276. Busquets S, García-Martínez C, Alvarez B, Carbó N, López-Soriano FJ, Argilés JM. Calpain-3 gene expression is decreased during experimental cancer cachexia. *Biochimica et Biophysica Acta (BBA) - General Subjects* 2000;**1475**:5–9.

277. Moore-Carrasco R, Busquets S, Almendro V, Palanki M, López-Soriano FJ, Argilés JM. The AP-1/NF-kappaB double inhibitor SP100030 can revert muscle wasting during experimental cancer cachexia. *Int J Oncol* 2007;**30**:1239–1245.

278. Carbó N, López-Soriano J, Costelli P, Busquets S, Alvarez B, Baccino FM *et al.* Interleukin-15 antagonizes muscle protein waste in tumour-bearing rats. *British Journal of Cancer* 2000;**83**:526–531.

279. Solomon V, Baracos V, Sarraf P, Goldberg AL. Rates of ubiquitin conjugation increase when muscles atrophy, largely through activation of the N-end rule pathway. *Proc Natl Acad Sci U S A* 1998;**95**:12602–12607.

280. Eley HL, Russell ST, Tisdale MJ. Attenuation of muscle atrophy in a murine model of cachexia by inhibition of the dsRNA-dependent protein kinase. *British Journal of Cancer* 2007;**96**:1216–1222.

281. Shum AMY, Fung DCY, Corley SM, McGill MC, Bentley NL, Tan TC *et al.* Cardiac and skeletal muscles show molecularly distinct responses to cancer cachexia. *Physiological Genomics* 2015;**47**:588–599.

282. Judge SM, Wu C-L, Beharry AW, Roberts BM, Ferreira LF, Kandarian SC *et al.* Genome-wide identification of FoxO-dependent gene networks in skeletal muscle during C26 cancer cachexia. *BMC Cancer* 2014;**14**:997.

283. Bonetto A, Aydogdu T, Kunzevitzky N, Guttridge DC, Khuri S, Koniaris LG *et al.* STAT3 Activation in Skeletal Muscle Links Muscle Wasting and the Acute Phase Response in Cancer Cachexia. *PLoS ONE* 2011;**6**:e22538.

284. Costelli P, Bossola M, Muscaritoli M, Grieco G, Bonelli G, Bellantone R *et al.* Anticytokine treatment prevents the increase in the activity of ATP-ubiquitin-and Ca2+-dependent proteolytic systems in the muscle of tumour-bearing rats. *Cytokine* 2002;**19**:1–5.

285. Llovera M, Garcia-Martinez C, Agell N, Lopez-Soriano FJ, Argiles JM. Muscle wasting associated with cancer cachexia is linked to an important activation of the atp-dependent ubiquitin-mediated proteolysis. *International Journal of Cancer* 1995;**61**:138–141.

286. Bonaldo P, Sandri M. Cellular and molecular mechanisms of muscle atrophy. *Disease Models & Mechanisms* 2013;**6**:25–39.

287. Masiero E, Agatea L, Mammucari C, Blaauw B, Loro E, Komatsu M *et al.* Autophagy Is Required to Maintain Muscle Mass. *Cell Metabolism* 2009;**10**:507–515.

288. Mammucari C, Milan G, Romanello V, Masiero E, Rudolf R, Del Piccolo P *et al.* FoxO3 Controls Autophagy in Skeletal Muscle In Vivo. *Cell Metabolism* 2007;**6**:458–471.

289. Zhao J, Brault JJ, Schild A, Cao P, Sandri M, Schiaffino S *et al.* FoxO3 Coordinately Activates Protein Degradation by the Autophagic/Lysosomal and Proteasomal Pathways in Atrophying Muscle Cells. *Cell Metabolism* 2007;**6**:472–483.

290. Marzetti E, Lorenzi M, Landi F, Picca A, Rosa F, Tanganelli F *et al.* Altered mitochondrial quality control signaling in muscle of old gastric cancer patients with cachexia. *Experimental Gerontology* 2017;**87**:92–99.

291. Ballarò R, Penna F, Pin F, Gómez-Cabrera MC, Viña J, Costelli P. Moderate Exercise Improves Experimental Cancer Cachexia by Modulating the Redox Homeostasis. *Cancers* 2019;**11**:285.

292. Hentilä J, Nissinen TA, Korkmaz A, Lensu S, Silvennoinen M, Pasternack A *et al.* Activin Receptor Ligand Blocking and Cancer Have Distinct Effects on Protein and Redox Homeostasis in Skeletal Muscle and Liver. *Front Physiol* 2019;**9**.

293. Deval C, Mordier S, Obled C, Bechet D, Combaret L, Attaix D *et al.* Identification of cathepsin L as a differentially expressed message associated with skeletal muscle wasting. *Biochemical Journal* 2001;**360**:143–150.

294. Milan G, Romanello V, Pescatore F, Armani A, Paik J-H, Frasson L *et al.* Regulation of autophagy and the ubiquitin–proteasome system by the FoxO transcriptional network during muscle atrophy. *Nature Communications* 2015;**6**:6670.

295. Sandri M, Sandri C, Gilbert A, Skurk C, Calabria E, Picard A *et al.* Foxo Transcription Factors Induce the Atrophy-Related Ubiquitin Ligase Atrogin-1 and Cause Skeletal Muscle Atrophy. *Cell* 2004;**117**:399–412.

296. Stitt TN, Drujan D, Clarke BA, Panaro F, Timofeyva Y, Kline WO *et al.* The IGF-1/PI3K/Akt pathway prevents expression of muscle atrophy-induced ubiquitin ligases by inhibiting FOXO transcription factors. *Mol Cell* 2004;**14**:395–403.

297. Johns N, Stretch C, Tan BHL, Solheim TS, Sørhaug S, Stephens NA *et al.* New genetic signatures associated with cancer cachexia as defined by low skeletal muscle index and weight loss. *Journal of Cachexia, Sarcopenia and Muscle* 2017;**8**:122–130.

298. Bartoli M, Richard I. Calpains in muscle wasting. *The International Journal of Biochemistry & Cell Biology* 2005;**37**:2115–2133.

299. Smith IJ, Aversa Z, Hasselgren P-O, Pacelli F, Rosa F, Doglietto GB *et al.* CALPAIN activity is increased in skeletal muscle from gastric cancer patients with no or minimal weight loss. *Muscle & Nerve* 2011;**43**:410–414.

300. Costelli P, Tullio RD, Baccino FM, Melloni E. Activation of Ca2+-dependent proteolysis in skeletal muscle and heart in cancer cachexia. *Br J Cancer* 2001;**84**:946–950.

301. Vainshtein A, Sandri M. Signaling Pathways That Control Muscle Mass. *Int J Mol Sci* 2020;**21**.

302. Le Moal E, Pialoux V, Juban G, Groussard C, Zouhal H, Chazaud B *et al.* Redox Control of Skeletal Muscle Regeneration. *Antioxidants & Redox Signaling* 2016;**27**:276–310.

303. Gomes-Marcondes MCC, Tisdale MJ. Induction of protein catabolism and the ubiquitin-proteasome pathway by mild oxidative stress. *Cancer Letters* 2002;**180**:69–74.

304. Aucello M, Dobrowolny G, Musarò A. Localized accumulation of oxidative stress causes muscle atrophy through activation of an autophagic pathway. *Autophagy* 2009;**5**:527–529.

305. McClung JM, Judge AR, Powers SK, Yan Z. p38 MAPK links oxidative stress to autophagy-related gene expression in cachectic muscle wasting. *Am J Physiol, Cell Physiol* 2010;**298**:C542-549.

306. Smuder AJ, Kavazis AN, Hudson MB, Nelson WB, Powers SK. Oxidation enhances myofibrillar protein degradation via calpain and caspase-3. *Free Radical Biology and Medicine* 2010;**49**:1152–1160.

307. Tan PL, Shavlakadze T, Grounds MD, Arthur PG. Differential thiol oxidation of the signaling proteins Akt, PTEN or PP2A determines whether Akt phosphorylation is enhanced or inhibited by oxidative stress in C2C12 myotubes derived from skeletal muscle. *The International Journal of Biochemistry & Cell Biology* 2015;**62**:72–79.

308. Yang SY, Hoy M, Fuller B, Sales KM, Seifalian AM, Winslet MC. Pretreatment with insulin-like growth factor I protects skeletal muscle cells against oxidative damage via PI3K/Akt and ERK1/2 MAPK pathways. *Laboratory Investigation* 2010;**90**:391–401.

309. Dodd SL, Gagnon BJ, Senf SM, Hain BA, Judge AR. Ros-mediated activation of NF-κB and Foxo during muscle disuse. *Muscle & Nerve* 2010;**41**:110–113.

310. Ramamoorthy S, Donohue M, Buck M. Decreased Jun-D and myogenin expression in muscle wasting of human cachexia. *American Journal of Physiology-Endocrinology and Metabolism* 2009;**297**:E392–E401.

311. Brzeszczyńska J, Johns N, Schilb A, Degen S, Degen M, Langen R *et al.* Loss of oxidative defense and potential blockade of satellite cell maturation in the skeletal muscle of patients with cancer but not in the healthy elderly. *aging* 2016;**8**:1690–1702.

312. Sullivan-Gunn MJ, Campbell-O'Sullivan SP, Tisdale MJ, Lewandowski PA. Decreased NADPH oxidase expression and antioxidant activity in cachectic skeletal muscle. *J Cachexia Sarcopenia Muscle* 2011;**2**:181–188.

313. Brown JL, Rosa-Caldwell ME, Lee DE, Blackwell TA, Brown LA, Perry RA *et al.* Mitochondrial degeneration precedes the development of muscle atrophy in progression of cancer cachexia in tumour-bearing mice. *Journal of Cachexia, Sarcopenia and Muscle* 2017;**8**:926–938.

314. Barreiro E, Puente B de la, Busquets S, López-Soriano FJ, Gea J, Argilés JM. Both oxidative and nitrosative stress are associated with muscle wasting in tumour-bearing rats. *FEBS Letters* 2005;**579**:1646–1652.

315. Deans D a. C, Tan BH, Wigmore SJ, Ross JA, de Beaux AC, Paterson-Brown S *et al.* The influence of systemic inflammation, dietary intake and stage of disease on rate of weight loss in patients with gastro-oesophageal cancer. *British Journal of Cancer* 2009;**100**:63–69.

316. O'Gorman P, McMillan DC, McArdle CS. Longitudinal Study of Weight, Appetite, Performance Status, and Inflammation in Advanced Gastrointestinal Cancer. *Nutrition and Cancer* 1999;**35**:127–129.

317. Scott HR, McMillan DC, Forrest LM, Brown DJF, McArdle CS, Milroy R. The systemic inflammatory response, weight loss, performance status and survival in patients with inoperable non-small cell lung cancer. *British Journal of Cancer* 2002;**87**:264–267.

318. Abbass T, Dolan RD, Laird BJ, McMillan DC. The Relationship between Imaging-Based Body Composition Analysis and the Systemic Inflammatory Response in Patients with Cancer: A Systematic Review. *Cancers* 2019;**11**:1304.

319. Scheede-Bergdahl C, Watt HL, Trutschnigg B, Kilgour RD, Haggarty A, Lucar E *et al.* Is IL-6 the best pro-inflammatory biomarker of clinical outcomes of cancer cachexia? *Clinical Nutrition* 2012;**31**:85–88.

320. Krzystek-Korpacka M, Matusiewicz M, Diakowska D, Grabowski K, Blachut K, Kustrzeba-Wojcicka I *et al.* Impact of weight loss on circulating IL-1, IL-6, IL-8, TNF-alpha, VEGF-A, VEGF-C and midkine in gastroesophageal cancer patients. *Clin Biochem* 2007;**40**:1353–1360.

321. Pfitzenmaier J, Vessella R, Higano CS, Noteboom JL, Wallace D, Corey E. Elevation of cytokine levels in cachectic patients with prostate carcinoma. *Cancer* 2003;**97**:1211–1216.

322. Penafuerte CA, Gagnon B, Sirois J, Murphy J, MacDonald N, Tremblay ML. Identification of neutrophil-derived proteases and angiotensin II as biomarkers of cancer cachexia. *British Journal of Cancer* 2016;**114**:680–687.

323. Lerner L, Tao J, Liu Q, Nicoletti R, Feng B, Krieger B *et al.* MAP3K11/GDF15 axis is a critical driver of cancer cachexia. *J Cachexia Sarcopenia Muscle* 2016;**7**:467–482.

324. Bossola M, Muscaritoli M, Bellantone R, Pacelli F, Cascino A, Sgadari A *et al.* Serum tumour necrosis factor-α levels in cancer patients are discontinuous and correlate with weight loss. *European Journal of Clinical Investigation* 2000;**30**:1107–1112.

325. Strassmann G, Fong M, Kenney JS, Jacob CO. Evidence for the involvement of interleukin 6 in experimental cancer cachexia. *J Clin Invest* 1992;**89**:1681–1684.

326. Zhou W, Jiang Z-W, Tian J, Jiang J, Li N, Li J-S. Role of NF-κB and cytokine in experimental cancer cachexia. *World J Gastroenterol* 2003;**9**:1567–1570.

327. Tessitore L, Costelli P, Baccino FM. Humoral mediation for cachexia in tumour-bearing rats. *Br J Cancer* 1993;**67**:15–23.

328. Dillon EL, Volpi E, Wolfe RR, Sinha S, Sanford AP, Arrastia CD *et al.* Amino acid metabolism and inflammatory burden in ovarian cancer patients undergoing intense oncological therapy. *Clin Nutr* 2007;**26**:736–743.

329. Prokopchuk O, Steinacker JM, Nitsche U, Otto S, Bachmann J, Schubert EC *et al.* IL-4 mRNA Is Downregulated in the Liver of Pancreatic Cancer Patients Suffering from Cachexia. *Nutr Cancer* 2017;**69**:84–91.

330. Gilabert M, Calvo E, Airoldi A, Hamidi T, Moutardier V, Turrini O *et al.* Pancreatic Cancer-Induced Cachexia Is Jak2-Dependent in Mice. *Journal of Cellular Physiology* 2014;**229**:1437–1443.

331. Costelli P, Muscaritoli M, Bossola M, Moore-Carrasco R, Crepaldi S, Grieco G *et al.* Skeletal muscle wasting in tumor-bearing rats is associated with MyoD down-regulation. *International Journal of Oncology* 2005;**26**:1663–1668.

332. Carbó N, Busquets S, van Royen M, Alvarez B, López-Soriano FJ, Argilés JM. TNF-α is involved in activating DNA fragmentation in skeletal muscle. *British Journal of Cancer* 2002;**86**:1012–1016.

333. Miller A, McLeod L, Alhayyani S, Szczepny A, Watkins DN, Chen W *et al.* Blockade of the IL-6 trans-signalling/STAT3 axis suppresses cachexia in Kras-induced lung adenocarcinoma. *Oncogene* 2017;**36**:3059–3066.

334. Baltgalvis KA, Berger FG, Pena MMO, Davis JM, Muga SJ, Carson JA. Interleukin-6 and cachexia in ApcMin/+ mice. *American Journal of Physiology-Regulatory, Integrative and Comparative Physiology* 2008;**294**:R393–R401.

335. McPherron AC, Lawler AM, Lee S-J. Regulation of skeletal muscle mass in mice by a new TGF-p superfamily member. *Nature* 1997;**387**:83–90.

336. Durieux A-C, Amirouche A, Banzet S, Koulmann N, Bonnefoy R, Pasdeloup M *et al.* Ectopic Expression of Myostatin Induces Atrophy of Adult Skeletal Muscle by Decreasing Muscle Gene Expression. *Endocrinology* 2007;**148**:3140–3147.

337. Han HQ, Zhou X, Mitch WE, Goldberg AL. Myostatin/activin pathway antagonism: Molecular basis and therapeutic potential. *The International Journal of Biochemistry & Cell Biology* 2013;**45**:2333–2347.

338. Amirouche A, Durieux A-C, Banzet S, Koulmann N, Bonnefoy R, Mouret C *et al.* Down-Regulation of Akt/Mammalian Target of Rapamycin Signaling Pathway in Response to Myostatin Overexpression in Skeletal Muscle. *Endocrinology* 2009;**150**:286–294.

339. Breitbart A, Scharf GM, Duncker D, Widera C, Gottlieb J, Vogel A *et al.* Highly Specific Detection of Myostatin Prodomain by an Immunoradiometric Sandwich Assay in Serum of Healthy Individuals and Patients. *PLoS ONE* 2013;**8**:e80454.

340. Talar-Wojnarowska R, Wozniak M, Borkowska A, Olakowski M, Malecka-Panas E. Clinical significance of activin A and myostatin in patients with pancreatic adenocarcinoma and progressive weight loss. *J Physiol Pharmacol* 2020;**71**.

341. Schuelke M, Wagner KR, Stolz LE, Hübner C, Riebel T, Kömen W *et al.* Myostatin Mutation Associated with Gross Muscle Hypertrophy in a Child. *New England Journal of Medicine* 2004;**350**:2682–2688.

342. Roberts EW, Deonarine A, Jones JO, Denton AE, Feig C, Lyons SK *et al.* Depletion of stromal cells expressing fibroblast activation protein-α from skeletal muscle and bone marrow results in cachexia and anemia. *J Exp Med* 2013;**210**:1137–1151.

343. Liu CM, Yang Z, Liu CW, Wang R, Tien P, Dale R *et al.* Myostatin antisense RNA-mediated muscle growth in normal and cancer cachexia mice. *Gene therapy* 2008;**15**:155.

344. Benny Klimek ME, Aydogdu T, Link MJ, Pons M, Koniaris LG, Zimmers TA. Acute inhibition of myostatin-family proteins preserves skeletal muscle in mouse models of cancer cachexia. *Biochemical and Biophysical Research Communications* 2010;**391**:1548–1554.

345. Zhong X, Pons M, Poirier C, Jiang Y, Liu J, Sandusky GE *et al.* The systemic activin response to pancreatic cancer: implications for effective cancer cachexia therapy. *Journal of Cachexia, Sarcopenia and Muscle* 2019;**10**:1083–1101.

346. Latres E, Mastaitis J, Fury W, Miloscio L, Trejos J, Pangilinan J *et al.* Activin A more prominently regulates muscle mass in primates than does GDF8. *Nature Communications* 2017;**8**:15153.

347. Lerner L, Gyuris J, Nicoletti R, Gifford J, Krieger B, Jatoi A. Growth differentiating factor-15 (GDF-15): A potential biomarker and therapeutic target for cancer-associated weight loss. *Oncology Letters* 2016;**12**:4219–4223.

348. Paajanen J, Ilonen I, Lauri H, Järvinen T, Sutinen E, Ollila H *et al.* Elevated Circulating Activin A Levels in Patients With Malignant Pleural Mesothelioma Are Related to Cancer Cachexia and Reduced Response to Platinum-based Chemotherapy. *Clinical Lung Cancer* 2020;**21**:e142–e150.

349. Matzuk MM, Finegold MJ, Mather JP, Krummen L, Lu H, Bradley A. Development of cancer cachexia-like syndrome and adrenal tumors in inhibin-deficient mice. *Proceedings of the National Academy of Sciences* 1994;**91**:8817–8821.

350. Otani T, Minami S, Yamoto M, Umesaki N. Production of Activin A in Hyperplasia and Adenocarcinoma of the Human Endometrium. *Gynecologic Oncology* 2001;**83**:31–38.

351. Wildi S, Kleeff J, Maruyama H, Maurer C, Buchler M, Korc M. Overexpression of activin A in stage IV colorectal cancer. *Gut* 2001;**49**:409–417.

352. Belizário JE, Lorite MJ, Tisdale MJ. Cleavage of caspases-1, -3, -6, -8 and -9 substrates by proteases in skeletal muscles from mice undergoing cancer cachexia. *Br J Cancer* 2001;**84**:1135–1140.

353. van Royen M, Carbó N, Busquets S, Alvarez B, Quinn LS, López-Soriano FJ *et al.* DNA Fragmentation Occurs in Skeletal Muscle during Tumor Growth: A Link with Cancer Cachexia? *Biochemical and Biophysical Research Communications* 2000;**270**:533–537.

354. Schmalbruch H, Hellhammer U. The number of nuclei in adult rat muscles with special reference to satellite cells. *The Anatomical Record* 1977;**189**:169–175.

355. Tedesco FS, Dellavalle A, Diaz-Manera J, Messina G, Cossu G. Repairing skeletal muscle: regenerative potential of skeletal muscle stem cells. *J Clin Invest* 2010;**120**:11–19.

356. Chapman K, Holmes M, Seckl J. 11β-Hydroxysteroid Dehydrogenases: Intracellular Gate-Keepers of Tissue Glucocorticoid Action. *Physiol Rev* 2013;**93**:1139–1206.

357. McCormick KL, Wang X, Mick GJ. Evidence that the 11 beta-hydroxysteroid dehydrogenase (11 beta-HSD1) is regulated by pentose pathway flux. Studies in rat adipocytes and microsomes. *J Biol Chem* 2006;**281**:341–347.

358. Timmermans S, Souffriau J, Libert C. A General Introduction to Glucocorticoid Biology. *Front Immunol* 2019;**10**.

359. Knapp ML, Al-Sheibani S, Riches PG, Hanham IWF, Phillips RH. Hormonal Factors Associated with Weight Loss in Patients with Advanced Breast Cancer. *Ann Clin Biochem* 1991;**28**:480–486.

360. Cala MP, Agulló-Ortuño MT, Prieto-García E, González-Riano C, Parrilla-Rubio L, Barbas C *et al.* Multiplatform plasma fingerprinting in cancer cachexia: a pilot observational and translational study. *J Cachexia Sarcopenia Muscle* 2018;**9**:348–357.

361. Flint TR, Janowitz T, Connell CM, Roberts EW, Denton AE, Coll AP *et al.* Tumor-Induced IL-6 Reprograms Host Metabolism to Suppress Anti-tumor Immunity. *Cell Metabolism* 2016;**24**:672–684.

362. Llovera M, García-Martínez C, Costelli P, Agell N, Carbo N, Lopez-Soriano FJ *et al.* Muscle hypercatabolism during cancer cachexia is not reversed by the glucocorticoid receptor antagonist RU38486. *Cancer Letters* 1996;**99**:7–14.

363. Russell ST, Tisdale MJ. The role of glucocorticoids in the induction of zinc- α 2 -glycoprotein expression in adipose tissue in cancer cachexia. *British Journal of Cancer* 2005;**92**:876–881.

364. Tanaka Y, Eda H, Tanaka T, Udagawa T, Ishikawa T, Horii I *et al.* Experimental Cancer Cachexia Induced by Transplantable Colon 26 Adenocarcinoma in Mice. *Cancer Res* 1990;**50**:2290–2295.

365. Crespigio J, Weidmann R, Macioszek MA, de Oliveira JF, de Souza M, Pignatelli D *et al.* Impaired Glucocorticoid Synthesis in Cancer Cachexia-Anorexia Syndrome in an Experimental Model. *Annals of Clinical & Experimental Metabolism* 2016;**1**:1008.

366. Ball HA, Samuels LT. Adrenal Weights in Tumor-Bearing Rats. *Proceedings of the Society for Experimental Biology and Medicine* 1938;**38**:441–443.

367. Sarason EL. Adrenal cortex in systemic disease: a morphologic study. *Arch Intern Med (Chic)* 1943;**71**:702–712.

368. Lofberg E, Gutierrez A, Wernerman J, Anderstam B, Mitch WE, Price SR *et al.* Effects of high doses of glucocorticoids on free amino acids, ribosomes and protein turnover in human muscle. *Eur J Clin Invest* 2002;**32**:345–353.

369. Tomas FM, Munro HN, Young VR. Effect of glucocorticoid administration on the rate of muscle protein breakdown in vivo in rats, as measured by urinary excretion of Nτ-methylhistidine. *Biochem J* 1979;**178**:139–146.

370. Kuo T, Lew MJ, Mayba O, Harris CA, Speed TP, Wang J-C. Genome-wide Analysis of Glucocorticoid Receptor-Binding Sites in Myotubes Identifies Gene Networks Modulating Insulin Signaling. *Proc Natl Acad Sci U S A* 2012;**109**:11160–11165.

371. Bodine SC, Furlow JD. Glucocorticoids and Skeletal Muscle. *Adv Exp Med Biol* 2015;**872**:145–176.

372. Schakman O, Kalista S, Barbé C, Loumaye A, Thissen JP. Glucocorticoid-induced skeletal muscle atrophy. *The International Journal of Biochemistry & Cell Biology* 2013;**45**:2163–2172.

373. Shimizu N, Yoshikawa N, Ito N, Maruyama T, Suzuki Y, Takeda S *et al.* Crosstalk between Glucocorticoid Receptor and Nutritional Sensor mTOR in Skeletal Muscle. *Cell Metabolism* 2011;**13**:170–182.

374. Watson ML, Baehr LM, Reichardt HM, Tuckermann JP, Bodine SC, Furlow JD. A cell-autonomous role for the glucocorticoid receptor in skeletal muscle atrophy induced by systemic glucocorticoid exposure. *Am J Physiol Endocrinol Metab* 2012;**302**:E1210–E1220.

375. Yamamoto D, Maki T, Herningtyas EH, Ikeshita N, Shibahara H, Sugiyama Y *et al.* Branched-chain amino acids protect against dexamethasone-induced soleus muscle atrophy in rats. *Muscle & Nerve* 2010;**41**:819–827.

376. Schakman O, Kalista S, Bertrand L, Lause P, Verniers J, Ketelslegers JM *et al.* Role of Akt/GSK-3β/β-Catenin Transduction Pathway in the Muscle Anti-Atrophy Action of Insulin-Like Growth Factor-I in Glucocorticoid-Treated Rats. *Endocrinology* 2008;**149**:3900–3908.

377. Shah OJ, Kimball SR, Jefferson LS. Acute attenuation of translation initiation and protein synthesis by glucocorticoids in skeletal muscle. *Am J Physiol Endocrinol Metab* 2000;**278**:E76-82.

378. Svaninger G, Gelin J, Lundholm K. Tumor-host wasting not explained by adrenal hyperfunction in tumor-bearing animals. *J Natl Cancer Inst* 1987;**79**:1135–1141.

379. Long CNH, Katzin B, Fry EG. The adrenal cortex and carbohydrate metabolism. *Endocrinology* 1940;**26**:309–344.

380. Weber G. Study and evaluation of regulation of enzyme activity and synthesis in mammalian liver. *Advances in Enzyme Regulation* 1963;**1**:1–35.

381. Malkawi AK, Masood A, Shinwari Z, Jacob M, Benabdelkamel H, Matic G *et al.* Proteomic Analysis of Morphologically Changed Tissues after Prolonged Dexamethasone Treatment. *International Journal of Molecular Sciences* 2019;**20**:3122.

382. Phuc Le P, Friedman JR, Schug J, Brestelli JE, Parker JB, Bochkis IM *et al.* Glucocorticoid Receptor-Dependent Gene Regulatory Networks. *PLoS Genet* 2005;**1**.

383. Bose SK, Hutson I, Harris CA. Hepatic Glucocorticoid Receptor Plays a Greater Role Than Adipose GR in Metabolic Syndrome Despite Renal Compensation. *Endocrinology* 2016;**157**:4943–4960.

384. Herzig S, Long F, Jhala US, Hedrick S, Quinn R, Bauer A *et al.* CREB regulates hepatic gluconeogenesis through the coactivator PGC-1. *Nature* 2001;**413**:179–183.

385. Lemberger T, Staels B, Saladin R, Desvergne B, Auwerx J, Wahli W. Regulation of the peroxisome proliferator-activated receptor alpha gene by glucocorticoids. *J Biol Chem* 1994;**269**:24527–24530.

386. Yoon JC, Puigserver P, Chen G, Donovan J, Wu Z, Rhee J *et al.* Control of hepatic gluconeogenesis through the transcriptional coactivator PGC-1. *Nature* 2001;**413**:131–138.

387. Magomedova L, Cummins CL. Glucocorticoids and Metabolic Control. *Handb Exp Pharmacol* 2016;**233**:73–93.

388. Dolinsky VW, Douglas DN, Lehner R, Vance DE. Regulation of the enzymes of hepatic microsomal triacylglycerol lipolysis and re-esterification by the glucocorticoid dexamethasone. *Biochem J* 2004;**378**:967–974.

389. Hemmer MC, Wierer M, Schachtrup K, Downes M, Hübner N, Evans RM *et al.* E47 modulates hepatic glucocorticoid action. *Nature Communications* 2019;**10**:306.

390. Lemke U, Krones-Herzig A, Diaz MB, Narvekar P, Ziegler A, Vegiopoulos A *et al.* The Glucocorticoid Receptor Controls Hepatic Dyslipidemia through Hes1. *Cell Metabolism* 2008;**8**:212–223.

391. Okun JG, Conway S, Schmidt KV, Schumacher J, Wang X, de Guia R *et al.* Molecular regulation of urea cycle function by the liver glucocorticoid receptor. *Molecular Metabolism* 2015;**4**:732–740.

392. Arias G, Asins G, Hegardt FG, Serra D. The effect of dexamethasone treatment on the expression of the regulatory genes of ketogenesis in intestine and liver of suckling rats. *Mol Cell Biochem* 1998;**178**:325–333.

393. Cole TG, Wilcox HG, Heimberg M. Effects of adrenalectomy and dexamethasone on hepatic lipid metabolism. *J Lipid Res* 1982;**23**:81–91.

394. Holroyde CP, Gabuzda TG, Putnam RC, Paul P, Reichard GA. Altered Glucose Metabolism in Metastatic Carcinoma. *Cancer Res* 1975;**35**:3710–3714.

395. Holroyde CP, Skutches CL, Boden G, Reichard GA. Glucose Metabolism in Cachectic Patients with Colorectal Cancer. *Cancer Res* 1984;**44**:5910–5913.

396. Leij-Halfwerk S, Dagnelie PC, Wilson JHP, Sijens PE. Hepatic sugar phosphate levels reflect gluconeogenesis in lung cancer: simultaneous turnover measurements and 31P magnetic resonance spectroscopy in vivo. *Clinical Science* 2000;**98**:167–194.

397. Leij-Halfwerk S, Dagnelie PC, van den Berg JWO, Wattimena JDL, Hordijk-Luijk CH, Wilson JP. Weight loss and elevated gluconeogenesis from alanine in lung cancer patients. *The American Journal of Clinical Nutrition* 2000;**71**:583–589.

398. Waterhouse C, Jeanpretre N, Keilson J. Gluconeogenesis from Alanine in Patients with Progressive Malignant Disease. *Cancer Res* 1979;**39**:1968–1972.

399. Lundholm K, Edström S, Karlberg I, Ekman L, Scherstén T. Glucose turnover, gluconeogenesis from glycerol, and estimation of net glucose cycling in cancer patients. *Cancer* 1982;**50**:1142–1150.

400. Tayek JA, Katz J. Glucose production, recycling, Cori cycle, and gluconeogenesis in humans: relationship to serum cortisol. *American Journal of Physiology-Endocrinology and Metabolism* 1997;**272**:E476–E484.

401. Farkas J, von Haehling S, Kalantar-Zadeh K, Morley JE, Anker SD, Lainscak M. Cachexia as a major public health problem: frequent, costly, and deadly. *J Cachexia Sarcopenia Muscle* 2013;**4**:173–178.

402. Laviano A, Molfino A. Cachexia: looking yet not seeing. *Journal of Cachexia, Sarcopenia and Muscle* 2016;**7**:510–511.

403. May RC, Kelly RA, Mitch WE. Metabolic acidosis stimulates protein degradation in rat muscle by a glucocorticoid-dependent mechanism. *J Clin Invest* 1986;**77**:614–621.

404. Wing SS, Goldberg AL. Glucocorticoids activate the ATP-ubiquitin-dependent proteolytic system in skeletal muscle during fasting. *Am J Physiol* 1993;**264**:E668-676.

405. Tiao G, Fagan J, Roegner V, Lieberman M, Wang JJ, Fischer JE *et al.* Energy-ubiquitin-dependent muscle proteolysis during sepsis in rats is regulated by glucocorticoids. *J Clin Invest* 1996;**97**:339–348.

406. Mitch WE, Bailey JL, Wang X, Jurkovitz C, Newby D, Price SR. Evaluation of signals activating ubiquitin-proteasome proteolysis in a model of muscle wasting. *Am J Physiol* 1999;**276**:C1132-1138.

407. Bodine SC, Latres E, Baumhueter S, Lai VK-M, Nunez L, Clarke BA *et al.* Identification of Ubiquitin Ligases Required for Skeletal Muscle Atrophy. *Science* 2001;**294**:1704–1708.

408. Gilson H, Schakman O, Combaret L, Lause P, Grobet L, Attaix D *et al.* Myostatin gene deletion prevents glucocorticoid-induced muscle atrophy. *Endocrinology* 2007;**148**:452–460.

409. Schakman O, Dehoux M, Bouchuari S, Delaere S, Lause P, Decroly N *et al.* Role of IGF-I and the TNFα/NF-κB pathway in the induction of muscle atrogenes by acute inflammation. *Am J Physiol Endocrinol Metab* 2012;**303**:E729-739.

410. Hu Z, Wang H, Lee IH, Du J, Mitch WE. Endogenous glucocorticoids and impaired insulin signaling are both required to stimulate muscle wasting under pathophysiological conditions in mice. *J Clin Invest* 2009;**119**:3059–3069.

411. Schneider CA, Rasband WS, Eliceiri KW. NIH Image to ImageJ: 25 years of image analysis. *Nature Methods* 2012;**9**:671–675.

412. World Health Organization. *WHO steps surveillance manual: the WHO stepwise approach to chronic disease risk factor surveillance*. WHO: Geneva; 2005.

413. Ware JE, Sherbourne CD. The MOS 36-item short-form health survey (SF-36). I. Conceptual framework and item selection. *Med Care* 1992;**30**:473–483.

414. Leplège A. *Le questionnaire MOS SF-36: manuel de l'utilisateur et guide d'interprétation des scores*. Editions ESTEM: Paris; 2001.

415. Bachasson D, Millet GY, Decorte N, Wuyam B, Levy P, Verges S. Quadriceps function assessment using an incremental test and magnetic neurostimulation: A reliability study. *Journal of Electromyography and Kinesiology* 2013;**23**:649–658.

416. van der Werf A, Langius J a. E, de van der Schueren M a. E, Nurmohamed SA, van der Pant K a. MI, Blauwhoff-Buskermolen S *et al.* Percentiles for skeletal muscle index, area and radiation attenuation based on computed tomography imaging in a healthy Caucasian population. *Eur J Clin Nutr* 2017;**72**:288–296.

417. Baxmann AC, Ahmed MS, Marques NC, Menon VB, Pereira AB, Kirsztajn GM *et al.* Influence of Muscle Mass and Physical Activity on Serum and Urinary Creatinine and Serum Cystatin C. *Clin J Am Soc Nephrol* 2008;**3**:348–354.

418. Schutte JE, Longhurst JC, Gaffney FA, Bastian BC, Blomqvist CG. Total plasma creatinine: an accurate measure of total striated muscle mass. *J Appl Physiol Respir Environ Exerc Physiol* 1981;**51**:762–766.

419. Fox KM, Brooks JM, G SR, Markus R, Chiou C. Clinical Study Estimation of Cachexia among Cancer Patients Based on Four Definitions. *Journal of oncology* 2009;**2009**:693458.

420. Hingorani SR, Wang L, Multani AS, Combs C, Deramaudt TB, Hruban RH *et al.* Trp53R172H and KrasG12D cooperate to promote chromosomal instability and widely metastatic pancreatic ductal adenocarcinoma in mice. *Cancer Cell* 2005;**7**:469–483.

421. Gagne D, Pons M, Philibert D. RU 38486: a potent antiglucocorticoid in vitro and in vivo. *J Steroid Biochem* 1985;**23**:247–251.

422. Breivik T, Gundersen Y, Gjermo P, Opstad P-K. Chronic treatment with the glucocorticoid receptor antagonist RU486 inhibits diabetes-induced enhancement of experimental periodontitis. *Journal of Periodontal Research* 2014;**49**:36–44.

423. Kumari R, Willing L, Jefferson LS, Simpson IA, Kimball SR. REDD1 (Regulated in DNA Damage and Development 1) Expression in Skeletal Muscle as a Surrogate Biomarker of the Efficiency of Glucocorticoid Receptor Blockade. *Biochem Biophys Res Commun* 2011;**412**:644–647.

424. Heikinheimo O, Pesonen U, Huupponen R, Koulu M, Lähteenmäki P. Hepatic metabolism and distribution of mifepristone and its metabolites in rats. *Hum Reprod* 1994;**9 Suppl 1**:40–46.

425. Das SK, Eder S, Schauer S, Diwoky C, Temmel H, Guertl B *et al.* Adipose Triglyceride Lipase Contributes to Cancer-Associated Cachexia. *Science* 2011;**333**:233–238.

426. Abstract. *Journal of Cachexia, Sarcopenia and Muscle* 2019;**10**:1378–1435.

427. Freire-Regatillo A, Argente-Arizón P, Argente J, García-Segura LM, Chowen JA. Non-Neuronal Cells in the Hypothalamic Adaptation to Metabolic Signals. *Front Endocrinol* 2017;**8**.

428. Langlet F, Levin BE, Luquet S, Mazzone M, Messina A, Dunn-Meynell AA *et al.* Tanycytic VEGF-A Boosts Blood-Hypothalamus Barrier Plasticity and Access of Metabolic Signals to the Arcuate Nucleus in Response to Fasting. *Cell Metab* 2013;**17**:607–617.

429. Czaja W, Nakamura YK, Li N, Eldridge JA, DeAvila DM, Thompson TB *et al.* Myostatin regulates pituitary development and hepatic IGF1. *American Journal of Physiology-Endocrinology and Metabolism* 2019;**316**:E1036–E1049.

430. Hayashi Y, Mikawa S, Ogawa C, Masumoto K, Katou F, Sato K. Myostatin expression in the adult rat central nervous system. *Journal of Chemical Neuroanatomy* 2018;**94**:125–138.

431. Ma K, Mallidis C, Bhasin S, Mahabadi V, Artaza J, Gonzalez-Cadavid N *et al.* Glucocorticoid-induced skeletal muscle atrophy is associated with upregulation of myostatin gene expression. *Am J Physiol Endocrinol Metab* 2003;**285**:E363-371.

432. Wang R, Jiao H, Zhao J, Wang X, Lin H. Glucocorticoids Enhance Muscle Proteolysis through a Myostatin-Dependent Pathway at the Early Stage. *PLOS ONE* 2016;**11**:e0156225.

433. Hulmi JJ, Oliveira BM, Silvennoinen M, Hoogaars WMH, Ma H, Pierre P *et al.* Muscle protein synthesis, mTORC1/MAPK/Hippo signaling, and capillary density are altered by blocking of myostatin and activins. *American Journal of Physiology-Endocrinology and Metabolism* 2012;**304**:E41–E50.

ABSTRACT

Role of the glucocorticoid pathway in skeletal muscle wasting and hepatic metabolism rewiring during cancer cachexia in *Apc*$^{Min/+}$ mice – Functional implication of myostatin gene invalidation

Cachexia affects about half of cancer patients and is characterized by a progressive body mass loss mainly resulting from skeletal muscle depletion. This loss of skeletal muscle mass together with a decrease in muscle force strongly contribute to reduce cancer patient quality of life, treatment efficiency and ultimately patient survival. Many factors are known to be involved in the regulation of skeletal muscle homeostasis. Among them, glucocorticoids are steroid hormones secreted under the control of the hypothalamic-pituitary axis that have been well described to promote skeletal muscle atrophy but also to exert systemic actions through activation or repression of gene expression in many tissues. We hypothesized that the glucocorticoid pathway could be activated during cancer cachexia in *Apc*$^{Min/+}$ mice, a mouse model of intestinal cancer. Here, we reported that activation of skeletal muscle catabolism was associated with a complete reprogramming of liver metabolism. Moreover, we showed an activation of the hypothalamus-pituitary axis that was associated with an increase in the level of corticosterone (the main glucocorticoid in rodent) in serum, quadriceps muscle and liver of advanced cancer cachectic mice. The transcriptional signature in quadriceps muscle and liver of advanced cancer cachectic mice significantly mirrored that observed in mice treated with dexamethasone, an analog glucocorticoid. Importantly, the inhibition of cancer cachexia by myostatin gene invalidation in *Apc*$^{Min/+}$ mice restored corticosterone levels and abolished skeletal muscle and liver gene reprogramming. Together, these data indicate that glucocorticoids drive a transcriptional program to coordinately regulate skeletal muscle mass loss and hepatic metabolism rewiring. The inhibition of this response by myostatin gene invalidation highlights the existence of a molecular dialog between skeletal muscle and liver.

Rôle de la voie des glucocorticoïdes dans la perte de masse musculaire et le remaniement du métabolisme hépatique pendant la cachexie associée au cancer dans les souris *Apc*$^{Min/+}$ – implications fonctionnelles de l'inactivation du gène de la myostatine

La cachexie affecte environ la moitié des patients atteints d'un cancer et est caractérisée par une perte progressive de la masse corporelle résultant principalement d'une perte de masse musculaire squelettique. Cette perte de masse musculaire squelettique associée à une perte de force musculaire contribue fortement à réduire la qualité de vie des patients, l'efficacité des traitements et à terme, la survie des patients. Plusieurs facteurs sont connus pour être impliqués dans la régulation de la masse musculaire. Parmi eux, les glucocorticoïdes sont des hormones stéroïdiennes sécrétées sous le contrôle de l'axe hypothalamo-hypophysaire qui sont connues pour induire l'atrophie musculaire mais aussi pour avoir une action systémique via l'activation ou l'expression de gènes dans plusieurs tissus. Nous faisons l'hypothèse que la voie des glucocorticoïdes pourrait être activée pendant la cachexie associée au cancer dans les souris *Apc*$^{Min/+}$, un model murin de cancer intestinal. Nous rapportons ici que l'activation du catabolisme musculaire était associée à une reprogrammation complète du métabolisme du foie. En outre, nous montrons une activation de l'axe hypothalamo-hypophysaire associée à une augmentation du niveau en corticostérone (le glucocorticoïde principal chez les rongeurs) dans le sérum, le muscle quadriceps et le foie des souris à un stade avancé de la cachexie associée au cancer. La signature transcriptionnelle dans le muscle quadriceps et le foie des souris à un stade avancé de la cachexie associée au cancer reflète celle observée dans des souris traitée avec de la dexaméthasone, un analogue des glucocorticoïdes. Il est important de souligner que l'inhibition de la cachexie associée au cancer par l'inactivation du gène de la myostatine dans les souris *Apc*$^{Min/+}$ a restauré les niveaux en corticostérone et abolit la reprogrammation génique dans le muscle squelettique et le foie. Ensemble, ces données indiquent que les glucocorticoïdes induisent un programme transcritptionnel pour réguler de façon coordonnée la perte de masse musculaire et le remaniement du métabolisme hépatique. L'inhibition de cette réponse par l'invalidation du gène de la myostatine souligne l'existence d'un dialogue moléculaire entre le muscle squelettique et le foie.